

**STUDIES OF HEPATITIS B VIRUS AND HEPATITIS C
VIRUS IN SCID/BEIGE-ALB/UPA CHIMERIC MICE**

by

Ran Chen

A thesis submitted in partial fulfillment of the requirements for the degree of

Doctor of Philosophy
in
Virology

Department of Medical Microbiology and Immunology
University of Alberta

© Ran Chen, 2014

Abstract

Both hepatitis C virus (HCV) and hepatitis B virus (HBV) infections represent major global public health problems. Interferon (IFN) has been an important factor in both resolution of infection and in the treatment of both infections. Clinical data on anti-HBV and anti-HCV innate immune responses, in particular the IFN response, during natural infection in patients are limited. This is, in part, because most of patients are asymptomatic during acute stages of infection. IFN has been used to treat both HBV and HCV infections for years. Unfortunately, many patients do not respond to the IFN therapy. The reason for the variable treatment outcomes, in particular, the nonresponsiveness to IFN therapy in both HBV and HCV infections still remains unclear. In this thesis, IFN responses in HBV and HCV infections were studied using the severe combined immunodeficiency (SCID) / beige (bg) - albumin (Alb) / urokinase-type plasminogen activator (uPA) chimeric mouse model.

The SCID/bg-Alb/uPA chimeric mouse model was initially reported in 2001. This model supports robust and sustained infection by clinical or tissue culture derived hepatitis viruses, such as hepatitis A virus (HAV), HBV and HCV. Evidence has shown that the antiviral response to IFN in the chimeric mouse often reflects closely the response of the identical virus in humans when treated with IFN.

A time course of HCV infection was performed in SCID/bg-Alb/uPA chimeric mice to study an induced endogenous IFN response. There was a peak of interferon-stimulated gene (ISG) response at day-10 post infection, but no

significant ISG upregulation was observed in long-term HCV infection in the mice.

I also investigated the contributions of viral and host factors on the response of HCV infection to IFN treatment using two HCV viral strains differing in their IFN-sensitivity. These studies were performed in chimeric mice produced using three hepatocyte donors, each with distinct interleukin (IL) 28B single nucleotide polymorphisms (SNPs) at both rs12979860 and rs8099917 loci. My results showed that virus factors were the key factors determining the outcome of IFN therapy, whereas, viral interference with host janus kinase - signal transducer and activator of transcription (JAK-STAT) pathway as well as host factors, such as polymorphisms at the IL28B loci and pre-treatment levels of intrahepatic ISG expression, were less important in determining the outcome of IFN therapy in chimeric mice than they are in the patients.

In addition, endogenous IFN response during the course of HBV in the SCID/bg-Alb/uPA chimeric mice was examined. No significant IFN or ISG response was detected in chimeric mice during the course of HBV infection.

Since both the HBV and HCV viruses used in my studies were nonresponsive to exogenous IFN treatment in chimeric mice, the molecular mechanism of IFN nonresponsiveness of the two viruses was compared in a cohort of donor-matched chimeric mice. I found that in HBV infected chimeric mice, but not in mice infected with HCV, the JAK-STAT pathway was inhibited by STAT1 nucleus translocation blockage and thus expression downregulation of ISGs in response to

exogenous IFN treatment.

Finally, two collaborative projects were completed during my PhD. In the first study, the potential antiviral activity of exogenous HCV pathogen-associated molecular pattern (PAMP) RNA was investigated in HCV-infected SCID/bg-Alb/uPA chimeric mice. My results suggested that HCV PAMP RNA administration elicited an innate immune response in the livers of chimeric mice, which limited HCV infection. In the second study, we found that HCV infection in chimeric mice enhanced microRNA-27 expression and resulted in upregulating hepatic lipid droplet (LD) biogenesis. These results represented a novel mechanism by which HCV induces steatosis in chronic carriers of HCV.

Preface

This thesis is an original work by Ran Chen with exceptions mentioned below. The research project, of which this thesis is a part, received research ethics approvals from the University of Alberta Research Ethics Board: “Hep B and Hep C viruses / animal model of HBV or HCV” Pro00001040 (Human Ethics) and “Studies of HAV, HBV and HCV in the chimeric mouse model” AUP00000348 (Animal Ethics).

The experiments presented in Table 3.2 in Chapter 3 were performed by Ms. Michelle Kobewka, a 499 project student in Dr. D. Lorne Tyrrell’s laboratory, under my supervision.

Section 5.1 in Chapter 5 of this thesis was part of a project, named “Functional Analysis of MAVS Function in Innate Immunity”, in collaboration with Dr. Yueh-Ming Loo in Dr. Michael Gale Jr. laboratory in Seattle, USA. I was responsible for the experiment performance and data analysis in the studies done in chimeric mice in this Chapter. Dr. D. Lorne Tyrrell and I were involved in experiment design and manuscript preparation.

Section 5.2 in Chapter 5 of this thesis has been published as *Singaravelu R, Chen R, Lyn RK, Jones DM, O'Hara S, Rouleau Y, Cheng J, Srinivasan P, Nasheri N, Russell RS, Tyrrell DL, Pezacki JP. Hepatitis C virus induced up-regulation of microRNA-27: A novel mechanism for hepatic steatosis. Hepatology. 2014 Jan;59(1):98-108.* I was responsible for the experiments conducted in the

chimeric mice and data analysis, which is composed of the major body of section 5.2. I also contributed to manuscript edits. Dr. D. Lorne Tyrrell was the supervisory author and both Dr. D. Lorne Tyrrell and I were involved with concept formation and manuscript composition.

Acknowledgements

First and foremost, I would like to acknowledge my supervisor, Dr. Lorne Tyrrell, for his constant support, patience, motivation and enthusiasm during my Ph.D. Over all these years, he taught me to be independent and stand optimistic for all the things I do. His valuable advice helped me in all the time of research and writing of this thesis. He has been and will continue to be a mentor and role model to me.

Second, I would like to show my greatest appreciation to past and present the members of the Tyrrell lab. It has been a great team to work with and I feel grateful to get to know and become friends with all these incredible people. I would especially like to thank Dr. Bill Addison for his critical comments on my thesis and manuscripts. Bill also helped me in many ways on my research projects. Additionally, I would like to thank Gerald Lachance for his great technical support on animal experiments, Justin Shields for his help with mouse surgery and all the ELISA tests, Suellen Lamb for preparing all my slides and Mike Joyce for introducing me into the projects. I also thank Bonnie Bock as a good friend and wonderful co-worker for all the years in the lab.

Furthermore, I would like to express my warm and sincere thanks to my supervisory committee: Dr. Kevin Kane and Dr. Edan Foley for their encouragement, constructive feedback and supports during my Ph.D years. I would also like to thank Dr. Qiang Liu and Dr. Luis Schang for taking the time to read my thesis and for serving on my examining committee at the defense.

Finally, I would like to give my special thanks to my family: my husband Zaikun Xu, my parents and my son Shawn Zihan Xu, for their love, unwavering support, and for always believing in me. I appreciate Zaikun's support over the years of my graduate school. He has been patient, encouraging and caring throughout it all. I owe my loving thanks to my son, Shawn, who has been the most valuable gift in my life, and who has reminded me of more important things of life than work.

Table of Contents

CHAPTER 1: Introduction	1
1.1 Interferons and antiviral interferon response	2
1.1.1 Interferons	2
1.1.2 Type I interferon production and downstream signal transduction in response to viral infections	4
1.1.2.1 Type I interferon production in response to viral infections	4
1.1.2.2 Type I interferon stimulated signaling pathways	11
1.1.2.3 Type III interferon production and downstream signal transduction in response to viral infections	13
1.1.2.4 Viral immune evasion	16
1.2 Hepatitis B virus	16
1.2.1 Virology of Hepatitis B virus	16
1.2.1.1 HBV virion structure and genome organization	17
1.2.1.2 The life cycle of hepatitis B virus	21
1.2.2 Hepatitis B disease	25
1.2.2.1 Hepatitis B	25
1.2.2.2 Treatment of HBV infection	27
1.2.2.3 HBV vaccine	29
1.2.3 Innate immune response in HBV infection	30
1.3 Hepatitis C virus	33
1.3.1 Virology of Hepatitis C virus	33
1.3.1.1 HCV virion structure and genome organization	34
1.3.1.2 The life cycle of hepatitis C virus	37
1.3.2 Hepatitis C disease	41
1.3.2.1 Hepatitis C	41
1.3.2.2 Treatments for HCV infection	42
1.3.2.3 HCV vaccine	45
1.3.3 Innate immune response in HCV infection	45
1.4 Experimental models for the study of hepatitis B and C viruses	50
1.4.1 Cell culture models for the study of hepatitis B and C viruses	50
1.4.2 Animal models for the study of hepatitis B and C viruses	52
1.5 Hypothesis and research objectives	57
CHAPTER 2: Materials and Methods	60
2.1 Reagents	61
2.1.1 Reagents	61
2.1.2 Commonly used buffers and solutions	63

2.1.3 Oligonucleotides	65
2.1.4 Antibodies	67
2.1.5 Cells, animals and viruses	68
2.1.5.1 Cells	68
2.1.5.2 Animals	68
2.1.5.3 Viruses	69
2.2 Methods	69
2.2.1 Generation of SCID/bg-Alb/uPA chimeric mice	69
2.2.2 Defrosting of human hepatocytes	73
2.2.3 Human albumin measurement in mouse serum	73
2.2.4 Viral infection	74
2.2.5 Exogenous interferon treatment	75
2.2.6 Tissue dissection and organ harvest	76
2.2.7 Total RNA isolation from snap-frozen liver samples	77
2.2.8 Genomic DNA isolation from snap-frozen liver samples	78
2.2.9 Human chimerism measurement	80
2.2.10 HCV titer quantification in mouse serum	80
2.2.11 Quantification of intrahepatic HCV RNA	82
2.2.12 HBV titer quantification in mouse serum	82
2.2.13 Quantification of intrahepatic HBV DNA	83
2.2.14 Quantification of intrahepatic HBV RNA	84
2.2.15 Analysis of human gene expression by RT-real time PCR	85
2.2.16 Poly(I:C) treatment in BALB/c mice	86
2.2.17 Protein gel electrophoresis and detection	87
2.2.18 HBV capsid western blot	89
2.2.19 Indirect immunofluorescence microscopy	90
2.2.20 RNA transfection in HCV infected chimeric mice	91
2.2.21 Quantification of miR-27mRNA levels by RT-PCR	92
2.2.22 Immunofluorescence and Oil Red O Staining of chimeric mouse livers	92
2.2.23 Statistics	93
CHAPTER 3: A Study Of Viral Versus Host Factors That Determine The Response To Interferon Alpha Treatment Of HCV Infection In SCID/Beige-Alb/uPA Chimeric Mice	95
3.1 Rationale	96
3.2 Results	99
3.2.1 Role of HCV viral factors in determining IFN α treatment outcome	99
3.2.2 Role of viral interference with host IFN signalling in determining the sensitivity of HCV to exogenous IFN α treatment	107
3.2.3 Effect of host pre-treatment ISG expression level on	111

response to IFN α treatment	
3.2.4 Host IL28B polymorphisms in determining IFN treatment outcome in chimeric mice infected with HCV	113
3.3 Discussion	118
3.4 Summary	128
CHAPTER 4: Mechanism Of Interferon Nonresponsiveness Of HBV And HCV In SCID/Beige-Alb/uPA Chimeric Mice	130
4.1 Rationale	131
4.2 Results	134
4.2.1 Time course of induced IFN response during HBV infection in chimeric mice	134
4.2.2 The IFN response induced during the course of HCV infection in chimeric mice.	141
4.2.3 Comparison of the response of HBV and HCV to exogenous IFN treatment	148
4.2.4 Nonresponsiveness to exogenous IFN treatment of HBV and HCV is due to different mechanisms	152
4.3 Discussion	159
4.3.1 The endogenous IFN response induced during HBV or HCV viral infections in chimeric mice	159
4.3.2 The mechanisms of nonresponsiveness to exogenous IFN treatment differ between HBV and HCV	162
4.4 Summary	166
CHAPTER 5: Collaborative Research Projects Using The SCID/Beige-Alb/uPA Chimeric Mice	167
5.1 The HCV PAMP RNA induces innate immune responses that limits HCV infection in chimeric mice	168
5.1.1 Rationale	169
5.1.2 Results	170
5.1.2.1 HCV PAMP RNA, but not XRNA, induced an innate response in chimeric mice	170
5.1.2.2 The innate response triggered by HCV PAMP RNA limits chimeric mice from HCV infection	174
5.1.3 Discussion	177
5.1.4 Summary	178
5.2 HCV infection in chimeric mice induced up-regulation of microRNA-27: a novel mechanism for hepatic steatosis	179
5.2.1 Rationale	180
5.2.2 Results	182
5.2.2.1 HCV Infection activates miR-27 expression in chimeric mice	182
5.2.2.2 HCV infection caused increased cellular LDs	186

in chimeric mice	
5.2.3 Discussion	190
5.2.4 Summary	192
CHAPTER 6: Project overview, Conclusion and Future Directions	193
6.1 Project overview and general discussion	194
6.2 Conclusion	200
6.3 Future directions and perspective	201
References	204

List of Tables

Table 2.1 Commercial sources of materials, chemicals, and reagents.....	61
Table 2.2 Molecular size standards.....	62
Table 2.3 DNA/RNA modifying enzyme.....	62
Table 2.4 Multi-component systems.....	63
Table 2.5 Detection systems.....	63
Table 2.6 Buffers and Solutions.....	63
Table 2.7 Oligonucleotides.....	65
Table 2.8 Primary antibodies.....	67
Table 2.9 Secondary antibodies.....	67
Table 3.1 Two HCV isolates with distinct sensitivities to IFN therapy.....	100
Table 3.2 Correlation of HCV response to pegIFN treatment in chimeric mice with the response of patients to the pegIFN and RBV therapy.....	106
Table 3.3 Three lines of chimeric mice populated with three different human Hepatocyte donors with distinct IL28B SNPs.....	115

List of Figures

Figure 1.1 PRRs-mediated signaling in response to viral infection.....	10
Figure 1.2 JAK-STAT signalling pathway.....	15
Figure 1.3 HBV viral structure.....	19
Figure 1.4 HBV genome organization.....	20
Figure 1.5A HBV life cycle.....	23
Figure 1.5B HBV transcripts during replication.....	24
Figure 1.6 Genome organization of HCV.....	36
Figure 1.7 The HCV replication cycle.....	40
Figure 2.1 Generation of SCID/bg-Alb/uPA chimeric mice.....	71
Figure 3.1 Sustained viremia by both HCV strains in chimeric mice populated with a single hepatocyte donor.....	101

Figure 3.2 Response of the two HCV strains to exogenous IFN α treatment in chimeric mice populated with a single hepatocyte donor.....	104
Figure 3.3 ISG expression upon exogenous IFN α treatment in HCV infected mouse livers in comparison to uninfected, saline-treated controls.....	109
Figure 3.4 Comparison of the effects of viral interference on ISG expression between the two HCV strains upon exogenous IFN α treatment.....	110
Figure 3.5 Endogenous IFN or ISG expression in chimeric mice (Hu8063) chronically infected with the two HCV strains.....	112
Figure 3.6 Effect of the non-responder genotypes of IL28B SNPs on response to IFN treatment in the two HCV strains.....	116
Figure 3.7 Effect of host IL28B SNPs on HCV sensitivity to IFN α treatment in the chimeric mouse model.....	117
Figure 3.8 Preliminary data of adoptive transfer of purified human pDCs into Chimeric mice infected with HCV.....	123
Figure 4.1. Kinetics of virological parameters during the course of HBV infection in SCID/bg-Alb/uPA chimeric mice.....	136
Figure 4.2 IFN response induced during the course of HBV infection in chimeric mice.....	138
Figure 4.3 ISG expression in mock-infected chimeric mice produced with hepatocytes Hu8063.....	139
Figure 4.4 ISG expression in long-term HBV-infected chimeric mice populated with a hepatocyte donor Hu8063.....	140

Figure 4.5 Kinetics of virological parameters during the course of HCV infection in SCID/bg-Alb/uPA chimeric mice.....	142
Figure 4.6 IFN response induced during the course of HCV infection in chimeric mice.....	144
Figure 4.7 ISG expression in long-term HCV-infected chimeric mice populated with a hepatocyte donor Hu8085.....	145
Figure 4.8 Examination of IFN response induction during chronic HCV infection in chimeric mice produced with two other hepatocyte donors.....	147
Figure 4.9 Response of HBV to exogenous IFN treatment.....	150
Figure 4.10 Response of HCV to exogenous IFN treatment.....	151
Figure 4.11 Potential suppression of ISG expression by HBV and HCV upon exogenous IFN treatment in chimeric mice.....	154
Figure 4.12 Transcriptional level change of STAT 1 and 2 in chimeric mice infected with HBV or HCV with/without IFN treatment.....	156
Figure 4.13 STAT1 nuclear translocation upon IFN treatment in chimeric mice infected with HBV or HCV.....	157
Figure 5.1 Expression of ISGs in chimeric mice transfected with HCV PAMP RNA or XRNA in comparison to the mice treated with PBS.....	172
Figure 5.2 Expression of IFNs in chimeric mice transfected with HCV PAMP RNA or HCV XRNA in comparison to the mice treated with PBS.....	173

Figure 5.3 HCV viremia change after administration of HCV PAMP RNA, HCV XRNA or PBS in chimeric mice infected with HCV.....	175
Figure 5.4 MiR-27 isoforms and conservation of sequence.....	183
Figure 5.5 HCV infection in chimeric mice.....	184
Figure 5.6 HCV infection enhances miR-27 expression in chimeric mice.....	185
Figure 5.7 MiR-27 regulates hepatic lipid homeostasis.....	188
Figure 5.8 Changes of cellular lipid levels by HCV infection in chimeric mice...	189

List of Nomenclature and Abbreviations

5'ppp	5' terminal triphosphate
aa	Amino acid
Alb	Albumin
ALT	Alanine transaminase
ANGPTL3	Angiotensin-like protein 3
anti-HBe	HBe antibody
APOBEC3G	Apolipoprotein B mRNA-editing enzyme catalytic polypeptide 3 protein G
BCA	Bicinchoninic acid
bg	Beige
BSA	Bovine serum albumin
Cardif	CARD adaptor inducing IFN β
CARDs	Caspase activation and recruitment domains
CARS	Coherent anti-Stokes Raman scattering
cccDNA	Covalently closed circular DNA
cDCs	Conventional DCs
cDNA	Complementary DNA
CETP	Cholesterol ester transfer protein
CHB	Chronic hepatitis B
CHC	Chronic hepatitis C
CK-18	Cytokeratin 18
CLDN-1	Claudin-1

CTL	Cytotoxic T cell
CXCL	Chemokine (C-X-C motif) ligand
DAAs	Direct-acting antiviral agents
DAI	DNA-dependent activator of IFN-regulatory factors
DAPI	4',6-diamidino-2-phenylindole
DCs	Dendritic cells
DHBV	Duck hepatitis B virus
DMEM	Dulbecco's modified Eagle's medium
DMSO	Dimethyl sulfoxide
ds	Double stranded
DTT	Dithiothreitol
ECL	Enhanced chemiluminescence
EDTA	Ethylenediaminetetraacetic acid
eIF2 α	Eukaryotic initiation factor 2 α subunit
ELISA	Enzyme-linked immunosorbent assay
ER	Endoplasmic reticulum
ERK	Extracellular-signal-regulated kinase
FASN	Fatty acid synthase
FBS	Fetal bovine serum
FDA	the Food and Drug Administration
GAGs	Glucosaminoglycans
GAPDH	Glyceraldehyde 3-phosphate dehydrogenase

GAS	IFN-gamma-activated site
GE	Genome equivalence
GSHV	Ground squirrel hepatitis virus
gt	Genotype
hApoB	Human apolipoprotein B
HAV	Hepatitis A virus
HBsAg	Hepatitis B surface antigen
HBV	Hepatitis B virus
HCC	Hepatocellular carcinoma
HCV	Hepatitis C Virus
HHBV	Heron hepatitis B virus
HIV	Human immunodeficiency virus
HPRT-1	Hypoxanthine Phosphoribosyltransferase 1
HRP	Horseradish peroxidase
HVR1	Hypervariable region 1
i.p	Intraperitoneal
i.v	Intravenous
IDUs	Injection drug users
IF	Immunofluorescence
IFI27	Interferon alpha -inducible protein 27
IFI6	Interferon alpha -inducible protein 6
IFIT1/2	Interferon-induced protein with tetratricopeptide repeats 1/2

IFITM1	Interferon-induced transmembrane protein 1
IFN	Interferon
IFNAR1	Interferon- α/β receptor 1
IKKi	The I κ B kinase i
IKK α	The inhibitor of NF- κ B kinase α
IL-10R β	IL10 receptor beta
IL28R α	IL28 receptor alpha subunit
IL29	Interleukin-29
IPS-1	IFN β promoter stimulator 1
IRAK4	Interleukin-1 receptor-associated kinase 4
IRES	Internal ribosome entry site
IRFs	Interferon-regulatory factors
IRRDR	The interferon/RBV-resistance-determining region
ISDR	IFN-sensitivity-determining region
ISG15	IFN-stimulated protein of 15 kDa
ISGF3	The IFN-stimulated gene factor 3
ISGs	IFN-stimulated genes
ISREs	IFN-stimulated response elements
IU	International unit
JAKs	Janus kinases
JFH-1	Japan Fulminant Hepatitis type 1
kb	Kilobase

LCMV	Lymphocytoid choriomeningitis virus
LDL	Low-density lipoprotein
LDLRs	Low-density lipoprotein receptors
LDs	Lipid droplets
LGP2	Laboratory of genetics and physiology gene 2
LHBs	Large HBV surface protein
LPA	Liner polyacrylamide
LRRs	Leucine-rich repeats
M-MLV	Moloney Murine Leukemia Virus
MAPKs	Mitogen-activated protein kinases
MAVS	Mitochondrial antiviral signaling
MDA5	Melanoma differentiation-associated gene 5
MHBs	Medium HBV surface protein
MHC	Major histocompatibility complex
miRNAs	microRNAs
MxA/Mx1	Myxovirus (influenza virus) resistance 1
MyD88	Myeloid differentiation factor 88
NANBH	non-A, non-B hepatitis
NF κ B	Nuclear factor kappa-light-chain-enhancer of activated B cells
NI	uninfected
NK	Natural killer
NLRs	Nucleotide-binding oligomerization domain receptors

NLS	Nuclear localization signal
NPCs	Nuclear pore complexes
NS	Non-structural
NTCP	Sodium taurocholate cotransporting polypeptide
NTFs	Nuclear transport factors
NTR	Non-translated region
Nups	Nuclear pore complex proteins
NVR	Non-virological response
OAS	2' 5-oligoadenylate synthetase
OCLN	Occludin
OCT	Optimal cutting temperature compound
OD	Optical density
ORFs	Open reading frames
ORO	Oil red O
p.i.	Post infection
p.t	Post transfer
PAMPs	Pathogen-associated molecular patterns
PBS	Phosphate buffered saline
PCR	Polymerase chain reaction
pDCs	Plasmacytoid DCs
pegIFN	Pegylated interferon alpha-2a
pgRNA	Pregenomic RNA

PI3K	Phosphatidylinositol 3-kinase
PIAS	Protein inhibitor of activated STAT1
PKR	Protein kinase R
PKRBD	PKR binding domain
pol	polymerase
poly(I:C)	Polyinosinic:polycytidylic acid
PPAR α	Peroxisome proliferator-activated receptor alpha
PRRs	Pathogen recognition receptors
PVDF	Polyvinylidene difluoride
qPCR	Quantitative polymerase chain reaction
RBV	Ribavirin
rcDNA	Relaxed circular DNA
RD	Repressor domain
RIG-I	Retinoic acid inducible gene I
RLRs	RIG-I-like receptors
RNaseL	Ribonuclease L
RSV	Respiratory syncytial virus
RT	Reverse transcription or Reverse transcriptase
RXR α	Retinoid X receptor α
s.c	Subcutaneous
SBEs	STAT3-binding elements
SCID	Severe combined immunodeficiency

SD	Standard deviation
SDS	Sodium dodecyl sulphate
SEM	The standard error of the mean
SHBs	Small HBV surface protein
SNPs	Single nucleotide polymorphisms
SOCS	Suppressor of cytokine signaling
SP110	SP110 nuclear body protein
SR-B1	Scavenger receptor type B1
SREBP1	Sterol regulatory element-binding protein 1
ss	Single stranded
STAT	Signal transducer and activator of transcription
SVP	Sub-viral particles
SVR	Sustained virological response
TBK1	TANK-binding kinase 1
TBS	Tris-buffered saline
TEMED	N,N,N',N',-tetramethylenediamine
TIR	Toll/IL-1 receptor homology
TLR	Toll-like receptor
TMB	3,3',5,5'-tetramethylbenzidine
TNFSF10	Tumor necrosis factor superfamily, member 10
TNF α	Tumor necrosis factor α
TRAF6	TNF receptor associated factor 6

TRIF	TIR-domain-containing adapter-inducing IFN- β
TRIM22/25	Tripartite motif-containing protein 22/25
TYK2	Tyrosine kinase 2
uPA	Urokinase-type plasminogen activator
USP18	Ubiquitin specific peptidase 18
VISA	Virus induced signaling adaptor
VLDL	Very-low density lipoprotein
WB	Western blot
WHO	World Health Organization
WHV	Woodchuck hepatitis virus
WMHV	Woolly monkey hepatitis B virus
XAF1	X-linked inhibitor of apoptosis protein associated factor 1

CHAPTER 1

Introduction

1.1 Interferons and antiviral interferon response

1.1.1 Interferons

Interferon was first discovered by Isaacs and Lindenmann in 1957 as an agent that protects cells from viral infection [1]. The interferons (IFNs) are a family of structurally related multifunctional cytokines made and released by host cells in response to a variety of stimuli. The IFN family is categorized into three classes, type I, II and III IFNs, according to their receptor specificity and functional properties. Only type I and III IFNs are discussed in the introduction of this thesis.

In humans, type I IFNs include 13 IFN α s and one single type of each of IFN β , ω , ϵ and κ [2]. All the genes that encode type I IFNs are clustered on chromosome 9 [3, 4]. All type I IFNs bind to a common receptor, the type I IFN receptor complex, which is widely expressed in almost all cell types and tissues and is composed of two subunits, the IFN α/β receptor 1 (IFNAR1) and IFNAR2 [5]. Although they interact with the same receptor, the type I IFNs exhibit a broad range of biological functions: antiviral activities, cell growth inhibition, control of apoptosis and immunomodulatory effects [6]. Differences in activity are regulated by many factors: specific subtypes of type I IFN, differential affinities for IFNARs [2], activation of cellular kinases in addition to Janus kinases, e.g. phosphatidylinositol-3 kinase (PI3K), patterns of activation of STATs in different cell types, and activation of many transcription factors other than STATs, such as the interferon-regulatory factors (IRFs) [7, 8]. Many of these actions make IFN a promising agent for the treatment of various diseases. However, therapeutic use of

IFNs is hampered by their side effects. The side effects of type I IFNs are related to the broad expression of IFNARs throughout the body. This results in activation of biological responses in tissues other than the targets. For example, in addition to liver cells, hematologic cell types, such as neutrophils and lymphocytes, express the IFNARs, and IFN α therapy for hepatitis C virus (HCV) infection often induces neutropenia and lymphopenia in a significant percentage of patients [9, 10]. In addition, expression of IFNARs in central nervous system causes psychiatric adverse events in chronic hepatitis C patients when treated with IFN therapy, which often lead to dose reductions or even discontinuation of the therapy [10].

In 2003, a new class of IFNs was discovered, the IFN λ molecules or type III IFNs: IFN λ 1, λ 2 and λ 3 [11, 12], which are also known in the literatures as interleukin (IL) 29, IL28A and IL28B, respectively. IFN λ s protect cells from virus infection and induce major histocompatibility complex (MHC) class I antigen expression, i.e. their antiviral activity is similar to type I IFNs [11, 12]. However, the immunomodulatory function of this novel class of cytokines is less well established. They bind a different cell surface receptor, which is composed of two chains, IL28 receptor alpha subunit (IL28R α) and IL10 receptor beta (IL10R β) [11, 12]. In contrast to the ubiquitous expression of the IFNAR receptor complex, IL28R α exhibits a more restricted tissue distribution, notably epithelial cells, e.g the stomach, intestine, liver and lungs [11, 13-15]. It has been suggested that the preferential expression of IFN λ receptors on epithelial cells may allow the host to rapidly eliminate viruses at the major portals of entry into the body before

infection is established without activating other arms of the immune system [16]. This is supported by a recent study showing that IFN λ s induce activation of janus kinase (JAK) - signal transducer and activator of transcription (STAT) signaling and a common set of interferon-stimulated genes (ISGs) in mouse and human hepatocytes but not in purified lymphocytes or monocytes [17]. However, the ability of immune cells to respond to IFN λ s remains a matter for debate. There are reports describing IFN λ signaling and receptor expression in some dendritic cells (DCs) and lymphocyte subsets [18-20]. Further clarification is required to determine if IFN λ s play a direct role in shaping the adaptive immune response like type I IFNs.

Most recently, a new member of type III IFN, IFN λ 4, has been discovered [21]. The IFN λ 4 gene harbors a dinucleotide variant (ss469415590, TT or Δ G), where the TT allele leads to a frame shift, thus inactivating the gene, while the Δ G allele results in a functional IFN λ 4 gene. In a large proportion of the human population, the TT allele renders the IFN λ 4 gene inactive [21]. *In vitro* studies show that the IFN λ 4 gene encodes an active type III IFN protein, which signals through the same IL28R α and IL10R β receptors as other IFN λ s [22]. Although its secretion is substantially lower than other IFN λ s, expression of IFN λ 4 has shown antiviral activity against HCV and coronaviruses at levels comparable to IFN λ 3 [22].

1.1.2 Type I interferon production and downstream signal transduction in response to viral infections

1.1.2.1 Type I interferon production in response to viral infections

Production of type I IFN is predominantly initiated in response to pathogens, such

as viruses, bacteria and their products. It is a hallmark of the innate immune responses of mammalian hosts to viral infection. Pathogens express a number of signature molecular structures, pathogen-associated molecular patterns (PAMPs), which are essential for their survival, and hence relatively conserved [23-25]. PAMPs are sensed as non-self by host sensors known as pathogen recognition receptors (PRRs). Recognition of PAMPs by PRRs rapidly activates an array of signal cascades and pathways resulting in the release of various inflammatory cytokines and chemokines as well as IFNs. These responses are also critical for the development of pathogen-specific, long-lasting adaptive immunity, which facilitates the clearance of the pathogen during the primary infection and during re-exposure [24, 26].

The PRRs are the first line of host recognition of both extracellular and intracellular pathogens. They are able to sense various classes of foreign molecules including proteins, lipids, carbohydrates and nucleic acids [27]. To date, several classes of PRRs, including Toll-like receptors (TLRs), retinoic acid inducible gene I (RIG-I) - like receptors (RLRs), nucleotide-binding oligomerization domain receptors (NLRs) and cytosolic DNA sensors, have been discovered [27]. Currently, the first three classes of these PRRs, TLRs, RLRs and NLRs, have been shown to recognize virus-specific components in infected cells [24, 27]. Among these three PRRs, TLRs and RLRs are important for the production of type I IFNs and pro-inflammatory cytokines, whereas NLRs are known to regulate IL1 β maturation through activation of caspase-1 [24, 27]. For the purpose of this thesis, only TLRs and RLRs will be discussed in detail.

TLRs are responsible for detecting viral components extracellularly and within cytoplasmic vacuoles after phagocytosis or endocytosis by the cells [27]. There are more than 10 TLRs in mammals. Among them, TLR2, TLR3, TLR4, TLR7, and TLR9 are involved in the recognition of viral components [24, 27, 28]. TLR2 and TLR4, located on the plasma membrane, sense viral envelope proteins on the cell surface [28]. While viral proteins recognized by these two surface TLRs trigger pro-inflammatory responses, their contribution to either protective or pathological immune responses largely depends on the type of virus, route of infection, and other host factors. TLR3, TLR7, and TLR9 are located on cytoplasmic vesicles, such as endosomes, and can be activated by nucleic acids [27, 28]. Although virtually all human cells are able to synthesize IFN α/β , expression of particular TLRs is more restricted among certain cell types. For example, TLR7 and TLR9, which recognize single stranded (ss) RNA and DNA with CpG motifs respectively, are highly expressed in plasmacytoid DCs (pDCs) [27, 28], a cell type well known to produce large amounts of type I IFNs in response to virus infection. TLR3 recognizes double stranded (ds) RNA and is expressed more widely, but is mainly expressed on conventional DCs (cDCs) and possibly on epithelial cells [27, 28].

TLRs are transmembrane proteins, composed of LRRs (leucine-rich repeats), a transmembrane domain, and a cytoplasmic domain designated the Toll/IL1 receptor homology (TIR) domain [29]. TLR signaling is mediated by the recruitment of TIR domain containing adaptor molecules, e.g myeloid differentiation factor 88 (MyD88) and TIR-domain-containing adapter-inducing

IFN β (TRIF), to the TIR domains of the TLRs [29]. All TLRs except TLR3 activate a common signaling pathway, the MyD88-dependent signaling pathway, leading to the production of pro-inflammatory cytokines and IFNs [27-29]. In pDCs stimulated with TLR7 and TLR9 PAMPs, MyD88 recruits various signaling proteins, such as IL1 receptor-associated kinase 4 (IRAK4), IRAK1, TNF receptor associated factor 6 (TRAF6), TRAF3, and/or the inhibitor of NF κ B kinase α (IKK α), which phosphorylate IRF7 to initiate the transcription of type I IFNs. On the other hand, TLR3 and TLR4 recruit the adaptor protein TRIF and initiate TRIF-dependent signaling to activate nuclear factor kappa-light-chain-enhancer of activated B cells (NF κ B) and IRF3 to induce production of pro-inflammatory cytokines and type I IFNs in response to PAMPs [27, 28]. A more detailed signaling transduction pathway is summarized in Figure 1.1.

The RLR family consists of three homologous DExD/H box RNA helicases: RIG-I, melanoma differentiation-associated gene 5 (MDA5), and laboratory of genetics and physiology gene 2 (LGP2) [27, 28]. RIG-I and MDA5 play a major role in recognition of RNA from RNA viruses or RNA intermediates of replicating DNA viruses, e.g hepatitis B virus (HBV) [30], in the cytoplasm of infected cells and induce inflammatory cytokines and type I IFNs in cDCs, macrophages and fibroblasts [27]. RIG-I binds 5'-triphosphorylated ssRNAs [31, 32] and short dsRNAs [33]. In addition, a polyU/C-containing RNA sequence in the 3' non-translated region (NTR) of HCV genomic RNA preferentially activates RIG-I compared to other sequences of HCV [34]. RIG-I mainly recognizes members of paramyxoviridae and flaviviridae families of viruses, such as Newcastle disease

virus, vesicular stomatitis virus, Japanese encephalitis virus and HCV [27]. In contrast, MDA5 preferentially recognizes longer dsRNA [33], including synthetic polyinosinic:polycytidylic acid [poly(I:C)]. The viruses of picornaviridae family, such as encephalomyocarditis virus, are targeted by MDA5 [27].

Both RIG-I and MDA5 contain two N-terminal tandem caspase activation and recruitment domains (CARDs), a DExD/H box RNA helicase domain, and a C-terminal repressor domain (RD) [35, 36]. The helicase and RD domains are important for the recognition of the RNA PAMPs, while the CARD domains are essential for triggering intracellular signaling cascades [35, 36]. LGP2 lacks the CARD domain, initially suggesting a negative regulatory role for LGP2 in RIG-I- and MDA5-mediated signaling [37]. However, recent evidence has shown that LGP2 acts as a positive regulator of RIG-I- and MDA5-mediated signaling through its ATPase domain [38]. In the cytoplasm, RIG-I and MDA5 sense cytosolic viral RNAs, which leads to conformational changes exposing their CARD domains. The CARD domains then interact with the CARD-containing adaptor protein, mitochondrial antiviral signaling (MAVS) [also known as IFN β promoter stimulator 1 (IPS-1), CARD adaptor inducing IFN β (Cardif), and virus induced signaling adaptor (VISA)] [39-41]. MAVS was initially found on mitochondria [40]. Recently, evidence has shown that MAVS is also present on peroxisomes [42]. Peroxisomal and mitochondrial MAVS act sequentially to create an antiviral cellular state. Upon viral infection, peroxisomal MAVS induces a rapid IFN-independent expression of defense factors that provide short-term protection by activating IRF1, whereas mitochondrial MAVS activates an IFN-

dependent signaling pathway with delayed kinetics through IRF3, which amplifies and stabilizes the antiviral response. As illustrated in Figure 1.1, upon recruitment of RIG-I and MDA5, MAVS activates the IKK-related kinase, TANK-binding kinase 1 (TBK1) / the I κ B kinase i (IKKi), which activates IRF3/IRF7 and the subsequent transcription of type I IFNs by TRAF3. MAVS also activates NF κ B for the expression of pro-inflammatory genes [39-41].

It is well known that innate immune responses are important for mounting adaptive immune responses to viral infections. However, it is not clear how the innate PRRs contribute to the activation of adaptive immunity. Three independent studies examined the roles of RLRs and TLRs in the activation of adaptive immune responses using different virus infection models. Studies with lymphocytic choriomeningitis virus (LCMV) [43] and influenza virus [44] found that TLRs (MyD88-dependent signaling), but not RLRs (MAVS-dependent signaling), are important for mounting cytotoxic T cell (CTL) responses in both infections. In a study of respiratory syncytial virus (RSV) infection [45], mice lacking both MAVS and MyD88 were still capable of mounting CTL responses to RSV infection, suggesting that RLR- and TLR-independent RNA virus recognition might be responsible for the activation of CTLs in the lung. Therefore, the experimental data so far support the notion that TLRs rather than RLRs are critical in priming the adaptive immune response. However, further studies are required, as these two PRR systems may contribute differently in different virus infection systems, and their contributions may also depend on the route of viral infection.

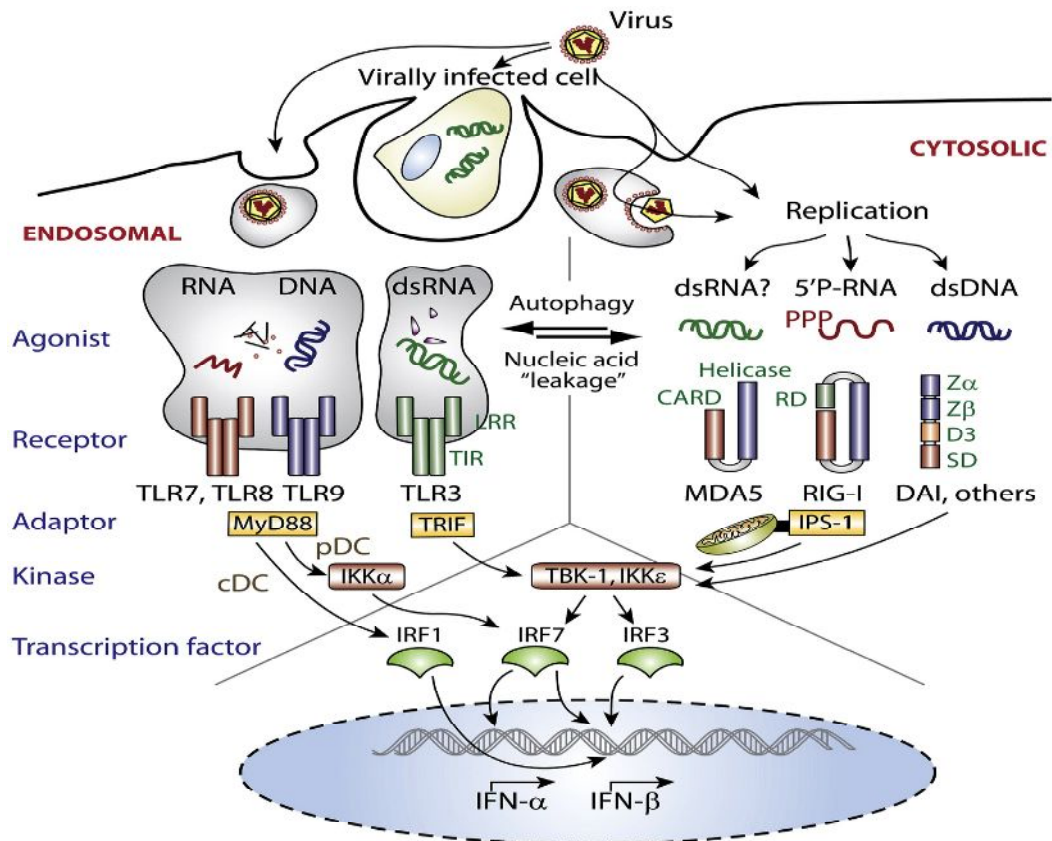


Figure 1.1 PRRs-mediated signaling in response to viral infection.

There are two classes of PRRs that signal the induction of IFN α and IFN β gene transcription upon virus recognition. In endosomes, the uptake of viruses or virus-infected cells delivers viral nucleic acids into endosomes, where the viral nucleic acids are detected by TLRs. In pDCs, TLR7, 8, and 9 signal through the adaptor MyD88 and the kinase IKK α to phosphorylate and activate the transcription factor IRF7, which regulates expression of the IFN α and IFN β genes. In the cytosol, viral RNAs are recognized by MDA5 and RIG-I, which signal through the mitochondrion-associated MAVS. MAVS activates the kinases TBK-1 and IKK ϵ to phosphorylate IRF3 and IRF7 and induce IFN α and IFN β gene transcription. Cytosolic DNA receptor(s) such as the DNA-dependent activator of IFN-regulatory factors (DAI) use an alternative adaptor to couple to TBK-1 and IKK ϵ , and IRF3 and IRF7. Figure is adapted from [46]. With permission by Elsevier, license number is 3326610999056.

1.1.2.2 Type I interferon stimulated signaling pathways

The action of type I IFNs is mediated through the heterodimer of IFNAR1 and IFNAR2. IFNAR1 and IFNAR2 are constitutively associated with JAK1 and non-receptor tyrosine kinase 2 (TYK2) [47, 48]. Binding the heterodimer of IFNAR1 and IFNAR2 by type I IFNs results in activation of JAK1 and TYK2, which leads to tyrosine phosphorylation and activation of several STAT family members, including STAT1, STAT2, STAT3 and STAT5 in most cell types [49]. Activation of STAT1 and STAT2 leads to the recruitment of IRF9 and the formation of a STAT1-STAT2-IRF9 complex, the IFN-stimulated gene factor 3 (ISGF3) complex [6, 49]. This complex then translocates to the nucleus and initiates transcription of ISGs through binding to IFN-stimulated response elements (ISREs) [6, 49]. In addition to the well-established ISGF3 complex, type I IFNs are shown to induce other types of STAT complexes. Examples include the formation of STAT1 homodimers which activate IFN-gamma-activated site (GAS) enhancer elements in the promoters of type II IFN associated ISGs [49]. Homodimers of phosphorylated STAT3 bind to STAT3-binding elements (SBEs) in the nucleus, resulting in the production of anti-inflammatory cytokines, such as IL10 [49, 50]. The JAK-STAT pathway stimulated by IFNs is summarized in Figure 1.2.

Besides the canonical JAK-STAT pathway, type I IFNs activate other STAT-independent signaling pathways that have crucial roles in their biological effects. For example, type I IFNs can induce activation of the PI3K signaling pathway [51, 52], which has an important role in mediating gene transcription in response

to both type I and type II IFNs. It has been also reported that the mitogen-activated protein kinases (MAPKs), especially extracellular-signal-regulated kinase (ERK) [53] and p38 MAPKs [54], are activated by type I IFNs and participate in the antiviral response induced by IFNs [55-57].

One of the important effects of IFN signaling cascades is induction of ISGs. The products of these ISGs exert numerous antiviral effector functions. Expression microarray studies have identified hundreds of ISGs induced by type I IFNs [58, 59]. While a limited number of ISGs, such as IFN-stimulated protein of 15 kDa (ISG15), protein kinase R (PKR), ribonuclease L (RNaseL), 2' 5-oligoadenylate synthetase (OAS), and Mx GTPases, have well defined antiviral mechanisms by studies in knockout mice [60], functions of most ISGs are poorly characterized, probably because of the difficulties involved in systematically overexpressing hundreds of genes. Recently, a large-scale antiviral ISG screen was conducted to identify novel antiviral effectors in the type I IFN system using a cell-based assay [61]. They found that some ISGs had broad activity against many viruses, while others were more restricted in specificity. A given virus seems preferentially inhibited by a particular subset of ISGs, its 'ISG profile', which is unique but partially overlaps with the profiles of other viruses, particularly those in the same family. The ISG members of these profiles block viral transcription, degrade viral RNA, inhibit translation and modify protein function to interfere with many steps of the viral life cycle. Another emerging paradigm for ISG-mediated activity is feedback into antiviral pathways. For example, major IFN signaling components, such as RIG-I, IRFs, and STAT1, are induced by IFNs [62].

On the other hand, over-induction of type I IFN genes could cause excessive IFN signaling and lead to tissue damage. A number of negative regulators, such as suppressor of cytokine signaling (SOCS), ubiquitin specific peptidase 18 (USP18) and the protein inhibitor of activated STAT1 (PIAS), play important roles in restraining the IFN response. In addition, refractoriness is another safety check of IFN signaling. Refractoriness is the phenomenon that cultured cells become rapidly unresponsive or refractory to continuous stimulation with IFN α as a result of negative feedback mechanisms in the JAK-STAT pathway [63]. Refractoriness has been observed not only in cultured cells, but also in the liver of mice injected with mouse IFN α [64]. Evidence shows that the early refractoriness requires SOCS, whereas prolonged unresponsiveness arises from long-lasting upregulation of USP18 [64]. However, refractoriness to human IFN α in human *in vivo* systems remains to be confirmed. In contrast to IFN α , IFN β signaling is not subject to refractoriness in the mouse liver, nor is IFN λ signaling [65].

1.1.2.3 Type III interferon production and downstream signal transduction in response to viral infections

Since their identification, the function of the IFN λ s was thought to resemble that of type I IFNs. However, emerging evidence suggests that the two antiviral systems do not entirely duplicate each other.

Co-expression of type I and type III IFNs in response to various viral infections was reported in both *in vitro* and *in vivo* studies (summarized in reference [66]). The similar expression patterns are due to the presence of common regulatory

elements in the promoters of the type I and type III IFN genes [67]. However, differences in the expression of these two types of IFNs have also been documented. Like IFN β , transcriptional regulation of the human IFN λ 1 gene is controlled by IRF3 and IRF7. In contrast, IFN λ 2/3 genes, like most IFN α genes, are more dependent on IRF7 [68]. In addition, it has been shown that expression of type III IFNs can also be induced through the independent action of IRFs or NF κ B [69]. This indicates that IFN λ s should be induced by a wider range of stimuli, and they may have a higher resistance barrier for viral immune evasion than type I IFN since both IRF and NF κ B signaling pathways would need to be simultaneously inhibited, whereas blocking IRFs is sufficient for the suppression of type I IFN production.

Despite signaling through distinct receptor complexes, type I and type III IFNs trigger similar downstream signaling cascades [70], including the canonical JAK-STAT pathway and the STAT-independent signaling pathways mentioned in the previous section. It should be noted that the intensity of STAT activation and subsequent biological activities in response to type III IFNs are generally weaker than in response to type I IFNs [71]. This may result from the lower level of IL28R α expression in cells, or from reduced ability to recruit and/or activate components of the intracellular signaling system. Another characteristic of type III IFNs is the restricted expression pattern of IL28R α : although all cells express receptors for type I IFNs, the type III IFN receptor is restricted to epithelial cells of the respiratory, intestinal including liver and reproductive tracts [11, 13-15].

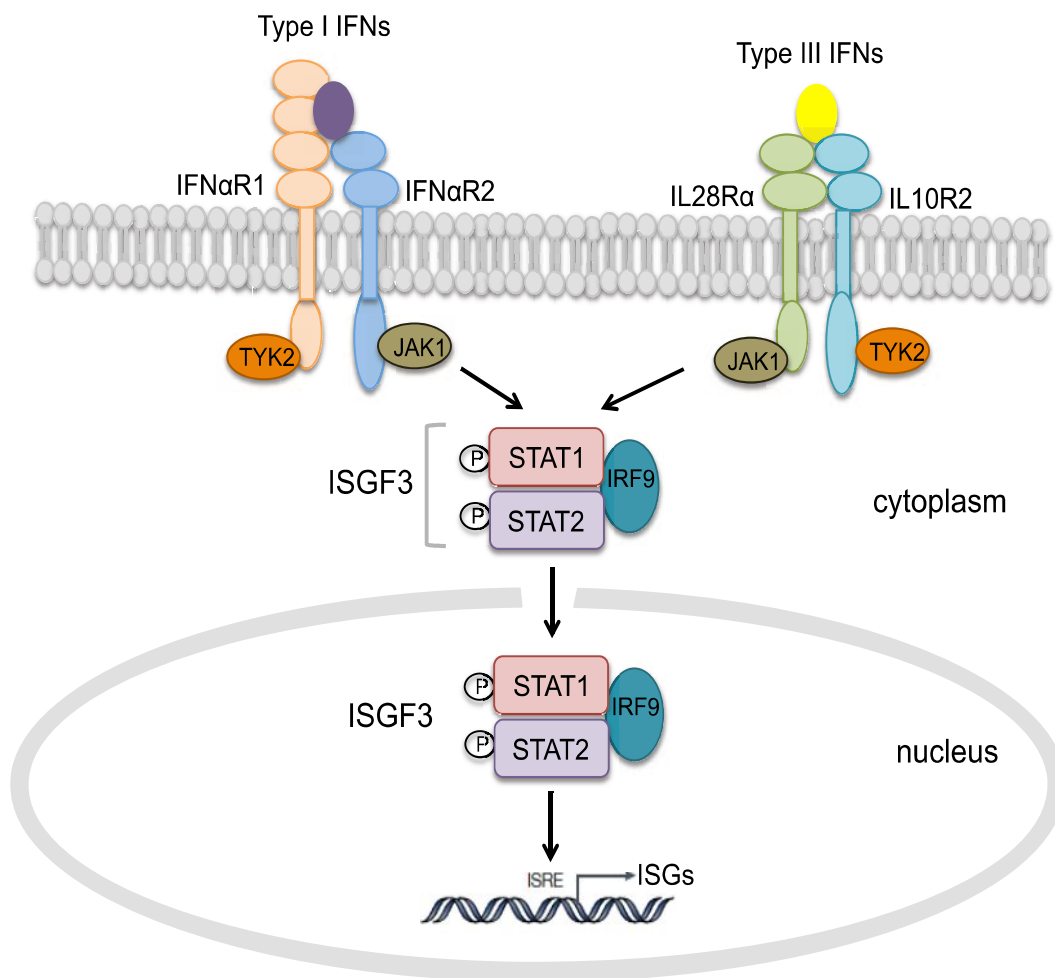


Figure 1.2 JAK-STAT signaling pathway.

Type I and III IFNs bind to their cell-surface specific receptors, IFNAR1/2 and IL28R α (or IFN λ R1) and IL10R β respectively, and activate the intracellular IFN signaling pathway, which involves mainly JAK1 and TYK2, and STAT1 and STAT2. The JAKs phosphorylate and activate the STATs, which homo- or hetero-dimerize and translocate to the nucleus to induce the expression of the ISGs.

1.1.2.4 Viral immune evasion

Viruses have been reported to block nearly all aspects of IFN production and the downstream IFN effector pathways. Evasion strategies include preventing initial virus detection by the disruption of the TLRs or RLRs, disrupting IFN production by disturbing IFN receptor or impeding JAK-STAT signaling events. In addition, specific ISGs can be selectively targeted for inhibition. Some viruses also disrupt IFN responses by up-regulating negative regulatory systems. Both HBV and HCV have been studied intensively for immune evasion mechanisms, which will be discussed in details in sections 1.2.3 and 1.3.3 respectively.

1.2 Hepatitis B virus

1.2.1 Virology of Hepatitis B virus

Hepatitis B virus is a member of the *Hepadnaviridae* family [72]. The hepadnaviruses are small, enveloped, spherical viruses with strict hepatic tropism. Their genomes are small (3-3.3 Kb), partially double-stranded DNA and are organized into 3 or 4 overlapping reading frames encoding viral proteins. One of the distinguishing features of the hepadnaviruses is that viral DNA is replicated by reverse transcription of an RNA intermediate by viral reverse transcriptase before release from an infected hepatocyte. These viruses have the ability to establish chronic infections without direct cellular cytopathic effects. A hallmark of hepadnaviral infection is the production of a large amount of surface antigen-containing, noninfectious particles from infected hepatocytes, which are released into the serum of infected individuals.

The Hepadnavirus family has two recognized genera, the orthohepadnaviruses that infect mammals, and the avihepadnaviruses that infect birds. Two major species have been assigned to the avihepadnaviruses, the duck hepatitis B virus (DHBV) and the heron hepatitis B virus (HHBV). The orthohepadnavirus genus includes four species - human HBV, woodchuck hepatitis virus (WHV), ground squirrel hepatitis virus (GSHV) and woolly monkey hepatitis B virus (WMHV). The prototype species is HBV that normally infects humans but can be used to experimentally infect chimpanzees. The HBV virus is divided into four major serotypes (adr, adw, ayr, ayw) based on epitopes present on its envelope proteins, and into eight genotypes (A-H) according to nucleotide sequence variation of the genome.

1.2.1.1 HBV virion structure and genome organization

As illustrated in Figure 1.3, there are three types of viral particles that can be detected in the serum of HBV infected patients [73]. The Dane particle is a spherical, double-shelled structure 42nm in diameter and is the infectious HBV virion. The outer shell of the virion consists of a lipid envelope containing virus-encoded surface antigens. Within the envelope is a nucleocapsid composed of HBV core antigen containing one copy of the virus encoded DNA polymerase/reverse transcriptase, covalently attached to the 5' end of the minus strand of the viral genome. The other two viral particle types found in serum are sub-viral particles (SVP), including small spherical structures with a diameter of 20nm and filaments of variable lengths with a width of 22nm. These spheres and

filaments are produced in 100-1000 fold excess of the Dane particles. They are composed of hepatitis B surface antigens (HBsAg) and host-derived lipids, but lack viral nucleic acids.

The HBV genome is partially double-stranded, circular DNA with approximately 3.2 kilobase (kb) pairs in length. The viral genome is remarkably compact and encodes four overlapping open reading frames (ORFs); S, C, P and X [73] as shown in Figure 1.4. The S ORF can be divided into three regions, pre-S1, pre-S2, and S, encoding three envelopes proteins, small HBV surface protein (SHBs) encoded by S region, medium HBV surface protein (MHBs) encoded by PreS2+S regions and large HBV surface protein (LHBsAg) encoded by PreS1+PreS2+S regions (Figure 1.5B). The C gene is subdivided into the precore and core regions, which encode HBcAg or HBeAg depending on where translation initiates (Figures 1.4 and 1.5B). The P ORF encodes the viral polymerase (pol). It has both RNA-dependent and DNA-dependent DNA polymerase activities as well as RNaseH activity. Finally the HBV X ORF encodes HBxAg, a protein with multiple functions in signal transduction, transcriptional activation, DNA repair, and inhibition of protein degradation pathways.

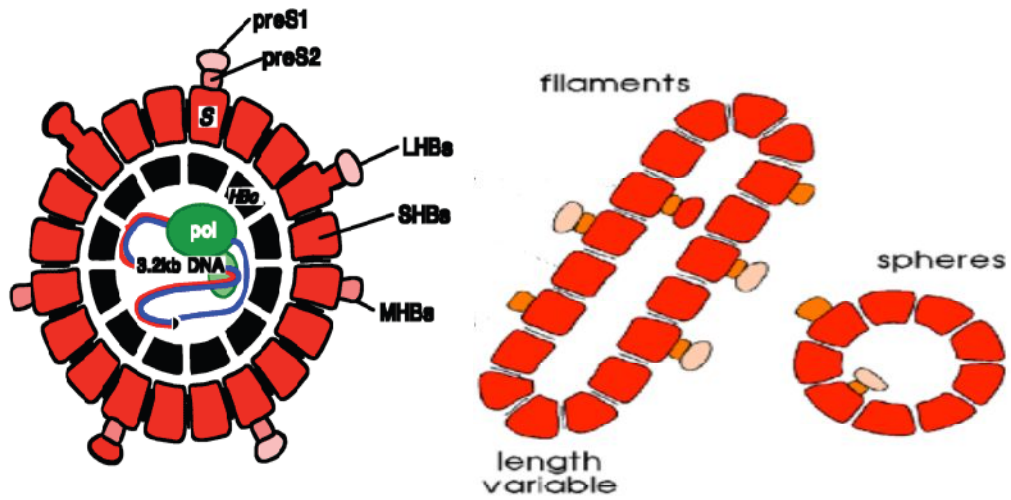


Figure 1.3 HBV viral structure.

The HBV Dane particle (left) as infectious virion and the filamentous or spherical HBsAg particles as noninfectious SVPs present in patient serum. Figure is modified from [74]. Permitted by BioMed Central, open access.

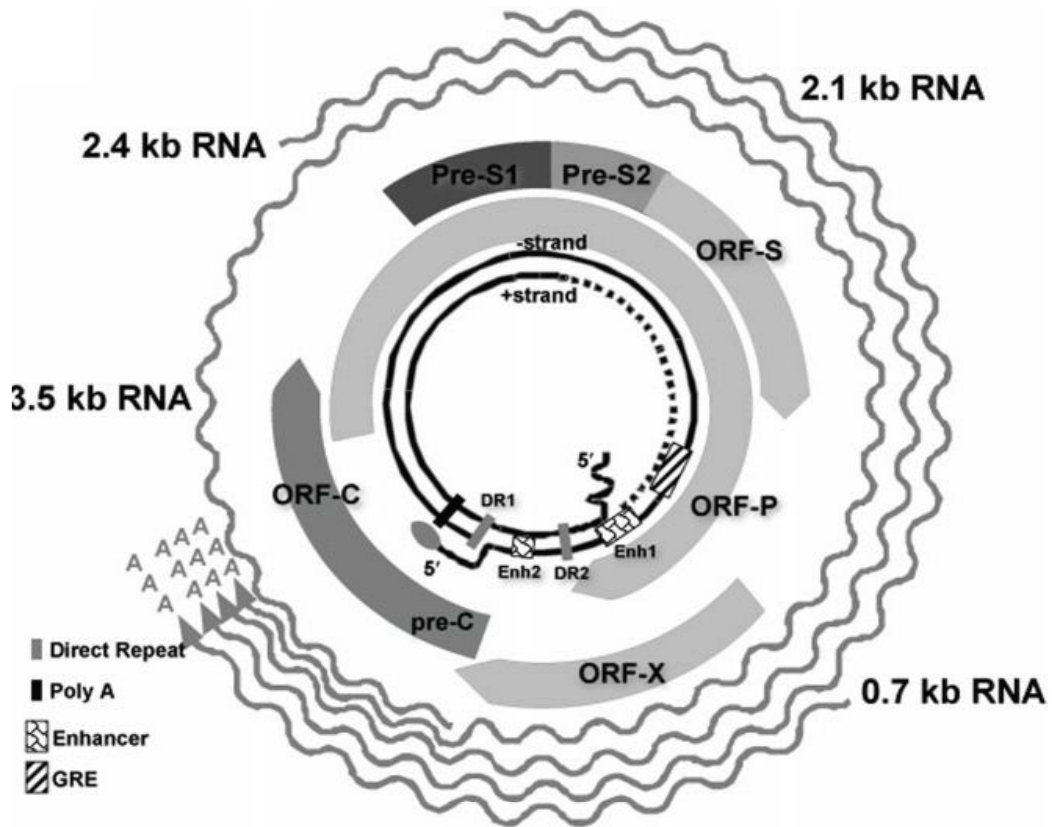


Figure 1.4 HBV genome organization.

HBV genome is partially double-stranded, circular DNA. It encodes four overlapping ORFs: S, C, P and X. Figure is adapted from [73]. Permitted by John Wiley and Sons, license number is 3326610575541.

1.2.1.2 The life cycle of hepatitis B virus

The HBV replication cycle, described in Figure 1.5A, starts with the attachment of the virus to a susceptible hepatocyte and binding to hepatocyte-specific receptor(s), e.g. sodium taurocholate cotransporting polypeptide (NTCP), a multiple transmembrane transporter predominantly expressed in the liver [75]. The entry of the virion is through endocytosis or fusion of the viral envelope at the plasma membrane [76]. The viral nucleocapsid containing the relaxed circular partially double stranded DNA (rcDNA) is then released into cytoplasm, followed by uncoating and delivery of virion rcDNA to the nucleus. Within the nucleus, the plus strand of incoming rcDNA is repaired by the attached viral polymerase and yet to be defined host factors [76], to generate a covalently closed circular DNA (cccDNA), which is complexed with host proteins in the nuclei to form a viral minichromosome [77, 78] and defines successful infection of a cell [79]. The cccDNA uses the cellular transcriptional machinery to produce all viral RNAs necessary for protein production and viral replication. There are four major RNA species produced during HBV replication cycle; the 3.5, 2.4, 2.1 and 0.7 kb viral RNA transcripts. They are transported to the cytoplasm to initiate translation of viral proteins. The pregenomic RNA (pgRNA, a 3.5 kb RNA) is translated to produce the core protein and the viral polymerase. The regulatory X protein and the three envelope proteins are translated from the subgenomic RNAs (refer to Figures 1.4 and 1.5B for the different viral RNA transcripts). The replication of HBV genomic DNA is initiated by packaging a pgRNA with the polymerase and assembling core protein to form an RNA-containing nucleocapsid. Reverse

transcription of HBV pgRNA into minus strand DNA is primed by the N terminal of HBV polymerase within the nucleocapsid. As the minus strand of HBV DNA is synthesized, the RNaseH activity of HBV polymerase digests the template HBV pgRNA. The minus strand DNA then serves as the template for positive strand DNA synthesis, which is primed by a capped small remnant of pgRNA, until the positive strand DNA reaches approximately 50-70% of the length of the minus strand [79]. A mature DNA-containing nucleocapsid is then formed. These nucleocapsids can be either re-imported into the nucleus to produce more cccDNA [76] or assemble with envelope proteins within membranes of the endoplasmic reticulum (ER) followed by transport through the Golgi apparatus for secretion as mature virions.

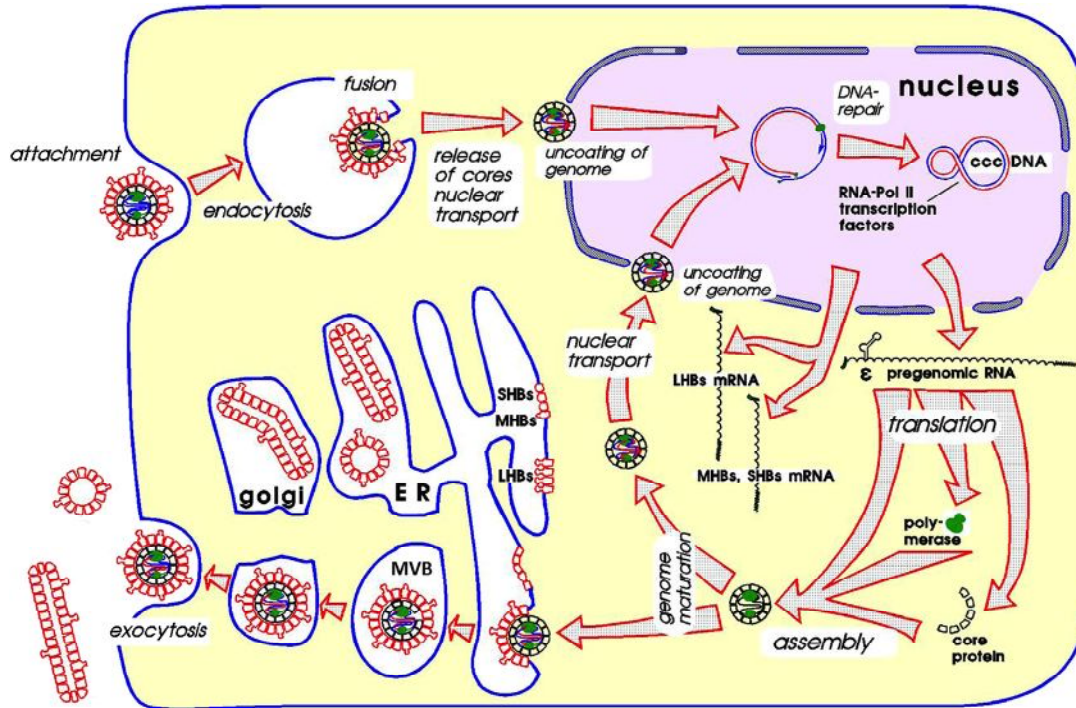


Figure 1.5A HBV life cycle.

Attachment to liver-specific receptors leads to endocytosis of HBV and release of HBV core particles. These are transported to the nucleus where the HBV genome is released. In the nucleus, the viral rcDNA is repaired to generate the cccDNA. In interaction with transcription factors, the cccDNA is transcribed to the pregenomic and subgenomic mRNAs. The mRNAs are transported to the cytoplasm. The two subgenomic mRNAs for the three HBV surface proteins are translated at the ER, assemble to subviral HBsAg particles and are secreted through the Golgi apparatus. In parallel, the pregenomic mRNA is translated in the cytosol to the HBV core protein and the viral polymerase, whereby the three components assemble to the immature core particle. The HBV genomes mature within the core particles through reverse transcription of the pregenomic mRNA to negative strand DNA and synthesis of the positive strand DNA by HBV pol. The mature core particles can migrate back to the nucleus or be enveloped by the surface proteins and secreted as mature virions. The figure is adapted from [74]. Permitted by BioMed Central, open access.

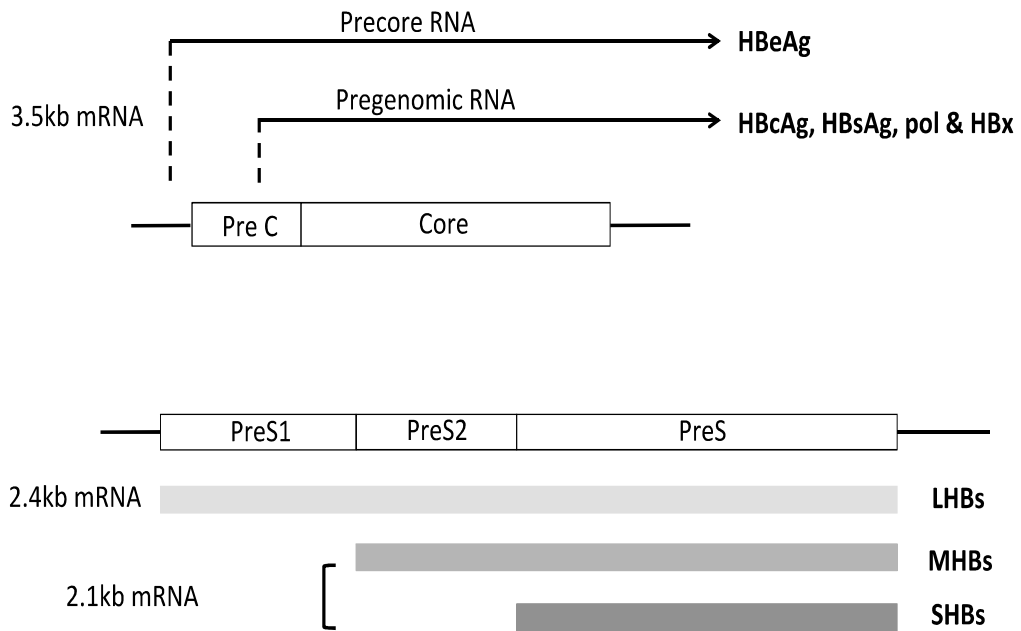


Figure 1.5B HBV transcripts during replication.

A list of the transcription start sites of various HBV transcripts and the proteins they encode.

1.2.2 Hepatitis B disease

1.2.2.1 Hepatitis B

Hepatitis B is a potentially life-threatening liver disease caused by the infection of HBV virus. It presents a major global health problem. According to the World Health Organization (WHO), more than 240 million persons worldwide are currently chronically infected with HBV [80]. About 600,000 people die every year due to the acute or chronic consequences of hepatitis B [80]. Hepatitis B infection leads to two primary adverse outcomes: cirrhosis and hepatocellular carcinoma (HCC).

Increasing evidence shows that the natural history of chronic HBV infection differs depending on HBV genotype and subgenotype. Currently, eight genotypes of HBV (A to H) have been identified that differ from each other by at least 8% in genome sequence [81]. Genotype A is found in Northern Europe. Genotypes B and C are common in Asian populations. Genotype D is the most common genotype found in Southern and Eastern Europe and is also common in the Middle East. Genotype F is found in native populations in North and South America. Genotype E, G, and H infections are uncommon and their epidemiology is not well characterized [82]. Hepatitis B prevalence is highest in sub-Saharan Africa and East Asia. High rates of chronic infections are also found in the Amazon and the southern parts of eastern and central Europe. Less than 1% of the population in western Europe and North America is chronically infected with HBV [80].

HBV infection can be cleared or causes a broad spectrum of clinical diseases, ranging from acute hepatitis to progressive chronic hepatitis. Infants are infected by HBV through vertical transmission at birth and 90-95% become chronic carriers. Adults infected with HBV become carriers in 3-5% of the cases. About two-thirds of patients with acute HBV infection are asymptomatic. Chronic hepatitis B (CHB) has a variable and dynamic course. In general, there are four phases in the natural history of CHB without therapy [82-86]; the first phase is the immune tolerant phase, which occurs most frequently in persons who are infected by perinatal transmission from HBV-DNA positive mothers. In this phase, HBeAg may promote immune tolerance and aid the virus in avoiding detection by the immune system [82]. This phase is characterized by positive HBeAg, high HBV DNA levels, normal alanine transaminase (ALT) levels and minimal liver injury. Some of these patients remain in this phase lifelong. The immune active phase is the second stage, when the host's immune system recognizes HBV as foreign and initiates an immune response that results in hepatocyte damage. Patients in this phase often have fluctuating HBV DNA and ALT levels. During this period, active liver inflammation and rapid progression to fibrosis can occur. Cirrhosis and HCC can also develop as a result of this liver damage, either of which can lead to death. Many patients in this phase undergo seroconversion from HBeAg positive to negative and develop HBe antibody (anti-HBe), which is associated with decreased viremia. However, about 20-40% of patients experience reactivation and enter HBeAg negative immune active phase (HBeAg negative CHB), with risk of cirrhosis or HCC. This phase is characterized with negative

HBeAg, positive anti-HBe and detectable HBV DNA. A mutation in the precore region of the HBV DNA, resulting in a lack of HBeAg production, is associated with this phase of CHB. Some patients will experience immune control, when liver inflammation is minimal, HBV DNA is undetectable or at a low level, but patients remain HBsAg positive. Patients in this phase are ‘inactive carriers’ of the infection. Inactive carriers represent the largest group of CHB patients and most of them remain in this inactive phase for life.

1.2.2.2 Treatment of HBV infection

The goal of therapy for CHB is to improve quality of life and survival by permanently suppressing HBV replication and preventing progression of the disease to cirrhosis, decompensated cirrhosis, end-stage liver disease, HCC and death [87]. Currently, seven drugs are approved for treatment of CHB by the FDA: two interferon preparations (standard IFN α -2b and pegylated interferon alpha-2a [pegIFN α -2a]), three nucleosides (lamivudine, telbivudine, entecavir) and two nucleotides (adefovir and tenofovir) [87, 88].

The IFN-based therapy offers a finite duration of therapy, with approximately 30% of HBeAg-positive patients achieving HBeAg seroconversion with 12 months of therapy [87, 89, 90], and 80% of these patients had a sustained virological response 5 years later [89]. Since 2005, pegIFN α -2a has replaced standard IFN α -2a due to its improved pharmacokinetic properties, a less demanding injection schedule, a more convenient dosing regimen and comparable or improved efficacy. But it is limited by the high cost, substantial side effects and

poor tolerability in some individuals. Attempts have been made to identify the patients who most likely will respond to IFN treatment. Studies suggested that criteria usually include high ALT ($> 2-5$ times upper limits of normal), low HBV DNA ($< 2 \times 10^8$ international unit/mL), and genotype A HBV virus [90]. However, the predictive ability is still quite limited. Since two single nucleotide polymorphisms (SNPs) of the IL28B gene have been identified as a potent predictor of the sustained virological response (SVR) in IFN treatment of hepatitis C patients [91-95], their effect on HBeAg-positive CHB patients has also been evaluated by a few studies [96-99]. Some studies support the predictive value of the SNPs in IFN therapy on CHB patients, but further confirmation is required. On the other hand, treatment with IFN therapy of CHB patients would be improved with more accurate predictors of outcomes and better benchmarks for termination of treatment. HBV DNA kinetics during the therapy has shown only limited utility [100]. An alternative way is to measure the intrahepatic level of cccDNA, persistence of which at the end of treatment is predictive of off-treatment relapse [101]. However, the measurement of intrahepatic cccDNA requires a liver biopsy, which is invasive and carries significant risk. Another more realistic approach is the measurement of serum HBsAg, which correlates well with intrahepatic cccDNA levels in both HBeAg-positive and HBeAg-negative patients [102]. Recent studies have shown that decline of HBsAg serum level during pegIFN α -2a therapy predicts off-treatment response more accurately than HBV DNA kinetics, both in HBeAg-positive and HBeAg-negative patients. However, the predictive value of HBsAg decline may not apply equally to all

HBV genotypes [103-105].

Compared to the IFN-based therapies, the nucleos(t)ide analogues offer the ease of oral administration, more consistent antiviral response, and more favorable side-effect profiles. All current five oral drugs act on HBV DNA polymerase and inhibit viral replication, thus can result in suppression of HBV DNA, HBeAg seroconversion, ALT normalization, and histological improvement. However, since none of them is targeting the cccDNA, long-term treatment is often required and virological relapse is common after cessation of therapy. In addition, drug resistance caused by mutations in viral polymerase could present additional challenge. For example, lamivudine, adefovir dipivoxil, and telbivudine are associated with higher risk of resistance [88, 106]. Encouragingly, entecavir and tenofovir are recognized as the most potent antiviral drugs with high genetic barrier resulting with the lowest risk of resistance to date. Drug resistance occurs in 1.2% at 6 years of entecavir treatment [107, 108] and no resistance after 4 years of tenofovir treatment [109]. Both of these drugs are purine analogues and the very early studies by Dr. Lorne Tyrrell and colleagues predicted better responses with purine analogues than pyrimidine analogues [110, 111]. In addition, the high genetic barrier to resistance is likely related to early blockage of the protein priming of HBV DNA [112].

1.2.2.3 HBV vaccine

A HBV vaccine has been available for decades. The vaccine provides a strong, protective and long-lasting anti-HBs response in about 95% of people immunized

[80]. It is the world's first subunit vaccine, the world's first licensed vaccine against human cancer and the world's first recombinant expressed vaccine [113]. However, it is worth noting that resistance to vaccine is rare but does exist due to viral mutations [114]. The resulting mutants are resistant to specific neutralizing antibodies and hepatitis B immunoglobulin used even at high concentrations [113, 115].

1.2.3 Innate immune response in HBV infection

Efficient control of virus infections requires coordination of both the innate and the adaptive immune responses. Innate immunity serves as a first line of defense that is rapid and effective in clearing most of the invading pathogens. It starts with the detection of PAMPs such as viral nucleic acids, viral proteins and tissue damage by PRRs as discussed in section 1.1. Recognition induces a series of cellular responses, such as production and release of type I IFN by infected cells, killing of viral infected cells by natural killer (NK) cells, and production of pro-inflammatory cytokines and chemokines to support the efficient maturation of adaptive immunity and recruitment of immune cells to the site of infection.

In the case of HBV infection, our knowledge of the anti-HBV innate immune response is limited. Clinical data obtained during natural infection in patients are limited because most of patients are asymptomatic at the earliest acute stages of HBV infection. Studies in chimpanzees are limited by ethical issues and high costs. Studies in woodchucks and the Pekin ducks are hampered by the lack of reagents to analyze immunological events. Nevertheless, other than one study

showing that HBV mediated an induction of ISGs through the MDA5 signaling independent of type I IFN in Huh-7 cells transfected with a HBV replicative plasmid as well as in the livers of mice hydrodynamically injected with the HBV replicative plasmid [30], it appears that there is limited or even absent activation of innate immunity during acute HBV infection. The study in chimpanzees by Chisari and colleagues has shown that there was no transcription of IFN-related genes that correlated with HBV entry and expansion during the early phase of HBV infection in the livers of experimental infected chimpanzees [116]. This implies the lack of a PRR-mediated innate cytokine response to HBV infection. In line with this observation, there was no induction of type I or type III IFNs detected in sera of acute HBV infected patients in clinical studies [117, 118].

The lack of an IFN response to early HBV infection could be explained by the fact that HBV is a “stealth virus” that cannot be detected by the host innate immunity sensors, such as PRRs, or the virus could efficiently inhibit the innate immune response very early after infection. The latter possibility is supported by evidence from both *in vitro* and *in vivo* studies. For example, the TLR-mediated innate immune response leading to IFN β production, induction of ISGs and activation of IRF3, NF κ B, and ERK1/2 was attenuated in murine parenchymal and nonparenchymal liver cells expressing HBsAg and HBeAg [119]. As for the RLR mediated signaling pathway, HBx protein is reported to interact with MAVS, and disrupts RIG-I-mediated signal transduction [120]. HBV polymerase inhibits RIG-I-induced signaling through interference with IRF3 phosphorylation, dimerization, and nuclear translocation, and suppresses the interaction between

TBK1/IKK ϵ and DDX3 (a DEAD-box RNA helicase) in human hepatocytes [121, 122]. HBV also dampens JAK-STAT signaling and ISGs expression: HBV prevents IFN α mediated signaling by inhibiting nuclear translocation of STAT1 and thus interferes with transcription of ISGs in chimeric mice [123]. This is most likely caused by HBV polymerase, which is shown to inhibit STAT1 nuclear translocation in an *in vitro* system [124]. Moreover, evidence suggests that HBV precore/core proteins are able to inhibit MxA gene expression by their interaction with the MxA promoter [125].

On the other hand, accumulating data demonstrate that experimental activation of the PRR-mediated innate immune response inhibits HBV replication. HBV replication is markedly inhibited, in a type I IFN-dependent manner, following intravenous injection of ligands for TLR3, TLR4, TLR5, TLR7, and TLR9 in HBV transgenic mice [126]. Guo, *et al.* demonstrated that in addition to TLR signaling, activation of RIG-I or MDA5 dramatically reduces HBV replication in hepatocyte-derived HepG2 and Huh-7 cells over-expressing MyD88 and TRIF, or MAVS [127]. In addition, systemic administration of IFN α or induction of IFN α through injection of poly(I:C) suppresses viral replication in the HBV transgenic mouse model [128, 129]. The mechanism of inhibition of HBV infection by activating the PRR signaling pathways has been suggested to be either caused by some ISGs, such as indoleamine 2, 3-dioxygenase [130] or by apolipoprotein B mRNA-editing enzyme catalytic polypeptide 3 protein G (APOBEC3G) [131, 132], exerting effects on various steps of HBV life cycles, or tumor necrosis factor α (TNF α) that interferes with HBV nucleocapsid formation and stability by

activating the NF κ B pathway [133, 134]. However, since these data are mostly based on *in vitro* over-expression or a transgenic mouse model, confirmation in an animal model infected with HBV is necessary. Nevertheless, all these data suggest that activation of the innate immune response holds great potential as therapeutic approaches for chronic HBV infection.

1.3 Hepatitis C virus

1.3.1 Virology of Hepatitis C virus

Originally termed non-A, non-B hepatitis (NANBH), HCV was first cloned and characterized by Dr. Michael Houghton's group in 1989 [135]. It is an enveloped RNA virus belonging to the *Hepacivirus* genus of the *Flaviviridae* family, typified by classical flaviviruses, such as dengue virus, west Nile virus and yellow fever virus. Humans are the only natural host of HCV. An important feature of the HCV genome is its high degree of genetic variability. This heterogeneity is primarily due to the high error rate of its RNA-dependent RNA polymerase. Seven HCV genotypes and a large number of subtypes have been identified to date. Genotypes differ in their nucleotide sequences by 31–33% and subtypes by 20–25% [136]. Subtype 1a is predominant in North America and Northern Europe and is usually associated with injection drug users (IDUs). Subtype 1b and 3b are common genotypes all over the world. Genotype 2 is predominant in Mediterranean countries and the Far East. Subtype 3b and genotype 6 are distributed mainly in Asia. HCV genotype 4 is found in the Middle East, Africa and Europe. Subtype 5a is mostly in South Africa and some parts of Europe. A

new genotype tentatively named subtype 7a, has been registered in the HCV databases, but awaits further published information [137]. Like many other RNA viruses, HCV circulates in infected individuals as a dynamic distribution of non-identical but closely related mutant and recombinant viral genomes subjected to a continuous process of genetic variation, competition and selection referred to as quasispecies [138], which contributes to immune evasion and resistance to antiviral therapy.

1.3.1.1 HCV virion structure and genome organization

The HCV virion consists of a single-stranded positive RNA genome, surrounded by an icosahedral protective capsid, and enveloped by a lipid bilayer derived from host membrane, within which two glycoproteins, E1 and E2, are embedded.

A hallmark of HCV particles is their tight association with cellular lipoproteins and lipids, which therefore determines both morphology and biophysical properties of HCV virions. Properties of HCV particles may vary depending on the host cells in which they are produced because *in vivo* liver cells of patients or experimental animal models and *in vitro* cultured human hepatoma cells can differ in their capability to produce lipoproteins [139].

The HCV genome is a single-stranded positive sense RNA molecule (Figure 1.6). It contains three regions: a short 5' NTR, a single ORF of approximately 9.6 kb nucleotides and a short 3' non-coding NTR [140]. The 5' NTR is divided into

two domains, a stem-loop structure involved in positive-strand priming during HCV replication and an internal ribosome entry site (IRES), the RNA structure responsible for attachment of the ribosome and polyprotein translation. The HCV 3' NTR is comprised of three regions: a variable region with potential secondary structure, a non-structured polyU/UC region containing polyuridine tracts interspersed with ribocytidine, and the terminal X tail containing three conserved stem-loop structures [141]. Both 5' and 3' NTRs bear highly conserved RNA structures essential for polyprotein translation and genome replication. The ORF is translated into a single precursor polyprotein, followed by cleavage to yield at least 10 mature viral proteins; three structural proteins (the capsid protein C and the two envelope glycoproteins E1 and E2) and the seven non-structural (NS) proteins (p7, NS2, NS3, NS4A, NS4B, NS5A, and NS5B).

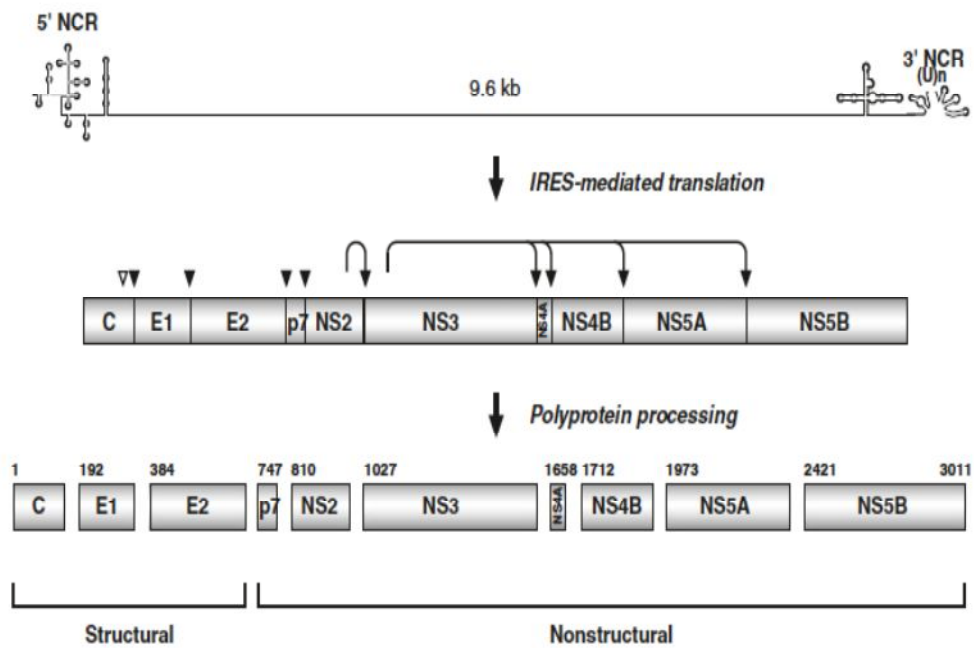


Figure 1.6 Genome organization of HCV.

The HCV polyprotein precursor is translated and processed into 10 mature proteins, which are divided into two groups: structural proteins including core protein, two glycoproteins E1 and E2, and NS proteins including p7, NS2, NS3, NS4A, NS4B, NS5A and NS5B. The figure is adapted from reference [142]. With permission by Springer, license number is 3326600678907.

1.3.1.2 The life cycle of hepatitis C virus

The life cycle of hepatitis C virus can be divided into 5 steps as illustrated in Figure 1.7: viral entry and uncoating, polyprotein synthesis, viral protein maturation, RNA replication and viral assembly.

During entry of HCV into host hepatocytes, the E2 envelope glycoprotein is the main viral factor responsible for receptor binding [143]. The number of cellular receptors that are important for HCV entry is increasing. To date, glucosaminoglycans (GAGs) and low-density lipoprotein receptors (LDLRs) on the liver cell surface are implicated as the initial docking site for HCV attachment [144, 145]. Entry factors scavenger receptor type B1 (SR-B1), CD81, and tight-junction proteins claudin-1 (CLDN-1) and occludin (OCLN) are essential for viral uptake and late stages in the entry process [143, 146].

Uncoating of HCV capsid releases the positive-strand genomic RNAs into the cell cytoplasm, where they serve as messenger RNAs for synthesis of the HCV polyprotein together with newly synthesized RNAs. Unlike cellular capped mRNA molecules, which are translated by a cap-dependent scanning mechanism, uncapped RNA viral genomes, such as those of the flaviviruses, are translated by a cap-independent IRES mediated process [143, 146]. The IRES of HCV is composed of part of the 5' untranslated region and the first 12-30 nucleotides of the core-coding region of the viral genome [143].

HCV RNA translation takes place at the rough ER. The translation product of the

HCV genome is a precursor polyprotein, about 3000 amino acids (aa) in length. The polyprotein is processed into at least 10 mature structural and nonstructural proteins by cellular and viral proteases. Junctions between HCV structural proteins are cleaved by at least two host cellular peptidases, signal peptidase and signal peptide peptidase [143, 146]. Two viral proteases are involved in the processing of HCV nonstructural proteins: NS2-3 protease cleaves the site between NS2 and NS3 by a rapid intramolecular reaction, whereas the cleavage of the remaining four junctions, NS3/NS4A, NS4A/NS4B, NS4B/NS5A and NS5A/NS5B, is catalyzed by the NS3/4A serine protease [143, 146].

HCV replication is catalyzed by the viral RNA-dependent RNA polymerase (the NS5B protein) and supported by other viral NS proteins, as well as by host factors, including cyclophilin A and the microRNA-122 [147]. As with other positive-strand RNA viruses, HCV replication starts with synthesis of a complementary negative-strand intermediate using the positive-strand genome as a template. Then, negative-strand RNA serves as a template to produce numerous positive-strand genomic RNAs, which will subsequently be used for polyprotein translation, synthesis of new intermediates of replication or packaging into new virions. During the replication of viral RNAs, all HCV viral proteins are directly or indirectly associated with ER-derived membranes. By the action of NS4B, presumably in conjunction with NS5A, membranous replication vesicles are induced and accumulate in the infected cell as distinct structures designated as the membranous web [148, 149]. The membranous web manifests as vesicle clusters, which result from massive rearrangements of intracellular membranes,

including the formation of double-membraned vesicles induced by HCV NS5A protein and possibly NS4B protein, presumably with support of host cell factors [150, 151]. Although the precise structure and function of the membranous web is unclear, a recent study suggests that in HCV infected cells, cytoplasmically positioned nuclear pore complexes (NPCs) are predicted to form channels across double membrane structures of the membranous web. These NPCs are proposed to facilitate movement of nuclear localization signal (NLS)-containing proteins, such as HCV core, NS2, NS3, NS5A and host nuclear proteins, from the surrounding cytoplasm across double membrane structures of the membranous web, while excluding proteins lacking NLS sequences, e.g. PRRs, from regions of HCV replication and assembly events [152].

HCV viral assembly is initiated with the formation of nucleocapsid by the interaction of the core protein with HCV RNA. Nucleocapsids are enveloped and matured in the Golgi apparatus before newly produced virions are released in the pericellular space by exocytosis. Cytoplasmic lipid droplets serve as virus assembly platforms. Several nonstructural proteins have been shown to play a role in the late steps of the HCV lifecycle, including p7, NS2, NS3 and NS5A [146]. The very low-density lipoprotein synthesis/secretion machinery is also believed to be involved in infectious HCV production [139].

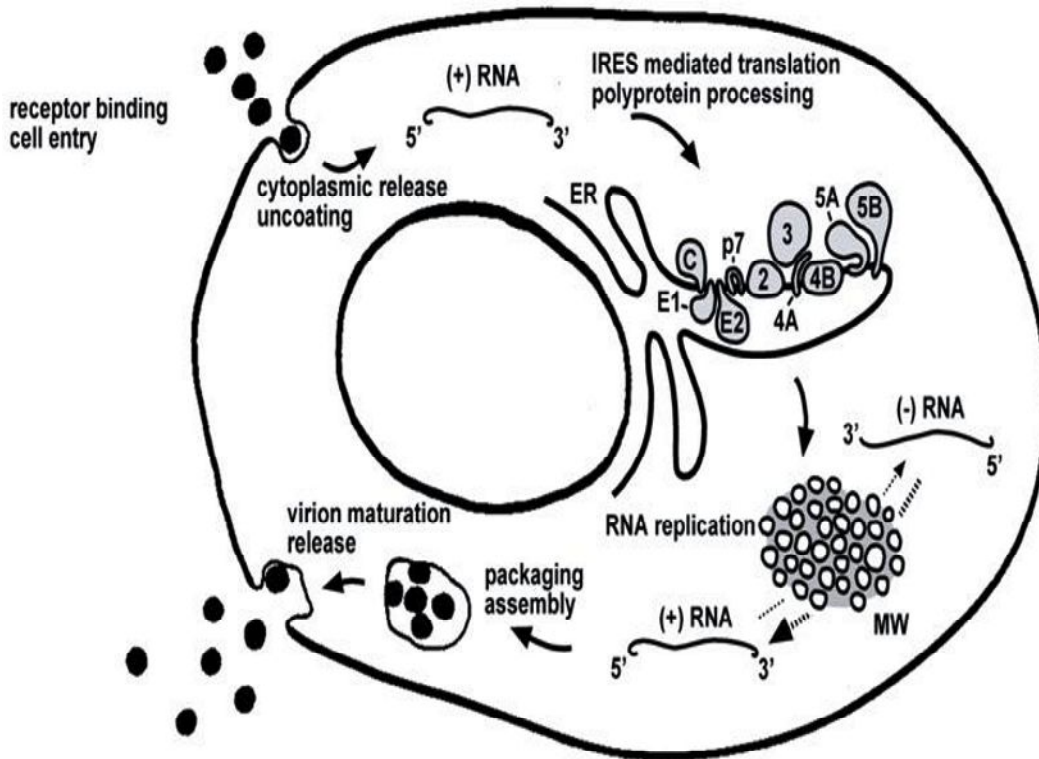


Figure 1.7 The HCV replication cycle.

Virion entry is initiated after the envelope protein E2 binds to cellular receptors, followed by receptor-mediated internalization of the virus. Uncoating of HCV capsid releases the positive-strand genomic RNAs into the cell cytoplasm. The viral RNA is translated into a single polyprotein at the ER membrane through IRES-mediated translation and cleaved into 10 mature proteins by viral and cellular proteases/peptidases. HCV replication is catalyzed by the viral RNA-dependent RNA polymerase in the membranous web. HCV viral assembly is initiated with the formation of nucleocapsid by the interaction of the core protein with HCV RNA. Cytoplasmic lipid droplets serve as virus assembly platforms. Nucleocapsids are enveloped and matured in the Golgi apparatus before newly produced virions are released in the pericellular space by exocytosis. The figure is adapted from reference [153]. Permitted by IJMS Publishing Team through email.

1.3.2 Hepatitis C disease

1.3.2.1 Hepatitis C

Hepatitis C is a worldwide liver disease that results from HCV infection. According to WHO, 3-4 million people are infected with HCV annually [154]. About 150 million people are chronically infected and at risk of developing liver cirrhosis and/or liver cancer. More than 350,000 people die from hepatitis C-related liver diseases each year. The disease is mainly transmitted through exposure to infectious blood, injection drug use, blood transfusion, hemodialysis, organ transplantation, or being born to a hepatitis C-infected mother. Sexual transmission is a less common means of transmission.

Hepatitis C can present as acute or chronic hepatitis. During the acute phase, the majority of patients are asymptomatic. Even in the patients with symptoms, the clinical course is mild and symptoms are nonspecific. In some patients HCV infection is a self-limited disease and HCV RNA becomes undetectable in these cases within three-four months after onset of infection. However, spontaneous clearance of HCV occurs only in a minority of patients, since 60-80% people with acute infection develop chronic infection [155-157]. Chronic hepatitis C (CHC) is defined by the persistence of HCV RNA six month after viral transmission [157, 158]. Once chronic HCV infection is established, spontaneous HCV clearance rarely occurs. Overall, 15-56% of patients with CHC will ultimately develop cirrhosis at some point, and a significant proportion will go on to develop HCC [156, 157]. CHC accounts for approximately 25% of the HCC cases worldwide

with particular high prevalence in East Asia [159].

1.3.2.2 Treatments for HCV infection

Until recently, the combination of pegIFN α and ribavirin (RBV) was the standard therapy for hepatitis C for more than 10 years regardless of the strain of the virus. This therapy, administered for 24 or 48 weeks, achieved sustained virological response (SVR) in approximately 70% of patients with HCV genotype 3, about 90% among patients infected with HCV genotype 2 and 45-55% among patients with genotype 1 and 4-6 [160]. SVR is the marker for HCV treatment success and it is defined as an undetectable HCV viral load test six months after completing a successful course of HCV treatment. Although new drugs have been approved for genotype 1 treatment, pegIFN α and RBV will continue to be an important component of genotype 1 HCV therapy until IFN-free therapy is approved, and pegIFN α and RBV may remain as an important component of the treatment options for infection with HCV of genotypes 2 and 3.

The limitations of this therapy are well recognized. It remains costly and side effects, such as fatigue, flu-like symptoms, anxiety, depression and gastrointestinal symptoms, are observed in almost 80% of patients during treatment. Side effects can be severe and 10-15% of patients discontinue treatment. Therefore, it would be useful if one could predict which patients will respond to antiviral therapy. Considerable effort has been directed at identifying factors predictive of IFN responsiveness. Both viral and host factors have been shown to influence treatment outcome. Among host factors, besides non-genetic

factors (such as age, alcohol and smoking), upregulation of pre-treatment liver gene expression of ISGs has been shown to be associated with non-response to IFN therapy [161, 162]. In addition, genetic polymorphisms in the human genome, e.g. two SNPs near the IL28B coding region rs12979860 and rs8099917 [91-95], are associated with IFN therapy outcome. At SNP rs12979860, CC is considered the responder allele, whereas CT and TT are non-responder alleles [92]. At SNP rs8099917, TT is the responder allele and GG and GT are the poor-responder alleles [91, 92]. Most recently, a new member of type III IFN, IFN λ 4, has been discovered [21]. Interestingly, evidence has shown that the inactivation of IFN λ 4 gene expression is strongly positively associated with HCV clearance as well as with positive pegIFN and RBV treatment outcome in patients [21, 163]. In addition, another recent study identified a functional SNP at rs4803217 in the 3' NTR of IFN λ 3 mRNA associated with clearance of HCV. The authors revealed that this SNP was critical in directing the outcome of HCV infection by controlling the stability of IFN λ 3 mRNA: IFN λ 3 mRNA bearing rs4803217-T/T 3' NTR (genotype associated with HCV persistence) decayed twice as fast as that bearing rs4803217-G/G 3' NTR (associated with HCV clearance) [164]. As for the viral factors, HCV genotype has been well accepted as the strongest predictor of IFN response [165-167]. In patients infected with HCV genotype 1 or 4, IFN therapy clears HCV infection in 45-55% patients, whereas in patients infected with HCV genotypes 2 or 3, pegIFN and RBV is effective in up to 80% patients [160]. The kinetics of serum HCV RNA level reduction during the first weeks of therapy is also strongly associated with the subsequent treatment outcomes [168-

171]. In addition, amino acid variation in the IFN-sensitivity-determining region within the NS5A region [172, 173] as well as at aa 70 or 91[174, 175] in the HCV core region are predictors of SVR and non-virological response (NVR). The degree of quasispecies' complexity and diversity of hypervariable region 1 (HVR1) is another marker, which is closely correlated with the responsiveness to interferon therapy in CHC patients [176-178].

Recently, new direct-acting antiviral agents (DAAs) that target specific HCV proteins are being developed. The first two NS3/4A oral protease inhibitors, telaprevir [179-182] and boceprevir [183, 184] were approved for the treatment of HCV genotype 1 infections when used in combination with pegIFN α and RBV in 2011. This was a major advance in the pharmacotherapy of chronic hepatitis C. With this new triple therapy regimen, SVR rates in patients with HCV genotype 1 infections were increased from 45-55% to approximately 70-80%, while significantly reducing treatment duration. However, these DAA-containing triple therapies are still associated with limitations. For examples, the spectrum of serious side effects associated with anti-HCV therapy has increased; the triple therapy is associated with a large pill-burden and complex dosing schedule; it is limited to genotype 1 infections; and resistant mutations do occur. While writing my thesis, two additional DAAs were approved by the *Food and Drug Administration* (FDA), sofosbuvir (HCV NS5B polymerase inhibitor) and simeprevir (a new HCV NS3/4A protease inhibitor). In addition, new HCV NS5A inhibitors appear very potent and will soon be approved [185]. This will result in therapeutic regimens that are more efficacious and convenient, better tolerated,

active on all viral genotypes, as well as with a high barrier to develop viral resistance.

1.3.2.3 HCV vaccine

There is no prophylactic or therapeutic vaccine available for HCV infection mainly due to its high viral genetic diversity, incomplete understanding of viral persistence and most importantly, lack of a suitable experimental animal model to HCV vaccine development [186] which will be further discussed in section 1.4.

1.3.3 Innate immune response in HCV infection

As mentioned previously, a number of PRRs sense viral pathogens as non-self within the host cells through recognition of specific PAMPs to activate innate immune signaling. Three PRRs are critical in HCV recognition, RIG-I, TLR3 and PKR. RIG-I has been shown able to recognize HCV infection within hours [187]. The PAMP substrate of RIG-I is identified as the polyU/UC region of the 3' NTR of the HCV RNA [34], along with an exposed 5' terminal triphosphate (5'ppp) moiety. Although the 5'-triphosphate and the 3' NTR are at opposite ends of the HCV genome, activation of RIG-I signaling can be initiated by known intragenome interactions, which bring both 5' and 3' ends of HCV replication intermediate into proximity [188]. The role of TLR3 in HCV recognition has been demonstrated in TLR3-reconstituted Huh-7 and Huh-7.5 cells [189, 190]. HCV replication is substantially reduced when TLR3 signaling is restored in these

hepatoma cells. The TLR3 ligand of HCV has recently been identified as HCV dsRNA replication intermediates that accumulate late during HCV replication [189]. In contrast to RIG-I, activation of TLR3 is not dependent on the nucleotide composition or genome position from which HCV dsRNAs derive. PKR has recently been reclassified as a genuine PRR for HCV, which activates and contributes to innate immune signaling and IFN production [191]. Studies in tissue culture systems suggest that dsRNAs generated during HCV replication activate PKR and induce specific ISGs and IFN β production before RIG-I is activated [191, 192]. The HCV ligand for PKR is the structured RNA at the IRES of the HCV RNA [191, 193]. Paradoxically, this early activation of a PKR-dependent host response seems to benefit the virus rather than the host, as phosphorylation of the α subunit of eukaryotic initiation factor 2 (eIF2 α), induced by PKR activation, arrests host mRNA translation, but not HCV translation [193, 194].

Although detection of HCV by host PRRs results in an antiviral innate immune response, the majority of people with acute HCV infection develop a chronic infection. Studies have shown that HCV has developed multiple strategies to evade and actively counteract host innate defenses. In particular, the NS3/4A protease of HCV is a crucial component of the strategy HCV uses to evade the innate immune response [195]. It targets both MAVS in the RIG-I signaling pathway [41, 196, 197] and TRIF in the TLR3 pathway [198] for proteolysis and effectively abrogates IFN induction. Other HCV proteins, such as NS3 [199], NS4B [200] and NS5A [201], impair the IFN induction pathways *in vitro* by

several mechanisms. In addition, intensive *in vitro* experiments have shown that HCV, especially HCV core and NS5A proteins [202, 203], blocks the JAK-STAT signaling pathway downstream of the IFN receptors. It is worth to note that most evidence on HCV evasion or impairment of host innate immunity is derived from studies in tissue culture systems. Further confirmation remains to be performed in an *in vivo* system.

Acute HCV infection in humans is mostly asymptomatic. As a result, very few patients are diagnosed during the first few months after infection. Most of our understanding of early events in acute HCV infection derives from liver biopsy studies in experimentally infected chimpanzees [204-208]. In the first 2 weeks of HCV infection, HCV titers increase rapidly, but then viral replication slows down. This reduction is believed due to the induction of type I IFN-related ISGs in the liver. Effective control of the HCV infection observed 8-12 weeks post-infection is related to IFN γ induction and upregulation of IFN γ -stimulated genes in the liver. In agreement with the observations from the chimpanzees, a strong activation of IFN γ signaling is seen in liver biopsy samples obtained 2-5 months after HCV infection in patients [209]. The source of IFN γ in the liver is the infiltrating CD8-positive T cells found in direct proximity of hepatocytes. In contrast to chronic HCV infections, the response rate in patients with acute hepatitis C is over 90% to treatment with pegIFN α [210, 211]. This is because IFN γ is the main source of ISG expression during the acute phase of HCV infection. No elevations in transcript or protein levels of USP18 were found in liver biopsy specimens of acute HCV infected patients [209] in contrast to USP18

mRNA and protein elevation seen in chronic HCV infected patients [212]. As mentioned in section 1.1.2.2, USP18 is an IFN signaling negative regulator. Prolonged upregulation of USP18 is associated with refractoriness to continuous IFN α stimulation. Therefore, refractoriness to IFN α -based therapies in acute HCV-infected patients is not as much an issue as in the CHC patients.

Clinical data in CHC patients show that HCV infection induces a strong ISG response (either type I or type III IFN stimulated) in the liver of patients who failed to respond to IFN α therapy [161, 162, 213]. In addition, the expression of intrahepatic chemokines is often elevated in hepatitis C patients, and the levels of some of these correlate with the outcome of HCV infection or severity of liver inflammation [214, 215]. It has been suggested that patients with pre-activated IFN system fail to respond to further stimulation with pegIFN α injection due to a refractory effect, which may arise from prolonged upregulation of USP18 [212]. It remains unclear why the activated endogenous IFN system of the pegIFN α non-responders was unable to clear the infection. One possible explanation is that HCV infection induces phosphorylation of PKR and eIF2 α , leading to a global down-regulation of cellular mRNA translation. As a result, the effector function of IFN-stimulated genes is hampered, while the IRES-dependent translation of HCV RNA is unaffected [194]. Another hypothesis relies on the cross-talk between HCV-infected cells and the uninfected bystander cells [212]. Within the liver of a HCV-infected patient, the majority of liver cells are virus free. It is possible that the strong ISG expression observed in the pre-therapy livers is the result of endogenous IFN stimulation of uninfected bystander cells, whereas high

levels viral replication block the IFN signaling and target ISG gene expression in cells harboring HCV. In fact, resident or infiltrating liver myeloid cells, including pDCs and Kupffer cells, could produce type I or type III IFN after stimulation by viral products released from infected hepatocytes. In particular, pDCs can produce large amount of type I and type III IFNs upon recognition of exosomal transfer of HCV RNA from neighboring hepatocytes [216, 217]. Cytokines produced by pDCs, Kupffer cells and infected hepatocytes within the liver could also have an impact on the recruitment of immune cells to the liver. This would likely determine the effectiveness of the following adaptive immune response, especially the generation of virus-specific cytotoxic T lymphocytes, resulting in changes in HCV-induced pathogenesis and varying outcomes of IFN therapy [195]. It has been suggested that this cross-talk between liver cell subtypes would be influenced by the genotype of patient's IFN λ 3 locus, e.g. those with the favorable genotype have increased immune cell function and better viral clearance [218]. In summary, it is becoming clear that liver is an immunological organ. The crosstalk between the resident and infiltrating liver cell subtypes is important to predicting IFN treatment outcomes as well as the way to direct an effective adaptive immunity to HCV infection.

It is worth noting that innate immunity can also be over-activated and may result in pathology over protection. Recently, two groups using LCMV infection in mice as a model found that, although acute type I IFN signals is antiviral and stimulates clearance of infection, when virus cannot be controlled, sustained IFN signaling induces immunosuppression and facilitates persistent virus infection [219, 220].

So interfering with type I IFN signaling restores multiple parameters of productive antiviral immunity, allowing for viral clearance. Accordingly, in chronic hepatitis C treatment, identifying the molecular basis for the antiviral versus immunomodulatory effects of IFN α could be helpful to selectively manipulate the undesired IFN effect. It will also be important to determine how the balance between antiviral and immunoregulatory effects varies during HCV infection over time, which allows appropriate decision to be made to modify treatment strategies accordingly.

1.4 Experimental models for the study of hepatitis B and C viruses

1.4.1 Cell culture models for the study of hepatitis B and C viruses

The restricted host range and the need of highly differentiated and polarized hepatocytes to establish HBV infection have strongly limited the development of cell-based systems that model HBV infection. The first generation of *in vitro* strategies was based on transfection of human hepatoma cell lines with vectors, which can be either plasmids or recombinant adenovirus or baculovirus vectors, carrying 1.1 to 3 HBV genome units. For examples, 2.2.15 cells [221] and HepAD38 cells [222] are most commonly used HepG2 derived cells producing HBV particles in laboratories. Even though these transfection-based *in vitro* systems has significantly contributed to elucidate several aspects of the HBV life cycle [221, 223], these systems do not permit assessment of viral infectivity or to test the ability of specific HBV isolates to cope with host defenses. Primary human hepatocytes have been shown to support HBV infection [224-227].

However, susceptibility to infection is often low, and primary human hepatocytes tend to lose their differentiation status within days and become non-permissive for HBV infection quickly after plating, which hampered long-term studies [226, 227]. HepaRG cell line is a highly differentiated cell line isolated in 2002 [228]. This cell line represents an experimental breakthrough in HBV studies since it supports the early steps of HBV infection and offers a new possibility to study the infectivity of clinical isolates and HBV variants [229].

Similarly with *in vitro* systems for HBV study, development of experimental culture systems for HCV has been challenging. Although infectious cDNA clones derived from chronic hepatitis C patients infect chimpanzees [230-233], none could be efficiently cultured *in vitro*. The first breakthrough for cell culture of HCV was the development of a subgenomic replicon system [234]. The subgenomic replicon is composed of the HCV-IRES, the neomycin phosphotransferase gene for selection purpose, the IRES of the encephalomyocarditis virus, which directs translation of HCV sequences from NS2 or NS3 up to NS5B, and the 3' NTR [234]. The replicon system proved to replicate at very high efficiency in the Huh-7 hepatoma cell line, the most permissive cell type for HCV RNA replication [235]. A second breakthrough was the discovery of a high-replication molecular clone, Japan Fulminant Hepatitis type 1 (JFH-1), by Dr. Wakita's group [236] from a "fulminant" hepatitis patient infected with genotype 2a HCV [237]. Transfection of Huh-7 and its derivatives, e.g. Huh-7.5 cells, with *in vitro*-transcribed full-length JFH-1 RNA, or recombinant chimeric genome of JFH-1 with another genotype 2a isolate, J6,

produced viral particles that were infectious to naïve Huh-7 cells, chimpanzees, and chimeric mice populated with human hepatocytes [238-241]. In addition to the infectious cell culture producing HCV based on the JFH-1 genome (termed HCVcc system), genotype 1a (H77) and genotype 1b (Con1) virus production systems have also been established [242, 243]. What's more, a current study done in our laboratory showed that culturing Huh-7.5 cells by supplementing tissue culture media with 2% human serum produces over 1000-fold more JFH-1 than the standard 10% FBS tissue culture conditions [244]. More importantly, the HCV virions produced with this method more closely resemble HCV present in serum of infected patients.

Most recently, a group in China has established a novel hepatoma cell line, HLCZ01 [245]. This cell line supports the entire life cycles of HBV and HCV produced both in cultured cells and clinically. Interestingly, HLCZ01 cells are able to mount an innate immune response to virus infection. The cell line holds promise as a powerful *in vitro* tool for addressing the HBV and HCV life cycles, the interactions between host and virus, as well as the development of novel antiviral agents and vaccines.

1.4.2 Animal models for the study of hepatitis B and C viruses

Both HBV and HCV have a very narrow host range. Human and chimpanzee are the only organisms naturally susceptible to these infections. Valuable *in vivo* data on virus-host interactions, viral immunity, and the viral pathogenesis of HBV and HCV infection have been obtained from clinical studies in humans or in

experimental studies in chimpanzees. However, clinical research is hampered by the heterogeneity of human study cohorts, restricted access to liver samples and limited control over critical experimental parameters. The chimpanzee has been an important tool for HBV and HCV research from the discovery of the HCV virus [135] to characterization of the natural clinical course of viral infection including the immune response induced to both infections [116, 204, 205, 208, 246-248]. Due to their ability to mount virus-specific immune responses, chimpanzees have been particularly useful in assessing the preclinical efficacy of vaccine candidates for both HBV [249-252] and HCV [253-257]. The chimpanzee model remains the gold standard for all other animal models in the field of HCV research. But high costs and ethical constraints limit access to the chimpanzee model. Chimpanzees have lower susceptibility to chronic HBV and HCV infections than humans, thus limiting the study of viral cirrhosis and hepatocellular carcinoma [248]. Therefore, the development of suitable alternative models is critical, particularly since the Institute of Medicine report on chimpanzee experimentation in 2011 recommended that the National Institute of Health no longer provides financial support to studies using chimpanzees [258].

The tree shrew (*Tupaia belangeri*) supports both HBV and HCV infection and has been used as a small animal model in HCV study. Some animals developed severe liver disease including steatosis, fibrosis, and cirrhosis 3 years after initial HCV infection [259]. However, experimental infection of tree shrews with HBV is not efficient and causes only a mild, transient infection with low viral titers in these animals [260, 261]. Drawbacks of this model are the limited availability of tupaia-

specific reagents and the inability to easily manipulate its genetics.

Other than exploring the infectivity of HBV and HCV in different animals, some closely related viruses have been proposed as surrogate models for the study of the two infections. For example, GB virus B [262, 263] and canine hepacivirus [264] for HCV studies, and DHBV [265] and WHBV [266] for HBV studies. These surrogate viruses, especially in HBV studies, have contributed greatly to the understanding of viral replication, chronic infection, hepatic carcinogenicity of hepadnaviruses and development of antiviral agents for HBV.

Mice and rats are the most frequently used laboratory animals due to their low colony maintenance cost and the availability of numerous inbred strains with genetic deficiencies as well as species-specific reagents to model human diseases. Mice and rats are not susceptible to HBV or HCV infection. However, by taking advantage of the genomic manipulation technologies, various approaches have been explored to model HBV or HCV infection and their pathogenesis in mice.

In HBV studies, transgenic mice expressing partial or complete copies of the HBV genome are developed [267-269]. They have been very useful in investigating the mechanism of HBV replication, to study specific viral genes for their oncogenic function *in vivo*, and to test the antiviral activity of various nucleoside analogues, cytokines and HBV-specific small interfering RNAs. However, HBV-transgenic mice are immunologically tolerant to HBV antigens and, therefore they do not develop liver disease. Alternatively, systems, in which the viral genome is introduced into mouse hepatocytes using recombinant

adenoviral particles or adenoviruses [270, 271] or by hydrodynamic injection of naked DNA [272], have been used to study tolerance to HBV antigens, mechanisms of viral clearance and for testing antiviral therapies.

In studies of HCV, a number of transgenic mice expressing individual or combinations of HCV gene products were developed mainly to study HCV-induced liver diseases and intrahepatic, virus-specific adaptive immune responses against HCV (reviewed in reference [273]). Attempts have also been made to build a genetically humanized mouse model, i.e expression of human host factors, such as virus entry receptors CD81 and OCLN, and/or inactivation of inhibitory murine molecules to support the HCV life cycle [274, 275]. However, this approach is challenging since the mechanisms for the narrow host range of HCV are incompletely understood and the viral life cycle is insufficiently supported at multiple steps in murine cells. Alternatively, a complementary approach is to promote the adaptation of HCV to efficiently use entry factor orthologs of murine origin, and to replicate and produce progeny virus in mouse cells by taking advantage of the remarkable mutational plasticity of HCV [276]. This method may have very limited usage in vaccine and therapy development since both of them require accurate assessment of human-specific target/virus in order to gain high efficacy.

Another humanization method is xenoengraftment of permissive human cells, such as hepatoma cell lines or primary hepatocytes, in mice. The common strategy shared by these models is to repopulate human-derived hepatocytes into

mice that are immunodeficient to prevent xenograft rejection and often suffering from an endogenous liver injury to promote hepatocyte proliferation and provide human donor cells a competitive growth advantage over mouse hepatocytes. Donor hepatocytes are usually injected intrasplenically from where they rapidly migrate through the portal venous system into the liver resulting in a more even distribution of donor cells throughout all liver lobes in contrast to localized intrahepatic injections. Numerous models have been established based on the xenoengraftment method. The severe combined immunodeficiency (SCID) / beige (bg) - albumin (Alb) / urokinase-type plasminogen activator (uPA) model transplanted with human hepatocytes was the first animal model to successfully support HCV infection and replication [277]. This is the key model I used to study HBV and HCV infection throughout my PhD program.

Overexpression of urokinase by the uPA transgene under the albumin promoter in the mice leads to sustained mouse liver injury and neonatal liver failure. The degeneration of mouse hepatocytes provides opportunity for engrafted primary human hepatocytes to populate the failing liver, and establish chimeric livers containing both mouse and human hepatocytes. This model supports robust and sustained infection by clinical or tissue culture derived hepatitis viruses, including HAV, HBV and HCV. The understanding of many aspects of HCV biology has been furthered by studies in this model, e.g. viral entry [278, 279]; the role of anti-HCV antibodies [280]; infectious particle composition [239, 281] and innate immune responses [282-284]. It is also a superior model for the pre-clinical evaluation of antiviral compounds over other small rodent models. The main

drawbacks of the SCID/bg-Alb/uPA mouse model are its lack of an adaptive immune system to study vaccines or viral infection clearance, inability to achieve a fully humanized liver and its laboriousness and high cost. One of the unique opportunities offered by this small animal model that particularly interested me is the ability to separate viral and host factors in studies of hepatitis viral infections; we can study infections by different viruses, such as different hepatitis viruses or different genotypes or strains of HCV, in animals repopulated with hepatocytes from the same donor (cryopreserved hepatocytes), or to use the same virus to infect the mice transplanted with hepatocytes from different donors. This enables us to control the variables in the examination of host-virus interactions and to dissect the contributions of host and viral factors in the response to antiviral treatment.

1.5 Research objectives

Since the discovery of HBV and HCV, the *in vitro* cultivation of these two viruses has been experimentally difficult. At the time my PhD thesis was started, the *in vitro* tissue culture systems that support a complete HCV or HBV life cycle were limited. The infectious HCV tissue culture systems now include JFH-1 (HCV genotype 2b) and H77 (HCV genotype 1a) in hepatoma Huh-7 cells or Huh-7 derived cells. *In vitro* HBV infection systems commonly used in laboratories includes HepAD38 cells and 2.2.15 cells stably expressing HBV (ayw subtype). In contrast, the SCID/bg-Alb/uPA mice engrafted with human hepatocytes are susceptible to the infection of both tissue culture derived and clinically isolated

HBV and HCV. More importantly, the SCID/bg-Alb/uPA mouse model offered me a unique opportunity to separate viral and host factors in studies of hepatitis viral infections which cannot be done in any of the current available tissue culture systems; viral factors can be studied by infecting hepatocyte donor-matched chimeric mice with different hepatitis viruses or viral strains, and host factors can be investigated by using the same virus to infect the chimeric mice transplanted with hepatocytes from different donors. This enables me to control the variables in the examination of host-virus interactions and to dissect the contributions of host and viral factors in the response to antiviral treatment.

As mentioned in previous sections in this chapter, interferon response is crucial to viral pathogenesis as well as treatment in both HBV and HCV infections. The main objective of this thesis was to study the role of interferon response in HBV and HCV infections in the SCID/bg-Alb/uPA chimeric mouse model. I first examined the contributions of viral and host factors to the response of HCV infection to exogenous IFN treatment by manipulating the SCID/bg-Alb/uPA chimeric mice with different HCV strains on donor-matched background or with different hepatocyte donors infected with the same HCV strains. The second study focused on detection of the endogenous interferon response induced during the course of HBV or HCV infection in SCID/bg-Alb/uPA chimeric mice. The third study was to compare the difference in molecular mechanisms by which HBV *versus* HCV resist to the treatment of exogenous IFN. Lastly, two collaborative projects were also included in this thesis: in collaboration with Dr. Yueh-Ming Loo in Dr. Michael Gale Jr. laboratory in Seattle, USA, I used the SCID/bg-

Alb/uPA chimeric mouse model to study the potential antiviral effect of HCV PAMP RNA by inducing innate immune responses; In collaboration with Rangunath Singaravelu in Dr. John Paul Pezacki laboratory in Ottawa, Canada, the role of miR-27 in HCV infection and hepatic lipid droplet (LD) biogenesis was studied in the SCID/bg-Alb/uPA chimeric mouse model.

CHAPTER 2

Materials And Methods

2.1 Reagents and Materials

2.1.1 Reagents

During completion of this work, the following reagents and supplies were utilized as recommended by the manufacturer, unless otherwise specified.

Table 2.1 Commercial sources of materials, chemicals, and reagents

<i>Name</i>	<i>Source</i>
10% buffered formalin phosphate	Thermo Fisher Scientific
2-Mercaptoethanol	Thermo Fisher Scientific
4',6-diamidino-2-phenylindole (DAPI)	Sigma-Aldrich
40% Acrylamide/Bis-acrylamide solution (29:1)	Bio-Rad
Acetone (Certified ACS)	Thermo Fisher Scientific
Agarose, ultrapure, electrophoresis grade	Invitrogen
Ampicillin	Sigma-Aldrich
Bovine serum albumin (BSA)	Sigma-Aldrich
Bromophenol blue	Sigma-Aldrich
Chloroform	Thermo Fisher Scientific
Complete TM EDTA-free protease inhibitors	Roche
Disodium phosphate	BDH Chemicals
Dithiothreitol (DTT)	Sigma-Aldrich
Ethanol	Commercial Alcohols
Ethidium bromide solution	Sigma-Aldrich
Ethylenediaminetetraacetic acid (EDTA)	EMD Chemicals
Fetal bovine serum (FBS)	Invitrogen
Formaldehyde, 37% (v/v)	Sigma-Aldrich
Glacial acetic acid	Thermo Fisher
Glucose	Thermo Fisher Scientific
Glycerol	Thermo Fisher Scientific
Glycine	EM Science
Human DNA	Promega G3041
Human IFN α -2b (INTRON® A)	MERCK
Human pegIFN α -2b (PEGSYS)	Roche
Hydrochloric acid	Thermo Fisher Scientific
Isopropanol	Commercial Alcohols
Isopropanol, molecular biology grade	Sigma-Aldrich
L-Glutamine	Invitrogen
Magnesium acetate	Thermo Fisher Scientific
Magnesium chloride	EMD Chemicals
Methanol	Thermo Fisher Scientific
Monopotassium phosphite	BDH Chemicals
Mouse DNA	Promega G3091
N,N,N',N',-tetramethylethylenediamine (TEMED)	Sigma-Aldrich

Table 2.1 (continued)

<i>Name</i>	<i>Source</i>
Paraffin wax for tissue embedding	Sigma-Aldrich
Paraformaldehyde	Thermo Fisher Scientific
Phenol, buffer saturated	Sigma-Aldrich
Phosphoric acid	Thermo Fisher Scientific
Poly(I:C)	Sigma-Aldrich
Potassium acetate	Anachemia
Potassium chloride	Becton, Dickinson & Company
Prolong gold mounting medium	Invitrogen
Random hexamer primers	Invitrogen
Restore [™] Western Blot Stripping Buffer	Pierce
Skim milk powder	Carnation
Sodium azide	Sigma-Aldrich
Sodium chloride	Sigma-Aldrich
Sodium dodecyl sulphate (SDS)	Bio-Rad
Sodium hydroxide	Sigma-Aldrich
Spermine	Sigma-Aldrich
Sucrose	EMD Chemicals
Tissue-Tek Optimal Cutting Temperature Compound (OCT)	Sakura
Tris base	VWR
Triton X-100	VWR
TRIZOL	Invitrogen
Tween 20	Thermo Fisher
UltraPure distilled water	Invitrogen
Xylene cyanol FF	Sigma-Aldrich

Table 2.2 Molecular size standards

<i>Marker</i>	<i>Source</i>
GeneRuler 1 kb DNA Ladder	Fermentas
PageRuler Pre-stained Protein Ladder (10-170 kDa)	Fermentas

Table 2.3 DNA/RNA modifying enzymes

<i>Enzyme</i>	<i>Source</i>
DNase I	Ambion
Moloney Murine Leukemia Virus Reverse Transcriptase (M-MLV RT)	Invitrogen
RNaseOut	Invitrogen
ThermoScript [™] reverse transcriptase	Invitrogen

Table 2.4 Multi-component systems

<i>System</i>	<i>Source</i>
High Pure Viral Nucleic Acid kit	Roche
Lipid based in vivo transfection reagent	Altogen Biosystems
MegaScript in vitro transcription kit	Ambion
Pierce BCA Protein Assay kit	Thermo Scientific
Platinum Taq PCR System	Invitrogen
Power SYBR® Green PCR Master Mix	Applied Biosystems
QIAprep spin miniprep kit	QIAGEN
QIAquick PCR Purification kit	QIAGEN
SuperScript III Reverse Transcriptase system	Invitrogen
TaqMan® Universal PCR Master Mix	Applied Biosystems

Table 2.5 Detection systems

<i>System</i>	<i>Source</i>
ABI 7900 Real Time PCR system	Applied Biosystems
Leica TCS SP5	Leica microsystems
NanoDrop ND-1000 Spectrophotometer	Thermo Scientific
PVDF membrane (0.45 µM)	Millipore
Rx film	Fuji
Supersignal West Pico chemiluminescent substrate	Thermo Scientific
TMB microwell peroxidase substrate system	KPL
Ultraviolet gel transilluminator	Thermo Fisher Scientific
XO-MAT Developer	Kodak

2.1.2 Commonly used buffers and solutions

Table 2.6 Buffers and Solutions

<i>Name</i>	<i>Composition</i>
1% agarose gel running buffer for HBV capsid WB	80 mM Tris H ₃ PO ₄ pH 7.5, 1 mM Mg(OAc) ₂ , 0.1 mM EDTA
5x Protein sample buffer	62.5 mM Tris-HCl (pH 6.8), 25% (v/v) glycerol, 2% (w/v) SDS, 0.01% (w/v) bromophenol blue, 5% (v/v) β-mercaptoethanol
6 x DNA gel loading buffer	40% (w/v) sucrose, 0.25% (w/v) bromophenol blue, 0.25% (w/v) xylene cyanol FF
Back extraction buffer	4M Guanidine Thiocyanate, 50mM Sodium Citrate, 1M Tris

Table 2.6 (continued)

<i>Name</i>	<i>Composition</i>
Coating buffer	4.21g NaHCO ₃ and 5.5g N ₂ CO ₃ in 1L distilled water.
Equilibration buffer	75% EtOH, 0.3M NaOAc, 10mM Mg(oAc) ₂ , 10mM Tris, pH8
Hepatocyte medium	DMEM supplemented with 10% FBS, 50IU/mL penicillin, 10µg/mL streptomycin and 10pg/mL hepatocyte growth factor
Orange G loading dye	0.35% Orange G, 15% Ficoll 400, dissolve in H ₂ O
Phosphate buffered saline (PBS)	137 mM NaCl, 2.7 mM KCl, 6.5 mM Na ₂ HPO ₄ , 1.5 mM KH ₂ PO ₄ (pH 7.15-7.4)
PBS-T	137 mM NaCl, 2.7 mM KCl, 6.5 mM Na ₂ HPO ₄ , 1.5 mM KH ₂ PO ₄ (pH 7.15-7.4), 0.05% (v/v) Tween-20
RIPA buffer	50 mM Tris-HCl (pH 7.5), 150 mM NaCl, 0.1% SDS, 1% Triton X-100, 1% sodium deoxycholate, 5 mM EDTA
SDS-PAGE resolving gel buffer	0.1% SDS, 374 mM Tris-HCl (pH 8.8)
SDS-PAGE running buffer	250 mM glycine, 0.1% SDS, 100 mM Tris Base (pH 8.3)
SDS-PAGE stacking gel buffer	0.1% SDS, 250 mM Tris-HCl (pH 6.8)
TAE	40 mM Tris acetate, 1 mM EDTA (pH 8.0)
Tris-buffered saline (TBS)	137 mM NaCl, 2.7 mM KCl, 24 mM Tris-HCl (pH 7.4)
TBS-T	137 mM NaCl, 2.7 mM KCl, 24 mM Tris-HCl (pH 7.4), 0.05% (v/v) Tween 20
TE solution	1 mM EDTA, 10 mM Tris-HCl, pH 7.5
Transfer buffer	200 mM glycine, 25 mM Tris base (pH 8.3), 20% (v/v) methanol, 0.1% (w/v) SDS
TritonX-100 lysis buffer	50 mM Tris-HCl (pH 7.2), 150 mM NaCl, 2 mM EDTA, 1% (v/v) TritonX-100, 1 mM fresh DTT

2.1.3 Oligonucleotides

Table 2.7 Oligonucleotides

Name	Forward primer (5'->3')	Probe (5'-FAM-TAMRA-3')	Reverse primer (5'->3')	Usage
IFN α 1	AACTCCCCTGATG AATGC	N/A	CTGCTCTGACAACC TCCC	RT-qPCR
IFN β	CAATTTTCAGTGTC AGAAGCTCC	CTGTGGCAATTGAAT GGGAGGCTT	AAAGTTCATCCTGT CCTTGAGG	RT-qPCR
IL28A+B	GACGCTGAAGGTT CTGGAG	CCACCGCTGACACTG ACCCA	ATATGGTGCAGGG TGTGAAG	RT-qPCR
IL29	CTGTCACCTTCAA CCTCTTCC	CCCATCGGCCACATA TTTGAGGTCT	GACGTTCTCAGACA CAGGTTC	RT-qPCR
HPRT1	CTTGGTCAGGCAG TATAATCCA	N/A	CAAATCCAACAAA GTCTGGCT	RT-qPCR
APOBEC3G	CAACCAGGCTCCA CATAAACAC	TTTCCTTGAAGGCCGC CATGCA	GGAATCACGTCCA GGAAGCA	RT-qPCR
CIG5/Viperin	AGATGTTTCTGAA GCGAGGA	TGGATTGGTAGAGCG GAAAGTGA	GCAGACAATGGCA GTTACTC	RT-qPCR
CXCL9	AGGAACCCAGTA GTGAGAAAGG	CCTGCATCAGCACCA ACCAAGGGA	GGTCTTTCAAGGAT TGTAGGTGGAT	RT-qPCR
CXCL10/IP10	TGAAAAAGAAGGG TGAGAAGAGATG	CTGAATCCAGAATCG AAGGCCATCAAGA	CCTTCCTTGCTAA CTGCTTTCAG	RT-qPCR
CXCL11	CCTCCATAATGTA CCCAAGTAACAAC T	AGGACAACGATGCCT AAATCCCAAATCG	TTTTTGATTATAAG CCTTGCTTGCT	RT-qPCR
IFI6	AAGGCCCTGACCT TCAT	AGGAGGACTCGCAGT CGCC	ATTCAGGATCGCA GACCA	RT-qPCR
IFI27	GTAGTTTTGCCCCT GGC	GACATCATCTTGCTG CT	TGTGATTGGAGGA GTTGTGGCTGT	RT-qPCR
IFIT2	AGGAAGATTTCTG AAGAGTGC	CACTGCAACCATGAG TGAGAACAATAAGAA	GTTCCAGGTGAAAT GGCA	RT-qPCR
IFITM1	TCCTCATGACCATT GGATTCATC	AGACTGTCACAGAGC CGAATACCA	CCGTTTTTCCTGTA TTATCTGTAACATA A	RT-qPCR
IRF1	CTGTCGCCATGTG CTGTCA	CAGCACTCTCCCCGA CTGGCACA	TGTCCGGCACAAC TCCA	RT-qPCR
IRF3	CCCTCACGACCCA CATAAAATC	CAGACACCTCTCCGG ACACCAATG	CCCAGTAACTCATC CAGAATGTC	RT-qPCR
IRF7	GTGAAGCTGGAAC CCTGG	AGCGCCAACAGCCTC TATGACG	CCATAAGGAAGCA CTCGATGTC	RT-qPCR
IRF9	GCCCTACAAGGTG TATCAGTTGCT	CCACCAGGAATCGTC TCTGGCCA	TCGCTTTGATGGTA CTTTCTGAGT	RT-qPCR
ISG15	TGGTGAGGAATAA CAAGGGC	N/A	CAGATTCATGAAC ACGGTGC	RT-qPCR
MAVS	ACCCACAGGGTCA GTTGTATCTACT	TTCTCCTCCTCATCC CTGGCTTGG	TCACTCTCTGCACC CTGTTTACC	RT-qPCR
MxA	ACCTGATGCCTA TCACCAG	N/A	TTCAGGAGCCAGCT GTAGGT	RT-qPCR
OAS1	TGTGTGTCCAAGG TGGTAAAGG	CCTCAGGCAAGGGCA CCACCCT	CAACCAGGTCAGC GTCAGATC	RT-qPCR
OAS2	GGTGAACACCATC TGTGACG	N/A	TGAACCCATCAAG GGACTTC	RT-qPCR
PKR	TTAGTGACCAGCA CACTCGC	N/A	ATGCCAAACCTCTT GTCCAC	RT-qPCR
RIG-I	GGACGTGGCAAAA CAAATCAG	ATTGTGATCTCCACTG GCTTTGA	ACACAGGAATGAC CCTCCCGGCA	RT-qPCR

Table 2.7 (continued)

Name	Forward primer (5'→3')	Probe (5'-FAM-TAMRA-3')	Reverse primer (5'→3')	Usage
SP110	CAAAGCGATGAGA TCCTGAG	CTTGTCATTGGTCACT GAAGTGCTTCT	CTGAGTCTTCTTCC GCATTC	RT-qPCR
STAT1	GTGGAAAGACAGC CCTGCAT	ACTGGACCCCTGTCTT CAAGAC	AACGCACCCTCAG AGGCCGC	RT-qPCR
STAT2	ACCAGTTGCTCAC TGAGGAGAATATA	GGTAGTAGCACCCAA AAGCTTCA	TGCGCTTCCTCTAT CCCCGAATCC	RT-qPCR
TNFSF10	TGCGTGCTGACGT GATCTT	TGCTCCTGCAGTCTCT CTGTGTGGCT	GTACTIONTCTGCA TCTGCTCA	RT-qPCR
TRIM22	GCAGGAGTTTGTG ACCAA	CCAAGGGAGCAGTGC AATGGATTT	AGAGGTTCTGTGAG GAGC	RT-qPCR
TRIM25	CCGAGGTGGAAC GAACCA	AAGCTGATAAAAGGC ATCCACCAGAGCA	TTCAGCTCGTTTTT GAGGTCTATG	RT-qPCR
USP18	TGGCCTACTGCCT GCAGAA	TGCAACGTGCCCTTGT TTGTCCA	GGTACAGTTGGGC AGCATCA	RT-qPCR
XAF1	CTTGAGCACCAGC AGG	TCATAAGGCCAATGA GTGCCAGGA	GCATGTCCAGTTTG CAGA	RT-qPCR
Mouse Mx1	TGCCTGGCAGAGA GACTGACT	AGCTCACCTCCCACAT CTGTAAATCACTGC	GCTTGCCTCTGAT GACTGCTATTT	RT-qPCR
Mouse OAS1a	CCCGGTCTCTGAG CTTCAAG	TGAGCGCCCCCATCT GCA	GCTGGCAGCACAT CAAATC	RT-qPCR
Mouse IFN α 4	GCCTCACACTTAT AACCTCGG	TTTGGATTCCCCTTGG AGAAGGTGG	GCCTTCTGGATCTG TTGGTTA	RT-qPCR
Mouse IFN β	CAGCCCTCTCCAT CAACTATAAG	CTCCAGCTCCAAGAA AGGACGAACAT	TCTCCGTCATCTCC ATAGGG	RT-qPCR
Mouse GAPDH	ACC ACA GTC CAT GCC ATC AC	N/A	TCC ACC ACC CTG TTG CTG TA	RT-qPCR
miR-27	GGCCGCTTACAGTG GCTAAGTTCTGCGTG ATTTTCACAGTGGCT AAGTTCTGCC	N/A	TCGAGGCAGAACTTA GCCACTGTGAAAATC ACGTAGAACTTAGCC ACTGTGAAGC	RT-qPCR
HBV	GGCCATCAGCGCA TGC	CTCTGCCGATCCATAC TGCGGAACTC	C/i5NitInd/GCTGCGA GCAAAACA	Titration
HCV	TCTGCGGAACCGG TGAGTA	CACGGTCTACGAGAC CTCCCGGGGCAC	GTGTTTCTTTTGGT TTTCTTTGAGGTT TAGG	Titration

2.1.4 Antibodies

Table 2.8 Primary antibodies

<i>Antibody</i>	<i>Application*</i>	<i>Source</i>
Goat anti-human albumin	ELISA, WB, IF	Cedarlane
Rabbit anti-HBcAg	WB, IF	DAKO
Rabbit anti- human CK18	WB, IF	Abcam
Mouse anti-human STAT1	IF	BD Biosciences
Rabbit anti-human ISG15	WB	Cell Signaling
Mouse anti-HCV core	WB	Thermo Scientific
Mouse anti-HCV NS5A	WB	Dr. Michael. Gale Jr. University of Washington

* WB: Westernblot; IF: immunofluorescence; ELISA: Enzyme-linked immunosorbent assay

Table 2.9 Secondary antibodies

<i>Antibody::Conjugate</i>	<i>Application*</i>	<i>Source</i>
Goat anti-mouse::HRP	WB	Invitrogen
Goat anti-rabbit::HRP	WB	Invitrogen
Goat anti-human albumin::HRP	ELISA	BETHYL
Goat anti-mouse::Alexa488	IF	Invitrogen
Goat anti-mouse::Alexa546	IF	Invitrogen
Goat anti-rabbit::Alexa488	IF	Invitrogen
Goat anti-rabbit::Alexa546	IF	Invitrogen

* WB: Westernblot; IF: immunofluorescence; ELISA: Enzyme-linked immunosorbent assay

2.1.5 Cells, animals and viruses

2.1.5.1 Cells

Cryopreserved human primary hepatocytes were purchased commercially. Each lot of hepatocytes represented a distinct donor. Hepatocyte donors with younger ages were intentionally selected due to their higher engraftment success rate. Since not every lot of hepatocytes produces chimeric mice with satisfactory engraftment, a trial study using 10-20 mice was performed before each lot of human hepatocytes was used for experiments. Five hepatocyte preparations were used in my studies: Hu8063, Hu8085 and Hu4109 were purchased from CellDirect Inc, USA. FLO cells were from BioreclamationIVT, USA. Hepatocytes Hu3111 were freshly isolated from a liver donor supplied by Dr. Norm Kneteman (A liver surgeon, University of Alberta Hospital). Informed consent was obtained from all local donors of human hepatocytes in accordance with the University of Alberta Faculty of Medicine Research Ethics Board guidelines.

2.1.5.2 Animals

All mice were housed and maintained in pathogen-free ventilated cages according to Canadian Council on Animal Care guidelines. All animal experiments were approved by the University of Alberta Animal Welfare Committee. The SCID-bg/Alb-uPA transgenic mice were produced by crossing B6SJL-TqN (Alb 1 p Plau) 144Br (Jackson, Bar Harbor, Maine) mice carrying the uPA gene linked to

an albumin promoter with C-b-17 Gbms Tac-SCID/bg immunodeficient mice (Taconic Farms Germantown, New York) [277]. Offspring were crossed back to homozygosity for both the SCID/bg trait and the Alb-uPA transgene (Figure 2.1).

2.1.5.3 Viruses

Two isolates of HCV viruses were used in my studies: HCV gt1a was from a null-responder hepatitis C patient and HCV gt2b was isolated from a patient who achieved a SVR after pegIFN and ribavirin treatment. One HBV stock virus isolated from a HBV positive patient was used in my studies. All three clinical viral isolates were collected from Dr. Lorne Tyrrell's clinic (University of Alberta, Edmonton, Alberta.). The collection and use of human sera in these studies were approved by the human ethics committee, Faculty of Medicine and Dentistry, University of Alberta.

2.2 Methods

2.2.1 Generation of SCID/bg-Alb/uPA chimeric mice

The generation of SCID/bg-Alb/uPA mice is illustrated in Figure 2.1. Briefly, mice were transplanted with human hepatocyte between 10-21 days of age. Animals were anesthetized with isoflurane/O₂ followed by a small left-flank incision to expose the spleen. Human hepatocytes ($0.5-1 \times 10^6$ per mouse) were then injected slowly into the inferior splenic pole for repopulation of the mouse liver. A single titanium clip was placed across the injection site for hemostasis, and the incision was closed. The transplantation procedure was performed under a

surgical microscope (Leica M275). After the surgery was completed, mice were closely monitored in a newly prepared cage until they were fully recovered. A red light was used to keep the animals warm during recovery. Pain-relief medication was offered if there was any sign of stress during recovery.

In order to produce the chimeric mice, I took an advanced surgery training course, microvascular surgery (SURG 555), offered by Department of Surgery, Faculty of Medicine and Dentistry, University of Alberta. As a result of this training, I experted in performing human hepatocyte transplantation into 5-21 day old mice to produce chimeric mice. The surgery for the vast majority of experimental mice used in my projects or in collaborative research projects during my PhD studies was performed by me with the help of a lab technician.

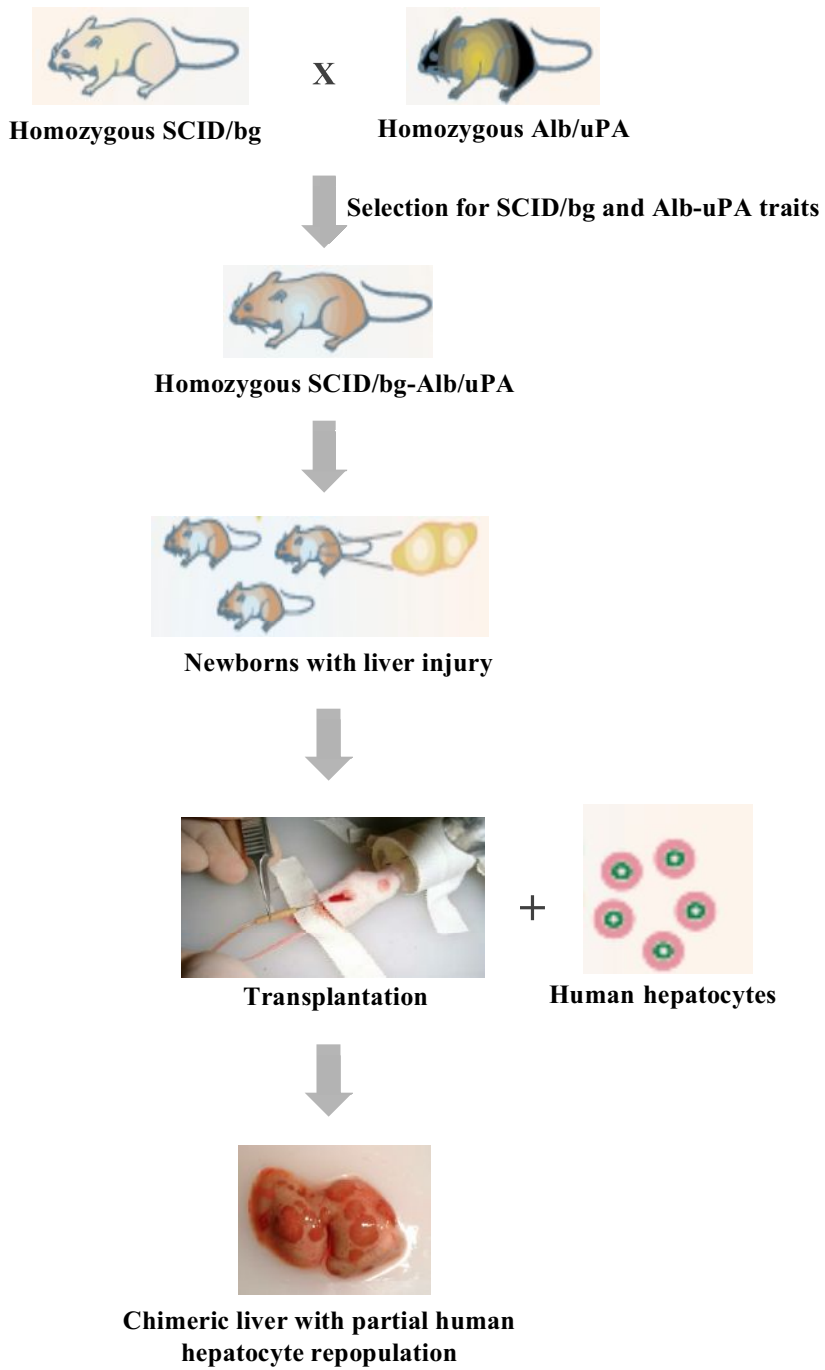


Figure 2.1 Generation of SCID/bg-Alb/uPA chimeric mice.

Alb-uPA transgenic mice were crossed with SCID/bg mice to obtain homozygosity for both traits [277]. The homogenous SCID trait causes severe combined immunodeficiency affecting both B and T lymphocytes, resulting the loss of B- and T-cell immunity [285]. The beige mutation in mice leads to impairment in NK cell function [286]. Expression of the Alb/uPA transgene results in urokinase overproduction in the liver that accelerates mouse hepatocyte death. Human hepatocytes were then transplanted into immunocompromised transgenic newborn mice with liver injury, resulting in a chimeric liver with partial population with human hepatocytes (Red nodules in the chimeric livers). The SCID trait could be followed by confirming the absence of mouse IgG in SCID homogenous mice. We originally used anti-NK antisera to simulate the beige trait. However, we are grateful to Dr. William Addison for developing a lysosome granule staining system to select for homogenous beige mice.

2.2.2 Defrosting of human hepatocytes

Before each surgery, vials containing cryopreserved human hepatocytes cells were removed from liquid nitrogen and incubated in 42°C water bath until 70-80% cells were thawed. Cells were then transferred into freshly prepared cold hepatocyte medium (Table 2.6) with at least 10 times volumes of the initial cell suspension and mixed well. Hepatocytes were spun down at 200xg for 5-10 minutes at room temperature and supernatant was discarded for the removal of dimethyl sulfoxide (DMSO) in the original cell suspension. The pellet was resuspended in cold hepatocyte medium with a volume of 200µL (0.5-1 million cells) for each mouse.

2.2.3 Human albumin measurement in mouse serum

Four and eight weeks after transplantation, the approximate human hepatocyte repopulation levels in transplanted mice were determined by measuring human albumin in mouse serum using a sandwich enzyme-linked immunosorbent assay (ELISA). Briefly, a 96-well ELISA plate was coated at 4°C overnight with a capture antibody, unlabeled goat anti-human albumin antibody, 1:800 diluted in coating buffer (Table 2.6). The next day, each well of the plate was blocked with 200µL of 1% gelatin in TBS-T (blocking solution) at room temperature for 30 minutes following 3 washes with TBS-T. A positive human serum control with known human albumin concentration (1:10,000 diluted in blocking solution), a negative control (1:150 diluted mouse serum in blocking solution), standards (serial dilutions of commercial human albumin with known concentrations) and

mouse serum samples 4-fold serially diluted from 1:5,000 in blocking solution were added to the ELISA plate at 100 μ L each well and incubated at room temperature for 1 hour. After washing in TBS-T 3 times, 100 μ L goat anti-human albumin antibody conjugated with horseradish peroxidase (HRP) diluted 1:80,000 in blocking solution was added to each well as the detection antibody. The plate was incubated at room temperature for 1 hour, washed with TBS-T for 3 times, and then 100 μ L of 3,3',5,5'-tetramethylbenzidine (TMB) microwell peroxidase substrate was added for HRP detection. The detection reaction was stopped by adding 100 μ L of 1M phosphoric acid in each well. The optical density (OD) for each well was read with a microplate reader (Spectra max plus 384, Molecular Devices) set to 450nm. Concentration of each chimeric mouse samples was calculated according to OD readings of the positive control and the standard curve in the same plate.

2.2.4 Viral infection

Animals with successful human engraftment at eight weeks post transplantation were used for HBV and HCV infection studies. A previous study by Steenburgen *et al.* in our lab showed that infection success by HCV in SCID/Alb-uPA chimeric mice was correlated with human hepatocyte engraftment success, whereas mice with lower engraftment that did not support HCV infection were susceptible to HBV infection [281]. In addition, other than a significant engraftment of mouse livers with human hepatocytes, humanization of lipoprotein profiles, such as expression of markers of human lipoprotein biosynthesis, human apolipoprotein B

(hApoB) and cholesterol ester transfer protein (CETP), was positively associated with HCV infection success [281]. Based on these results as well as my experience working with HBV and HCV infections in the chimeric mice, chimeric mice with human albumin levels higher than 1,000 μ g/mL at 8-week post transplantation were used for HBV infection and mice with albumin higher than 5,000 μ g/mL were used for HCV infection studies.

Mice with greater than 5,000 μ g/mL serum human albumin level were infected intravenously (i.v) with 100 μ L of human serum containing at least 10^5 genome equivalence of HCV per mL. Chimeric mice with human albumin level at 1,000 μ g/mL and above received a single intraperitoneal (i.p) injection of 100 μ L HBV-positive human patient serum (greater than 10^5 genome equivalence). For the mock-infected controls, age- and hepatocyte donor-matched chimeric mice with the similar range of human chimerism received 100 μ L of serum from a HBV-negative, HCV-negative and human immunodeficiency virus (HIV)-negative healthy donor through i.v or i.p injection.

2.2.5 Exogenous interferon treatment

Human IFN α -2b (INTRON® A) was used in all my experiments unless otherwise specified due to that both HBV and HCV infection takes place in human hepatocytes in the chimeric liver. Exogenous IFN treatment was performed by subcutaneous (s.c) injections, the same route as in patients, daily for 14 days at 1,350 international unit (IU)/gram body weight. The injection was prepared in PBS to a final concentration of 1,350 IU/ μ L. The volume of IFN α -2b was

determined by the weight of each mouse. Six hours after the last IFN injection at day 14, mice were sacrificed and samples/tissues were collected for further analysis (see section 2.2.6). Animals injected s.c with an equivalent volume of PBS were used as control animals. For the treatment with pegylated IFN α -2b (Pegasys, Roche), mice were given 875ng of pegIFN once a week by s.c injection. After 4 weeks, treatment was discontinued and animals were kept as treatment-free for two weeks to monitor potential relapse before termination.

2.2.6 Tissue dissection and organ harvest

Infected chimeric mice were euthanized and tissues and organs were harvested at pre-determined endpoints. Mice were first anesthetized by isoflurane at 5% vaporiser concentration. Ethanol (70%) was used to sanitize the mouse abdomen followed by a laparotomy using surgical scissors to gain access into the abdominal cavity. The diaphragm was penetrated and blood was collected through an apical puncture of the heart by a 25-gauge needle and syringe. The liver was dissected, rinsed in cold PBS and cut into small pieces using a scalpel. The liver pieces were divided into 3 groups: one group was placed in a tissue cassette and fixed in 10% buffered formalin phosphate for paraffin embedding and sectioning, one group was placed into a labeled mold with Tissue-Tek OCT and snap-frozen in liquid nitrogen for cryostat sectioning, and the last group was directly snap-frozen in liquid nitrogen for future DNA/RNA/protein analysis. Snap-frozen tissues were transferred for long-term storage in a -80°C freezer. Blood was centrifuged at 1500xg for 10 minutes at room temperature and the serum was

divided into small aliquots and stored in a -80°C freezer for future analysis.

Tissue for paraffin embedding was fixed in 10% buffered formalin phosphate overnight on a shaker. They were processed in increasing concentration of ethanol, 70% to 90% to 100%, for 60-90 minutes each concentration, followed by replacement in 100% butanol-1 overnight. Tissues were paraffin embedded by vacuum infiltration and sectioned at 4 microns by a Shandon Histocentre 2 microtome for histological analysis.

The cryostat tissues in OCT were stored in a -80°C freezer or in liquid nitrogen for long-term storage. Before each experiment, the tissues were cut into 4 microns by a Shandon Histocentre 2 microtome on glass slides and used for indirect immunofluorescence staining.

2.2.7 Total RNA isolation from snap-frozen liver samples

The snap-frozen liver samples harvested in experimental chimeric mice, as described in section 2.2.6, were powdered in a mortar and pestle containing liquid nitrogen and divided into 4-5 cryopreservation vials. One mL of TRIzol reagent was added to one vial of liver powder for total RNA isolation according to the manufacturer's specifications. The homogenate was incubated on a shaker for 30 minutes at room temperature to permit the complete dissociation of the nucleoprotein complexes. Chloroform (0.3mL) was added to the homogenate and mixed vigorously by vortexing for 15 seconds. Samples were incubated at room temperature for 3-5 minutes then centrifuged at $12000\times g$ for 15 minutes at 4°C ,

which separates the mixture into a lower red phenol phase, interphase and colorless upper aqueous phase containing total RNA. The aqueous phase was transferred into a new tube and 0.5mL of chloroform was added to remove the traces of phenol. The samples were vortexed for 15-20 seconds and incubated on a shaker for two minutes before centrifugation at 12000xg for 15 minutes at 4°C. The aqueous phase was collected and mixed with 250µL isopropanol to precipitate the RNA. Samples were incubated at -20°C overnight. Samples were then centrifuged at 12000xg for 30 minutes at 4°C. The supernatant was removed and the RNA pellet was washed by adding 1mL of 75% (v/v) ethanol prepared with RNase-free water and centrifuged for 5 minutes at 4°C. The RNA pellet was air-dried at room temperature and 50µL of RNase-free water was used to resuspend the pellet by pipetting up and down several times and incubating at 55°C until dissolved completely. The quantity and purity of total RNA (1:30 diluted in RNase-free water) was measured by A_{260} and A_{260}/A_{280} ratio readings on a NanoDrop spectrophotometer and the final total RNA concentration was calculated by multiplying dilution factor of 30.

2.2.8 Genomic DNA isolation from snap-frozen liver samples

After complete removal of the aqueous phase containing RNA as described in section 2.2.7, genomic DNA was isolated in the interphase and phenol phase from the initial homogenate. Specifically, 0.5mL of back extraction buffer (Table 2.6) was added to the tube. Samples were incubated at room temperature on a shaker for 10 minutes and centrifuged at 12,000xg for 30 minutes at 4°C. The upper

aqueous phase was transferred into a new tube, 15µg of liner polyacrylamide (LPA), a RNA carrier, and 0.5mL of isopropanol were added for DNA precipitation. Samples were incubated at -20°C overnight, followed by centrifugation at 12,000xg for 15 minutes at 4°C. Supernatant was removed and pellet containing DNA was washed twice by adding 1mL of 75% (v/v) ethanol prepared with DNase-free water, incubating at room temperature for 10 minutes on a shaker and then centrifuging for 5 minutes at room temperature. Ethanol was removed and DNA was air-dried on bench and dissolved in 200µL TE solution (Table 2.6). Additionally, 1/10 volume (20µL) of 0.1M spermine (dissolved in water) was added to the DNA samples. The precipitation of DNA with spermine is useful for removing many contaminations that normally co-precipitate with DNA [287]. Samples were incubated on ice for 15 minutes and centrifuged at 13,000xg for 5 minutes at room temperature. Supernatant was discarded. The precipitate was incubated in 0.5mL of equilibration buffer (Table 2.6) at room temperature for at least 1 hour to remove the spermine. Samples were centrifuged at 13,000xg for 5 minutes at room temperature and supernatant was discarded. DNA pellets were washed 2-3 times in 1mL of 75% (v/v) ethanol prepared with DNase-free water and finally dissolved in 50µL of DNase-free water. The quantity and purity of isolated genomic DNA (diluted 1:10 in DNase-free water) was quantified by A_{260} and A_{260}/A_{280} ratio readings on a NanoDrop spectrophotometer.

2.2.9 Human chimerism measurement

This method was developed by Dr. William Addison, a research scientist in Dr. Lorne Tyrell's laboratory. Purified genomic DNA (A_{260}/A_{280} ratio was ~ 1.9) isolated from each chimeric mouse liver sample (described in section 2.2.8) was diluted to a final concentration of $5\text{ng}/\mu\text{L}$ with 1/10 TE solution. The average human cell content of chimeric liver was determined using a TaqMan Copy Number Reference Assay, which targets the single copy human RNase P gene (Applied Biosystems). Each polymerase chain reaction (PCR) reaction contained $10\mu\text{L}$ of Taqman Universal PCR master mix, $1\mu\text{L}$ of RNaseP reference assay (20x stock), $4\mu\text{L}$ of genomic DNA (20ng) and $5\mu\text{L}$ of water. Each sample was run in triplicates. The reaction conditions were 50°C for 2 minutes, 95°C for 10 minutes, and 40 times of a PCR cycle (95°C for 15 seconds and 60°C for 1 minute). A standard curve for the TaqMan assay was constructed using known-ratio mixtures of quantified commercial human/mouse genomic DNA ratio: 0%, 2%, 10%, 20%, 30%, 50% and 70% of human DNA with the balance of mouse DNA.

2.2.10 HCV titer quantification in mouse serum

HCV RNA was extracted from $30\mu\text{L}$ mouse serum samples using High Pure Viral Nucleic Acid kit according to manufacturer's directions. Extracted RNA samples were dried by vacuum centrifugation for 1.5 hours at 2000rpm, followed by reverse transcription using HCV specific primer (HCV reverse primer in Table 2.7) and ThermoScript™ reverse transcriptase according to manufacturer's directions. Briefly, mixture of $1\mu\text{L}$ of 10mM RNase-free dNTPs and $1\mu\text{L}$ of $2\mu\text{M}$

HCV specific primer with RNase-free water up to a total volume of 13 μ L was added to the dried HCV RNA. The sample was mixed gently and transferred into a 0.2mL PCR tube. The sample was heated to 65°C for 5 minutes and quickly chilled on ice. Then 4 μ L of 5X cDNA synthesis buffer, 1 μ L of 0.1M DTT, 1 μ L of RNaseOUT (40U/ μ L) and 1 μ L of ThermoScript™ reverse transcriptase (15U/ μ L) were added to the PCR tube. The contents were mixed gently and incubated at 50°C for 60 minutes. The reaction was stopped by heat inactivation at 85°C for 15 minutes. The resulting complementary DNA (cDNA) was used for the preparation of a reaction mixture for real-time quantitative PCR. Briefly, 900nM of each HCV specific primer (2.25 μ L of 10 μ M stocks) and 250nM of probe (2.5 μ L of 2.5 μ M stock) (Table 2.7) and 12.5 μ L of TaqMan universal master mix were mixed in one well of a 96-well PCR plate with water added to make the final volume of 22.5 μ L. HCV cDNA (2.5 μ L) was added to the well before the PCR plate was sealed to prevent vaporization. The PCR was performed on an ABI 7900 Real Time PCR machine. The reaction conditions were 50°C for 2 minutes, 95°C for 10 minutes, and 40 times of a PCR cycle (95°C for 15 seconds and 60°C for one minute). Known amounts (10^1 to 10^7 copies/mL) of cloned HCV genomic cDNA (supplied by Dr. Michael Joyce in Dr. Lorne Tyrrell lab) were amplified in parallel to establish a standard curve for quantification. The PCR efficiency was determined by the slope of the standard curve. Viral load was determined using the Applied Biosystems SDS Software 2.3 (Applied Biosystems).

In order to maintain consistency for each HCV RNA isolation and RT-PCR quantification, a negative control and a positive control were included from the

beginning of HCV RNA extraction. The negative control was 30µL human serum isolated from a known HCV negative individual. The positive control was 30µL serum from a HCV positive patient with known HCV RNA quantities. The HCV RNA copy numbers of the positive control was obtained from ProVLab Alberta.

2.2.11 Quantification of intrahepatic HCV RNA

Total RNA was isolated from snap-frozen mouse liver samples as described in section 2.2.7. Reverse transcription was performed using 2µg total RNA with a HCV specific primer (the HCV reverse primer in Table 2.7) and ThermoScript™ reverse transcriptase as described in section 2.2.10. The generated cDNA was used for HCV qPCR following the same protocol described in section 2.2.10. In addition, the amount of human total RNA was quantified by measuring the mRNA level of a house-keeping gene, human HPRT-1 (Hypoxanthine Phosphoribosyltransferase 1), in the same cDNA samples for HCV qPCR. The detailed procedure for human HPRT-1 mRNA quantification is described in section 2.2.15. The intrahepatic HCV RNA levels were presented as HCV genome equivalence relative to expression levels of human HPRT-1.

2.2.12 HBV titer quantification in mouse serum

As the procedure of HCV viral RNA isolation from mouse serum described in section 2.2.10, HBV viral DNA was extracted from 30µL mouse serum samples using High Pure Viral Nucleic Acid kit (Roche). Viral DNA, dissolved in 50µL elution buffer provided by the kit, was then used for the preparation of HBV

qPCR reaction. Briefly, 900nM of each HBV specific primer (2.25µL of 10µM stock) and 250nM of probe (2.5µL of 2.5µM stock) (Table 2.7) [288] and 12.5µL of TaqMan universal master mix and 2µL HBV DNA were mixed in one well of a 96-well PCR plate. Water was added to make the reaction volume to 25µL in total. The PCR was performed on an ABI 7900 Real Time PCR machine. The reaction conditions were 50°C for two minutes, 95°C for 10 minutes, and 40 times of a PCR cycle (95°C for 15 seconds and 60°C for one minute). Known references (10^1 to 10^7 copies/mL) of cloned HBV genomic DNA (provide by Mr. Karl Fischer in Dr. Tyrrell lab) were amplified in parallel to establish a standard curve for quantification. Viral load was determined using the Applied Biosystems SDS Software 2.3 (Applied Biosystems).

In addition, both negative and positive controls were included in HBV DNA extraction. The negative control was 30µL serum from a known HBV negative individual. The positive control was 30µL serum from a HBV positive patient with known HBV DNA quantities. The HBV DNA copy numbers of the positive control sample was obtained from ProvLab Alberta.

2.2.13 Quantification of intrahepatic HBV DNA

Intrahepatic HBV DNA levels were quantified using genomic DNA isolated from snap-frozen mouse liver samples as described in section 2.2.8. The PCR reaction was prepared by mixing 900nM of each HBV specific primer (2.25µL of 10µM stock) and 250nM of probe (2.5µL of 2.5µM stock) (Table 2.7), 12.5µL of TaqMan universal master mix and 2µg of genomic DNA in one well of a 96-well

PCR plate. Water was added to make the reaction volume to 25 μ L in total. The reaction conditions were the same as described in section 2.2.12. HBV genome equivalence was determined according to the standard curve and positive control in the same PCR plate. The intrahepatic HBV DNA level was shown as HBV genome equivalence per μ g of genomic DNA.

2.2.14 Quantification of intrahepatic HBV RNA

Intrahepatic HBV RNA level was quantified using total RNA sample of each chimeric mouse liver. The extraction of total RNA was described in section 2.2.7. Total RNA was treated with DNase I to remove HBV DNA contamination prior to cDNA synthesis. Reverse transcription was performed using 2 μ g total RNA with a HBV specific primer (HBV reverse primer in Table 2.7) and ThermoScript™ reverse transcriptase as described in section 2.2.10. Besides the water control, a minus RT control which contained all the components except the reverse transcriptase in the reverse transcription reaction preparation was included to confirm the absence of HBV DNA contamination in DNase I treated RNA samples. The generated cDNA was used for HBV qPCR reaction, which included 900nM of each HBV specific primer (2.25 μ L of 10 μ M stock), 250nM of probe (2.5 μ L of 2.5 μ M stock) (Table 2.7), 12.5 μ L of TaqMan universal master mix and 2 μ L of generated cDNA in one well of a 96-well PCR plate, with water to make the reaction volume to 25 μ L in total. The reaction conditions were described in section 2.2.12 including the minus RT control. HBV genome equivalence was determined according to the standard curve and positive control in the same PCR

plate. Additionally, the mRNA level of human HPRT-1 was measured in the same cDNA samples for HBV qPCR. The detailed procedure for human HPRT-1 mRNA quantification is described in section 2.2.15. The intrahepatic HBV RNA levels were presented as HBV genome equivalence relative to expression levels of human HPRT-1.

2.2.15 Analysis of human gene expression by RT-real time PCR

To determine expression levels of genes related to IFN signaling in human hepatocytes, oligonucleotides specifically recognizing human transcripts and not cross-reacting with murine genes, were designed using Primer Express 3.0 (Applied Biosystems) and validated by blasting the primer sequences to the NCBI mouse genome database as well as by performing RT-real-time PCR using intrahepatic total RNA isolated from BALB/c mice treated with poly(I:C) (described in section 2.2.16). These targeted genes are listed in Table 2.7.

Reverse transcription was performed using 2µg total RNA with random hexamer primers and M-MLV RT according to manufacturer's specifications. Specifically, in a 0.2mL PCR tube, 0.15µL of random hexamer primers (3µg/µL stock), 1µL of RNase-free dNTPS (10mM stock), 0.2µL of 10mg/mL RNase-free BSA, 2µL of 0.1M DTT, 0.8µL of RNaseOUT (40U/µL), 1µL of M-MLV RT (200U/µL) and 2µg of total RNA were combined with RNase-free water up to a total volume of 20µL. The sample was mixed gently and loaded in a PCR machine. The reaction started at 22°C for 5 minutes, followed by incubation at 37°C for 1 hour. The M-MLV RT was heat inactivated at 85°C for 15 minutes at the end of reaction.

The resulting cDNA was then used for gene expression realtime PCR assay. Briefly, each reaction includes 900nM of specific primers (0.9 μ L of 10 μ M stocks) for each gene-of-interest and 250nM of specific probe (1 μ L of 2.5 μ M stock) (Table 2.7) and 5 μ L of TaqMan universal master mix mixed in one well of a 96-well PCR plate with water added to a total volume of 8 μ L. cDNA samples (2 μ L) were then added to the well before the PCR plate was sealed. If the gene-of-interest had no probe for detection, 150 μ M of primers (0.3 μ L of 5 μ M stock) and 2x Tagman *Power* SYBR Green PCR Master Mix were used. The real-time PCR was performed in an ABI 7900 Real Time PCR system. Each target was run in duplicate. The reaction conditions were 50°C for two minutes, 95°C for 10 minutes, and 40 times of a PCR cycle (95°C for 15 seconds and 60°C for one minute). For assays with SYBR green, disassociation curves were included in the assay to monitor the specific amplification of resulting PCR products. Transcript levels were normalized relative to the human HPRT-1. For data analysis, the $2^{-\Delta\Delta Ct}$ method was used and mean fold changes in expression were shown relative to the expression of the same gene in total RNA extracted from control mice [289]. The sequences of human specific primers and probes are listed in Table 2.7.

2.2.16 Poly(I:C) treatment in BALB/c mice

In order to ensure the human specificity of the oligos I designed for gene expression RT-PCR assays, four BALB/c mice received one i.v injection of 100 μ g of poly(I:C) dissolved in 50 μ L PBS (2 mice) or 50 μ L of PBS only (2 mice). Mice were sacrificed 4 hours after poly(I:C)/PBS injection. BALB/c mouse

livers were snap-frozen in liquid nitrogen and total RNA was isolated using the same procedure described in section 2.2.7. cDNA was generated using M-MLV RT and random hexamer primers as described in section 2.2.15. Induction of an IFN response in BALB/c mouse livers resulting from poly(I:C) treatment was confirmed by measuring mouse specific IFNs (IFN α 4 and IFN β , listed in Table 2.7) and ISGs (OAS1a and Mx1, listed in Table 2.7) in comparison to PBS treated mice using Taqman realtime PCR (PCR procedure was described in section 2.2.15). Synthesized oligos were considered human specific if no significant similarity was detected by blasting to mouse genome database and no amplification was observed in a Taqman realtime PCR assay using cDNA samples from BALB/c mice treated with poly(I:C) as the template.

2.2.17 Protein gel electrophoresis and detection

One vial of powdered mouse liver tissue processed from snap-frozen liver samples as described in section 2.2.7 was lysed in 0.5mL RIPA buffer (Table 2.6) containing a cocktail of protease inhibitors (Sigma) including 2mM AEBSF, 0.3 μ M Aprotinin, 130 μ M Bestatin, 1mM EDTA, 1 μ M E-64 and 1 μ M Leupeptin. Tissue lysates were incubated on ice for 30 minutes and then centrifuged at 12,000xg for 15 minutes at 4°C, after which protein concentrations in the supernatants were quantified by Pierce™ bicinchoninic acid (BCA) protein assay kit (Thermo Scientific) according to the manufacturer's recommendation.

Equivalent amounts of human protein (15-20 μ g/sample) of each sample,

calculated according to results of human chimerism measurement as described in section 2.2.9, were separated by discontinuous gel electrophoresis (5% stacking gel and 10-15% resolving gels). Stacking gels were prepared by adding acrylamide/bis-acrylamide, to final concentration of 5%, to the stacking gel buffer (Table 2.6). Resolving gels were prepared by combining acrylamide /bisacrylamide, to 10-15%, in the resolving gel buffer (Table 2.6). Mouse liver lysates were mixed with 5x protein sample buffer (Table 2.6) and denatured at 95°C for 10 minutes. Electrophoresis was performed using the Bio-Rad Mini-Protean II system with SDS-PAGE running buffer (Table 2.6) at 80-150 volts.

Once the electrophoresis was completed, the gel was transferred to a dish containing semi-dry transfer buffer (Table 2.6) and soaked for 5 minutes. At the same time, two Whatman 3MM filter pieces and a nitrocellulose membrane (Hybond-ECL) were soaked in semi-dry transfer buffer for 5 minutes. The Western transfer was set up using a semi-dry transfer apparatus (Fischer Brand FB-SDB-2020) where the gel and the membrane were sandwiched between the two filter papers, and the membrane was on the top of the gel, closest to the positive panel of the apparatus. The lid of the apparatus was closed, attached to a power pack (Bio-Rad Model 200/2.0 Power Supply) and run for 1 hour with a limit of 500-mA and a maximum voltage of 29-V.

Following completion of the transfer, the membranes were blocked in PBS-T (Table 2.6) containing 5% (w/v) skim milk powder for at least 1 hour on a rocking device. Membranes were incubated with 10mL primary antibodies diluted at

desired concentration in PBS-T containing 1% (w/v) skim milk powder for 2-3 hours at room temperature or overnight at 4°C. After three washes with PBS-T at room temperature for a total of 1 hour, the membranes were incubated in 10mL secondary antibody diluted at optimal concentrations in PBS-T for 1 hour at room temperature. The membranes were washed three times with PBS-T for a total of 1 hour and then incubated in Supersignal West Pico chemiluminescent substrate (Table 2.5) for 1 minute, after which they were exposed to Rx film in dark. The film was developed using the Kodak M35A XOMAT Processor.

2.2.18 HBV capsid western blot

This method was developed by Dr. William Addison in Dr. L. Tyrell's laboratory. Briefly, chimeric mouse liver tissue was homogenized and lysed in TritonX-100 buffer. Protein concentration of the tissue lysate was quantified by BCA protein assay and 20-30µg of protein was mixed in Orange G loading dye (Table 2.6) without denaturation. Intracellular HBV capsids were separated by electrophoresis the tissue lysate through a 1% agarose gel made with running buffer (Table 2.6) at 85V for about 2 hours. The separated samples were blotted onto a nitrocellulose membrane as for a Southern blot overnight at room temperature. After blocking with 5% skim milk, the membrane was incubated with 10mL of primary antibodies, including rabbit anti-HBcAg antibody (1:10,000 diluted in 1% skim milk in PBS-T) or goat anti-human albumin antibody (1:5,000 diluted in 1% skim milk in PBS-T) as a human protein loading control. The secondary antibodies (1:10,000 diluted in PBS-T), 10mL goat anti-

rabbit conjugated with HRP and 10mL chicken anti-goat HRP, were used for the detection of HBV capsid and human albumin respectively. The membrane was treated with Supersignal West Pico chemiluminescent substrate reagent and exposed to film to visualize the capsid bands. The film was developed using the Kodak M35A XOMAT Processor.

2.2.19 Indirect immunofluorescence microscopy

Frozen liver sections of 4 micron thickness were fixed in freshly made 4% paraformaldehyde for 30 minutes, followed by 5 minutes PBS rinse to remove excess paraformaldehyde. Fixed slides were then permeabilized in PBS containing 0.5% TritonX-100 for 10 minutes and blocked in PBS with 10% normal goat serum for 1 hour. One hundred microliters of a cocktail of 1/100 diluted primary antibodies in PBS-T, including a rabbit monoclonal antibody recognizing human cytokeratin 18 (CK-18) and a mouse monoclonal antibody against human STAT1, was applied to the liver sections and incubated at 4°C overnight in a sealed container. The next day, primary antibodies were detected by 100µL of a secondary antibody cocktail (1/200 diluted in PBS-T), including Alexa Fluor 488-conjugated goat anti-mouse, Fluor 546-conjugated goat anti-rabbit and DAPI for nucleus staining, for 1 hour at room temperature in dark. After 3 exchange of PBS, slides were air dried, mounted with prolong gold mounting medium (Invitrogen) and covered with coverslips. Samples were examined under Leica TCS SP5 confocal microscope. Captured images were processed using LAS AF Lite software.

2.2.20 RNA transfection in HCV infected chimeric mice

This protocol was established for the collaborative project “The HCV PAMP RNA induces innate immune responses that limits HCV infection in chimeric mice” (described in section 5.1 in Chapter 5) with Dr. Michael Gale Jr. laboratory in Seattle, USA. As mentioned in Chapter 1, the HCV 3’ NTR is comprised of three regions: a variable region, a non-structured polyU/UC region, and the terminal X region. The 100-nucleotide polyU/UC region has been found as the HCV PAMP motif that triggers RIG-I-dependent signaling of innate antiviral immunity, whereas the X region of HCV 3’ NTR was shown not a potent PAMP [34]. HCV XRNA and polyU/UC PAMP RNA were generated by Dr. Yueh-Ming Loo in Dr. Michael Gale Jr. laboratory, using the MegaScript *in vitro* transcription kit (Ambion) as described by Saito, *et al* [34]. SCID/bg-Alb/uPA mice, populated with a single hepatocyte donor Hu8085, received a single intravenous injection of 100µL serum (HCV genotype 2b). Infected animals were bled at days 7, 10 and 14 post-infection for confirmation of HCV infection as well as viremia level measurement. On day 11 post infection, HCV viremia positive animals were divided into 3 groups: the first group received an i.p. delivery of 150µg HCV PAMP RNA in total volume of 200µL in PBS with the lipid-based *in vivo* transfection reagent from Altogen Biosystems; the second group of mice were transfected with 150µg XRNA with the same lipid-based *in vivo* transfection reagent in PBS with total volume of 200µL; the third group of animals received 200µL of PBS in lipid-based *in vivo* transfection reagent as a control. Eight hours after final transfection, all three groups of animals were terminated, and the livers

were excised, dissected into small pieces, and then snap frozen in liquid nitrogen for further histological and molecular analyses. For gene expression analyses, uninfected mice that received the same treatments as infected mice were terminated 8 hours after RNA transfection and the livers were removed and sectioned as described in section 2.2.5.

2.2.21 Quantification of miR-27 mRNA levels by RT-PCR

This assay was performed by Ragu Nath Singaravelu in Dr. John Paul Pezacki laboratory for the collaborative project named “HCV infection in chimeric mice induced up-regulation of microRNA-27: a novel mechanism for hepatic steatosis” (described in details in section 5.2 in Chapter 5) with Dr. John Paul Pezacki laboratory in Ottawa, Canada. MiR-27 levels were quantified using the Taqman MicroRNA Assay (Applied Biosystems, Foster City, CA). In brief, 10ng of total RNA was reverse transcribed using the TaqMan MicroRNA Reverse Transcription Kit. MiR-27 levels were analyzed using the Taqman real-time (qRT-PCR) method [290]. Each PCR sample included 1X Universal Taqman PCR Master Mix (Applied Biosystems), 0.2mM TaqMan probes against miR-27a/b (Applied Biosystems), and 1.5mM forward/reverse primers. Sequences of forward and reverse primers of miR-27 are listed in Table 2.7.

2.2.22 Immunofluorescence and Oil Red O Staining of chimeric mouse livers

I established this protocol for the collaborative project “HCV infection in chimeric mice induced up-regulation of microRNA-27: a novel mechanism for

hepatic steatosis” (section 5.2 in Chapter 5) with Dr. John Paul Pezacki laboratory in Ottawa, Canada. Briefly, chimeric mouse liver frozen sections (at 4 μ m thickness) were fixed in 4% freshly made paraformaldehyde for 30 minutes, followed by 5 minutes PBS rinse to remove excess paraformaldehyde. Fixed slides were then permeabilized in PBS containing 0.5% Triton X-100 for 10 minutes and blocked in PBS with 10% normal goat serum for 1 hour at room temperature. The 1/100 diluted primary rabbit monoclonal antibody specifically recognizing human CK-18 was applied to the liver sections and incubated at 4°C overnight. The next day liver sections were incubated in secondary antibody, Alexa Fluor 488-conjugated goat anti-rabbit, together with DAPI, for 1 hour at room temperature in the dark. After 3 washes of PBS, slides were immersed in oil red O (ORO) working solution (freshly prepared in 30% triethyl-phosphate) [291], for 30 minutes in dark, followed by 3 rinses with distilled water. Finally, slides were rinsed in the dark for 10 minutes, air dried, mounted with prolong gold mounting medium, and coverslipped. Samples were examined with a Leica TCS SP5 confocal microscope. ORO staining of lipids was visualized at far-red wavelength: 633nm (excitation spectrum) and 647nm (emission spectrum). Images were processed using LAS AF Lite software.

2.2.23 Statistics

Statistical analysis was performed with Prism software for Mac OS X version 5.0. Majority data were expressed as means \pm standard deviation (SD) or median with range where appropriate. The one-way ANOVA tests (to compare ≥ 3 groups) or

un-paired t tests (to compare 2 groups) were used for nonparametric pair wise comparisons. P values <0.05 were considered significant.

CHAPTER 3

A Study Of Viral Versus Host Factors That Determine The Response To Interferon Alpha Treatment Of HCV Infection In SCID/Beige-Alb/uPA Chimeric Mice

3.1 Rationale

When I began this study, the standard treatment for chronic HCV infection was a combination of pegIFN α and RBV. This combination cleared the infection in a genotype-dependent manner: 45-55% of patients infected with HCV genotypes 1 or 4, in up to approximately 70% of those infected with HCV genotype 3, and 80-90% in patients infected with genotype 2 [160]. However, in about 50% of genotype 1 HCV infected patients, a SVR was not achieved with this therapy since patients failed to clear the virus or relapsed after treatment was stopped. Two HCV NS3/4A protease inhibitors, boceprevir [183, 184] and telaprevir [179-182], were licensed in 2011. They work as DAAs and provide treatment options with improved rates of viral clearance for individuals infected with HCV genotype 1, the most common genotype in North America and Europe. However, problems remain with the application of DAA therapy in ‘real-life’ situations, such as the rapid emergence of drug resistant variants, adverse side effects and additional costs to healthcare budgets. Therefore, the continued use of pegIFN α and RBV will likely remain as a component of HCV treatment regimens for some HCV genotypes for some years to come. Consequently, even in the exciting new era of HCV treatments, understanding the reasons for a lack of response to IFN therapy remains an important question to be addressed.

In the past decade, intensive efforts have been made using clinical data to identify factors that are predictive of interferon responsiveness. Both viral and host factors have been shown to be involved in determining treatment outcome. Among host

factors, besides non-genetic factors (such as age, alcohol, obesity, smoking), upregulation of pre-treatment intrahepatic expression of certain ISGs, such as Viperin/CIG5, ISG15 and interferon-induced protein with tetratricopeptide repeats 1 (IFIT1), has been shown to be associated with poor-response to IFN therapy [161, 162]. In addition, polymorphisms, especially the alleles of two SNPs near the IL28B coding region, rs12979860 and rs8099917, have improved our ability to predict the likelihood of a SVR to IFN therapy [91-95]. As for viral factors, HCV genotypes are well accepted as the strongest predictor of IFN response. Rapid reduction of serum HCV RNA level during the first 4 weeks of therapy is also strongly predictive of a positive SVR response. In addition, amino acid variation in the IFN-sensitivity-determining region within the NS5A protein [172, 173] as well as at aa 70 or 91 in the HCV core protein [174, 175] are predictors of SVR and NVR. Early change of HCV quasispecies, e.g. the degree of quasispecies' complexity and diversity of hypervariable region 1, is another marker, which is closely correlated with the responsiveness to interferon therapy in CHC patients [176-178].

Assaying these host and viral factors in clinical situations is complex because each patient presents with a unique set of viral and host components that may interfere their response to IFN therapy. The first non-primate small animal model to support HCV infection, the SCID/bg-Alb/uPA chimeric mouse model, was developed at the University of Alberta in 2001 [277]. Taking advantage of the immunodeficiency of this animal (SCID/bg) and the sub-acute liver failure induced by the homozygous expression of the transgene (Alb/uPA), newborn

pups of this SCID/bg-Alb/uPA transgenic mouse can be transplanted with freshly isolated or cryopreserved human hepatocytes by intrasplenic injection (refer to section 2.2.1 in Chapter 2). The resulting chimeric mouse livers are successfully populated with human hepatocytes, and if there is sufficient chimerism (human albumin level in mouse serum is $>5,000\mu\text{g/mL}$), the animals become susceptible to long-term infection by HCV.

One of the unique opportunities offered by this system is the ability to study both viral and host factors in the response of HCV to IFN therapy. Infections by different viruses, with different genotypes or derived from different HCV infected patients, can be studied in animals populated with hepatocytes from a single donor. This allowed me to study some of the viral factors in response to IFN therapy in an identical human hepatocyte background. It could not happen or be reproduced in any clinical setting and could not be achieved in cultured cells as very few HCV viruses can be grown in cell cultures. Up to date, only JFH-1 (genotype 2a HCV), H77 (genotype 1a) and Con1 (genotype 1b) can be grown in Huh-7 and its derived cells. Conversely, a single strain of virus can be used to infect the chimeric mice transplanted with hepatocytes from different donors. This allows me to study the response to IFN in the setting of an identical virus in mice with various host backgrounds. The control of these variables allows me to dissect the contributions of both host and viral factors to the responsiveness of HCV infection to IFN α treatment.

3.2 Results

3.2.1 Role of HCV viral factors in determining IFN α treatment outcome

Two HCV strains were selected of different genotypes (Table 3.1), genotype 1a and genotype 2b, from two chronic hepatitis C patients. One HCV strain, the genotype (gt) 2b, responded to pegIFN α /RBV therapy, whereas the second HCV strain, HCV gt1a, was from a known null-responder.

In order to exclude the host variable, all chimeric mice in this part of the study were populated with human hepatocytes derived from a single donor, Hu8063 (CellDirect, USA). First, I examined the ability of the two viral strains to infect the chimeric mice to rule out any possibility that the difference in IFN response would be attributed to differences in the ability to sustain a chronic infection in these mice by the two HCV strains. Three or four mice were infected by intravenous injection of 100 μ L serum containing $>10^5$ genome equivalence of each strain followed for 7 weeks during which the serum viremia of each mouse was monitored. For both HCV strains, viral serum titer reached stable levels 2-3 weeks post infection (p.i) and remained at relatively constant levels for 7 weeks (Figure 3.1).

Table 3.1 Two HCV isolates with distinct sensitivities to IFN therapy.

HCV strains	genotype	response in patient to IFN therapy
HCVgt1a	1a	Null responder
HCVgt2b	2b	SVR

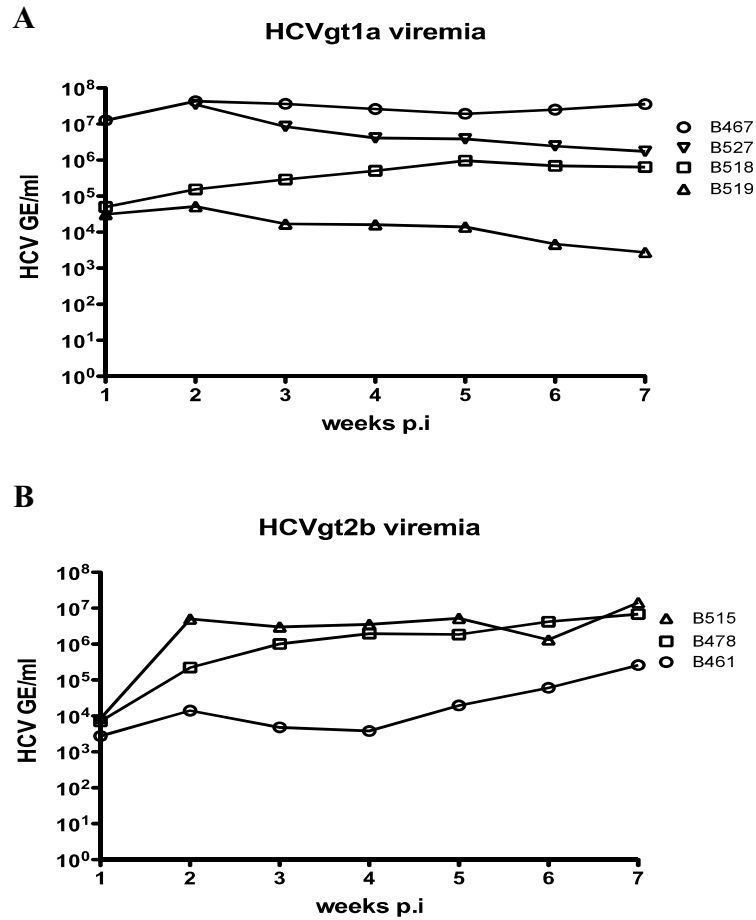


Figure 3.1 Sustained viremia of both HCV strains in chimeric mice populated with a single hepatocyte donor.

Age-matched mice produced with a single hepatocyte donor Hu8063 were infected with two HCV strains through intravenous injection: (A) HCVgt1a strain in 4 mice, (B) HCVgt2b strain in 3 mice. Animals were bled weekly for 7 weeks after inoculation and viremia titer was measured by RT-qPCR. Each sample was quantified in duplicate.

Following confirmation of stable and comparable levels of viremia with both HCV strains in chimeric mice, I next examined the response of HCV in chimeric mice infected with each of HCV strains to exogenous IFN α treatment. Two groups of chimeric mice were infected, one group with HCVgt1a strain (9 mice) and another one with HCVgt2b strain (8 mice) for 5 weeks to reach stable viremia. Then each group was divided in two subgroups with one subgroup receiving exogenous IFN α at 1,350IU/gram/day for 2 weeks and a control subgroup receiving 30 μ L of saline. Viremia levels were measured during the course of IFN α treatment. Data in Figure 3.2 show that the two HCV strains responded to IFN α treatment differently. Strain HCVgt1a had a minimal response to two weeks of IFN α treatment. The mice in this group showed that the serum viral level declined by less than 1 log during therapy (Figure 3.2 A and E). On the other hand, chimeric mice infected with strain HCVgt2b showed more than 3 log decline of serum viral RNA levels with 2 weeks IFN α treatment (Figure 3.2 C and E). The viremia of one mouse became undetectable with this short course of therapy. To rule out the possibility that the viremia change was due to a dramatic change in the human hepatocyte numbers in the chimeric liver, the level of human albumin in serum of each animal, a marker of human chimerism, was measured by ELISA. During the course of infection and IFN α treatment, there was no significant decrease in the human content of the chimeric livers based on serum albumin levels (Figure 3.2 B and D). At the end of the experiment, HCV RNA copy numbers were measured in chimeric mouse livers. Mirroring the serum viremia results (Figure 3.2E), the HCVgt2b strain showed a significant decrease

in intrahepatic HCV levels upon IFN α treatment, whereas the livers of chimeric mice infected with HCVgt1a did not show a significant decrease of HCV RNA with IFN treatment (Figure 3.2F).

To further address the significant effect of viral factors on HCV response to IFN therapy, we infected chimeric mice through intravenous injection of more HCV isolates from patients with various response outcomes to pegIFN and RBV treatment. In order to gain a closer comparison between chimeric mice and patients, pegIFN α -2b rather than IFN α was used in this experiment. We did not use RBV because of its toxic effect on chimeric mice. Mice stably infected with HCV isolates were treated with a weekly s.c injection of pegIFN (875ng/mouse) for 4 weeks followed by two-week treatment-free period before the mice were sacrificed. The viremia level changes of each mouse were monitored. Our result in Table 3.2 showed a good correlation of viral response to pegIFN treatment in chimeric mice with the response observed in patients, supporting the key role of viral factors in predicting the response to IFN therapy.

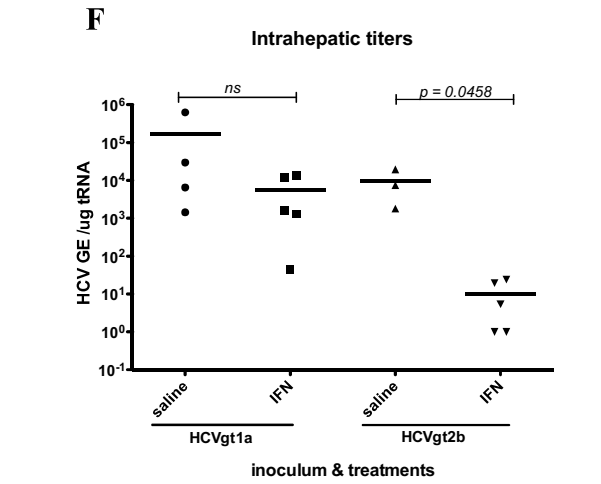
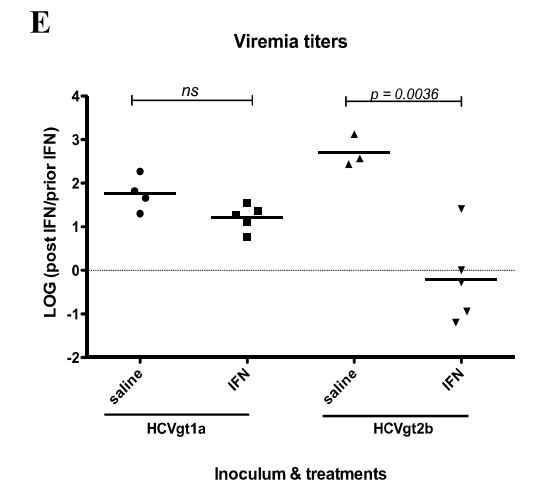
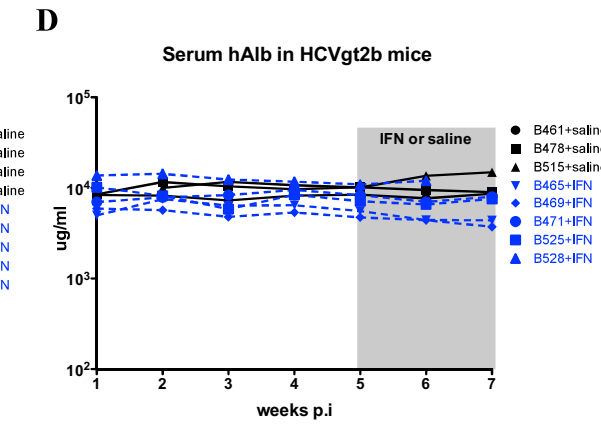
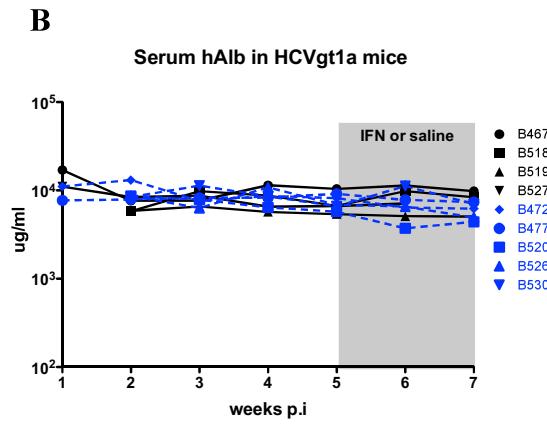
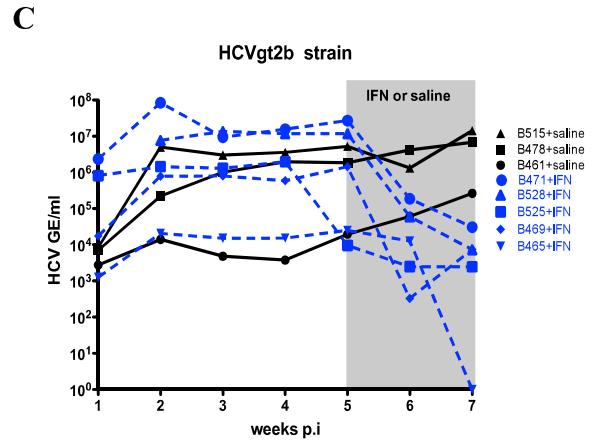
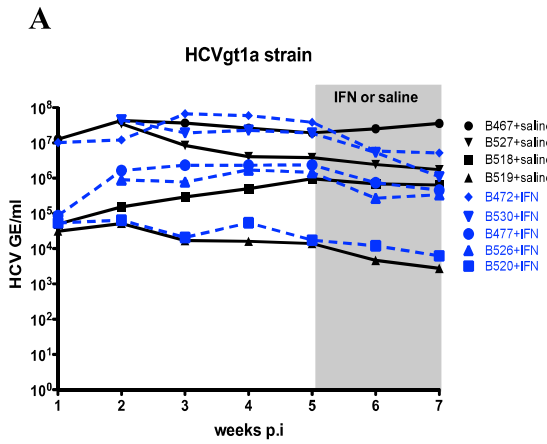


Figure 3.2 Response of the two HCV strains to exogenous IFN α treatment in chimeric mice populated with a single hepatocyte donor.

Chimeric mice, produced with a single hepatocyte donor Hu8063, were infected with 2 HCV strains for 5 weeks. Exogenous IFN α -2b was then injected subcutaneously daily at 1,350 IU/gram for 14 days. Control animals were treated with saline. Mice were bled weekly for viremia and serum human albumin measurements. Six hours after the last IFN α injection, mice were terminated and intrahepatic viral load was measured. Mice treated with saline are presented in black solid lines and mice treated with IFN α are presented in blue dashed lines in Figures A-D. The period of IFN α /saline treatment is shaded.

(A) HCVgt1a viremia titer over the course of infection and IFN α treatment. Each line represents a single mouse.

(B) Human albumin level in the same mouse serum samples assayed for HCVgt1a RNA in (A).

(C) HCVgt2b viremia titer over the course of infection and IFN α treatment.

(D) Serum human albumin levels in mouse serum samples assayed for HCV gt2b RNA in (C).

(E) Serum HCV RNA level comparison between saline-treated and IFN treated mouse groups at week 7. *P*-values were calculated by unpaired t-test. Ns= not significant.

(F) Comparison of intrahepatic HCV RNA levels in the experimental groups at week 7. *P*-values were calculated by unpaired t-test. Ns= not significant.

Table 3.2 Correlation of HCV response to pegIFN treatment in chimeric mice with the response of patients to the pegIFN and RBV therapy.

HCV isolates	HCV genotype	Mouse ID	Hepatocyte donor	Mouse response to pegIFN	Patient response to pegIFN+RBV	SVR in patient?
UA110	1a	B1379	Hu8063	NR	NR	No
		B1369	Hu8063	NR		
UA164	1	B1242	Hu8085	NR	NR	No
		B1270		NR		
UA174	1a	B1305	Hu8085	NR	NR	No
UA176	1	B1310	Hu8085	Partial	NR	No
UA131	2	B1268	Hu8085	R	R	Yes
UA141	1a	B1478	FLO	R	R	Side effects
		B1486	FLO	R		No
UA143	1a	B1485	FLO	R	R	Yes
UA159	5a	B1483	FLO	R	R	Yes
UA166	2	B1490	Hu8085	R	R	Yes
		B1488	Hu8085	R		
UA167	1a	B1464	Hu8085	R	Partial R	No
		B1491	Hu8085	R		
UA177	3a	B1482	FLO	R	R	Yes
UA178	1a	B1462	FLO	R	R	Yes
		B1471	FLO	R		

R-Responder, NR-Non-responder

Note: The experiments presented in Table 3.2 were performed by Ms. Michelle Kobewka, a 499 project student in Dr. L. Tyrrell's laboratory, under my supervision.

3.2.2 Role of viral interference with host IFN signaling in determining the sensitivity of HCV to exogenous IFN α treatment

The two HCV strains differ in their response to exogenous IFN α treatment in chimeric mice produced with identical donor cells. It is known that HCV infection can block the IFN innate response in HCV infected cells *in vitro* (reviewed in reference [292]). I thus hypothesized that the different sensitivities of the two HCV strains to IFN α was possibly caused by differences in each strain's ability to interfere with the IFN α signaling, e.g the JAK-STAT pathway, which transduces exogenous IFN α signals from the IFN receptors on the cell surface to the cell's transcription apparatus. The same set of mice infected with both HCV strains and treated with IFN α for two weeks as shown in Figure 3.2 was sacrificed 6 hours after the last IFN α injection and chimeric mouse livers were harvested for analysis. Activation of JAK-STAT pathway was assayed by measuring the changes in expression levels of a number of human-specific intrahepatic ISGs using RT- realtime PCR. The changes in IFN-induced ISGs were first compared to age-matched, donor-matched mice but uninfected and treated with saline (Figure 3.3). Significant upregulation of most of the ISGs tested was observed in mice infected with either of the viral strains and treated with exogenous IFN α (Figure 3.3), indicating that the mouse model used in this study can respond to IFN α treatment. This upregulation of ISGs in response to IFN treatment was observed in both sets of chimeric mice infected with the two HCV stains, however, the upregulated ISGs induced a significant drop in HCV viremia only in animals infected with the HCVgt2b strain (Figure 3.2E).

In order to compare the suppressive effect on the JAK-STAT pathway by the two HCV strains, I measured ISG expression levels in chimeric mice infected with each of these HCV strains and compared the levels to ISG expression in uninfected control chimeric mice treated with IFN α in Figure 3.4. My hypothesis was that differences in sensitivity to IFN α treatment were determined by differences in the ability of HCV strains to interfere with the JAK-STAT pathway. If this was correct, I would expect to see more inhibition of ISG expression in mice infected with the IFN nonresponsive HCVgt1a strain than the inhibition of ISGs in mice infected with the IFN responsive HCVgt2b strain. Surprisingly, data in Figure 3.4B show that the ISG expression in response to exogenous IFN treatment in chimeric mice infected with the HCVgt2b strain was not significantly different than the ISG expression in mice infected with the HCVgt1a strain. In fact, there were more ISGs with significantly lower levels of mRNA in animals infected with HCVgt2b in comparison to the control mice than in mice infected with HCVgt1a, which was opposite to what I expected. This result indicates that intrinsic viral factors rather than viral interference with host IFN signaling are the critical determinant of the response to IFN in HCV infection in this chimeric mouse model.

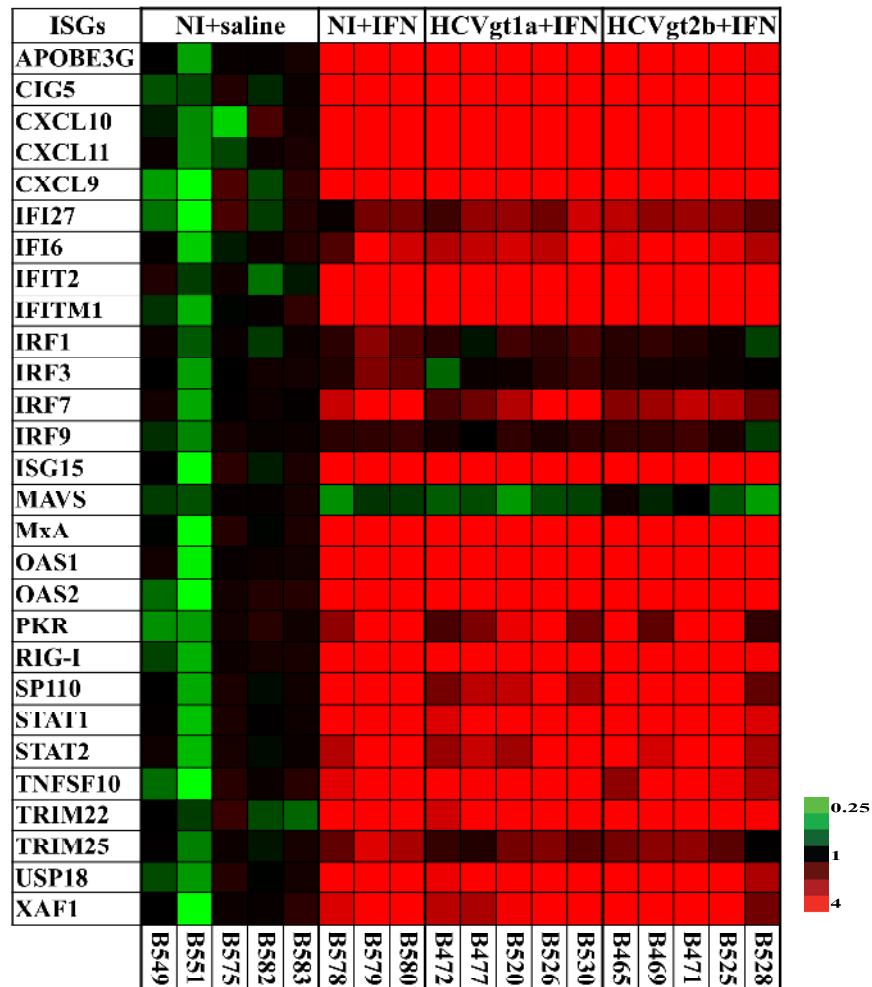
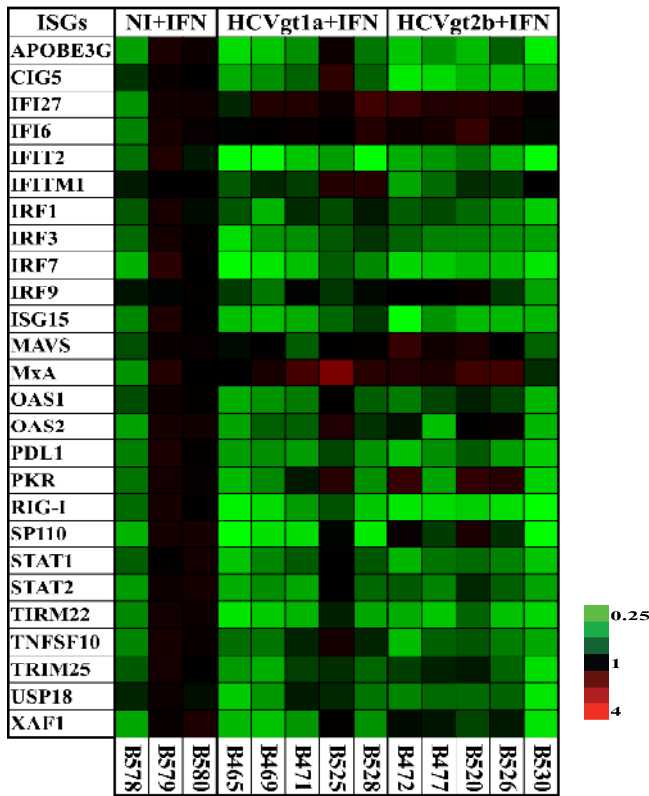


Figure 3.3 ISG expression upon exogenous IFN α treatment in HCV infected mouse livers in comparison to uninfected, saline-treated controls.

Total RNA isolated from IFN α -treated, uninfected mice or mice infected with HCV were examined for intrahepatic expression of ISGs by RT-realtime PCR. All mice were populated with a single hepatocyte donor, Hu8063. Results are shown as fold change relative to the ISG expression in uninfected, saline-treated controls. Each column represents a single mouse in the respective treatment group as indicated at the bottom of the heatmap. Increased and decreased expression of specific genes compared to the control is shown by red (Fold >1 - \geq 4) and green (Fold <1 - \leq 0.25), respectively, black indicates no change (Fold =1).

A



B

ISGs	HCV gt1a + IFN			HCV gt2b + IFN		
	mean fold	p-value	p-value summary	mean fold	p-value	p-value summary
APOBE3G	0.7	0.22	ns	0.5	0.05	*
CIG5	0.8	0.08	ns	0.4	0.02	*
IFI27	1.4	0.23	ns	1.5	0.10	ns
IFI6	1.2	0.54	ns	1.3	0.25	ns
IFIT2	0.3	0.01	**	0.5	0.03	*
IFITM1	1.1	0.76	ns	0.8	0.13	ns
IRF1	0.8	0.18	ns	0.7	0.05	*
IRF3	0.6	0.06	ns	0.6	0.02	*
IRF7	0.5	0.08	ns	0.4	0.04	*
IRF9	0.9	0.16	ns	0.9	0.53	ns
ISG15	0.6	0.07	ns	0.5	0.02	*
MAVS	1.0	0.81	ns	1.2	0.47	ns
MxA	1.7	0.16	ns	1.5	0.19	ns
OAS1	0.7	0.08	ns	0.7	0.08	ns
OAS2	0.9	0.56	ns	0.8	0.43	ns
PKR	0.8	0.50	ns	1.2	0.77	ns
RIG-I	0.5	0.02	*	0.3	0.00	**
SP110	0.5	0.08	ns	1.0	0.68	ns
STAT1	0.7	0.13	ns	0.6	0.02	*
STAT2	0.7	0.15	ns	0.7	0.15	ns
TNFSF10	1.0	0.58	ns	0.7	0.06	ns
TRIM22	0.5	0.05	ns	0.5	0.02	*
TRIM25	0.7	0.07	ns	0.8	0.19	ns
USP18	0.7	0.07	ns	0.6	0.01	*
XAF1	0.7	0.17	ns	0.9	0.43	ns

Figure 3.4 Comparison of the effects of viral interference on ISG expression between the two HCV strains in chimeric mice treated with IFN α .

ISG expression data of IFN-treated animals presented in Figure 3.3 were reanalyzed. The uninfected, IFN α treated animal controls were set as the baseline for comparison. The difference between expression levels of ISGs in uninfected IFN-treated mice and in mice infected with either HCVgt1a or HCVgt2b treated with IFN was analyzed. Each column in the heat map (A) represents a biological repeat in each group. *P*-values in Figure B were calculated by unpaired t-test. Significantly ($p < 0.05$) upregulated and downregulated expression of ISGs in Figure B is indicated by highlighting the tables in red and green respectively. No highlighting shows no significant difference in comparison to the uninfected (NI), IFN-treated control.

3.2.3 Effect of host pre-treatment ISG expression level on response to IFN α treatment

In chronically infected HCV patients, high ISG expression before therapy begins is usually associated with poor response to pegIFN α /RBV treatment. Conversely, ISG expression in liver biopsies of SVR patients is usually comparable to that of healthy adults before treatment [161, 162]. In light of these findings, I studied pre-treatment ISG expression in mice infected by IFN nonresponsive and responsive HCV strains (Table 3.1) in donor-matched chimeric mice.

The uninfected (NI) animals and chimeric mice infected with the two HCV strains without the treatment of IFN α in experiment of Figure 3.1 were euthanized and chimeric liver tissues were collected. The mRNA levels of type I IFNs (IFN α 1 and IFN β), type III IFNs (IFN λ 1-3) and ISGs were measured in mice infected with the two HCV strains using RT-qPCR and compared to the mRNA levels of the same genes in uninfected chimeric mice. I found that there was no significant upregulation of endogenous IFN (Figure 3.5A) or ISG (Figure 3.5B) expression in the liver of donor-matched chimeric mice chronically infected with the two HCV strains in comparison to the uninfected controls. This result indicated that without IFN treatment, there was no IFN response present during the chronic phase of HCV infection in this *in vivo* chimeric mouse model, a result consistent with the findings in tissue culture systems using an infectious HCV virus, JFH-1 [194, 293].

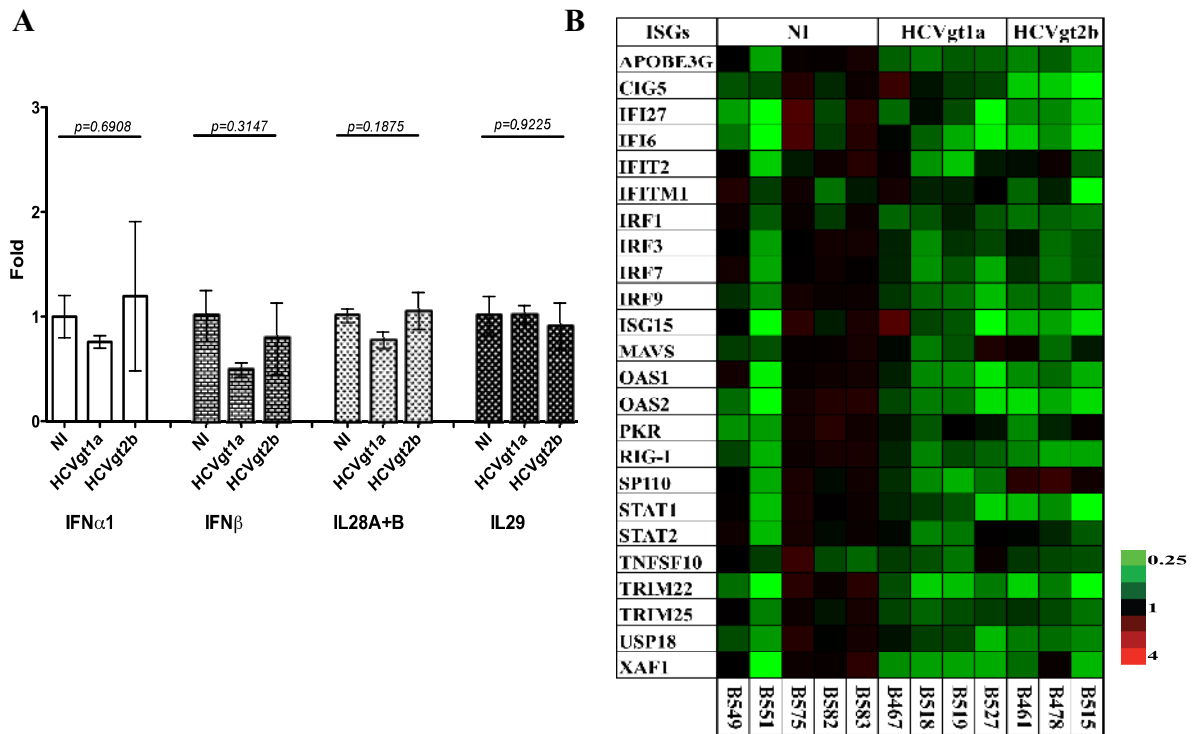


Figure 3.5 Endogenous IFN or ISG expression in chimeric mice (Hu8063) chronically infected with the two HCV strains.

Mice produced with hepatocyte donor Hu8063 were infected with either HCVgt1a or HCVgt2b as shown in Figure 3.1. Seven weeks p.i, the mice were sacrificed. Total RNA extracted from liver tissue of each animal was subjected to RT-qPCR. The expression levels of each human specific endogenous IFN genes (A) and ISGs (B) relative to a house-keeping gene HPRT-1 was determined using the $2^{-\Delta\Delta C_t}$ method. In uninfected donor-matched animals, the mean value of each gene mRNA level was normalized to 1. Data in Figure A were indicated as mean \pm the standard error of the mean (SEM); n = 3-5. P-values were determined by one-way ANOVA calculation. In Figure B, each column represents an experimental mouse whose ID was indicated at the bottom of the map. Increased and decreased expression of specific genes compared to the uninfected control is shown by red (Fold >1 - ≥ 4) and green (Fold <1 - ≤ 0.25), respectively, whereas black indicates no change (Fold =1).

3.2.4 Host IL28B polymorphisms in determining IFN treatment outcome in chimeric mice infected with HCV

Polymorphism of 2 SNPs, rs12979860 and rs8099917, upstream of the IL28B coding region is the best characterized host factors predictive of responses to IFN treatment in chronic HCV infection so far. It has been recently reported in a number of studies published almost simultaneously [91-95]. At SNP rs12979860, CC is considered the responder genotype, whereas CT and TT are poor-responder genotypes [92, 94]. At SNP rs8099917, TT is the responder genotype and GG and GT are the poor-responder genotypes [91, 92].

The experiments described in section 3.2.1 as shown in Figure 3.2 were done in mice transplanted with hepatocytes donor Hu8063, which has responder genotypes at both IL28B SNPs (Table 3.3). To investigate the impact of host IL28B polymorphisms on outcome of IFN treatment of HCV infection in the chimeric mouse model, I produced chimeric mice populated with 2 other hepatocyte donors, Hu4109 (CellDirect, USA) and FLO (BioreclamationIVT, USA), carrying poor-responder genotypes of IL28B SNPs as listed in Table 3.3. Chimeric mice produced with the different hepatocyte donors were infected with the same two HCV strains differing in IFN sensitivity (Table 3.1), followed by IFN α treatment at 1,350 IU/gram/day for 2 weeks. HCV viremia was quantified by RT-qPCR and compared between saline-treated and IFN-treated groups. If the IL28B SNPs were a critical determinant of the outcome of IFN therapy in these chimeric mice, I hypothesized that the decline in viremia would be rapid in mice

with the responder hepatocyte donor Hu8063 (rs12979860 CC and rs8099917 TT) and a slower decrease or no change of HCV titers in chimeric mice with in the poor-responder hepatocyte donors Hu4109 (rs12979860 TT and rs8099917 GG) or FLO (rs12979860 CT and rs8099917 TG) in response to exogenous IFN α treatment. However, this hypothesis was not supported by my results, which showed that the IFN-nonresponsive HCVgt1a strain remained nonresponsive to IFN treatment in chimeric mice produced with either IL28B responder (Figure 3.2 A and E) or poor-responder (Figure 3.6 A and C) genotype hepatocytes. The IFN-sensitive strain HCVgt2b had similar sensitivities in both sets of chimeric mice produced with IL28B poor-responder genotype hepatocytes (Figure 3.6 B and D). This response was as good or better than the response of this HCVgt2b strain in chimeric mice produced with hepatocytes of IL28B responder genotype as shown in Figure 3.2 C and E. Surprisingly, the viremia decline of the IFN-sensitive HCV strain was more rapid and more profound in chimeric mice populated with the poor-responder Hu4109 and FLO hepatocytes than in chimeric mice produced with responder Hu8063 hepatocytes as illustrated in Figure 3.7. These results suggest that viral factors are more important determinant of a response to IFN therapy than the SNPs of IL28B in hepatocytes in HCV infected chimeric mice.

Table 3.3 Three lines of chimeric mice populated with three different human hepatocyte donors with distinct IL28B SNPs.

donors	rs12979860	rs8099917	genotype
Hu8063	CC	TT	responder
Hu4109	TT	GG	non-responder
FLO	CT	TG	non-responder

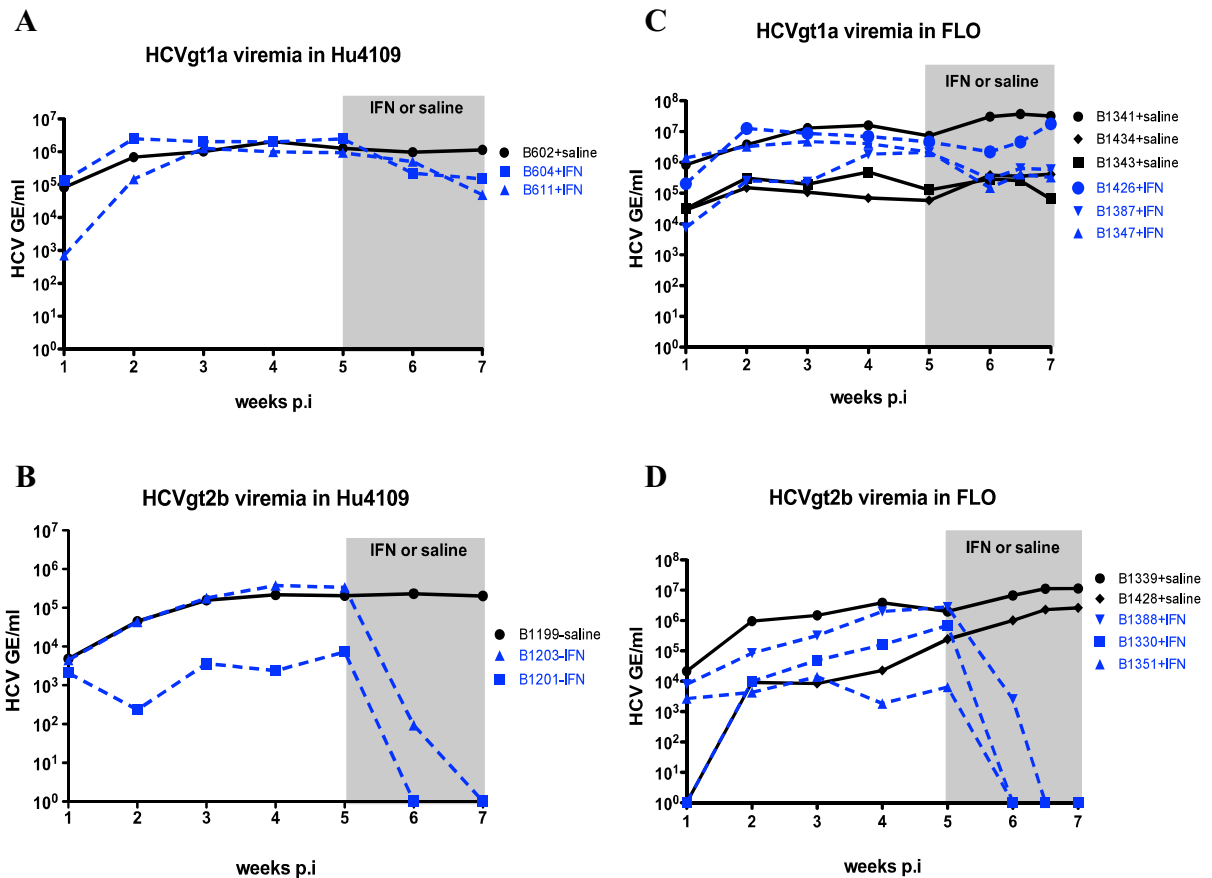


Figure 3.6 Effect of the non-responder genotypes of IL28B SNPs on response to IFN treatment in the two HCV strains.

Animals populated with two hepatocyte donors, Hu4109 (A+B) and FLO (C+D), were infected with HCVgt1a (A+C) or HCVgt2b (B+D). Exogenous IFN α -2b treatment was initiated subcutaneously daily for 14 days at 5 weeks post infection. Control animals received saline at the same schedule. Mice were bled weekly for viremia measurements. Mice treated with saline are presented in black solid lines and animals with IFN α are in blue dashed lines. The period of IFN α /saline treatment is shaded.

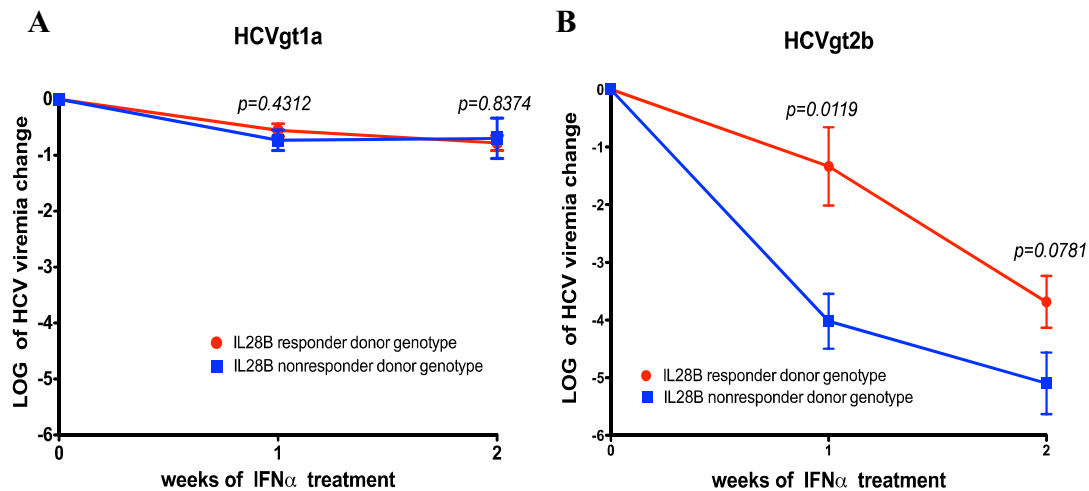


Figure 3.7 Effect of host IL28B SNPs on HCV sensitivity to IFN α treatment in the chimeric mouse model.

The rate of reduction of viremia in response to exogenous IFN treatment in chimeric mice produced with different hepatocyte donors was examined. Three hepatocyte donors with different IL28B SNPs were divided into 2 groups; responder donor genotype (Hu8063) *versus* nonresponsive donor genotypes (combined with data of Hu4109 and FLO). The two HCV strains with different sensitivities to IFN treatment were used to infect chimeric mice populated with different hepatocyte donors: (A) IFN nonresponsive strain HCVgt1a in chimeric mice produced with IL28B responder *versus* nonresponder genotype hepatocytes; (B) IFN sensitive strain HCVgt2b in chimeric mice produced with IL28B responder *versus* nonresponder genotype hepatocytes. Viral titer reduction at each time point was calculated on the basis of 4-5 mice. Error bars represent standard error of the mean. *P*-values were calculated by unpaired t-test.

3.3 Discussion

Less than 50% of patients infected with genotype 1 HCV response to pegIFN α and RBV combination therapy. It is important to understand the basis of this lack of response to overcome it or to identify factors predictive of patient response to the treatment. Clinical evidence shows that some combination of host and viral factors results in response or nonresponse to therapy.

Among viral factors responsible for non-response to IFN treatments, HCV genotype is the strongest predictor [165-167]. In my studies, I used two HCV strains belonging to different genotypes, HCV gt1a from a null responder and HCV gt2b from a SVR patient. When these two strains infected chimeric mice with the same hepatocyte background, I observed that each viral strain retained the same IFN sensitivity as it displayed in the patient from whom the virus was derived, suggesting an important role of viral factors in determining IFN therapy treatment outcomes. To further demonstrate the critical role of viral factors, more HCV clinical isolates from patients with variable treatment results were used to infect chimeric mice and pegIFN was administered for 4 weeks. We found that although the patient hepatocyte background was not possible to replicate in the chimeric mice, the response of each HCV isolate to IFN therapy in patients could be correlated in the HCV-infected chimeric mice treated with IFN. This indicates that viral factors are likely more dominant factors determining response outcomes to IFN treatment. It is also worth noting that in our results in the chimeric mice, HCV strains of the same genotype responded differently to pegIFN treatment

(Table 3.2), for example, eight genotype 1 HCV strains were used in our study, four strains responded and four were non-responsive to pegIFN treatment. This correlated well with the history of treatment of these viruses and their response in patients treated with pegIFN and RBV. This result indicates that although HCV genotype is very important, there are intrinsic viral factors that have a profound effect on the response to IFN treatment.

A known characteristic of HCV viruses is their significant genetic diversity, resulting from the lack of proofreading activity in RNA-dependent RNA polymerase and high level of viral replication during HCV infection. It is reasonable to assume that HCV sensitivity to IFN treatment is affected by the generation of escape mutants through selection pressure during IFN-based therapy treatment. This leads to the selection of a viral population/mutants resistant to IFN becoming dominant. Indeed, certain amino acid sequence variations in some regions of HCV genome have been associated with IFN treatment outcomes. For example, substitutions of R70Q and/or L91M in the core region of HCV genome are found to be common in null-responders, especially in patients of HCV genotype 1b [174, 175]. Amino acid variations in the IFN-sensitivity-determining region (ISDR) [173, 294-296], the interferon/RBV-resistance-determining region (IRRDR) [297], and the PKR binding domain (PKRBD) [298-301] within the NS5A protein are predictors of SVR. In addition, with the introduction of ultra-deep sequencing technology, identification of rare minority mutants among the diverse and complex HCV genome populations in a patient, i.e. quasispecies, is feasible. Evidence has shown HCV strains with an inherent resistance to IFN exist

prior to IFN treatment in patients who subsequently experienced a viral breakthrough or relapse on IFN therapy [302, 303]. There are also studies showing that early change of HCV quasispecies, e.g. decreases in the degree of quasispecies' complexity and diversity of HVR1 located in the putative HCV E2 region during the initial few weeks of therapy, is closely correlated with the responsiveness to interferon therapy in CHC patients, especially patients infected with HCV genotype 1b [176-178].

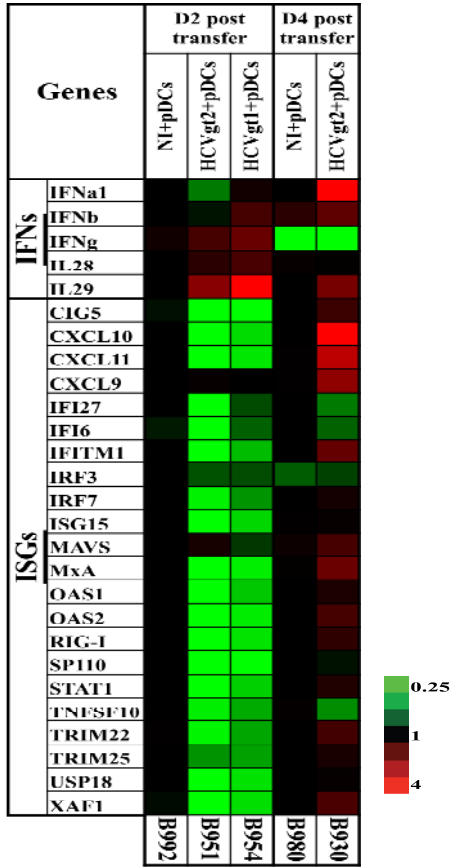
The data about the molecular mechanism underlying HCV sensitivity to IFN α therapy are very limited, but evidence that HCV antagonizes the host IFN response pathway suggests the hypothesis that the lack of response of the non-responder HCV strains to IFN therapy may result from their more effective suppression of the host JAK-STAT pathway. I tested this idea by measuring ISG transcription levels in infected hepatocytes after IFN treatment. Surprisingly, my results showed that mice infected with the IFN-nonresponsive HCV strain had no lower mRNA level of ISG than the ISG expression in mice infected with the IFN-sensitive strain, suggesting that both strains had minimal effects on the IFN response pathway in the chimeric mouse model. Thus, HCV sensitivity to IFN α therapy is not critically associated with viral interference with host IFN signaling downstream of IFN receptors in this mouse model.

In terms of host factors affecting IFN therapy treatment outcomes, two factors were examined in the present study; liver ISG expression prior to IFN therapy and the hepatocyte donor SNPs at two IL28B loci.

Gene expression analyses in HCV patient liver biopsies have been assessed by real-time PCR and microarray studies. Pre-treatment gene expression patterns in responders and non-responders were compared in a few studies [161, 162]. These authors found that up-regulation of a subset of ISGs before treatment was strongly associated with nonresponse to exogenous IFN therapy. Liver biopsy samples from the patients contain mixtures of several cell types besides hepatocytes. The clinical data thus represent the IFN response from the mixture of cell types residing within the liver. In the chimeric mouse livers, human hepatocytes are the primary human cell type present. My results showed that there was no significant upregulation of human endogenous type I and III IFNs or ISGs in response to long-term infection by either of the two HCV strains in chimeric mice. This observation suggested that the upregulation of ISGs seen in patient liver biopsy studies could be the result of ISG expression in other cell types rather than in hepatocytes or the result of direct or indirect interactions between hepatocytes and other cell types. In fact, the finding that pDCs can sense HCV infected Huh-7.5 cells and produce large amount of type I and type III IFNs upon recognition of exosomal transfer of HCV RNA from neighboring hepatocytes provides supporting evidence for the latter idea [216, 217, 304]. In order to test whether human pDCs are responsible for the upregulated ISGs in the liver of CHC patients, I performed a pilot study of adoptive transferring unstimulated human pDCs isolated from healthy volunteers into chimeric mice chronically infected with HCV. Briefly, five chimeric mice were produced with the same hepatocyte donor Hu8085. Three mice were chronically infected (8 weeks) with two clinical

isolated HCV viruses listed in Table 3.1; two mice infected with HCVgt2b, one mouse infected with HCVgt1a, and the rest two mice were left uninfected as controls. All mice received a single i.p injection of 4×10^5 viable unstimulated pDCs purified from healthy adults. One mouse of each group was euthanized 2 days after pDC transfer and the remaining mice were euthanized 4 days after transfer. Chimeric mouse serum and liver samples were collected. HCV viremia titer and expression of human specific IFNs and ISGs were measured by RT-qPCR as described previously. As illustrated in Figure 3.8A, my preliminary data showed that induction of some IFNs, such as IFN β and IFN λ s, was observed as early as 2 days after pDC transfer, whereas at day 4 post transfer (p.t), more IFNs and ISGs were upregulated in HCV-infected chimeric mice in comparison to the uninfected mice. In addition, a decline of HCV viremia was observed in all HCV-infected mice receiving pDCs over a short 2-day or 4-day experiment (Figure 3.8B). These preliminary results suggested that the cross-talk between HCV-infected hepatocytes and human pDCs led to an antiviral IFN response.

A



B

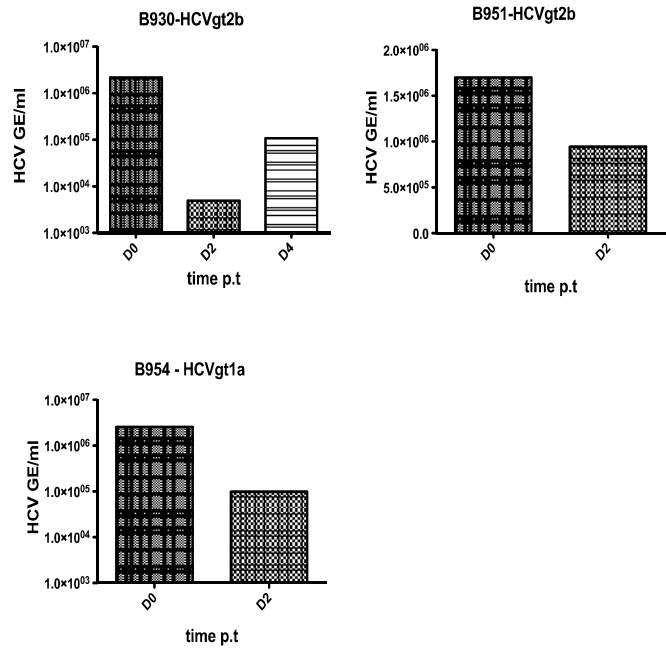


Figure 3.8 Preliminary data of adoptive transfer of purified human pDCs into chimeric mice infected with HCV.

(A) Expression of human IFNs and ISGs in chimeric mouse liver receiving pDC transfer in comparison to uninfected (NI) mice receiving pDC transfer. Each column in the heatmap represents a single mouse. Increased and decreased expression of specific genes compared to the control is shown by red (Fold >1 - ≥ 4) and green (Fold <1 - ≤ 0.25), respectively, whereas black indicates no change (Fold =1).

(B) HCV viremia change before and after pDC transfer. Each plot represents a single mouse. The top two mice were infected with HCVgt2b strain and the bottom one was infected with HCVgt1a strain.

In line with the pDC results, a recent study evaluated the acute response to pegIFN α *in vivo* after the first 24 hours of treatment in patients with HCV genotype 1 infection using liver biopsy samples and modeled this response *in vitro* [305]. Their results suggested that Kupffer cells, the residing macrophages in the liver, were a possible source of hepatic IFN in CHC patient through local exposure to HCV and that constant exposure of surrounding hepatocytes to local IFN β produced by Kupffer cells may drive a state of pretreatment tolerance to ISG function in these hepatocytes, which likely mitigated the cellular response to IFN, thus attenuating IFN actions and reducing the efficacy of therapy. Studies by another group also investigated the cell-type-specific expression pattern of certain ISGs among CHC patients with different response outcomes to IFN therapy [306, 307]. By staining MxA or ISG15 protein in different cell types in patient liver biopsy tissues, the authors discovered that the levels of MxA or ISG15 immunostaining in hepatic macrophages correlated inversely with those of hepatocytes. A strong MxA or ISG15 cell staining in macrophages is characteristic of treatment responders, whereas strong MxA or ISG15 expression in hepatocytes is characteristic of nonresponders. Therefore, it has become clear that tissue- and cell-specific response compartmentalization is important to the response to IFN therapy among patients with HCV.

On the other hand, I found that no significant ISG upregulation induced during long-term HCV infection in chimeric mice, which was unexpected as we had previously observed an ISG response in HCV infected chimeric mice [284]. It was difficult to understand the differences in these studies. However, I believe

there were two important factors. First, the production of successful human hepatocyte engraftment in the chimeric mice became more difficult in our lab over time. A key factor in this problem was that although we followed the detection of the SCID trait, as it was monitored by IgG levels in mouse sera, the level of the beige trait was more difficult to monitor. Dr. William Addison, a research scientist in Dr. L. Tyrrell laboratory, was able to develop a system to follow the beige trait. The mice I used in my PhD studies were confirmed to carry both the SCID and beige traits, whereas a portion of the chimeric mice used in the previous study [284] may have lost their beige trait. Lack of the beige trait resulted in more mouse NK cell function, which may have contributed to a stronger ISG response. Second, the previous study [284] used fresh human hepatocytes isolated from liver tissues taken at the time of liver surgery (by Dr. Norm Kneteman). Although these cell preparations contained primarily human hepatocytes, the preparation almost certainly contained other liver cell types that may have been important in the production of an ISG response.

Large-scale genome-wide association studies have been used to identify host markers associated with responsiveness to IFN treatment of HCV infection. Two SNPs upstream of the IL28B coding region are identified: at rs12979860, CC genotype is associated with responsiveness to IFN treatment while CT and TT are predictive of poor response. At rs8099917, TT is associated with good response and CG or GG is with poor response [91, 92, 94, 95]. Recently, a Japanese group found no significant difference in HCV RNA reduction in response to IFN treatment in chimeric mice sera between favourable and unfavourable IL28B

genotypes of host hepatocytes [308]. However, the three HCV inocula the authors used were very close to each other in terms of their IFN-sensitivities, which may have obscured the effects of the polymorphisms at the IL28B locus. On the other hand, using a similar chimeric mouse model, another group reported that the favourable IL28B genotype was associated with earlier reduction in HCV RNA [309]. In my study, I used two HCV isolates with distinct IFN-sensitivities and infected mice produced with hepatocyte donors carrying three different genotypes at two IL28B SNPs including both “favorable” and “unfavorable” IFN response genotypes. I found the IFN-nonresponsive HCV strain isolated from a null-responder remained non-responsive to IFN treatment in all three hepatocyte backgrounds. The IFN-sensitive HCV strain was sensitive in all three host backgrounds. These results suggested that the variants of the IL28B SNPs in donor hepatocytes had little or no influence on the response to IFN treatment under immunosuppressive conditions of the SCID/beige trait in our chimeric mice, which is in agreement with the observations by Watanabe, *et al* [308]. On the other hand, the published data from patient studies consistently addressed the association of IL28B “favorable” SNPs with early HCV decline in response to IFN treatment [91, 92, 94, 95]. Therefore, my results suggest that the association of IL28B SNPs with response to IFN treatment found in patient studies may require a complete immune system. Interestingly, I even observed more rapid and profound viremia reduction in “unfavorable” than in the “favorable” donor hepatocytes. This suggests that the association of IL28B SNPs with IFN response may vary among different types of cells. The effects seen in patient studies likely

occur in cells types other than hepatocytes, such as immune cells, whereas in hepatocytes, my data showed that the association was opposite to what has been observed in patients. The magnitude of effect in those immune cells is likely greater than in hepatocytes, resulting in a stronger association between IL28B SNPs and IFN response in immunocompetent patients. In addition, two previous studies of HCV infection in different hepatocyte donors carrying different IL28B SNPs in chimeric mice showed controversial results regarding intrahepatic ISG expression. One study, that supports the correlation between host IL28B genotypes and early reduction in HCV RNA levels, showed response to IFN was associated with higher expression levels of ISGs, e.g intrahepatic ISG expression levels were significantly higher in IL28B responder donors than IL28B non-responder donors in response to IFN treatment [309]. However, no significant difference in ISG expression levels was observed between favourable and unfavourable IL28B donor genotypes upon IFN administration in the study by Watanabe, *et al.* [308]. The latter study did not find a correlation between donor IL28B SNPs with HCV response to IFN treatment, which is consistent with my results.

Finally, it has been suggested that refractoriness could be one mechanism underlying the lack of response to pegIFN α in CHC patients who already had an active ISG response [212]. Refractoriness has been observed not only in cultured cells, but also in the liver of mice injected with mouse IFN α [64]. However, after two weeks of daily administration of exogenous IFN α , intense upregulation of ISG gene expression was observed in the chimeric mouse livers, suggesting there

was no refractoriness to IFN treatment in the chimeric mouse system. Most importantly, since the two HCV strains with different response outcomes to IFN therapy retained their sensitivities in response to exogenous IFN treatment in our chimeric mice in absence of the refractoriness effect, my results indicate that refractoriness is not likely the main cause of IFN non-responsiveness in humans. Instead, an “innate immune tolerance model” described by Lau, *et al* [305] provides an alternative explanation for the nonresponsiveness of CHC patients who already had an upregulated ISG response to IFN therapy. The model proposes that endogenous IFN β produced by myeloid cells, e.g Kupffer cells, drives basal ISG expression among hepatocytes through paracrine signaling. ISGs exert antiviral actions through multiple processes, which are often cytotoxic with prolonged exposure. ISGs, therefore, must be tolerated for the cell to survive. As the cell becomes tolerized to the actions of IFN, the efficacy of IFN therapy is reduced.

3.4 Summary

In this study, host and viral factors, which may contribute to the outcome of IFN therapy, were investigated in the SCID/bg-Alb/uPA chimeric mouse model. The response of two HCV strains with distinct IFN-sensitivities to IFN α treatment was studied in mice transplanted with hepatocytes from three donors carrying different IL28B SNPs. I found that intrinsic viral factors were the key determinants of the response to IFN therapy, whereas viral interaction with host IFN signaling to induce ISGs and host factors, such as polymorphism at the IL28B locus and pre-

treatment levels of intrahepatic ISG expression, were not important factors in determining the outcome of IFN therapy in HCV infection in chimeric mice.

CHAPTER 4

Mechanism Of Interferon Nonresponsiveness Of HBV And HCV In SCID/Beige-Alb/uPA Chimeric Mice

4.1 Rationale

Although HBV and HCV are very different viruses, they share the same hepatic tropism. Both viral infections represent major global public health problems. End-stage liver diseases caused by these viruses are the common causes for liver transplantation in the western world. Interferon alpha has been a major component in treatments for both HBV and HCV infections for more than two decades. Importantly, a significant proportion of treated patients with either CHB or CHC do not respond to IFN therapy. This nonresponsiveness has been a major problem in the management of both infections.

In CHB patients, about 30% of patients respond to IFN therapy. In HBeAg positive patients, female gender, older age, HBV genotype A, high levels of ALT, low levels of HBV DNA in serum, a rapid decline in serum HBsAg and HBV DNA levels during therapy are associated with a SVR [90]. Recent studies suggest that in CHB patients, SNPs near IL28B correlate with serologic response to pegIFN [96-99], while the absence of precore and basal core promoter mutants in the virus may also predict a SVR [310]. As discussed in Chapter 3, in patients with chronic HCV infection, IFN therapy has been used in combination with ribavirin. Host factors, such as host IL28B SNPs [91-95] and pre-treatment hepatic ISG expression level [161, 162], are associated with responsiveness or non-responsiveness in patients to IFN therapy. Other viral factors, such as viral genotype [165], amino acid substitution at aa 70 or 91 of HCV core [175] or the

IFN-sensitivity-determining region of HCV NS5A [173], are critically important in predicting the response to pegIFN and RBV therapy.

In addition, many viruses block or suppress the IFN signaling downstream of the IFN receptors to escape the antiviral effects of IFNs. Both HBV and HCV have evolved such strategies to block the type I IFN signaling through modification of key molecules in the JAK-STAT pathway. Evidence suggests that HBV precore/core proteins downregulate MxA gene expression by their interaction with the MxA promoter [125]. A recent study using humanized mice showed that HBV prevented IFN α mediated signaling by inhibiting nuclear translocation of STAT1, thus interfered with transcription of ISGs [123]. The inhibition of STAT1 nuclear translocation is most likely mediated by HBV polymerase. It has been shown in an *in vitro* culture system that ectopic expression of HBV polymerase suppressed IFN α -induced STAT1 serine 727 phosphorylation and STAT1/2 nuclear accumulation [124].

On the other hand, studies done in cultured cell transfected with HCV proteins suggest that HCV impairs the JAK-STAT pathway through various mechanisms (reviewed in reference [292]). For examples, after transfection into cells, both HCV core and NS5A proteins interacted with STAT1 and impaired IFN-induced STAT1 phosphorylation, resulting in inhibition of downstream ISG transcription [202, 203]. HCV core was also found to interfere with STAT1 nuclear translocation [311, 312] or binding of ISGF3 to the ISRE in ISG promoters [313]. However, data from HCV-infected hepatoma cells do not support the inhibitory

effects of HCV proteins on the JAK-STAT pathway. In Huh-7 cells infected with JFH-1 virus, overexpression of individual components of the dsRNA-signaling pathway indicated that HCV inhibited IFN β promoter activity by proteolytically cleaving MAVS, while leaving the IFN-induced JAK-STAT signaling pathway intact [293]. In addition, in response to exogenous IFN β treatment, JFH-1 infection in Huh-7 cells triggered phosphorylation and activation of PKR, which inhibited eIF2 α and attenuated ISG protein expression, however ISG mRNAs were induced at similar levels as in uninfected cells, suggesting the JAK-STAT pathway was not affected [194]. Therefore, more studies in the context of HCV infection *in vivo* were undertaken in an attempt to address these inconsistencies.

Previously, the lack of small animal models supporting HBV and HCV infections hampered the *in vivo* investigation of the molecular mechanisms responsible for the ineffectiveness of IFN therapy. The SCID/bg-Alb/uPA chimeric mouse model supports long-term infections by HCV and HBV. Evidence in Chapter 3 and other studies [314] has shown that the antiviral response to IFN in the chimeric mice often reflects the response of the identical virus to IFN therapy in humans.

Based on the current knowledge of immune evasion by HBV and HCV, the main objective of the study in this Chapter was to compare the molecular mechanisms of interferon nonresponsiveness of HBV and HCV in parallel, in particularly the potential differences in the evasion of the JAK-STAT signaling between the two viruses in the SCID-bg/Alb-uPA chimeric mouse model.

4.2 Results

4.2.1 Time course of induced IFN response during HBV infection in chimeric mice

(A) Time course of HBV infection in chimeric mice

Most studies on HBV infection in patients and the chimeric mouse model have focused on its chronic phase. However, Wieland, *et al.* have performed a longitudinal analysis of the activation of cellular genes on liver biopsy specimens from three experimentally infected chimpanzees [116]. Surprisingly, they were not able to detect any change of ISG expression that related to the entry and expansion of the virus during acute HBV infection. In this chapter, I performed a detailed investigation of the time course of HBV infection and measured IFN response over the course of HBV infection for 8 weeks in the SCID-bg/Alb-uPA chimeric mouse model. This study was performed in chimeric mice produced with a hepatocyte donor Hu8063 (Table 3.3). Chimeric mice were infected with a clinical HBV isolate (genotype C) by i.p. injection [10^5 - 10^6 genome equivalence (GE) /animal]. Three to six animals were euthanized at 5 time points during HBV infection: 6-hour, 2-day, 14-day, 28-day and 56-day post infection. HBV viral DNA levels in mouse serum and liver were measured by qPCR. Data in Figure 4.1 A and B show that both HBV viremia and hepatic DNA levels rose in parallel starting at day 2 post infection. The HBV viremia at the early time point, e.g. 6 hours p.i, likely represented inoculum virus rather than a true infection, since after 6-hour time point the HBV titer in both serum and liver fell by day 2 p.i and then

began to rise indicating active HBV replication (Figure 4.1 A and B). The level of HBV viremia and intrahepatic DNA level continued to increase until they plateaued after 28 days p.i. to establish a long-term stable infection, which was maintained until the experiment was terminated at day-56 p.i.. This increase in HBV DNA in mouse sera was paralleled by the intrahepatic HBV RNA measurements in Figure 4.1C.

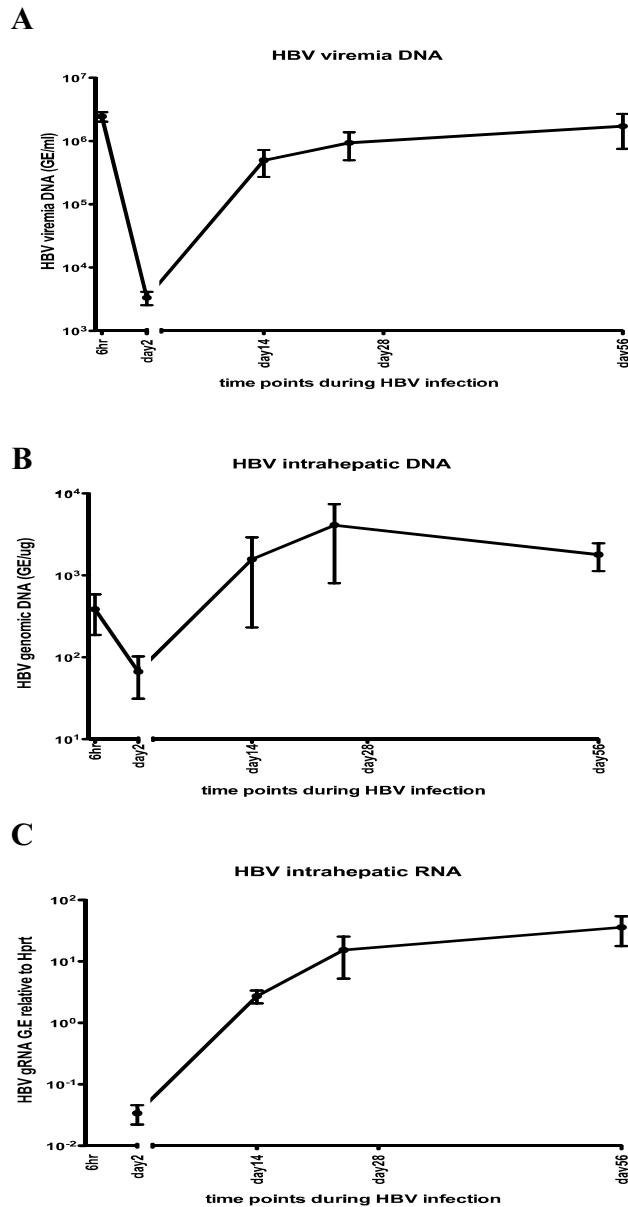


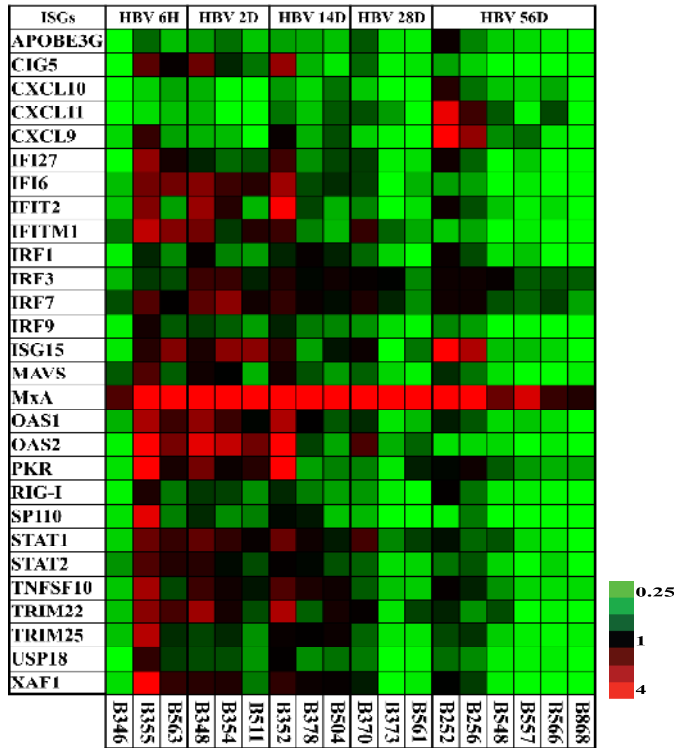
Figure 4.1. Kinetics of virological parameters during the course of HBV infection in SCID/bg-Alb/uPA chimeric mice.

A time course study of HBV infection was performed in chimeric mice populated with a single human hepatocyte donor Hu8063. Five time points were examined; 6-hour, 2-day, 14-day, 28-day and 56-day p.i. Levels of HBV viremia DNA (A), intrahepatic viral DNA (B) and intrahepatic viral RNA (C) were measured at these time points by realtime qPCR or RT-qPCR. At each time point, 3-6 mice were sacrificed. Data are represented as mean \pm standard deviation.

(B) Time course of induced IFN response during HBV infection in chimeric mice

During the course of viral infection, intrahepatic expression of human specific ISGs, as an indicator of IFN signaling activation, was measured by RT-realtime PCR in chimeric mouse livers. Only 3 ISG genes were significantly upregulated at 6-hour and day-2 after HBV inoculation (Figure 4.2B). However, since elevation of the same ISGs at 6 hour and day 2 post-inoculation was also observed in mock-infected animals as compared to hepatocyte donor-matched uninfected controls (Figure 4.3B), this very early upregulation of ISG expression was unrelated to HBV infection. There was no significant induction of IFN or ISGs observed at the later time point (day-56 p.i) of HBV infection in chimeric mice as shown in Figure 4.4A and B respectively. In fact, a number of ISGs were expressed at significantly lower levels than the levels of these ISGs in the uninfected control mice (Figure 4.4B), which was not observed in chimeric mice infected with HCV (refer to Figure 4.7). In this study, HBV did not induce IFN or ISG mRNA upregulation in the chimeric mice over the time course of a 56-day infection.

A



B

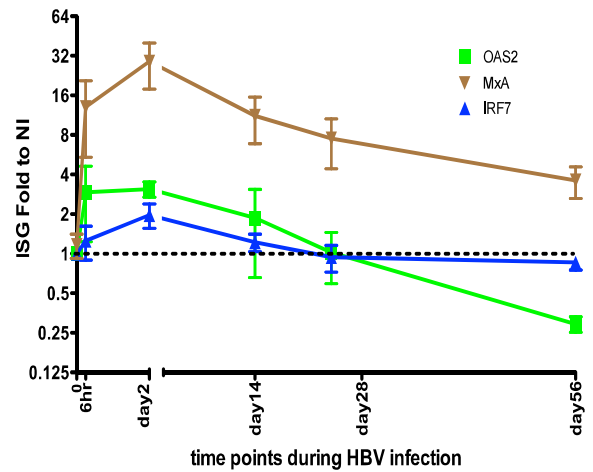
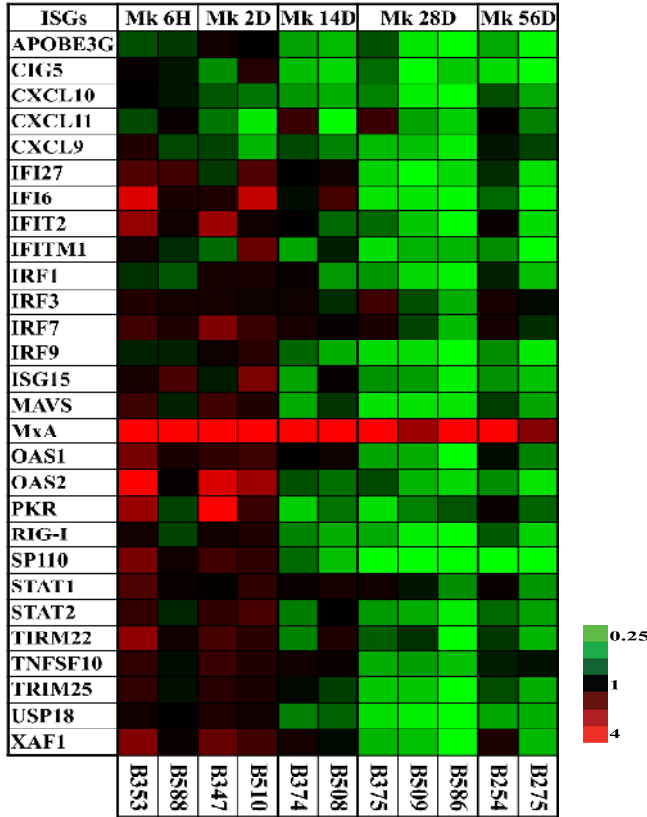


Figure 4.2 IFN response induced during the course of HBV infection in chimeric mice.

Intrahepatic expression levels of ISGs were analyzed in chimeric mouse liver samples over the time course of HBV infection by RT-real time PCR. Oligos for each gene of interest were designed human specific. Expression of each gene was relatively quantified by normalizing to a human-specific housekeeping gene HPRT-1 and gene expression calculation was carried out according to the $2^{-\Delta\Delta Ct}$ method. Data in the heatmap (A) are shown as fold change compared to the donor-matched uninfected controls (data not shown). Each column in the heat map represents a single mouse. Increased and decreased expression of specific genes is shown by red (Fold >1 - ≥ 4) and green (Fold <1 - ≤ 0.25), respectively, black indicates no change (Fold =1). Only the ISGs that were significantly upregulated ($P < 0.05$) in comparison to donor-matched NI controls (“0” on the X axis in the figure) during the course of HBV infection were shown in (B). Significance was determined by one-way ANOVA calculation.

A



B

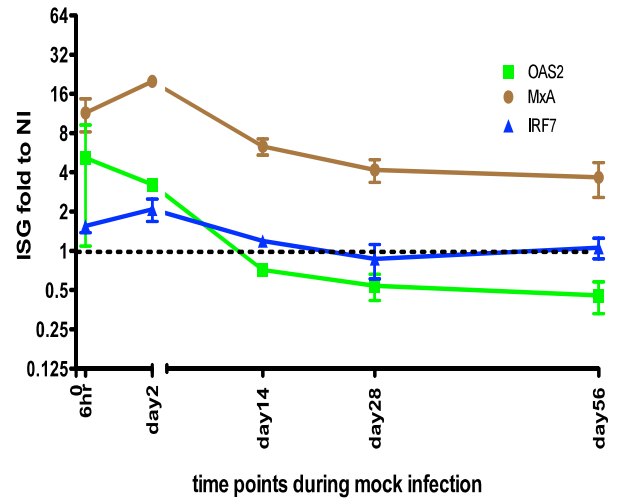
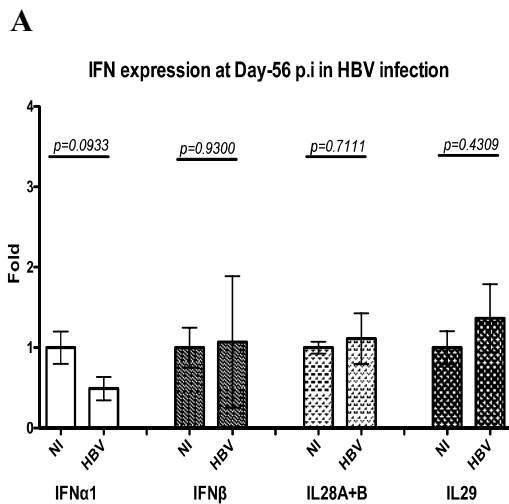


Figure 4.3 ISG expression in mock-infected chimeric mice produced with hepatocytes Hu8063.

Chimeric mice produced with hepatocyte donor Hu8063 were mock-infected with a serum sample isolated from a healthy adult (HBV, HCV and HIV negative). Five time points, 6-hour, 2-day, 14-day, 28-day and 56-day post inoculation, were examined. At each time point, 2-5 mice were sacrificed. Intrahepatic expression levels of human specific ISGs were measured by RT-realtimePCR. Data in the heatmap (A) are shown as fold change compared to the donor-matched uninfected controls (data not shown). Each column represents a single mouse. ISGs, that were significantly induced by mock infection compared to the donor-matched NI controls (“0” on the X axis in the figure), were shown in (B). Results were represented as mean \pm standard deviation. Significance was determined by one-way ANOVA calculation.



B

ISGs	Mean fold to NI	p-value	p-value summary
APOB3G	0.51	0.0263	*
CIG5	0.24	0.0003	***
CXCL10	0.59	0.0984	ns
CXCL11	1.26	0.9504	ns
CXCL9	1.70	0.5053	ns
IFI27	0.49	0.0806	ns
IFI6	0.30	0.0206	*
IFIT2	0.53	0.0397	*
IFITM1	0.28	0.0004	***
IRF1	0.52	0.0243	*
IRF3	0.94	0.5348	ns
IRF7	0.86	0.2618	ns
IRF9	0.32	0.0009	***
ISG15	2.10	0.6614	ns
MxA	3.60	0.0539	ns
OAS1	0.49	0.0180	*
OAS2	0.29	0.0064	**
PKR	0.74	0.1804	ns
RIG-I	0.47	0.0230	*
SP110	0.27	0.0008	***
STAT1	0.55	0.0297	*
STAT2	0.44	0.0053	**
TNFSF10	0.60	0.0619	ns
TRIM22	0.47	0.0420	*
TRIM25	0.48	0.0065	**
USP18	0.39	0.0042	**
XAF1	0.45	0.0275	*

Figure 4.4 ISG expression in long-term HBV-infected chimeric mice populated with a hepatocyte donor Hu8063.

In chimeric mice (hepatocyte donor Hu8063) chronically infected with HBV (56-day p.i.), intrahepatic expression of human specific IFNs (A) and ISGs (B) were examined by reverse transcription - realtime PCR. Results in (A) are represented as mean \pm standard deviation, n=3-6. In Figure B, ISG expression was compared to that of NI control animals. *P*-values were calculated by unpaired t-test. Significantly ($p < 0.05$) upregulated and downregulated expression of ISGs is indicated by highlighting the tables in red and green colors respectively. No highlighting shows no significant difference ($p \geq 0.05$) in comparison to the NI control.

4.2.2 The IFN response induced during the course of HCV infection in chimeric mice

(A) Time course of HCV infection in chimeric mice

Similar to the experiments described in the previous section, the course of HCV infection at 6 different time points; 6-hour, 1-day, 2-day, 10-day, 21-day and 49-day p.i., was examined in chimeric mice populated with a single hepatocyte donor Hu8085. At each time point, 3-5 animals were sacrificed. HCV viral RNA levels in mouse serum and in chimeric mouse liver were quantified by RT-qPCR. Data in Figure 4.5 show that active HCV replication started between day 2 -10 p.i and plateaued at day 10 p.i. The HCV viremia remained stable up to day 49 p.i or longer.

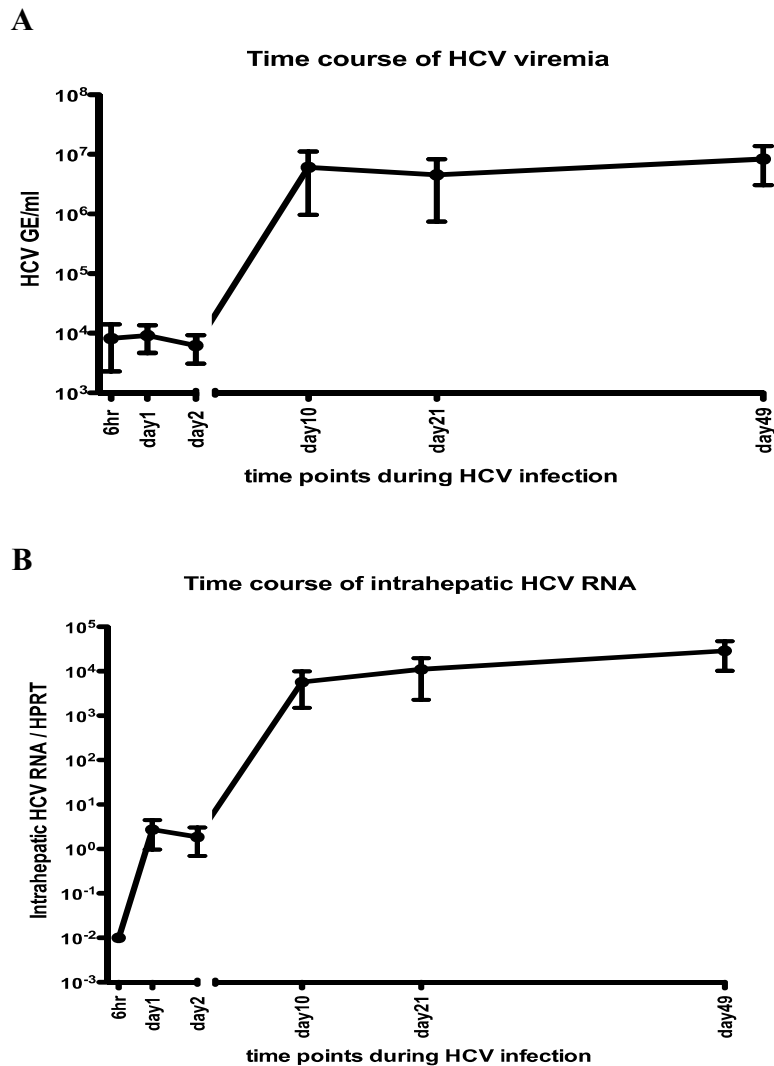


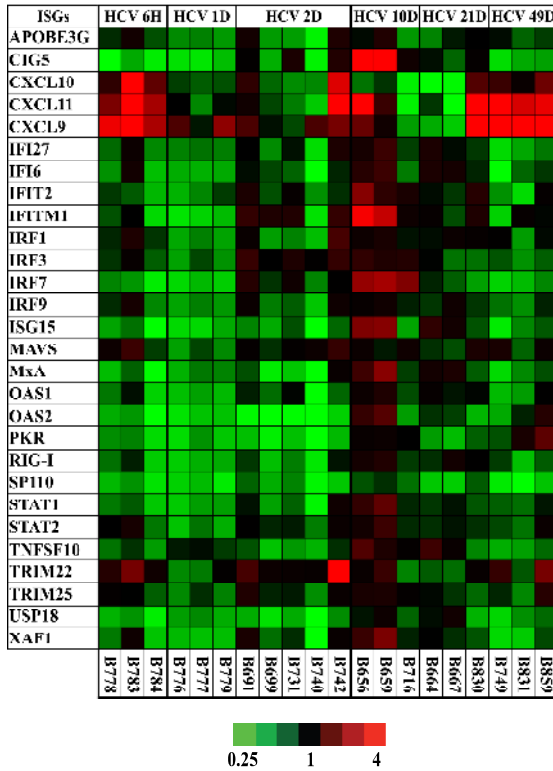
Figure 4.5 Kinetics of virological parameters during the course of HCV infection in SCID/bg-Alb/uPA chimeric mice.

Six time points: 6-hour, 1-day, 2-day, 10-day, 21-day and 49-day, were examined during HCV infection in chimeric mice produced with a single hepatocyte donor Hu8085. HCV viral RNA levels in both serum (A) and liver (B) were determined by realtime RT-qPCR. At each time point, 3-5 mice were sacrificed as biological repeats. Data are represented as mean \pm standard deviation.

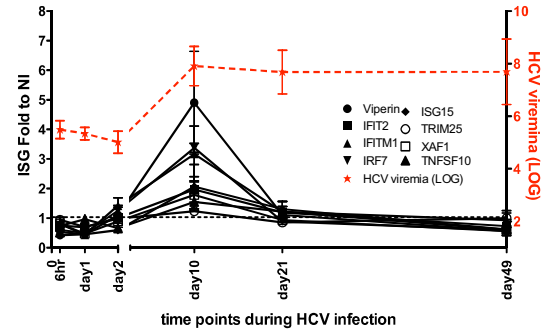
(B) Time course of induced IFN response during HCV infection in chimeric mice

Intrahepatic expression profile of human specific ISGs over the course of HCV infection in chimeric mice was examined by RT-real time PCR. As illustrated in Figure 4.6 A and B, there was a significant peak of IFN response at day 10 p.i during HCV infection course. The possibility of nonspecific induction due to other content in the inoculum was excluded by measuring the same ISGs, that were elevated at day-10 p.i in HCV infection, in chimeric mice inoculated with mock serum as shown in Figure 4.6C. There was no significant IFN or ISG upregulation during long-term HCV infection (≥ 28 days) (Figure 4.7 A and B). Out of 25 human specific ISGs examined, the majority of ISGs remained at levels comparable with those in uninfected animals produced with the same hepatocytes. These data are consistent with the observation in Chapter 3 (Figure 3.5).

A



B



C

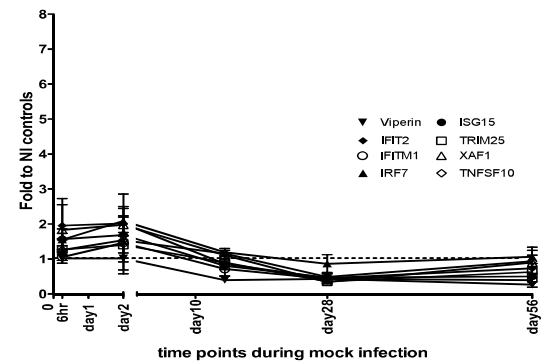
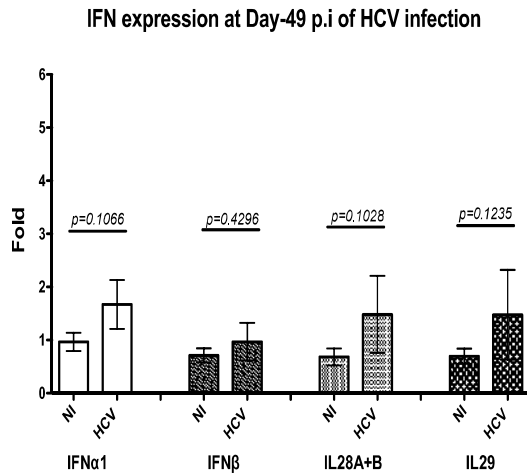


Figure 4.6 IFN response induced during the course of HCV infection in chimeric mice.

Intrahepatic expression levels of ISGs were analyzed in mouse liver total RNA samples from the time course study of HCV infection by RT-real time PCR. Data in the heatmap (A) are shown as fold change compared to the donor-matched uninfected controls (data not shown). Each column in the heat map represents a single mouse. Only the ISGs that were significantly upregulated ($p < 0.05$) in comparison to donor-matched NI controls (“0” on the X axis in the figure) during the course of HCV infection are shown in Figure B in correlation with HCV viremia change (red dashed line). Significance was determined by one-way ANOVA calculation. (C) The same ISGs observed in Figure B were measured in mock-infected chimeric mice produced with hepatocyte donor Hu8063 in comparison to donor-matched uninfected controls (as described in Figure 4.3). Data are represented as mean \pm standard deviation.

A



B

ISGs	Mean fold to NI	p-value	p-value summary
APOBE3G	0.91	0.51	ns
CIG5	0.56	0.30	ns
IFI27	0.55	0.06	ns
IFI6	0.65	0.17	ns
IFIT2	0.73	0.23	ns
IFITM1	0.93	0.62	ns
IRF1	0.91	0.52	ns
IRF3	0.73	0.19	ns
IRF7	0.59	0.29	ns
IRF9	0.75	0.15	ns
ISG15	0.61	0.14	ns
MAVS	1.10	0.84	ns
MxA	0.72	0.33	ns
OAS1	0.69	0.08	ns
OAS2	1.20	0.89	ns
PKR	1.63	0.38	ns
RIG-I	0.71	0.16	ns
SP110	0.50	0.47	ns
STAT1	0.84	0.38	ns
STAT2	0.88	0.38	ns
TNFSF10	0.61	0.06	ns
TRIM22	1.73	0.09	ns
TRIM25	1.00	0.91	ns
USP18	0.59	0.06	ns
XAF1	0.56	0.06	ns

Figure 4.7 ISG expression in long-term HCV-infected chimeric mice populated with a hepatocyte donor Hu8085.

Intrahepatic expression of IFNs (A) and ISGs (B) in mice chronically infected with HCV (49-day p.i.) were examined in comparison to donor-matched NI controls. Results in (A) were represented as mean \pm standard deviation. $n=3-6$. In (B), p -values were calculated by unpaired t-test. Significantly ($p<0.05$) upregulated and downregulated expression of ISGs is indicated by highlighting the tables in red and green colors respectively. No highlighting shows no significant difference (ns, $p\geq0.05$) in comparison to the NI control.

As mentioned in section 3.2.3, these results were in contrast to published data in chronically HCV infected patients or chimpanzees in which chronic HCV infection is mostly associated with significantly upregulated intrahepatic ISGs [161, 162, 208]. In order to confirm the lack of ISG upregulation in chronically infected chimeric mice, I repeated these experiments in two additional sets of chimeric mice produced with two different hepatocyte donors, Hu3111 and Hu8063. In comparison to the donor-matched uninfected control animals, neither of these additional studies showed significant IFN or ISG upregulation at day-49 post infection (Figure 4.8). This confirmed the lack of an IFN response in long-term HCV infection in the chimeric mice produced with cryopreserved human hepatocytes.

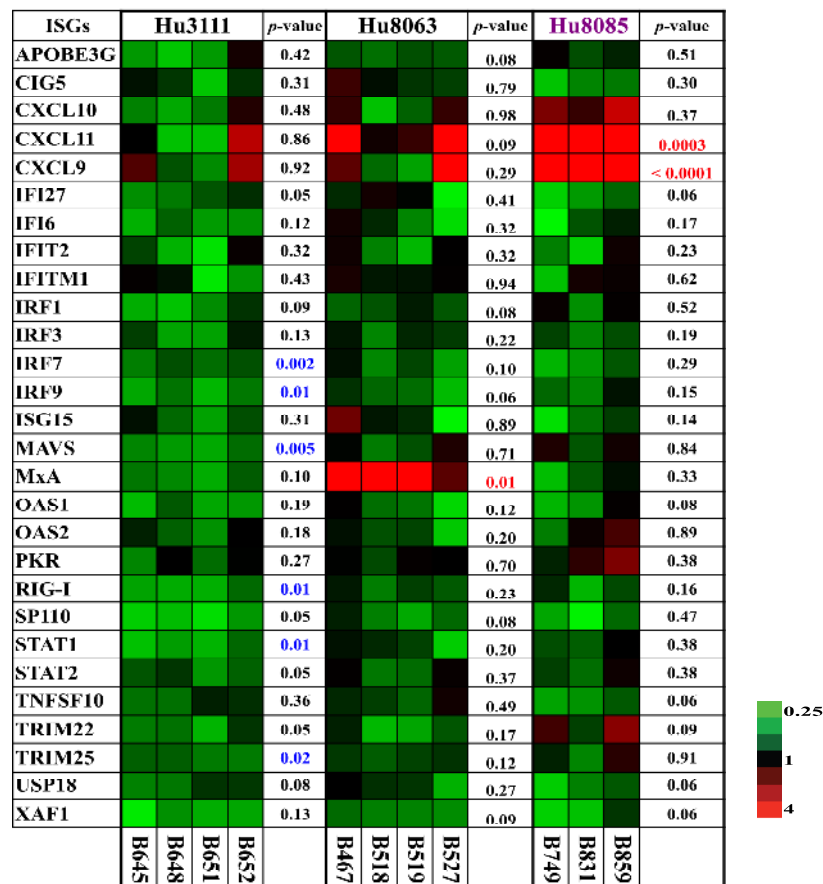


Figure 4.8 Examination of IFN response induced during chronic HCV infection in chimeric mice produced with two hepatocyte donors.

Animals populated with two additional hepatocyte donors, Hu8063 & Hu3111, in addition to Hu8085 (purple) that was used for experiment in Figure 4.7, were infected with HCVgt1a for 49 days. Total RNA was isolated from chimeric mouse livers and analyzed by RT-realtime PCR for expression of human ISGs. Data are shown as fold change compared to the donor-matched uninfected controls (data not shown). Each column in the heat map represents a single mouse. Increased and decreased expression of specific genes is shown by red (Fold >1 - ≥ 4) and green (Fold <1 - ≤ 0.25), respectively, whereas black indicates no change (Fold =1). *P*-values were calculated by unpaired t-test. Significantly ($p < 0.05$) upregulated and downregulate expression of ISGs is indicated by text-highlighting *p*-values in red and blue colors respectively. *P*-values in black represent no significant difference ($p \geq 0.05$) in comparison to the NI control.

4.2.3 Comparison of the response of HBV and HCV to exogenous IFN treatment

Data for HCV in this section are the same as in Chapter 3 (HCVgt1a data in response to exogenous IFN treatment), but repeated here to compare with the HBV infection. We knew that the HCV strain used in this study was isolated from a hepatitis C patient who was a null responder to pegIFN/RBV treatment (refer to Table 3.1 in Chapter 3). The sensitivity of the HBV strain to IFN was unknown.

I first tested the response of the two viruses to exogenous IFN treatment in chimeric mice produced with a single hepatocyte donor, Hu8063. Two groups of chimeric mice were infected, one with HBV and one with HCV. After stable infections were established (8 weeks p.i in HBV infected mice and 5 weeks p.i in chimeric mice infected with HCV), each group was split in two groups with one group received subcutaneous injection of exogenous IFN α daily at 1,350IU/gram for 2 weeks (blue in Figure 4.9 and Figure 4.10) and the control group received 30uL of saline subcutaneously (black in Figure 4.9 and Figure 4.10). After IFN α was administrated, both HBV and HCV viremia declined less than 1 log (Figures 4.9A and 4.10A), indicating that neither HBV nor HCV used in this study was responsive to IFN α treatment. In addition, the serum level of human albumin in each animal during the course of infection and IFN α treatment was measured by ELISA. No significant change in serum human albumin levels was observed with infection or IFN treatment (Figures 4.9B and 4.10B). This ruled out the possibility that there was a dramatic change in the human hepatocytes engraftment of the chimeric liver during therapy with IFN. At the end of the treatment period of 14

days, HBV RNA and HCV viral RNA copy numbers were measured in the chimeric mouse livers (Figures 4.9C and 4.10C). The intrahepatic viral RNA levels in both infections did not differ between IFN treated and saline-treated groups, confirming that both HBV and HCV viruses used in this study were nonresponsive to exogenous IFN treatment in the chimeric mice.

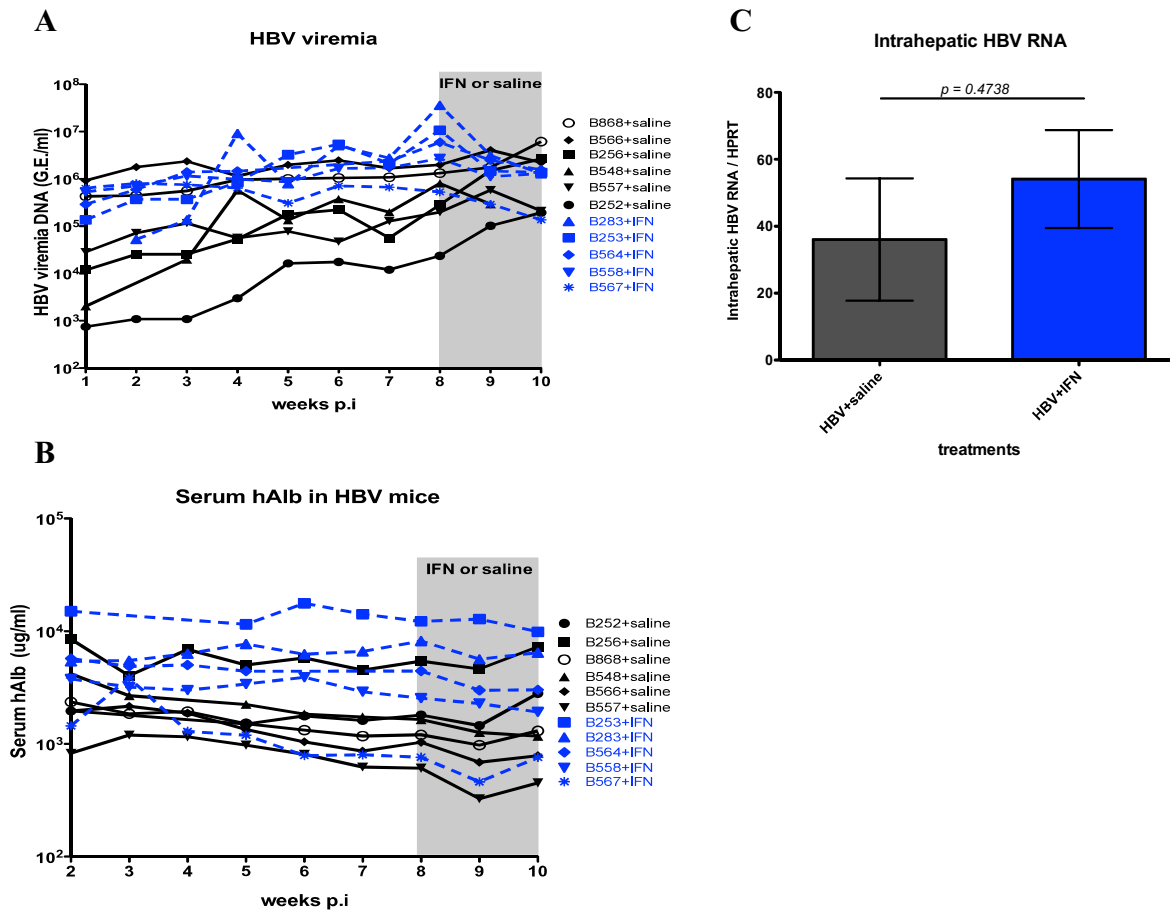


Figure 4.9 Response of HBV to exogenous IFN treatment.

Chimeric mice produced with Hu8063 were chronically infected with HBV. Exogenous IFN α -2b treatment was delivered subcutaneously daily for 14 days. Control animals were injected with saline. Mice were bled weekly for viremia and serum human albumin measurements. Six hours after last IFN injection, mice were sacrificed and intrahepatic viral loads were measured and compared to the intrahepatic viral loads in saline treated controls. Mice treated with saline are presented in black solid lines and mice treated with IFN are in blue dashed lines. (A) HBV viral DNA levels over the course of infection and IFN treatment. Each line represents a single mouse. (B) Human albumin levels in mouse serum in parallel with the HBV viral DNA change in (A). The period of IFN α /saline treatment is shaded. (C) HBV RNA levels in mouse livers upon termination. Data were normalized with human specific HPRT-1 and indicated as mean \pm standard deviation; n = 4-5. *P*-values were calculated by unpaired t-test.

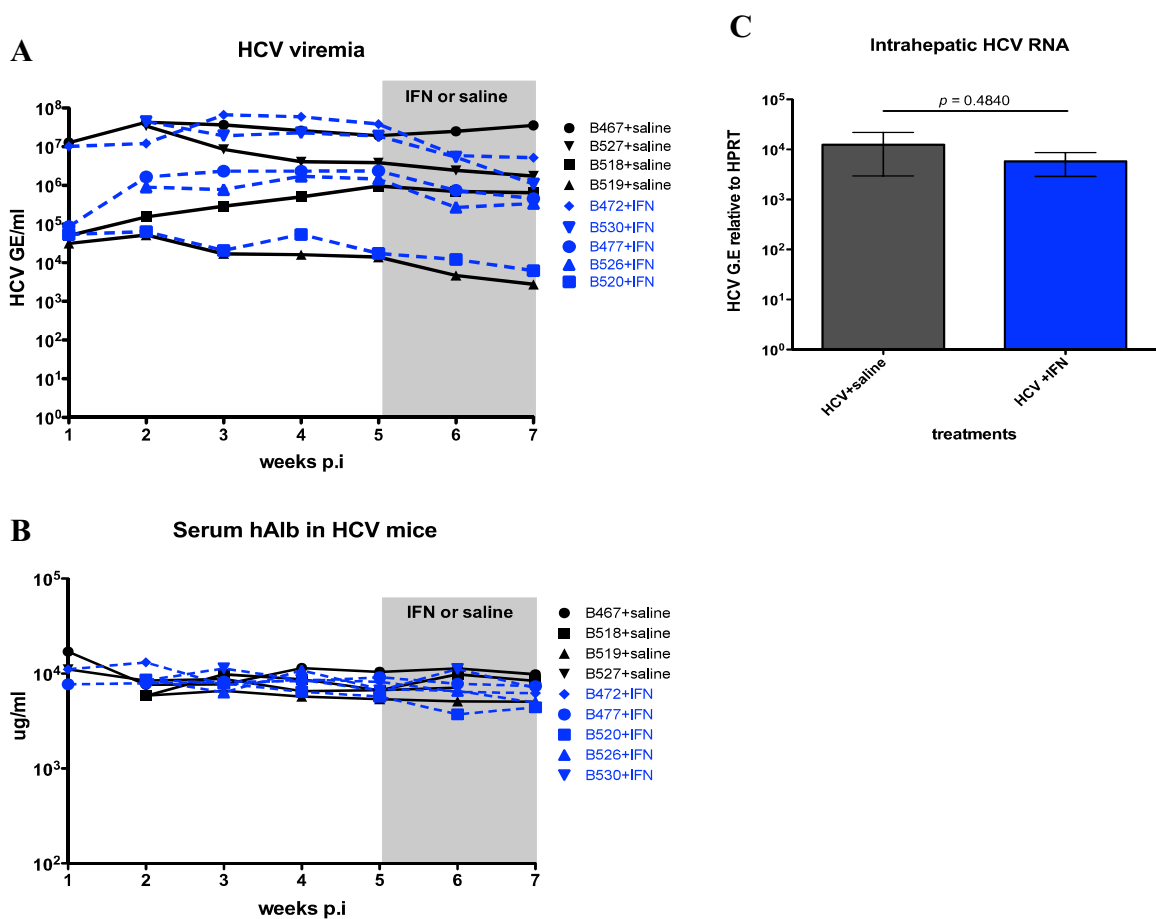


Figure 4.10 Response of HCV to exogenous IFN treatment.

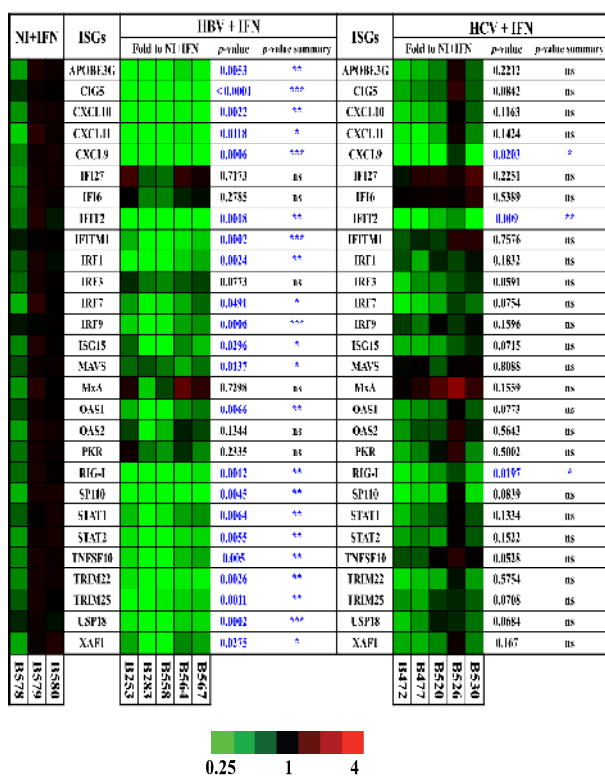
Chimeric mice produced with Hu8063 were chronically infected with HCV. Exogenous IFN α -2b was administered subcutaneously daily for 14 days. Control animal were injected with saline. Mice were bled weekly for viremia and serum human albumin measurements. Six hours after the last IFN injection, mice were terminated and intrahepatic viral load was measured and compared to the saline treated controls. Mice treated with saline are presented in black solid lines and mice treated with IFN are in blue dashed lines. Figures A-C: HCV viremia RNA levels (A), serum human albumin levels (B) and intrahepatic HCV RNA levels (C) in mice infected with HCV at various time points are illustrated. *P*-values in (C) were calculated by unpaired t-test. The period of IFN α /saline treatment is shaded in A and B.

4.2.4 Nonresponsiveness to exogenous IFN treatment of HBV and HCV is due to different mechanisms

Having shown the relative lack of IFN response in both long-term HCV and HBV infections in chimeric mice as well as their nonresponsiveness to exogenous IFN treatment, it is possible that host IFN signaling was strongly suppressed by both viruses. I next examined the changes in expression of human ISGs in infected chimeric mice upon IFN treatment using the same mice as described in section 4.2.3. To illustrate the potential suppressive effect of either HBV or HCV infection on JAK-STAT pathway, the ISG expression levels of IFN-treated HBV or HCV infected mice was compared to that of the IFN-treated uninfected control mice in Figure 4.11A. Data in Figure 4.11A showed that the extent of the upregulation of ISG expression was significantly lower in HBV infected mice for 22 out of 28 ISGs compared to the response to exogenous IFN treatment in uninfected control mice. A similar comparison in HCV infected mice showed that there were only 3 ISGs that were expressed at significantly lower levels compared to the levels of ISG expression in IFN-treated uninfected mice. Although I observed no evidence of HCV blocking the IFN response at the transcriptional level, suppression could also occur at the protein translation levels. It has been demonstrated that in JFH-1 infected Huh-7 cells treated with IFN β , although ISG mRNAs were induced, HCV triggered phosphorylation and activation of PKR, which inhibited eIF2 α and attenuated ISG protein expression [194]. One of the representative ISGs that were significantly increased at transcriptional level in HCV-infected mice treated with IFN compared to uninfected and saline-treated

controls was ISG15 (refer to Figure 3.3 in Chapter 3). I examined the protein level of ISG15 by western blot and found that the protein expression of ISG15 in the livers of HCV-infected chimeric mice treated with IFN was strongly induced in comparison to the HCV-infected saline-treated controls (Figure 4.11B). This result suggests that the nonresponsiveness of HCV virus to IFN treatment in this study was likely not due to active blockage of host protein translation.

A



B

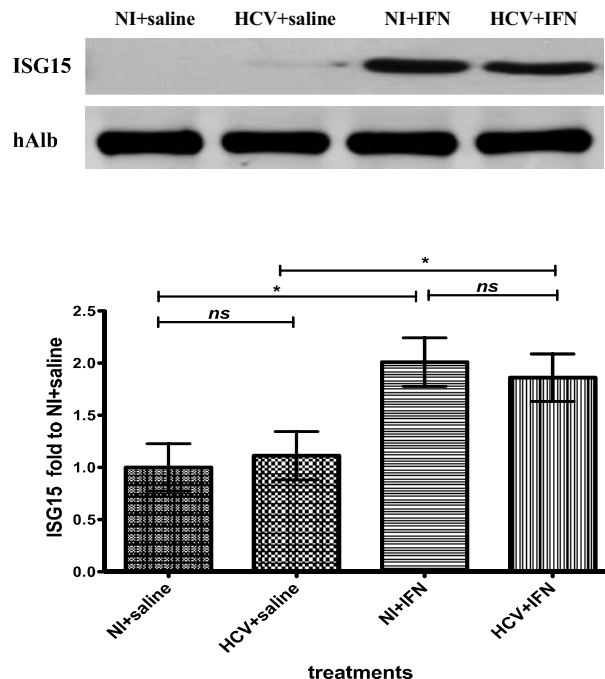


Figure 4.11 Potential suppression of ISG expression by HBV and HCV upon exogenous IFN treatment in chimeric mice.

All mice were produced with a single hepatocyte donor Hu8063. ISG expression in mice infected with HBV *versus* HCV and treated with IFN were analyzed in comparison to the uninfected, IFN treated controls in Figure A. *P*-values were calculated by unpaired t-test. ISGs in (A) that were expressed at significantly higher levels than uninfected and IFN treated controls are highlighted in blue. Figure B: Top: A representative mouse liver from each treatment group was lysed and analyzed by WB for human ISG15 detection. Human albumin was examined as protein loading control. Bottom: Relative levels of ISG15 (normalized to human albumin) from three independent experiments. Protein levels were quantified using ImageFauge V4.22. Bars indicate standard error values. *P*-values were calculated by one-way ANOVA.

Two important molecules required for successful expression of ISGs during IFN signal transduction are STAT1 and STAT2, as described in section 1.1.2.2. They both are ISGs and their protein activation by phosphorylation and nuclear translocation determines whether downstream ISG expression is properly initialized. I firstly examined STAT1 and STAT2 at transcriptional level in the same groups of mice used in the experiment described in section 4.2.3. Data in Figure 4.12 show that genes of STAT1 and STAT2 were always expressed at significantly lower levels in HBV-infected mice in comparison to uninfected controls both without and with IFN treatment. Whereas in IFN-treated chimeric mice infected with HCV, expression of STAT1 and STAT2 remained at comparable levels to the levels in uninfected controls treated with IFN. Moreover, immunofluorescence staining of STAT1, shown in Figure 4.13, indicated that in livers of HBV-infected chimeric mice, the nuclear translocation of STAT1 upon IFN stimulation was impaired, whereas nuclear staining of STAT1 was detectable in both uninfected and HCV infected animals treated with IFN.

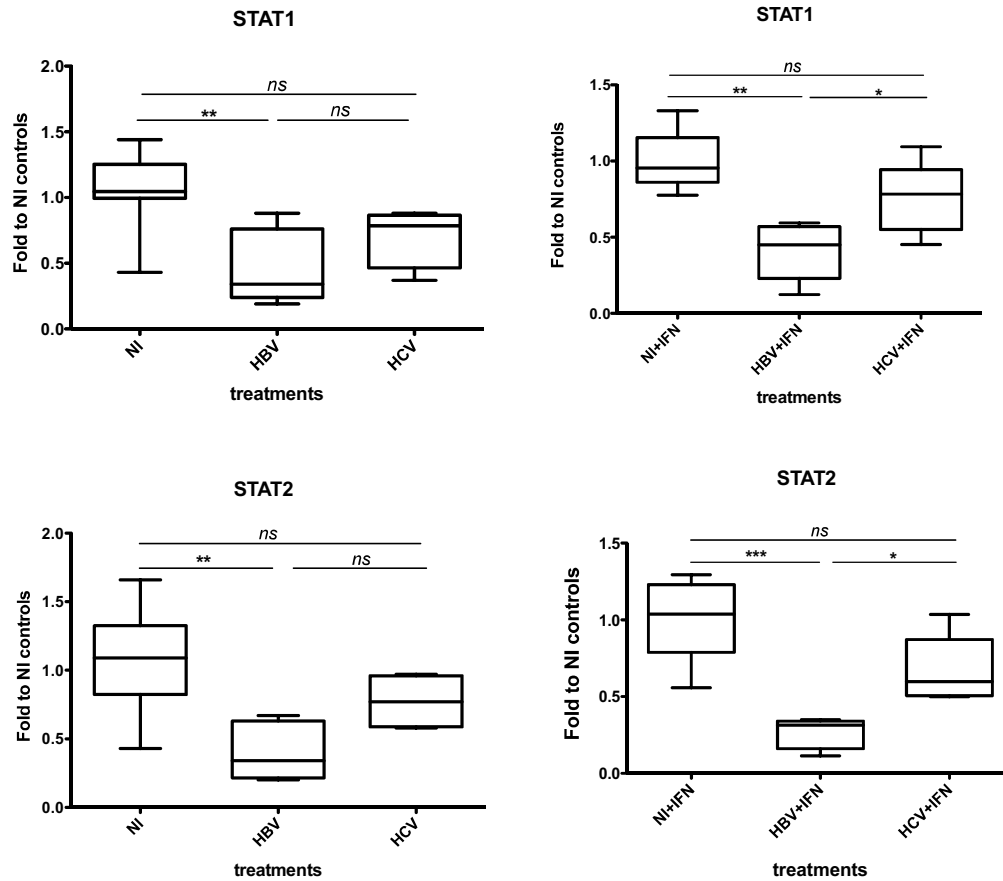


Figure 4.12 Transcriptional level change of STAT 1 and 2 in chimeric mice infected with HBV or HCV with/without IFN treatment.

Uninfected mice or mice infected with HBV or HCV, treated with or without IFN were examined for intrahepatic expression of human STAT1 and STAT2 by RT-realtime PCR. All mice were populated with a single hepatocyte donor Hu8063. Results are shown as mean fold change compared to the ISG expression in uninfected, untreated controls. n= 3-5. *P*-values were calculated by one-way ANOVA.

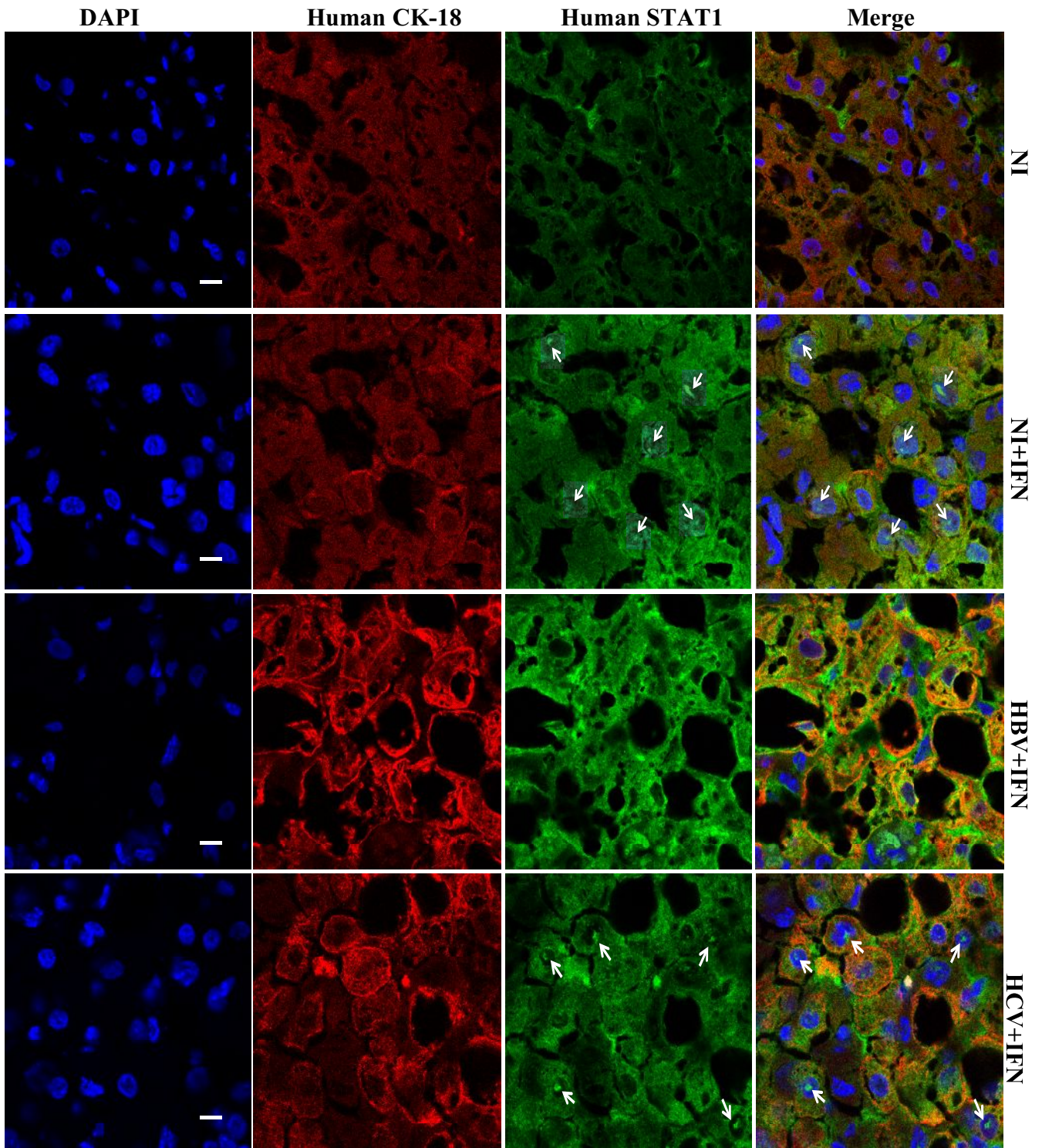


Figure 4.13 STAT1 nuclear translocation upon IFN treatment in chimeric mice infected with HBV or HCV.

Cryopreserved liver sections from donor-matched, IFN-treated uninfected, HCV-infected or HBV-infected chimeric mice were processed for indirect immunofluorescence using mouse anti-STAT1 and rabbit anti-CK-18 monoclonal antibodies. Human CK-18 protein was detected as a marker for human content in chimeric mouse liver. Primary antibodies were detected using goat anti-mouse Alexa488 and goat anti-rabbit Alexa546 secondary antibodies. Nuclei were counter stained with DAPI. Images were captured using a Leica TCS SP5 confocal scanning microscope. Arrows indicate the staining of human STAT1 in the nucleus of human hepatocytes. Bar=10 μ m. For each treatment, at least three regions of interest in 2-3 mice with the same treatment were analyzed.

4.3 Discussion

4.3.1 The endogenous IFN response induced during HBV or HCV viral infections in chimeric mice

The majority of patients acutely infected with HBV or HCV are asymptomatic, thus current knowledge of the immune response induced at early stages of viral infection in HBV and HCV patients is poorly documented. In this chapter, I compared endogenous IFN induction throughout the courses of infections by HBV and HCV in chimeric mice produced with two different hepatocytes donors, Hu8063 and Hu8085 respectively. My results showed that the two viruses differ in the induction of endogenous IFN response in chimeric mice: HCV induced a spike of significant ISG response 10 days after inoculation, whereas no significant ISG response was detected throughout the entire course of HBV infection.

Although it is possible that some ISG expression was below the detection limit of RT-real time PCR, the lack of IFN response during the course of HBV infection in chimeric mice could be explained by the following scenarios: HBV in chimeric mice is a “stealth” virus that cannot be detected by the PRRs in human hepatocytes, and/or HBV efficiently suppresses the innate IFN response very early following infection. As mentioned in section 1.2.1.2 in Chapter 1, some aspects of the HBV life cycle support the concept that HBV behaves as a “stealth” virus because viral nucleic acid could “hide” from the host innate sensing machinery. For example, HBV viral replication occurs within nucleocapsids and the cccDNA is complexed with its host proteins in the nuclei to form a viral

minichromosome. However, HBV RNAs and proteins are expressed in the cytoplasm and would be accessible to cellular PRRs. Thus, it is possible that in addition to being “stealth”, HBV is able to actively block cellular defences.

Consistent with my results, intrahepatic gene expression profiling from liver biopsy samples taken from acutely HBV-infected chimpanzees showed that HBV failed to induce gene expression of any ISGs that relate to the entry and expansion of the virus [116], implicating the lack of PRR-mediated innate response during the early phase of HBV infection. In line with this observation, there was no induction of type I or type III IFNs in the sera of acutely infected HBV patients in clinical studies [117, 118]. However, the presence of innate immune responses following exposure to HBV is controversial. Activation of NK cells and NKT cells, measured by the expression of activation markers, such as CD69 and NKG2D, on cell surface, or NK and NKT cell cytotoxicity and IFN γ production, were observed before maximal HBV DNA elevation in two acute hepatitis B patients [118]. However there is also evidence suggesting that there was transient inhibition of NK and T-cell responses at the early stage of acute HBV infection in 21 patients, which may be attributed to the induction of the immunosuppressive cytokine IL-10 accompanying HBV viremia [117]. The NK and T-cell responses would be missed in our mouse model since a functioning human immune system is absent in the chimeric mice.

The intrahepatic immune response during the acute phase of HCV infection has been primarily studied in experimentally infected chimpanzees [204, 205, 208].

Induction of type I IFN ISGs was detected 5-8 weeks after inoculation in HCV infected chimpanzees. The extent and duration of ISG induction showed a positive correlation with viral load [208]. This is comparable to my observations in the chimeric mice that a spike of ISG expression upregulation was detected in chimeric mice 10 days after HCV infection, which was just before HCV levels in mouse sera stabilized (Figure 4.6B).

On the other hand, a subset of type I and III ISGs are constantly expressed at high levels in the liver of chronic hepatitis C patients, especially the patients not responding to pegIFN therapy [161]. I did not observe significant ISG upregulation or endogenous IFN induction during HCV long-term infection in the chimeric mice. This lack of IFN response in HCV-infected chimeric mice may be attributed to several factors. First, a complete immune system is absent in the chimeric mice as discussed in Chapter 3. Second, HCV replication occurs in subcellular compartments that are not accessible to host TLR dependent and/or RIG-I dependent sensory systems or antiviral ISG proteins. For example, the membranous web, in particular the double-membraned vesicles, has been described as an intracellular membrane structure where HCV replication takes place [150, 151]. A recent study investigating the roles of nuclear pore complex proteins (Nups) and nuclear transport factors (NTFs) in the membranous web during HCV infection suggested that in HCV infected cells, cytoplasmically positioned NPCs were predicted to form channels across double membrane structures of the membranous web. These NPCs are proposed to facilitate movement of NLS-containing proteins, such as HCV core, NS2, NS3, NS5A and

host nuclear proteins, from the surrounding cytoplasm across double membrane structures of the membranous web while excluding proteins lacking NLS sequences, such as PRRs, from regions of HCV replication and assembly events [152]. Third, HCV effectively antagonizes host antiviral responses by either directly blocking IFN signaling pathway with viral proteins or up-regulating cellular negative regulators to inhibit the IFN response. Many lines of evidence supporting the inhibitory effect of HCV on the innate immune response are derived from *in vitro* experiments in hepatoma cell lines. Evidence shows that the cleavage of MAVS in RIG-I signaling and TRIF in TLR3 pathway by NS3/4A protease of HCV is a crucial strategy HCV uses to evade the innate immune response [41, 196-198]. In our chimeric mice, HCV infection could have triggered ISG induction during early stages of HCV infection (< 10 days p.i). However, since during early time points, the human hepatocytes infected with HCV were only small proportion of the chimeric liver, gene transcription change in this relatively small number of infected cells may not be readily detected with the PCR method used in my study until day 10 p.i. Whereas after day 10 p.i, while increasing number of hepatocytes were infected by HCV, more HCV NS3/4A protein accumulated in the cells. Efficient inhibition of RIG-I and TLR3 pathways by HCV NS3/4A in the chimeric mouse livers could result in the lack of IFN and ISG response during long-term HCV infection.

4.3.2 The mechanisms of nonresponsiveness to exogenous IFN treatment differ between HBV and HCV

Interferon has been an important component in the treatment of both HBV and

HCV infections. IFN treatment is successful in a proportion of patients, but in majority of patients chronically infected with either HBV or HCV, IFN therapy alone is not effective.

The basic theory of IFN therapy is that administration of exogenous IFN activates the JAK-STAT pathway and leads to the establishment of an antiviral status, thereby eradicating the viral infection. The JAK-STAT signaling induces the expression of a large number of ISGs. The products of these ISGs are responsible for IFN α antiviral effects through two distinct yet complementary mechanisms: first, an antiviral effect resulting in direct inhibition of viral replication and second, immunomodulatory effects that enhance the host's adaptive antiviral immune response and may accelerate the clearance of infected cells. Evidence has shown that both HBV and HCV actively antagonizes host JAK-STAT pathway using various strategies summarized in section 1.1. In the chimeric mouse model, no significant ISG gene expression was detected during long-term infections with HBV or HCV. For the strains of HBV and HCV viruses I used in this study, neither of viruses responded to exogenous IFN treatment. Thus I investigated the molecular mechanisms of IFN nonresponsiveness of these two viruses in chimeric mice produced with an identical hepatocyte donor.

Several HBV proteins can interfere with JAK-STAT signaling and ISGs expression when overexpressed in cells: HBV surface and X proteins upregulate protein phosphatase 2A which inhibits IFN α signaling [315]; HBV precore/core proteins interact with the MxA promoter and inhibit its expression [316]. In line

with these results, I found that HBV infection resulted in significantly less upregulation of a number of ISGs in response to exogenous IFN treatment in chimeric mice than IFN treatment in uninfected controls. Two molecules that are important for successful expression of ISGs in the JAK-STAT pathway are STAT1 and STAT2. I examined the changes in the expression of these two genes in HBV-infected chimeric mice in comparison to the changes in uninfected control mice. Lower expression levels of both STAT1 and STAT2 were also observed not only in long-term HBV infected chimeric mouse livers, but also in HBV infected mice treated with exogenous IFN. Furthermore, immunohistological staining of human STAT1 in mouse livers showed that the nuclear translocation of STAT1, which was normally seen with IFN treatment, was inhibited in HBV infected mice but not in IFN-treated uninfected chimeric mice. The effect we observed in IFN-treated HBV infected chimeric mice were consistent with the observations in tissue cultures [317], liver biopsies of patients [124] and previously reported in chimeric mice [123]. My results support that HBV has evolved strategies to suppress type I IFN response and it is not simply a “stealth” virus.

In contrast to the studies of the HBV effect on the induction of ISGs, I did not observe inhibition of STAT1 transcription or blockage of STAT1 nuclear translocation in HCV-infected animals treated with IFN in donor-matched chimeric mice. This is not in agreement with the results in tissue culture systems, which showed that transient expression of full-length HCV and HCV subgenomic constructs corresponding to each of structural and the nonstructural proteins

impaired STAT1 activation by degradation of STAT1 protein [318] or inhibition of nuclear translocation of phosphorylated STAT1 [312]. It could be that our *in vivo* study system, which used an infectious clinical HCV strain, is different from the *in vitro* cell cultures where there is higher expression of viral proteins. My results suggested that the lack of response of this clinical HCV strain to IFN treatment was not the result of inactivation of JAK-STAT signaling transduction. It is possible that HCV replication occurs in subcellular compartments that are not accessible to antiviral proteins induced by IFNs, or there are certain viral intrinsic factors, such as IFN resistant mutations located at NS5A and core regions, which are responsible for the non-responsiveness of HCV to IFN treatment. Since the percentage of human hepatocytes infected with HCV in the liver of chimeric mice is most likely low, it is also possible that in chimeric mice, nuclear translocation of STAT1 was inhibited by HCV, but due to these infected cells were rare, they were not specifically addressed in mouse liver sections stained with antibodies against STAT1 and a human cytokeratin marker CK-18 in the confocal microscopy experiments (Figure 4.13). Confirmation by co-staining STAT1 with a HCV viral protein, such as HCV core or NS5A, is necessary. However, generation of a satisfactory laboratory protocol for HCV staining in my experimental samples presented challenges; I have tried five different HCV antibodies under various conditions, but in spite of the ability to see HCV infected cells in cultured cells, I could not make these antibodies work in the liver samples from chimeric mice. It could be that the HCV strain used in my experiments was a clinical isolate belonging to genotype 1a, whereas currently available antibodies

targeting HCV proteins are mostly raised against the JFH-1 strain (genotype 2a). I am continuing to look for anti-HCV sera that will work in our chimeric mice.

4.4 Summary

In this study, I did a comparative examination of HBV and HCV in the SCID/bg-Alb/uPA mouse model. Both of the two viral isolates used in this study were non-responsive to exogenous IFN treatment. I performed a detailed time course to investigate the induction of type I IFNs and ISGs in the chimeric mice for each infection. I found that there was no IFN or ISG response to HBV infection. In HCV infected animals, there was a peak of ISG response at day 10 p.i, but there was no significant IFN response detected in long-term HCV infection. A donor-matched mouse cohort was designed to compare the nonresponsiveness of each virus to exogenous IFN treatment. My results showed that there were differences in the way the two viruses blocked the host response to IFN treatment. One mechanism used by HBV was to actively antagonize host JAK-STAT pathway activation by suppressing expression of STAT1/2 and to block STAT1 nucleus translocation, thus controlling the upregulated expression of ISGs. Conversely, there was very little difference in the upregulation of the ISG expression observed in HCV infected chimeric mice treated with IFN compared to the uninfected control with IFN treatment. There was no significant change in STAT1/2 mRNAs or inhibition of STAT1 nucleus translocation detected, indicating that the nonresponsiveness of this HCV strain to IFN therapy was associated with intrinsic viral factors, which is consistent with the conclusion from Chapter 3.

CHAPTER 5

Collaborative Research Projects Using The SCID/Beige- Alb/uPA Chimeric Mice

5.1 The HCV PAMP RNA Induces Innate Immune Responses That Limit HCV Infection In Chimeric Mice

- The work is part of a collaborative project, named “*Functional Analysis of MAVS Function in Innate Immunity*” with Dr. Yueh-Ming Loo in Dr. Michael Gale Jr. laboratory in Seattle, USA.

5.1.1 Rationale

Innate immune defense is essential for the control of virus infection and is triggered through host recognition of viral macromolecular motifs known as PAMPs. HCV infection is regulated by hepatic immune defense triggered by the cellular RIG-I helicase [319]. RIG-I binds PAMP RNA and signals IRF3 activation to induce the expression of type I IFNs and ISGs that limit infection [320]. The HCV 3' NTR is comprised of three regions: a variable region with potential secondary structure, a non-structured polyU/UC region containing polyuridine with interspersed ribocytidine, and the terminal X region containing three conserved stem-loop structures [141]. It has been found that the 100-nucleotide polyU/UC region located in the 3' NTR of the HCV genome is the HCV PAMP motif that specifically engages and triggers RIG-I-dependent signaling of innate antiviral immunity [34]. As mentioned in Chapter 1, the helicase and repressor domain (RD) domains of RIG-I are important for the recognition of its RNA targets, while the CARD domains are essential for triggering intracellular signaling cascades. Interestingly, the structure of human RIG-I helicase-RD in complex with dsRNA was recently reported by Jiang, *et al* [321]. Their results show that the helicase-RD organizes into a ring around dsRNA, capping one end, while contacting both strands to recognize dsRNA. Limited proteolysis and differential scanning fluorimetry indicate that RIG-I is in an extended and flexible conformation that compacts upon binding RNA. On the other hand, it has also been found that double-stranded RNA regions of the HCV RNA, such as 5' NTR and X region of 3' NTR (XRNA), are not potent PAMPs

[34]. Our hypothesis is that HCV-infected SCID/bg-Alb/uPA chimeric mice treated with HCV 3' NTR polyU/UC as HCV PAMP, but not the infected mice treated with HCV XRNA, will mount innate immune responses that decreases the serum HCV RNA levels.

5.1.2 Results

5.1.2.1 HCV PAMP RNA, but not XRNA, induced an innate response in chimeric mice

An innate response induced by viral infection is characterized by the production of type I IFNs and the expression of ISGs with direct antiviral activity or the ability to modulate the immune response to effectively limit and control virus infections. In this study, the ability to induce an innate response with each of the RNA constructs administrated in chimeric mice was examined at intrahepatic levels in uninfected chimeric mice populated with hepatocyte donor Hu8085. Mice of matching age and hepatocyte donor were divided into 3 groups, each group received an i.p injection of 150µg of HCV XRNA, 150µg of HCV PAMP RNA or the same volume of PBS mixed in lipid-based *in vivo* transfection reagent. Eight hours after injection, mice were euthanized. The dosages for HCV PAMP RNA and XRNA as well as the timeline for termination of animals were determined based on the studies of west Nile virus infection in C57Bl/6 mice by Dr. Yueh-Ming Loo (unpublished data). The intrahepatic transcription level of ISGs or IFNs was measured by RT-PCR. Significant upregulation of ISGs was observed in chimeric mice transfected with HCV PAMP RNA in comparison to

the PBS control (Figure 5.1). In contrast, the delivery of the same amount of HCV XRNA showed no significant increase compared to the PBS treated control mice (Figure 5.1). Expression of endogenous IFNs was also examined. Upregulated expression of all three types of IFNs was consistently observed in chimeric mice transfected with HCV PAMP RNA in comparison to the mice treated with HCV XRNA or PBS, although the difference among these three groups was not statistically significant (Figure 5.2). The reason for this may have been because the IFN transcripts peaked earlier than most of ISGs and the 8-hour post treatment termination time point was too late to catch the very early IFN peak responses. In summary, these results suggest that *in vivo* introduction of HCV PAMP RNA induced an innate antiviral response in chimeric mice, whereas this response was not observed in chimeric mice treated with the same amount of XRNA.

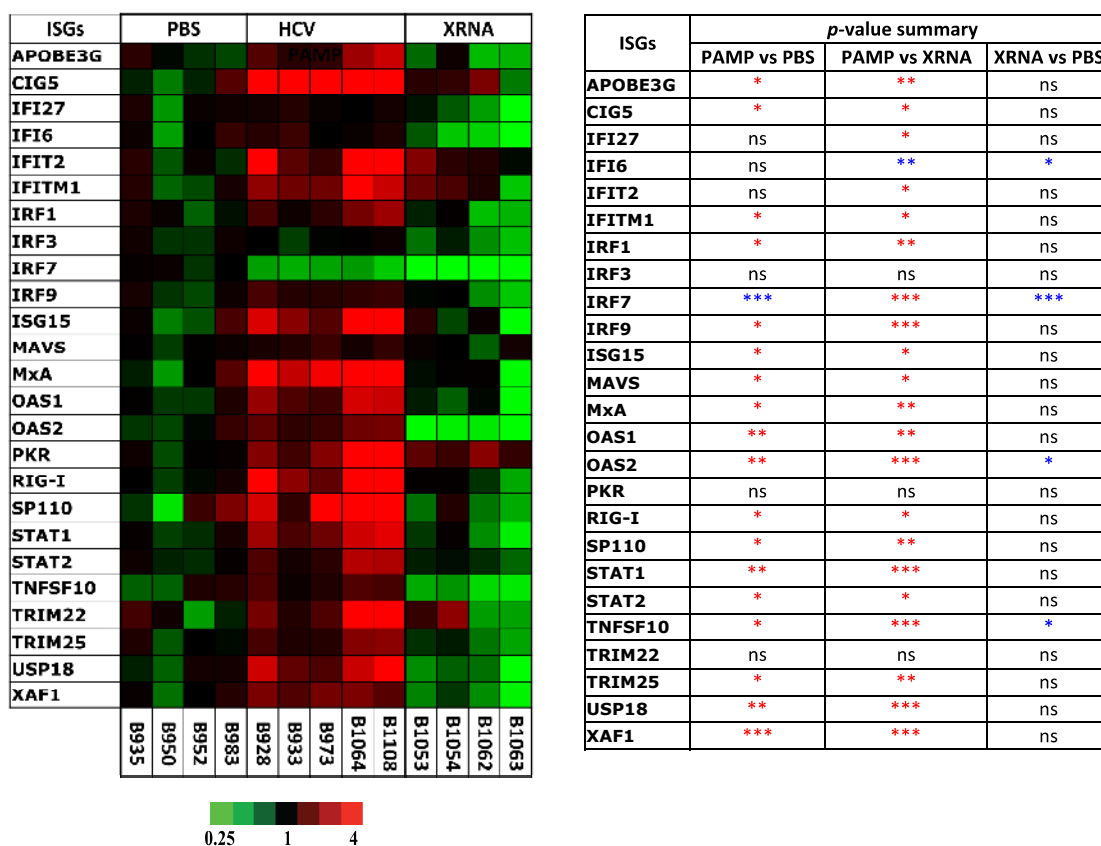


Figure 5.1 Expression of ISGs in chimeric mice transfected with HCV PAMP RNA or XRNA in comparison to the mice treated with PBS.

Total RNA isolated from the livers of chimeric mice transfected with HCV PAMP RNA, XRNA or PBS were examined for intrahepatic expression of ISGs by RT-realtime PCR. Oligos designed for each ISG are human specific. All mice were populated with a single hepatocyte donor, Hu8085. Results are shown as fold change relative to ISG expression in PBS-treated mouse controls. Left panel: Each column in the heatmap represents a single mouse in the respective treatment group. Increased and decreased expression of specific genes compared to the control is shown by red (Fold >1 - ≥4) and green (Fold <1 - ≤0.25), respectively, whereas black indicates no change (Fold =1). Right panel: *P*-values for each comparison were calculated by one-way ANOVA. Significantly upregulated and downregulate expression ($p < 0.05$) of ISGs is indicated by text-highlighting the *P*-value summary in red and blue respectively. Black shows no significant difference ($p \geq 0.05$).

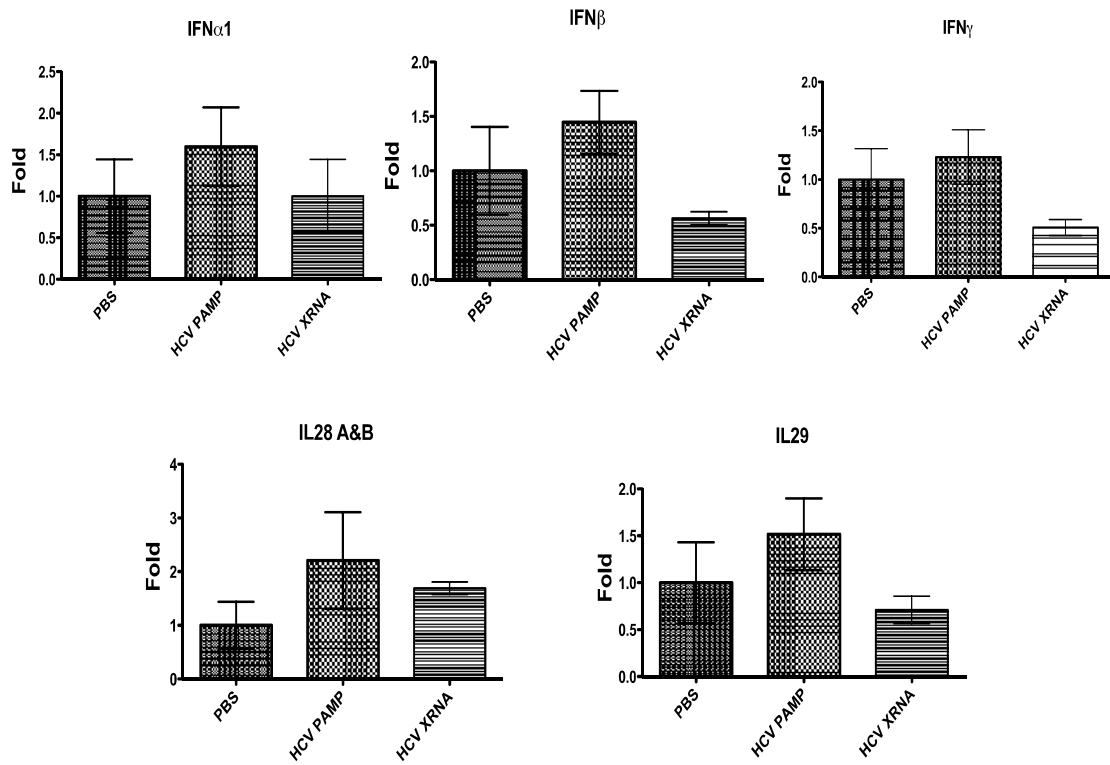


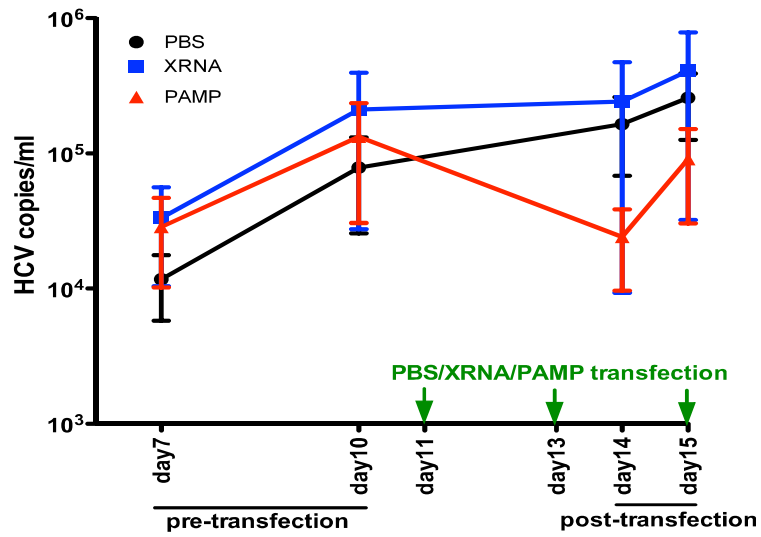
Figure 5.2 Expression of IFNs in chimeric mice transfected with HCV PAMP RNA or HCV XRNA in comparison to the mice treated with PBS.

The same mouse liver RNA samples from Figure 5.1 were analyzed for intrahepatic expression of IFNs. Oligos designed for each IFN are human specific. Results are shown as fold change relative to IFN expression in PBS-treated mice. Data were indicated as mean \pm SEM; n = 4-5.

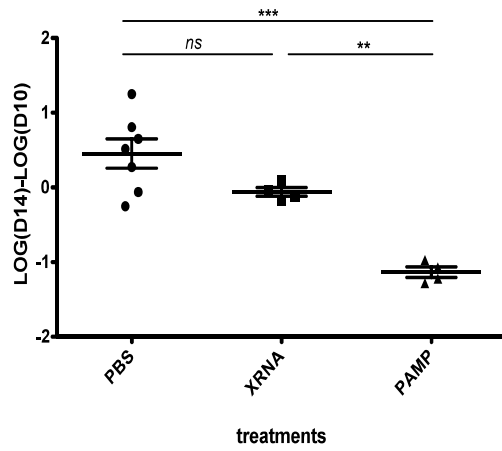
5.1.2.2 The innate response triggered by HCV PAMP RNA limits chimeric mice from HCV infection

HCV PAMP RNA, as a RIG-I agonist, triggers an innate immune response in chimeric mice. We next hypothesized that the HCV PAMP RNA might be useful as an antiviral therapy in treating HCV infection. To test this hypothesis, chimeric mice populated with the same hepatocyte donor, Hu8085, as described in section 5.1.2.1, were inoculated with an IFN sensitive HCV strain, HCV gt2b (Table 3.1). The infected mice were transfected with 150µg of HCV PAMP RNA, 150µg of HCV XRNA or equal volume of PBS mixed in lipid-based *in vivo* transfection reagent at days 11, 13 and 15 post-infection. HCV serum RNA levels were measured by RT-qPCR. A significant decline of HCV viremia, after administration of HCV PAMP RNA at day 14 (Figure 5.3B) and day 15 (Figure 5.3C) p.i in comparison to the viremia prior to treatment at day 10 p.i., was observed in infected mice transfected with HCV PAMP RNA. This decline was not seen in HCV-infected chimeric mice treated with XRNA or PBS (Figure 5.3), indicating the innate response induced by HCV PAMP RNA may play a role in limiting HCV infection in the chimeric mouse livers.

A



B



C

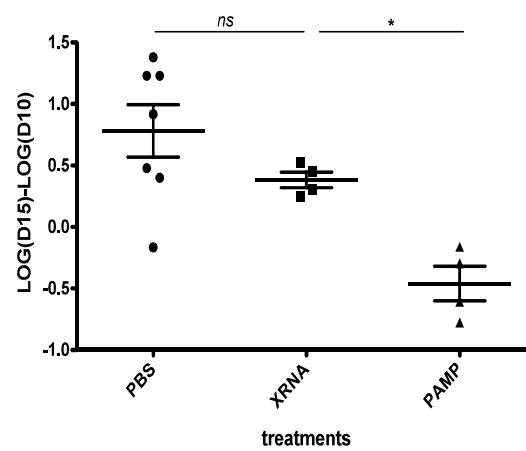


Figure 5.3 HCV viremia change after administration of HCV PAMP RNA, HCV XRNA or PBS in chimeric mice infected with HCV.

Chimeric mice, produced with a single hepatocyte donor Hu8085, were infected with HCVgt2b strain for 10 days. Three dosages of PBS, HCV XRNA or HCV PAMP RNA were then administrated in mixture with lipid-based *in vivo* transfection reagent by i.p injection every other day starting at day-11 p.i.. Mice were bled at days 7, 10, 14 and 15 p.i for viremia measurements by RT-qPCR. Each sample was quantified in duplicate. Data are presents as mean \pm SEM. n= 4-7. *P*-values were calculated by one-way ANOVA.

(A) HCV serum RNA changes from day-7 to day-15 p.i. of HCV infection in chimeric mice. Three treatments with PBS/HCV XRNA/HCV PAMP RNA are indicated by green arrows. Day-7 and 10 are prior to treatments, and day-14 and 15 are after treatment.

(B) Statistical comparison of HCV viremia change in each treatment between day-10 and day-14 p.i of HCV infection in chimeric mice.

(C) Statistical comparison of HCV viremia change in each treatment between day-10 and day-15 p.i of HCV infection in chimeric mice.

5.1.3 Discussion

A number of studies have shown that RIG-I signaling is essential for the control of virus infection and immunity *in vivo* [322, 323]. In this study, we have provided evidence that by selectively triggering RIG-I-dependent signaling with a RIG-I-specific agonist, HCV PAMP RNA, an antiviral response can be effectively elicited in the livers of chimeric mice to limit HCV infection.

Compared to the treatment with exogenous IFN on chimeric mice infected with the same HCVgt2b strain in experiments described in Chapter 3, HCV viremia decline was not as dramatic in mice treated with HCV PAMP RNA. It is likely that the three dosages of HCV PAMP RNA administration over the course of five days were not as effective in treatment of HCV infection as daily injection of exogenous IFN for two weeks. As described in section 1.3.3 in Chapter 1, three PRRs, RIG-I, TLR3 and PKR, are critical in HCV recognition to active an innate immune signaling and type I IFN production. It could also be that activation of TLR3 and/or PKR pathways is indispensable besides RIG-I signaling for effective control of HCV replication. In addition, HCV NS3/4A protease is a crucial component HCV uses to evade the innate immune response by targeting both MAVS in the RIG-I signaling pathway and TRIF in the TLR3 pathway. Based on the study of endogenous IFN response induced during the course of HCV infection in chimeric mice in Chapter 4, ISG expression elevated at day-10 p.i and then decreased to the levels of ISGs seen in uninfected controls during the later stages of the infection. This result suggested that it required about 10 days for

HCV to produce enough amount of NS3/4A protease to effectively control the IFN signaling. Administration of HCV PAMP RNA in mice infected with HCV at days 11, 13 and 15 p.i was most likely at the same time when sufficient amount NS3/4A was generated to antagonize host innate response. This therefore may also contribute to the fact that treatment with HCV PAMP RNA was less effective than treatment with exogenous IFN in this time interval.

5.1.4 Summary

In this study, the potential antiviral activity of exogenous HCV PAMP RNA was investigated in HCV-infected SCID/bg-Alb/uPA chimeric mice. We first examined the innate immune response induced by transfecting HCV PAMP RNA into uninfected chimeric mice in comparison to the control HCV RNA of equivalent length, HCV XRNA. As expected, increased IFN transcripts and significant upregulation of ISGs were observed in chimeric mice transfected with HCV PAMP RNA, but not in mice receiving XRNA. The potential antiviral effect of HCV PAMP RNA was then studied in donor-matched chimeric mice infected with HCV. Significant viremia decline was only observed in HCV-infected chimeric mice when HCV PAMP RNA was administered as compared to administration of XRNA or PBS to HCV-infected chimeric mice. In summary, our data suggest that HCV PAMP RNA administration can elicit an innate immune response in the livers of chimeric mice, which limits HCV infection. These results provide evidence that HCV PAMP RNA could be a good therapeutic agent for the development of novel antiviral treatments.

5.2 HCV Infection in Chimeric Mice Induced Up-Regulation of MicroRNA-27: A Novel Mechanism for Hepatic Steatosis

- This work is part of a collaborative project with Ragunath Singaravelu, a PhD student in Dr. John Paul Pezacki laboratory in Ottawa, Canada.

- A version of this data are published in: *Singaravelu R, Chen R, Lyn RK, Jones DM, O'Hara S, Rouleau Y, Cheng J, Srinivasan P, Nasheri N, Russell RS, Tyrrell DL, Pezacki JP. Hepatitis C virus induced up-regulation of microRNA-27: A novel mechanism for hepatic steatosis. Hepatology. 2014 Jan;59(1):98-108.*

5.2.1 Rationale

MicroRNAs (miRNAs) are a class of endogenously synthesized small non-coding RNAs approximately 20-25 nucleotides in length. They regulate gene expression by targeting mRNAs for translational repression or degradation by cleavage. Due to their regulatory function, miRNAs can help to shape host transcriptomes and proteomes, and thus play a critical role in cellular physiology. They are involved in the fine-tuning and modulation of host genes in a broad range of biological pathways in the eukaryotic cell, including cellular development, differentiation, proliferation, metabolism, maintenance, immunity, and death [324-326]. Because of their understood role in numerous crucial cellular functions, dysregulation of miRNAs is associated with a variety of human diseases including cancer and virally induced illnesses [327, 328].

Several viruses, such as HIV and HCV, modulate the host miRNAs for their pathogenesis. One such miRNA involved in HCV life cycle is miR-122. The miR-122 is a liver-specific miRNA that makes up approximately 70 % of all miRNAs in the liver [329, 330]. The miR-122 has been identified as a host factor required for efficient replication and viral production of HCV [331, 332]. Besides miR-122, other host miRNAs, such as miR-199a [333], miR-141 [334], miR-196 [335], miR-29 [336], Let-7b [337], and miR-130a [338], are also reported to be modulated by HCV to promote its replication or pathogenesis. Hepatic miRNAs can influence HCV either through direct interactions with the viral genome or regulation of HCV-associated host pathways.

HCV is described as a lipotropic virus because of its close association with serum lipoprotein. HCV-induced modulations of lipid metabolism include increased cellular triglyceride and cholesterol storage to facilitate viral replication [339-341]. HCV utilizes the low-density lipoprotein (LDL) receptor for cellular entry [342-344] and forms replication complexes on lipid rafts [345]. The HCV core protein surrounds and binds LDs [346]. Moreover, HCV particle assembly and secretion also use components of the very-low density lipoprotein (VLDL) pathway [347]. In addition, steatosis is often observed in CHC in liver tissue histology.

However, miRNAs that regulate lipid metabolism and HCV replication have not been reported until recently [348]. MiR-27 represents another liver-abundant miRNA [349]. Its role in HCV pathogenesis is poorly understood. MiR-27 regulates lipid metabolism in adipocytes and macrophages and is implicated in atherosclerosis [350]. In hepatoma cells, miR-27 has been shown to regulate many lipid metabolism-related transcription factors, such as retinoid X receptor α (RXR α), peroxisome proliferator-activated receptor alpha (PPAR α), PPAR γ , *fatty acid synthase* (FASN), sterol regulatory element-binding protein 1 (SREBP1) and SREBP2 [348]. Furthermore, miR-27 is deregulated in liver metabolic disorders [351-353], suggesting it plays a role in hepatic lipid metabolism, a critical host pathway hijacked by HCV to facilitate its lifecycle and pathogenesis [339, 340].

Due to this intimate association of both HCV and miR-27 with hepatic metabolism, the hypothesis of this study was that HCV infection in chimeric mice

enhances miR-27 expression and results in upregulating hepatic LD biogenesis.

5.2.2 Results

5.2.2.1 HCV infection activates miR-27 expression in chimeric mice

There are two isoforms of miR-27, miR-27a and miR-27b, encoded by separate gene loci and differing by one nucleotide (Figure 5.4). The single nucleotide difference in miR-27 sequences is conserved across species (Figure 5.4). We first examined whether HCV infection induces the expression of either miR-27 isoform in SCID/bg-Alb/uPA chimeric mice. As shown in Figure 5.5, two HCV clinical isolates of different genotypes, HCVgt1a and HCVgt2b (described in Table 3.1 in Chapter 3), were used to infect 10 chimeric mice populated with two different hepatocyte donors, Hu8063 (4 mice) and Hu8085 (6 mice). Chimeric mice of matching age and hepatocyte donor were mock infected with serum from a healthy adult (HBV-, HCV- and HIV-negative) as controls. Mock- or HCV-infected chimeric mice were terminated at two different infection time points, 21-day and 7-week p.i. Successful HCV infection was confirmed by measuring HCV serum and intrahepatic RNA levels using RT-qPCR (Figure 5.5). Expression levels of miR-27a and miR-27b in chimeric mouse livers were analyzed by RT-qPCR. Our result revealed a 2.9-fold upregulation in miR-27b levels 7 weeks after HCV infection was initiated (Figure 5.6A). This increase was conserved across both HCV genotypes examined. There was also a 2-fold increase in miR-27a levels (Figure 5.6B) in HCV-infected chimeric mouse livers in comparison to the mock controls. In summary, our results showed that HCV infection in chimeric mice enhanced intrahepatic expression levels of both miR-27a and miR-27b.

<i>hsa-miR-27a</i>	uucacaguggcuaaguuccgc
<i>mmu-miR-27a</i>	uucacaguggcuaaguuccgc
<i>rno-miR-27a</i>	uucacaguggcuaaguuccgc
<i>ptr-miR-27a</i>	uucacaguggcuaaguuccgcc
<i>cfa-miR-27a</i>	uucacaguggcuaaguuccg
<i>hsa-miR-27b</i>	uucacaguggcuaaguucugc
<i>mmu-miR-27b</i>	uucacaguggcuaaguucugc
<i>rno-miR-27b</i>	uucacaguggcuaaguucugc
<i>ptr-miR-27b</i>	uucacaguggcuaaguucugc
<i>cfa-miR-27b</i>	uucacaguggcuaaguucugc

Figure 5.4 MiR-27 isoforms and conservation of sequence.

Sequences of both isoforms of miR-27 (a and b) are depicted. The single nucleotide difference in miRNA-27 sequences is conserved across species and is highlighted.

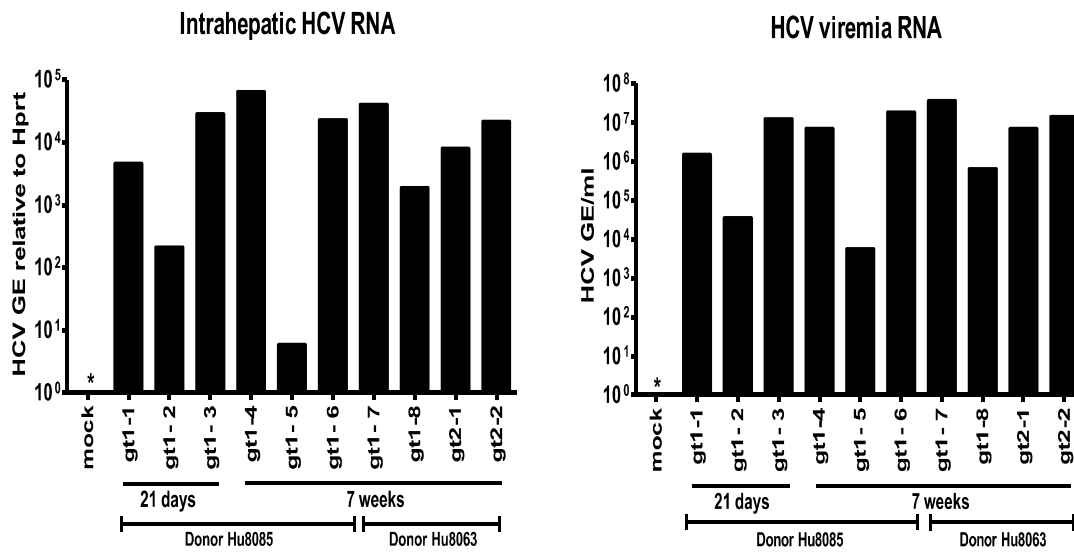


Figure 5.5 HCV infection in chimeric mice.

Chimeric mice were infected with two clinical isolates of HCVgt1a or HCVgt2b and serum/liver samples were taken at either 21 days or 7 weeks p.i. Each bar corresponds to an individual infected mouse. Chimeric mice produced with two sets of donor hepatocytes, Hu8085 and Hu8063, were used for this study. Viremia RNA levels are shown in GE/mL while intrahepatic HCV RNA levels were normalized by HPRT-1 expression levels, as described in Chapter 2.

Left panel :Intrahepatic HCV RNA.

Right panel: HCV viremia RNA.

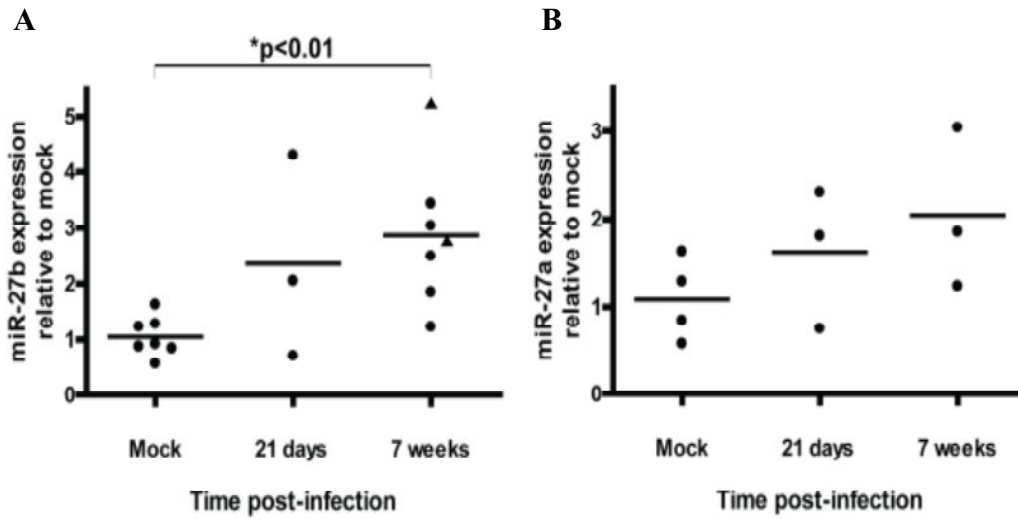


Figure 5.6 HCV infection enhances miR-27 expression in chimeric mice.

Chimeric mice were infected with clinical isolates of HCV genotypes 1a(●) and 2b (▲). Total RNA was isolated from mock- or HCV-infected mice 21 days and 7 weeks postinfection, and RT-qPCR was used to measure the relative expression of miR-27b (A) and miR-27a (B). Expression levels for each trial were normalized to the average for mock-infected mice. Results are displayed in a vertical scatterplot with the average expression denoted by a horizontal line.

Note: this experiment was performed by our collaborator, Ragunath Singaravelu.

5.2.2.2 HCV infection caused increased cellular LDs in chimeric mice

As mentioned in Rationale, miR-27 regulates lipid metabolism. Dysregulation of miR-27 results in liver metabolic disorders, suggesting it plays a role in hepatic lipid metabolism.

Our collaborator, Ragunath Singaravelu, examined whether miR-27 plays a regulatory role for lipid metabolism in Huh7 cells by transfecting with control or miR-27 mimics and inhibitors and measuring the effects. He used coherent anti-Stokes Raman scattering (CARS) microscopy, a modern multiphoton imaging method, to image miR-27 influence on hepatic lipid content in a highly effective manner [354]. CARS has been used extensively for label-free imaging and quantification of hepatic lipid content in biological systems, thereby avoiding perturbations and artifacts that can be introduced by added dyes and staining protocols [354, 355]. His results showed that transfection of miR-27a and miR-27b mimics in Huh-7 cells induced an increase in both the size and abundance of LDs (Figure 5.7), demonstrating a correlation between accumulation of hepatic LDs with increased expression of miR-27.

Having known that HCV infection in chimeric mice induces miR-27 expression, and in cultured hepatoma cells, increased expression of miR-27 is associated with the accumulation of hepatic LDs. I was interested to study whether HCV infection in chimeric mice causes increased LD accumulation. I used a classic histochemical stain, oil red O, to visualize LDs in chimeric mouse livers in combination with immunolabelling a human specific marker CK-18 [291]. Frozen

sections of liver samples from mock- or HCVgt1a-infected chimeric mice were used for staining. Two time points were examined for HCV infection, 21 days and 7 weeks p.i. Accumulation of cellular LDs was visualized in the livers of HCV infected chimeric mice in comparison to the mock-infected animals (Figure 5.8). A correlation of increased amount of intrahepatic LDs with longer period of HCV infection was also observed. In summary, our results indicated an association between HCV infection and increased LD accumulation in chimeric mice.

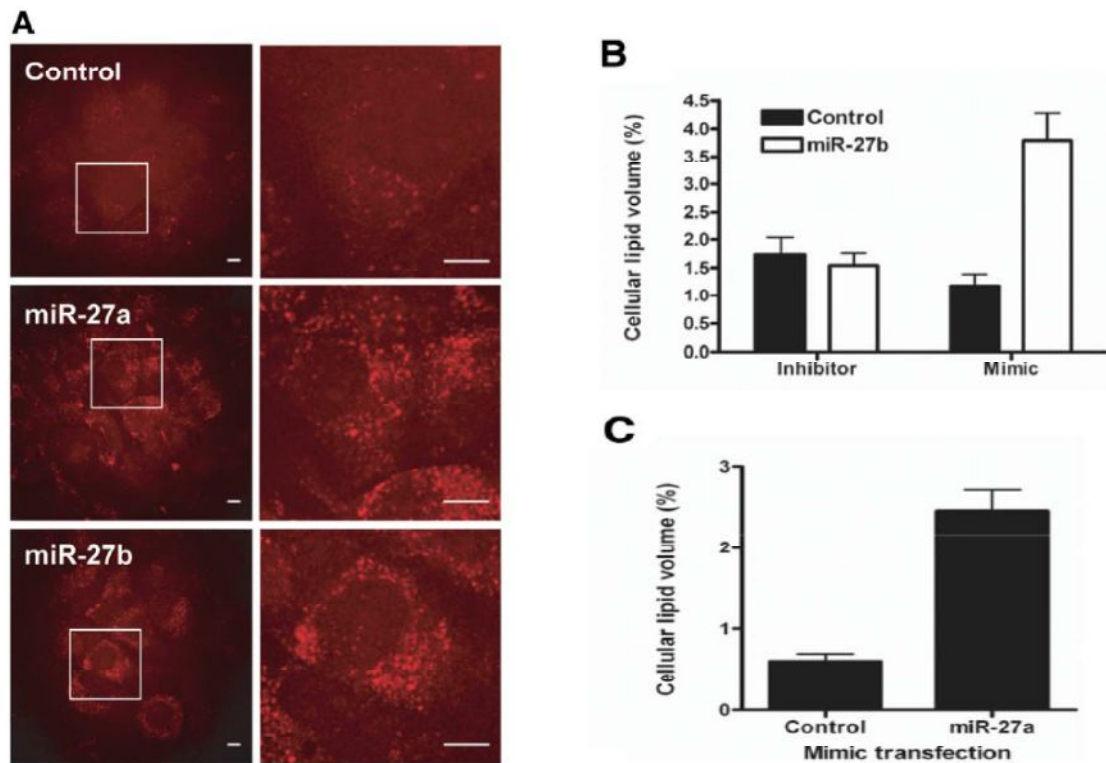


Figure 5.7 MiR-27 regulates hepatic lipid homeostasis.

Huh7 cells were transfected with 20nM miR-27a, miR-27b, or control mimics and inhibitors. Cells were fixed 48 hours posttransfection. (A) Representative CARS images of mimic transfected cells are shown. Scale bars =10 μ m. The results of voxel analysis are shown in (B,C) as percentage cellular lipid volume. Voxel analysis is representative of $n \geq 75$ cells from two biological replicates. Error bars represent the standard error of the mean.

Note: this experiment was performed by our collaborator, Ragunath Singaravelu.

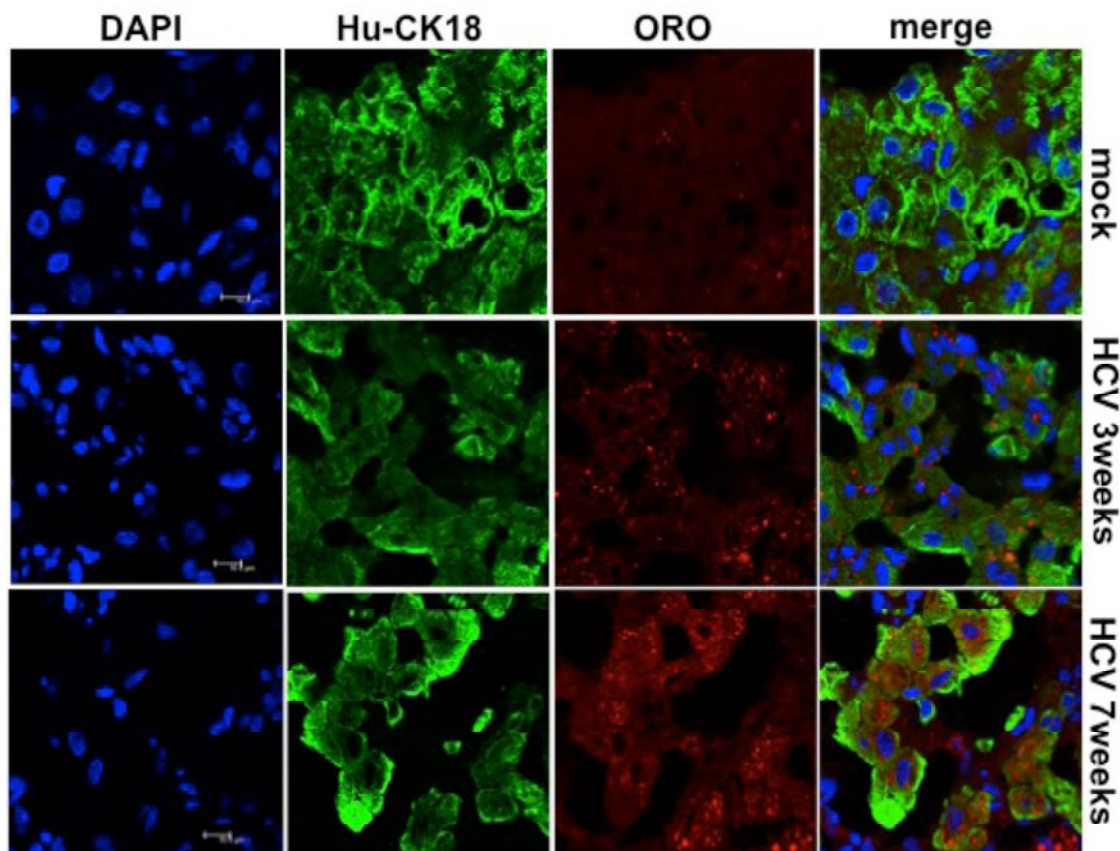


Figure 5.8 Changes of cellular lipid levels by HCV infection in chimeric mice. Oil red O staining of LDs in mice liver cross-sections are shown in red. Human CK-18 immunostaining was used as marker of human hepatocytes (green). Nuclear DNA was stained with DAPI (blue). Images were acquired with a confocal microscope. Scale bars =10 μ m. Representative images are shown from three mice. For each mouse, at least three regions of interest were analyzed.

5.2.3 Discussion

MiRNAs play an important role in various biological processes, and are also involved in infections and diseases, such as HCV infection. Several host miRNAs have been identified in relationships with the HCV life cycle to promote its replication or pathogenesis as mentioned previously in rationale section. However, miRNAs that regulate lipid metabolism and HCV replication are poorly understood. To date, miR-27 is the only one that has been reported [348, 356]. In this study, we have shown that HCV infection in chimeric mice upregulated miR-27 expression, which led to upregulated hepatic LD biogenesis.

Two target genes of miR-27, PPAR- α and angiopoietin-like protein 3 (ANGPTL3), were predicted by a computer software and further confirmed experimentally by measuring the change of mRNA levels of PPAR- α and ANGPTL3 in Huh-7.5 cells transfected with miR-27b mimics by our collaborators. They found decreased mRNA levels of PPAR- α and ANGPTL3 in cells overexpressing miR-27 mimics, suggesting miR-27 regulated PPAR- α or ANGPTL3 at the RNA level. It is known that both PPAR- α and ANGPTL3 are associated with lipid metabolism signaling pathways. PPAR- α is a key nuclear receptor that transcriptionally activates genes associated with fatty acid oxidation [357]. ANGPTL3 is expressed by the liver [358] and secreted into circulation [359]. Studies have shown that ANGPTL3 suppresses the activity of lipoprotein lipase, which regulates triglyceride levels in circulation [360]. Based on the observations made by us using chimeric mice and by our collaborators using

Huh7.5 cells, a novel mechanism was proposed, by which HCV-induced miR-27 overexpression promoted steatosis. In this model, HCV infection induces miR-27 overexpression, which leads to down-regulation of miR-27 mRNA targets: ANGPTL3 and PPAR- α . Antagonism of PPAR- α signaling by miR-27 results in increased cellular triglyceride content. Decreased ANGPTL3 levels by increased miR-27 expression in HCV infection would result in increased activity of lipoprotein lipase, which regulates triglyceride levels. The latter mechanism could also account for further accumulation of triglycerides.

In agreement with our results, another group studying activation of miR-27a expression by HCV infection observed that the expression of miR-27a was upregulated more in CHC liver than in CHB liver and identified a correlation between miR-27a expression and severity of steatosis in CHC patients [348]. They also showed that the expression of many lipid metabolism-related genes, including PPAR- α , was repressed by miR-27 in Huh-7.5 cells [348]. In addition, it is interesting to note that the assessment of miR-27a expression in patients receiving pegIFN and RBV therapy by the same group showed that CHC patients with high miR-27a levels in the liver had a more favorable treatment response [348]. They also demonstrated that miR-27a significantly enhanced IFN signaling in Huh-7.5 cells [348]. Therefore, they suggested that miR-27 might have therapeutic benefits in combination with IFN therapy, especially in patients with the IFN-nonresponsive IL-28B genotype, who show a more severe steatosis than those with the IFN-sensitive IL-28B genotype [361-365].

Finally, to the best of our knowledge, our study represents the first report visualizing HCV-induced hepatic lipid accumulation in SCID/bg-Alb/uPA mice, highlighting the utility of the model for studying HCV-associated steatosis.

5.2.4 Summary

In this study, we have shown that HCV infection enhanced miR-27 expression in chimeric mice, and this was conserved across genotypes. HCV infection was also associated with increased accumulation of hepatic LDs in chimeric mice. Together with the data from our collaborators, our results suggested that HCV-induced miR-27 expression, and the resultant down-regulation of PPAR- α and ANGPTL3, represented a novel mechanism by which HCV induced steatosis.

CHAPTER 6

Project Overview, Conclusion and Future Directions

6.1 Project overview and general discussion

Both HCV and HBV infections represent major global public health problems. According to WHO 2013 data sheets [80, 154], more than 240 million and 150 million people worldwide are currently chronically infected with HBV and HCV respectively. About 1 million people die every year due to acute or chronic HBV and HCV infections primarily from the adverse outcomes of cirrhosis and HCC. Interferon response has been shown to be crucial to viral pathogenesis. In addition, interferon has been a significant component of the treatment for both HBV and HCV infections. In this thesis, the role of interferon responses in HBV and HCV infections were studied using the SCID/bg-Alb/uPA chimeric mouse model.

The majority of patients acutely infected with HCV are asymptomatic, thus current knowledge of the immune response induced at early stages of viral infection in HCV patients is poorly documented. A detailed time course study of HCV infection was performed in SCID/bg-Alb/uPA chimeric mice to detect an induced endogenous IFN response by measuring changes in the transcription of human ISGs in correlation with the changes of viral parameters. I did not observe any significant ISG stimulation in HCV infection other than a spike of ISG response at day-10 post infection in HCV infected chimeric mice. The upregulated ISG response detected in chimeric mice 10 days after HCV inoculation is comparable to the observations made in HCV infected chimpanzees in which induction of type I IFN ISGs was detected 5-8 weeks after inoculation

and the extent and duration of ISG induction was positively correlated with viral load [208].

However, the lack of an IFN response in long-term HCV infection in the chimeric mice in my studies is in contrast to our previous observations in the chimeric mice by *Walters, et al.* showing an ISG response in HCV infected chimeric mice [284]. The difference between these two studies may be accounted for the lack of beige trait in the study by *Walters, et al.*, which led to more mouse NK cell function. In addition, different human hepatocyte sources were used: commercial cryopreserved human hepatocytes were used in my studies, whereas fresh human hepatocytes isolated from liver tissues were used in *the study by Walters, et al.* Fresh human hepatocytes preparations may contain other liver cell types, such as dendritic cells and Kupffer cells, that may have been important in the production of an ISG response.

The absence of significant ISG upregulation during long-term HCV infection in chimeric mice is also in contrast to the results of upregulated ISG expression reported in CHC patient studies [161]. These results of HCV infection in my studies may be due to the lack of a functional immune system in the mouse model.

Despite the lack of ISG upregulation in chimeric mice chronically infected with HCV, administration of HCV PAMP RNA elicited a significant ISG response in the livers of chimeric mice. These observations suggested that HCV virus could effectively inhibit host antiviral response, which is most likely contributed by

HCV NS3/4A protease that targets both MAVS in the RIG-I signaling pathway and TRIF in the TLR3 pathway. Although HCV NS3/4A protease is a crucial component that HCV uses to evade the innate immune response, evidence from my studies in chimeric mice showed that HCV PAMP RNA administration limited HCV infection. This is most likely because administration of HCV PAMP RNA induced IFN signaling not only in the hepatocytes infected with HCV, which are only a proportion of human hepatocytes where HCV NS3/4A protease was able to execute its inhibitory function on IFN signaling, but also in cells that were virus-free. IFNs released from these HCV-free cells bind to IFNARs presented on hepatocytes infected with HCV and stimulated JAK-STAT pathway that controlled HCV infection.

However, in comparison to the treatment with exogenous IFN on HCV-infected chimeric mice, HCV viremia decline was not as much in mice infected with the same HCV strain and treated with HCV PAMP RNA. This could be due to the fact that effective control of HCV infection requires activation of three pathways, TLR3, PKR and RIG-I pathways. HCV PAMP RNA activates only RIG-I pathway. Alternatively, HCV PAMP RNA activates RIG-I signaling which is targeted by HCV NS3/4A protease in HCV-infected hepatocytes, whereas exogenous IFN treatment stimulates signal transduction from IFNARs which is downstream of RIG-I signaling and not inhibited by HCV NS3/4A protease.

Interferon has been used in treatments for HCV infection for years. Unfortunately, a good proportion of patients do not respond adequately to IFN therapy. What

causes the nonresponsiveness to IFN therapy during HCV infection remains unclear. Evidence suggests that factors determining the response to IFN therapy likely include both host and viral factors. However, it has been a great challenge to evaluate the relative contributions of these host and viral factors to IFN nonresponsiveness in HCV infection. One of the unique opportunities offered by the SCID/bg-Alb/uPA mouse model that particularly interested me is the ability to separate viral and host factors in studies of HCV infection; we can study infections by different strains of HCV in animals populated with hepatocytes from the same donor, or to use the same HCV virus to infect the mice transplanted with hepatocytes from different donors. This enabled me to control the variables in the examination of virus-host interactions and to dissect the contributions of host and viral factors in the response to IFN treatment. Several HCV clinical isolates differing in their genotype and IFN-sensitivity were used to investigate the contributions of viral factors to IFN treatment response in the SCID/bg-Alb/uPA mouse model. I found that although it was not possible to produce chimeric mice with hepatocytes from individual patients, the response of each patient HCV isolate to IFN therapy showed a good correlation to the IFN response in the HCV-infected chimeric mice produced with cryopreserved human hepatocytes. This suggested that intrinsic viral factors had a profound effect on the response to IFN treatment. I had predicted that distinct sensitivity of HCV strains to IFN α therapy would be due to different suppressive effects of nonresponsive and responsive HCV strains on the host JAK-STAT pathway. Surprisingly, my results showed that both IFN-nonresponsive and IFN-sensitive HCV strains had minimal

inhibitory effects on the JAK-STAT pathway in the chimeric mouse model. This result was also supported by the observations described in Chapter 4 that IFN treatment led to significant upregulation of STAT1/2 mRNAs and nuclear translocation of STAT1 in the livers of chimeric mice infected with an IFN-nonresponsive HCV strain. Therefore, my results suggested that HCV sensitivity to IFN α therapy was not critically associated with viral interference with host IFN signaling downstream of IFN receptors in this mouse model. In addition, host factors affecting IFN therapy treatment outcomes, such as liver ISG expression prior to IFN therapy and the hepatocyte donor SNPs at two IL28B loci, were studied. In contrast to the results found in patients, where an up-regulation of a subset of ISGs before treatment is strongly associated with nonresponsiveness to exogenous IFN therapy, there was no significant upregulation of human endogenous type I and III IFNs or ISGs in chimeric mice chronically infected by either of the IFN-nonresponsive and IFN-sensitive HCV strains. This observation suggested that the upregulation of ISGs in chronically infected HCV patients could be the result of ISG expression in other cell types rather than in hepatocytes, such as pDCs and Kupffer cells, or the result of direct or indirect interactions between hepatocytes and other cell types. In the studies on the effects of the hepatocyte donor SNPs at two IL28B loci on IFN therapy treatment outcomes, I used two HCV isolates with distinct IFN-sensitivities and infected mice produced with hepatocyte donors carrying three different IL28B SNPs including both “favorable” and “unfavorable” IFN response genotypes. Surprisingly, the variants of the IL28B SNPs in donor hepatocytes had little or no

influence on the response outcome to IFN treatment under immunosuppressive conditions of the SCID/beige trait in our chimeric mice, suggesting that the association of IL28B SNPs with response to IFN treatment found in patient studies may be very dependent on a complete immune system.

In addition to the functional analysis of IFN response in chimeric mice infected with HCV, the role of IFN response in HBV infection was also investigated in chimeric mice in this thesis.

Similarly to the HCV study, a time course of HBV infection was performed in SCID/bg-Alb/uPA chimeric mice to detect an induced endogenous IFN response. No significant ISG stimulation was observed during the entire course of HBV infection, which is consistent with the studies in HBV-infected chimpanzees [116] and humans [117, 118]. The lack of IFN response during the course of HBV infection in chimeric mice could be because HBV in chimeric mice is a “stealth” virus that cannot be detected by the PRRs in human hepatocytes, and/or HBV efficiently suppresses the innate IFN response very early following infection.

Lastly, the molecular mechanism responsible for nonresponsiveness of HBV and HCV to exogenous IFN treatment was investigated in a cohort of donor-matched chimeric mice. Nonresponsiveness to exogenous IFN treatment was mediated by different distinct mechanisms by the two viruses: HBV inhibited STAT1 transcription and nuclear translocation upon IFN stimulation, and thus downregulated the expression of ISGs. Whereas, no significant downregulation of ISG expression was observed in HCV-infected mouse livers upon IFN treatment,

nor was a change in STAT1 transcription or nuclear translocation detected. These results suggest that there are certain viral intrinsic factors, which are responsible for the non-responsiveness of HCV to IFN treatment.

In addition, response to IFN treatment in CHC and CHB patients show different patterns. Patients infected with HCV that respond usually show a rapid viremia decline within 2-4 weeks, whereas response to IFN treatment in HBV patients with chronic infection often do not show significant viral load decrease until 8-12 weeks after the initiation of IFN. In HBV patients responding to IFN therapy, viremia decline is usually correlated with a spike of liver enzymes, indicating stimulated hepatotoxicity, followed by normalized enzyme levels and drop in HBV load. These observations suggest that the effect of IFN therapy on HBV and HCV infections in patients is likely through different mechanisms: innate response elicited in the liver by IFN therapy is critical in eliminating responsive strains of HCV, whereas the IFN effect on HBV in chronically infected patients is not affected by the innate response directly and very dependent on an adaptive immunity.

6.2 Conclusion

A robust interferon response is crucial to the clearance of viral infections, including HBV or HCV infection of the liver.

Induced endogenous IFN response was studied during the course of HCV infection in chimeric mice. Other than a spike of ISG response at day-10 post

infection, no significant ISG stimulation in HCV infected chimeric mice was observed. Several host and viral factors that have been shown associated with the outcome to IFN therapy in CHC patients were evaluated in chimeric mice. I found that viral interference with host IFN signaling as well as host factors, such as polymorphisms at the IL28B loci and pre-treatment levels of ISG expression, had less impact than the HCV intrinsic viral factors in determining the response to exogenous IFN treatment in the chimeric mouse model.

In chimeric mice infected with HBV, no induced endogenous IFN response was detected during the entire course of HBV infection.

The molecular mechanism responsible for nonresponsiveness of HBV and HCV to exogenous IFN treatment was also investigated. HBV actively antagonized host JAK-STAT signal transduction, whereas the non-responsiveness of HCV to exogenous IFN treatment appeared to be primarily associated with intrinsic viral factors. Since the SCID/bg-Alb/uPA chimeric mouse model used in my studies is immunocompromised, my results suggested that effective control of HBV or HCV infection may require coordination or cross-talk between hepatocytes and other types of cells, in particularly immune cells residing in the liver or infiltrated to the liver during infections.

6.3 Future directions and perspective

My data have showed that HBV suppresses IFN response by antagonizing gene transcription of STAT1 and STAT2 and protein activation of STAT1. It will be

interesting to perform immunostaining of STAT2 in liver sections from HBV infected chimeric mice treated with IFN to determine if protein activation of STAT2 is also impaired by HBV in response to IFN treatment. In addition, many molecules, such as IFNAR1/2, JAK1 and TYK2, are involved in the JAK-STAT signaling pathway other than STAT1 and STAT2. Future studies will examine whether HBV infection exerts suppressive effects on any of these molecules. As discussed in Chapter 4, in order to further test the different effects of HBV compared to HCV on the JAK-STAT pathway, particularly on STAT1 protein activation, co-staining human STAT1 with viral proteins, such as HBV or HCV core protein, in liver sections from HBV infected chimeric mice treated with exogenous IFN is ongoing.

My studies have demonstrated that the nonresponse of HCV to exogenous IFN treatment is mostly associated with intrinsic viral factors in chimeric mice. Evidence has shown that amino acid variation in IFN-sensitivity-determining region (ISDR) within the HCV NS5A region [172, 173] as well as in the HVR1 located in HCV E2 region [176-178] and at aa 70 or 91 in the HCV core region [174, 175] are predictors of SVR and NVR to IFN therapy. Future studies will focus on determining if these sequence variations are present in the IFN-nonresponsive HCVgt1a strain prior to and post IFN treatment in mouse serum using direct sequencing or the next generation sequencing strategy. I attempted the next generation sequencing experiments, however, due to the limited amount of mouse serum samples available for analysis as well as the highly variable nature of HCV quasispecies in clinical samples, challenges are significant from

viral RNA isolation for library construction to final sequence analysis in mice. I will continue to explore next generation sequencing technologies to address these questions.

Host factors, such as IL28B SNPs, will be re-evaluated in HCV-infected hepatocytes co-cultured with immune cells carrying different IL28 SNPs. My preliminary experiments, by introducing unstimulated pDCs isolated from healthy adults into chimeric mice chronically infected with HCV, have showed that the cross-talk between infected hepatocytes and pDCs did lead to production of type I IFNs (Figure 3.8 in Chapter 3). The effect of different immune cells on the induction of an IFN response in uninfected and HCV infected chimeric mice deserves further study.

REFERENCES

1. Isaacs, A. and J. Lindenmann, *Virus interference. I. The interferon*. Proc R Soc Lond B Biol Sci, 1957. **147**(927): p. 258-67.
2. Borden, E.C., G.C. Sen, G. Uze, R.H. Silverman, R.M. Ransohoff, G.R. Foster, and G.R. Stark, *Interferons at age 50: past, current and future impact on biomedicine*. Nat Rev Drug Discov, 2007. **6**(12): p. 975-90.
3. Trent, J.M., S. Olson, and R.M. Lawn, *Chromosomal localization of human leukocyte, fibroblast, and immune interferon genes by means of in situ hybridization*. Proc Natl Acad Sci U S A, 1982. **79**(24): p. 7809-13.
4. Diaz, M.O., H.M. Pomykala, S.K. Bohlander, E. Maltepe, K. Malik, B. Brownstein, and O.I. Olopade, *Structure of the human type-I interferon gene cluster determined from a YAC clone contig*. Genomics, 1994. **22**(3): p. 540-52.
5. Mogensen, K.E., M. Lewerenz, J. Reboul, G. Lutfalla, and G. Uze, *The type I interferon receptor: structure, function, and evolution of a family business*. J Interferon Cytokine Res, 1999. **19**(10): p. 1069-98.
6. Stark, G.R., I.M. Kerr, B.R. Williams, R.H. Silverman, and R.D. Schreiber, *How cells respond to interferons*. Annu Rev Biochem, 1998. **67**: p. 227-64.
7. Takaoka, A. and H. Yanai, *Interferon signalling network in innate defence*. Cell Microbiol, 2006. **8**(6): p. 907-22.
8. van Boxel-Dezaire, A.H., M.R. Rani, and G.R. Stark, *Complex modulation of cell type-specific signaling in response to type I interferons*. Immunity, 2006. **25**(3): p. 361-72.
9. Ghany, M.G., D.B. Strader, D.L. Thomas, and L.B. Seeff, *Diagnosis, management, and treatment of hepatitis C: an update*. Hepatology, 2009. **49**(4): p. 1335-74.
10. McHutchison, J.G., E.J. Lawitz, M.L. Shiffman, A.J. Muir, G.W. Galler, J. McCone, L.M. Nyberg, W.M. Lee, R.H. Ghalib, E.R. Schiff, J.S. Galati, B.R. Bacon, M.N. Davis, P. Mukhopadhyay, K. Koury, S. Noviello, L.D. Pedicone, C.A. Brass, J.K. Albrecht, and M.S. Sulkowski, *Peginterferon*

- alfa-2b or alfa-2a with ribavirin for treatment of hepatitis C infection.* N Engl J Med, 2009. **361**(6): p. 580-93.
11. Sheppard, P., W. Kindsvogel, W. Xu, K. Henderson, S. Schlutsmeyer, T.E. Whitmore, R. Kuestner, U. Garrigues, C. Birks, J. Roraback, C. Ostrander, D. Dong, J. Shin, S. Presnell, B. Fox, B. Haldeman, E. Cooper, D. Taft, T. Gilbert, F.J. Grant, M. Tackett, W. Krivan, G. McKnight, C. Clegg, D. Foster, and K.M. Klucher, *IL-28, IL-29 and their class II cytokine receptor IL-28R.* Nat Immunol, 2003. **4**(1): p. 63-8.
 12. Kotenko, S.V., G. Gallagher, V.V. Baurin, A. Lewis-Antes, M. Shen, N.K. Shah, J.A. Langer, F. Sheikh, H. Dickensheets, and R.P. Donnelly, *IFN-lambdas mediate antiviral protection through a distinct class II cytokine receptor complex.* Nat Immunol, 2003. **4**(1): p. 69-77.
 13. Sommereyns, C., S. Paul, P. Staeheli, and T. Michiels, *IFN-lambda (IFN-lambda) is expressed in a tissue-dependent fashion and primarily acts on epithelial cells in vivo.* PLoS Pathog, 2008. **4**(3): p. e1000017.
 14. Mordstein, M., E. Neugebauer, V. Ditt, B. Jessen, T. Rieger, V. Falcone, F. Sorgeloos, S. Ehl, D. Mayer, G. Kochs, M. Schwemmle, S. Gunther, C. Drosten, T. Michiels, and P. Staeheli, *Lambda interferon renders epithelial cells of the respiratory and gastrointestinal tracts resistant to viral infections.* J Virol, 2010. **84**(11): p. 5670-7.
 15. Pulverer, J.E., U. Rand, S. Lienenklaus, D. Kugel, N. Zietara, G. Kochs, R. Naumann, S. Weiss, P. Staeheli, H. Hauser, and M. Koster, *Temporal and spatial resolution of type I and III interferon responses in vivo.* J Virol, 2010. **84**(17): p. 8626-38.
 16. Ank, N. and S.R. Paludan, *Type III IFNs: new layers of complexity in innate antiviral immunity.* Biofactors, 2009. **35**(1): p. 82-7.
 17. Dickensheets, H., F. Sheikh, O. Park, B. Gao, and R.P. Donnelly, *Interferon-lambda (IFN-lambda) induces signal transduction and gene expression in human hepatocytes, but not in lymphocytes or monocytes.* J Leukoc Biol, 2013. **93**(3): p. 377-85.

18. Dai, J., N.J. Megjugorac, G.E. Gallagher, R.Y. Yu, and G. Gallagher, *IFN-lambda1 (IL-29) inhibits GATA3 expression and suppresses Th2 responses in human naive and memory T cells*. Blood, 2009. **113**(23): p. 5829-38.
19. Megjugorac, N.J., G.E. Gallagher, and G. Gallagher, *Modulation of human plasmacytoid DC function by IFN-lambda1 (IL-29)*. J Leukoc Biol, 2009. **86**(6): p. 1359-63.
20. Mennechet, F.J. and G. Uze, *Interferon-lambda-treated dendritic cells specifically induce proliferation of FOXP3-expressing suppressor T cells*. Blood, 2006. **107**(11): p. 4417-23.
21. Prokunina-Olsson, L., B. Muchmore, W. Tang, R.M. Pfeiffer, H. Park, H. Dickensheets, D. Hergott, P. Porter-Gill, A. Mumy, I. Kohaar, S. Chen, N. Brand, M. Tarway, L. Liu, F. Sheikh, J. Astemborski, H.L. Bonkovsky, B.R. Edlin, C.D. Howell, T.R. Morgan, D.L. Thomas, B. Rehermann, R.P. Donnelly, and T.R. O'Brien, *A variant upstream of IFNL3 (IL28B) creating a new interferon gene IFNL4 is associated with impaired clearance of hepatitis C virus*. Nat Genet, 2013. **45**(2): p. 164-71.
22. Hamming, O.J., E. Terczynska-Dyla, G. Vieyres, R. Dijkman, S.E. Jorgensen, H. Akhtar, P. Siupka, T. Pietschmann, V. Thiel, and R. Hartmann, *Interferon lambda 4 signals via the IFNlambda receptor to regulate antiviral activity against HCV and coronaviruses*. EMBO J, 2013. **32**(23): p. 3055-65.
23. Janeway, C.A., Jr. and R. Medzhitov, *Introduction: the role of innate immunity in the adaptive immune response*. Semin Immunol, 1998. **10**(5): p. 349-50.
24. Iwasaki, A. and R. Medzhitov, *Toll-like receptor control of the adaptive immune responses*. Nat Immunol, 2004. **5**(10): p. 987-95.
25. Janeway, C.A., Jr., *Approaching the asymptote? Evolution and revolution in immunology*. Cold Spring Harb Symp Quant Biol, 1989. **54 Pt 1**: p. 1-13.
26. Medzhitov, R., *Recognition of microorganisms and activation of the immune response*. Nature, 2007. **449**(7164): p. 819-26.

27. Kumar, H., T. Kawai, and S. Akira, *Pathogen recognition by the innate immune system*. Int Rev Immunol, 2011. **30**(1): p. 16-34.
28. Takeuchi, O. and S. Akira, *Innate immunity to virus infection*. Immunol Rev, 2009. **227**(1): p. 75-86.
29. Akira, S., S. Uematsu, and O. Takeuchi, *Pathogen recognition and innate immunity*. Cell, 2006. **124**(4): p. 783-801.
30. Lu, H.L. and F. Liao, *Melanoma differentiation-associated gene 5 senses hepatitis B virus and activates innate immune signaling to suppress virus replication*. J Immunol, 2013. **191**(6): p. 3264-76.
31. Hornung, V., J. Ellegast, S. Kim, K. Brzozka, A. Jung, H. Kato, H. Poeck, S. Akira, K.K. Conzelmann, M. Schlee, S. Endres, and G. Hartmann, *5'-Triphosphate RNA is the ligand for RIG-I*. Science, 2006. **314**(5801): p. 994-7.
32. Pichlmair, A., O. Schulz, C.P. Tan, T.I. Naslund, P. Liljestrom, F. Weber, and C. Reis e Sousa, *RIG-I-mediated antiviral responses to single-stranded RNA bearing 5'-phosphates*. Science, 2006. **314**(5801): p. 997-1001.
33. Kato, H., O. Takeuchi, E. Mikamo-Satoh, R. Hirai, T. Kawai, K. Matsushita, A. Hiiragi, T.S. Dermody, T. Fujita, and S. Akira, *Length-dependent recognition of double-stranded ribonucleic acids by retinoic acid-inducible gene-I and melanoma differentiation-associated gene 5*. J Exp Med, 2008. **205**(7): p. 1601-10.
34. Saito, T., D.M. Owen, F. Jiang, J. Marcotrigiano, and M. Gale, Jr., *Innate immunity induced by composition-dependent RIG-I recognition of hepatitis C virus RNA*. Nature, 2008. **454**(7203): p. 523-7.
35. Yoneyama, M., M. Kikuchi, T. Natsukawa, N. Shinobu, T. Imaizumi, M. Miyagishi, K. Taira, S. Akira, and T. Fujita, *The RNA helicase RIG-I has an essential function in double-stranded RNA-induced innate antiviral responses*. Nat Immunol, 2004. **5**(7): p. 730-7.
36. Kang, D.C., R.V. Gopalkrishnan, Q. Wu, E. Jankowsky, A.M. Pyle, and P.B. Fisher, *mda-5: An interferon-inducible putative RNA helicase with*

- double-stranded RNA-dependent ATPase activity and melanoma growth-suppressive properties*. Proc Natl Acad Sci U S A, 2002. **99**(2): p. 637-42.
37. Saito, T., R. Hirai, Y.M. Loo, D. Owen, C.L. Johnson, S.C. Sinha, S. Akira, T. Fujita, and M. Gale, Jr., *Regulation of innate antiviral defenses through a shared repressor domain in RIG-I and LGP2*. Proc Natl Acad Sci U S A, 2007. **104**(2): p. 582-7.
38. Satoh, T., H. Kato, Y. Kumagai, M. Yoneyama, S. Sato, K. Matsushita, T. Tsujimura, T. Fujita, S. Akira, and O. Takeuchi, *LGP2 is a positive regulator of RIG-I- and MDA5-mediated antiviral responses*. Proc Natl Acad Sci U S A, 2010. **107**(4): p. 1512-7.
39. Kawai, T., K. Takahashi, S. Sato, C. Coban, H. Kumar, H. Kato, K.J. Ishii, O. Takeuchi, and S. Akira, *IPS-1, an adaptor triggering RIG-I- and Mda5-mediated type I interferon induction*. Nat Immunol, 2005. **6**(10): p. 981-8.
40. Seth, R.B., L. Sun, C.K. Ea, and Z.J. Chen, *Identification and characterization of MAVS, a mitochondrial antiviral signaling protein that activates NF-kappaB and IRF 3*. Cell, 2005. **122**(5): p. 669-82.
41. Meylan, E., J. Curran, K. Hofmann, D. Moradpour, M. Binder, R. Bartenschlager, and J. Tschopp, *Cardif is an adaptor protein in the RIG-I antiviral pathway and is targeted by hepatitis C virus*. Nature, 2005. **437**(7062): p. 1167-72.
42. Dixit, E., S. Boulant, Y. Zhang, A.S. Lee, C. Odendall, B. Shum, N. Hacohen, Z.J. Chen, S.P. Whelan, M. Fransen, M.L. Nibert, G. Superti-Furga, and J.C. Kagan, *Peroxisomes are signaling platforms for antiviral innate immunity*. Cell, 2010. **141**(4): p. 668-81.
43. Jung, A., H. Kato, Y. Kumagai, H. Kumar, T. Kawai, O. Takeuchi, and S. Akira, *Lymphocytoid choriomeningitis virus activates plasmacytoid dendritic cells and induces a cytotoxic T-cell response via MyD88*. J Virol, 2008. **82**(1): p. 196-206.
44. Koyama, S., K.J. Ishii, H. Kumar, T. Tanimoto, C. Coban, S. Uematsu, T. Kawai, and S. Akira, *Differential role of TLR- and RLR-signaling in the*

- immune responses to influenza A virus infection and vaccination.* J Immunol, 2007. **179**(7): p. 4711-20.
45. Bhoj, V.G., Q. Sun, E.J. Bhoj, C. Somers, X. Chen, J.P. Torres, A. Mejias, A.M. Gomez, H. Jafri, O. Ramilo, and Z.J. Chen, *MAVS and MyD88 are essential for innate immunity but not cytotoxic T lymphocyte response against respiratory syncytial virus.* Proc Natl Acad Sci U S A, 2008. **105**(37): p. 14046-51.
 46. Pichlmair, A. and C. Reis e Sousa, *Innate recognition of viruses.* Immunity, 2007. **27**(3): p. 370-83.
 47. Novick, D., B. Cohen, and M. Rubinstein, *The human interferon alpha/beta receptor: characterization and molecular cloning.* Cell, 1994. **77**(3): p. 391-400.
 48. Colamonici, O.R., H. Uyttendaele, P. Domanski, H. Yan, and J.J. Krolewski, *p135tyk2, an interferon-alpha-activated tyrosine kinase, is physically associated with an interferon-alpha receptor.* J Biol Chem, 1994. **269**(5): p. 3518-22.
 49. Gonzalez-Navajas, J.M., J. Lee, M. David, and E. Raz, *Immunomodulatory functions of type I interferons.* Nat Rev Immunol, 2012. **12**(2): p. 125-35.
 50. O'Shea, J.J. and R. Plenge, *JAK and STAT signaling molecules in immunoregulation and immune-mediated disease.* Immunity, 2012. **36**(4): p. 542-50.
 51. Uddin, S., L. Yenush, X.J. Sun, M.E. Sweet, M.F. White, and L.C. Platanius, *Interferon-alpha engages the insulin receptor substrate-1 to associate with the phosphatidylinositol 3'-kinase.* J Biol Chem, 1995. **270**(27): p. 15938-41.
 52. Kaur, S., A. Sassano, A.M. Joseph, B. Majchrzak-Kita, E.A. Eklund, A. Verma, S.M. Brachmann, E.N. Fish, and L.C. Platanius, *Dual regulatory roles of phosphatidylinositol 3-kinase in IFN signaling.* J Immunol, 2008. **181**(10): p. 7316-23.

53. David, M., E. Petricoin, 3rd, C. Benjamin, R. Pine, M.J. Weber, and A.C. Larner, *Requirement for MAP kinase (ERK2) activity in interferon alpha- and interferon beta-stimulated gene expression through STAT proteins*. Science, 1995. **269**(5231): p. 1721-3.
54. Uddin, S., B. Majchrzak, J. Woodson, P. Arunkumar, Y. Alsayed, R. Pine, P.R. Young, E.N. Fish, and L.C. Plataniias, *Activation of the p38 mitogen-activated protein kinase by type I interferons*. J Biol Chem, 1999. **274**(42): p. 30127-31.
55. Li, Y., A. Sassano, B. Majchrzak, D.K. Deb, D.E. Levy, M. Gaestel, A.R. Nebreda, E.N. Fish, and L.C. Plataniias, *Role of p38alpha Map kinase in Type I interferon signaling*. J Biol Chem, 2004. **279**(2): p. 970-9.
56. Ishida, H., K. Ohkawa, A. Hosui, N. Hiramatsu, T. Kanto, K. Ueda, T. Takehara, and N. Hayashi, *Involvement of p38 signaling pathway in interferon-alpha-mediated antiviral activity toward hepatitis C virus*. Biochem Biophys Res Commun, 2004. **321**(3): p. 722-7.
57. Wang, F., Y. Ma, J.W. Barrett, X. Gao, J. Loh, E. Barton, H.W. Virgin, and G. McFadden, *Disruption of Erk-dependent type I interferon induction breaks the myxoma virus species barrier*. Nat Immunol, 2004. **5**(12): p. 1266-74.
58. Der, S.D., A. Zhou, B.R. Williams, and R.H. Silverman, *Identification of genes differentially regulated by interferon alpha, beta, or gamma using oligonucleotide arrays*. Proc Natl Acad Sci U S A, 1998. **95**(26): p. 15623-8.
59. Liu, S.Y., D.J. Sanchez, R. Aliyari, S. Lu, and G. Cheng, *Systematic identification of type I and type II interferon-induced antiviral factors*. Proc Natl Acad Sci U S A, 2012. **109**(11): p. 4239-44.
60. Sadler, A.J. and B.R. Williams, *Interferon-inducible antiviral effectors*. Nat Rev Immunol, 2008. **8**(7): p. 559-68.
61. Schoggins, J.W., S.J. Wilson, M. Panis, M.Y. Murphy, C.T. Jones, P. Bieniasz, and C.M. Rice, *A diverse range of gene products are effectors of the type I interferon antiviral response*. Nature, 2011. **472**(7344): p. 481-5.

62. Schoggins, J.W. and C.M. Rice, *Interferon-stimulated genes and their antiviral effector functions*. *Curr Opin Virol*, 2011. **1**(6): p. 519-25.
63. Larner, A.C., A. Chaudhuri, and J.E. Darnell, Jr., *Transcriptional induction by interferon. New protein(s) determine the extent and length of the induction*. *J Biol Chem*, 1986. **261**(1): p. 453-9.
64. Sarasin-Filipowicz, M., X. Wang, M. Yan, F.H. Duong, V. Poli, D.J. Hilton, D.E. Zhang, and M.H. Heim, *Alpha interferon induces long-lasting refractoriness of JAK-STAT signaling in the mouse liver through induction of USP18/UBP43*. *Mol Cell Biol*, 2009. **29**(17): p. 4841-51.
65. Makowska, Z., F.H. Duong, G. Trincucci, D.F. Tough, and M.H. Heim, *Interferon-beta and interferon-lambda signaling is not affected by interferon-induced refractoriness to interferon-alpha in vivo*. *Hepatology*, 2011. **53**(4): p. 1154-63.
66. Donnelly, R.P. and S.V. Kotenko, *Interferon-lambda: a new addition to an old family*. *J Interferon Cytokine Res*, 2010. **30**(8): p. 555-64.
67. Kotenko, S.V., *IFN-lambdas*. *Curr Opin Immunol*, 2011. **23**(5): p. 583-90.
68. Osterlund, P.I., T.E. Pietila, V. Veckman, S.V. Kotenko, and I. Julkunen, *IFN regulatory factor family members differentially regulate the expression of type III IFN (IFN-lambda) genes*. *J Immunol*, 2007. **179**(6): p. 3434-42.
69. Thomson, S.J., F.G. Goh, H. Banks, T. Krausgruber, S.V. Kotenko, B.M. Foxwell, and I.A. Udalova, *The role of transposable elements in the regulation of IFN-lambda1 gene expression*. *Proc Natl Acad Sci U S A*, 2009. **106**(28): p. 11564-9.
70. Onoguchi, K., M. Yoneyama, A. Takemura, S. Akira, T. Taniguchi, H. Namiki, and T. Fujita, *Viral infections activate types I and III interferon genes through a common mechanism*. *J Biol Chem*, 2007. **282**(10): p. 7576-81.
71. Meager, A., K. Visvalingam, P. Dilger, D. Bryan, and M. Wadhwa, *Biological activity of interleukins-28 and -29: comparison with type I interferons*. *Cytokine*, 2005. **31**(2): p. 109-18.

72. Seeger C. Mason WS, Z.F., *Hepadnaviruses*, in *Fields Virology*, H. Knipe DM, Editor 2006, Lippincott, Williams & Williams: Philadelphia. p. 2977-3029.
73. Liang, T.J., *Hepatitis B: the virus and disease*. *Hepatology*, 2009. **49**(5 Suppl): p. S13-21.
74. Gerlich, W.H., *Medical virology of hepatitis B: how it began and where we are now*. *Virol J*, 2013. **10**: p. 239.
75. Yan, H., G. Zhong, G. Xu, W. He, Z. Jing, Z. Gao, Y. Huang, Y. Qi, B. Peng, H. Wang, L. Fu, M. Song, P. Chen, W. Gao, B. Ren, Y. Sun, T. Cai, X. Feng, J. Sui, and W. Li, *Sodium taurocholate cotransporting polypeptide is a functional receptor for human hepatitis B and D virus*. *Elife*, 2012. **1**: p. e00049.
76. Urban, S., A. Schulze, M. Dandri, and J. Petersen, *The replication cycle of hepatitis B virus*. *J Hepatol*, 2010. **52**(2): p. 282-4.
77. Bock, C.T., P. Schranz, C.H. Schroder, and H. Zentgraf, *Hepatitis B virus genome is organized into nucleosomes in the nucleus of the infected cell*. *Virus Genes*, 1994. **8**(3): p. 215-29.
78. Newbold, J.E., H. Xin, M. Tencza, G. Sherman, J. Dean, S. Bowden, and S. Locarnini, *The covalently closed duplex form of the hepadnavirus genome exists in situ as a heterogeneous population of viral minichromosomes*. *J Virol*, 1995. **69**(6): p. 3350-7.
79. Locarnini, S. and F. Zoulim, *Molecular genetics of HBV infection*. *Antivir Ther*, 2010. **15 Suppl 3**: p. 3-14.
80. WHO, H.f., <http://www.who.int/mediacentre/factsheets/fs204/en/index.html>, 2013.
81. Fung, S.K. and A.S. Lok, *Hepatitis B virus genotypes: do they play a role in the outcome of HBV infection?* *Hepatology*, 2004. **40**(4): p. 790-2.
82. McMahon, B.J., *The natural history of chronic hepatitis B virus infection*. *Hepatology*, 2009. **49**(5 Suppl): p. S45-55.

83. Shi, Y.H. and C.H. Shi, *Molecular characteristics and stages of chronic hepatitis B virus infection*. World J Gastroenterol, 2009. **15**(25): p. 3099-105.
84. Deny, P. and F. Zoulim, *Hepatitis B virus: from diagnosis to treatment*. Pathol Biol (Paris), 2010. **58**(4): p. 245-53.
85. Custer, B., S.D. Sullivan, T.K. Hazlet, U. Iloeje, D.L. Veenstra, and K.V. Kowdley, *Global epidemiology of hepatitis B virus*. J Clin Gastroenterol, 2004. **38**(10 Suppl 3): p. S158-68.
86. McMahon, B.J., *Natural history of chronic hepatitis B*. Clin Liver Dis, 2010. **14**(3): p. 381-96.
87. Tujios, S.R. and W.M. Lee, *Update in the management of chronic hepatitis B*. Curr Opin Gastroenterol, 2013. **29**(3): p. 250-6.
88. Ayoub, W.S. and E.B. Keeffe, *Review article: current antiviral therapy of chronic hepatitis B*. Aliment Pharmacol Ther, 2011. **34**(10): p. 1145-58.
89. Perrillo, R., *Benefits and risks of interferon therapy for hepatitis B*. Hepatology, 2009. **49**(5 Suppl): p. S103-11.
90. Liver., E.A.F.T.S.O.T., *EASL clinical practice guidelines: Management of chronic hepatitis B virus infection*. J Hepatol, 2012. **57**(1): p. 167-85.
91. Suppiah, V., M. Moldovan, G. Ahlenstiel, T. Berg, M. Weltman, M.L. Abate, M. Bassendine, U. Spengler, G.J. Dore, E. Powell, S. Riordan, D. Sheridan, A. Smedile, V. Fragomeli, T. Muller, M. Bahlo, G.J. Stewart, D.R. Booth, and J. George, *IL28B is associated with response to chronic hepatitis C interferon-alpha and ribavirin therapy*. Nat Genet, 2009. **41**(10): p. 1100-4.
92. Tanaka, Y., N. Nishida, M. Sugiyama, M. Kurosaki, K. Matsuura, N. Sakamoto, M. Nakagawa, M. Korenaga, K. Hino, S. Hige, Y. Ito, E. Mita, E. Tanaka, S. Mochida, Y. Murawaki, M. Honda, A. Sakai, Y. Hiasa, S. Nishiguchi, A. Koike, I. Sakaida, M. Imamura, K. Ito, K. Yano, N. Masaki, F. Sugauchi, N. Izumi, K. Tokunaga, and M. Mizokami, *Genome-wide association of IL28B with response to pegylated interferon-alpha*

- and ribavirin therapy for chronic hepatitis C*. Nat Genet, 2009. **41**(10): p. 1105-9.
93. Thomas, D.L., C.L. Thio, M.P. Martin, Y. Qi, D. Ge, C. O'Huigin, J. Kidd, K. Kidd, S.I. Khakoo, G. Alexander, J.J. Goedert, G.D. Kirk, S.M. Donfield, H.R. Rosen, L.H. Tobler, M.P. Busch, J.G. McHutchison, D.B. Goldstein, and M. Carrington, *Genetic variation in IL28B and spontaneous clearance of hepatitis C virus*. Nature, 2009. **461**(7265): p. 798-801.
94. Ge, D., J. Fellay, A.J. Thompson, J.S. Simon, K.V. Shianna, T.J. Urban, E.L. Heinzen, P. Qiu, A.H. Bertelsen, A.J. Muir, M. Sulkowski, J.G. McHutchison, and D.B. Goldstein, *Genetic variation in IL28B predicts hepatitis C treatment-induced viral clearance*. Nature, 2009. **461**(7262): p. 399-401.
95. Rauch, A., Z. Kutalik, P. Descombes, T. Cai, J. Di Iulio, T. Mueller, M. Bochud, M. Battegay, E. Bernasconi, J. Borovicka, S. Colombo, A. Cerny, J.F. Dufour, H. Furrer, H.F. Gunthard, M. Heim, B. Hirschel, R. Malinverni, D. Moradpour, B. Mullhaupt, A. Witteck, J.S. Beckmann, T. Berg, S. Bergmann, F. Negro, A. Telenti, and P.Y. Bochud, *Genetic variation in IL28B is associated with chronic hepatitis C and treatment failure: a genome-wide association study*. Gastroenterology, 2010. **138**(4): p. 1338-45, 1345 e1-7.
96. Tseng, T.C., M.L. Yu, C.J. Liu, C.L. Lin, Y.W. Huang, C.S. Hsu, C.H. Liu, S.F. Kuo, C.J. Pan, S.S. Yang, C.W. Su, P.J. Chen, D.S. Chen, and J.H. Kao, *Effect of host and viral factors on hepatitis B e antigen-positive chronic hepatitis B patients receiving pegylated interferon-alpha-2a therapy*. Antivir Ther, 2011. **16**(5): p. 629-37.
97. Sonneveld, M.J., V.W. Wong, A.M. Woltman, G.L. Wong, Y. Cakaloglu, S. Zeuzem, E.H. Buster, A.G. Uitterlinden, B.E. Hansen, H.L. Chan, and H.L. Janssen, *Polymorphisms near IL28B and serologic response to peginterferon in HBeAg-positive patients with chronic hepatitis B*. Gastroenterology, 2012. **142**(3): p. 513-520 e1.

98. Wu, X., Z. Xin, X. Zhu, L. Pan, Z. Li, H. Li, and Y. Liu, *Evaluation of susceptibility locus for response to interferon-alpha based therapy in chronic hepatitis B patients in Chinese*. *Antiviral Res*, 2012. **93**(2): p. 297-300.
99. Lampertico, P., M. Vigano, C. Cheroni, F. Facchetti, F. Invernizzi, V. Valveri, R. Soffredini, S. Abrignani, R. De Francesco, and M. Colombo, *IL28B polymorphisms predict interferon-related hepatitis B surface antigen seroclearance in genotype D hepatitis B e antigen-negative patients with chronic hepatitis B*. *Hepatology*, 2013. **57**(3): p. 890-6.
100. Fried, M.W., T. Piratvisuth, G.K. Lau, P. Marcellin, W.C. Chow, G. Cooksley, K.X. Luo, S.W. Paik, Y.F. Liaw, P. Button, and M. Popescu, *HBeAg and hepatitis B virus DNA as outcome predictors during therapy with peginterferon alfa-2a for HBeAg-positive chronic hepatitis B*. *Hepatology*, 2008. **47**(2): p. 428-34.
101. Sung, J.J., M.L. Wong, S. Bowden, C.T. Liew, A.Y. Hui, V.W. Wong, N.W. Leung, S. Locarnini, and H.L. Chan, *Intrahepatic hepatitis B virus covalently closed circular DNA can be a predictor of sustained response to therapy*. *Gastroenterology*, 2005. **128**(7): p. 1890-7.
102. Sonneveld, M.J., V. Rijckborst, C.A. Boucher, L. Zwang, M.F. Beersma, B.E. Hansen, and H.L. Janssen, *A comparison of two assays for quantification of Hepatitis B surface Antigen in patients with chronic hepatitis B*. *J Clin Virol*, 2011. **51**(3): p. 175-8.
103. Moucari, R., A. Korevaar, O. Lada, M. Martinot-Peignoux, N. Boyer, V. Mackiewicz, A. Dauvergne, A.C. Cardoso, T. Asselah, M.H. Nicolas-Chanoine, M. Vidaud, D. Valla, P. Bedossa, and P. Marcellin, *High rates of HBsAg seroconversion in HBeAg-positive chronic hepatitis B patients responding to interferon: a long-term follow-up study*. *J Hepatol*, 2009. **50**(6): p. 1084-92.
104. Brunetto, M.R., F. Moriconi, F. Bonino, G.K. Lau, P. Farci, C. Yurdaydin, T. Piratvisuth, K. Luo, Y. Wang, S. Hadziyannis, E. Wolf, P. McCloud, R. Batrla, and P. Marcellin, *Hepatitis B virus surface antigen levels: a guide*

- to sustained response to peginterferon alfa-2a in HBeAg-negative chronic hepatitis B.* Hepatology, 2009. **49**(4): p. 1141-50.
105. Rijckborst, V., B.E. Hansen, Y. Cakaloglu, P. Ferenci, F. Tabak, M. Akdogan, K. Simon, U.S. Akarca, R. Flisiak, E. Verhey, A.J. Van Vuuren, C.A. Boucher, M.J. ter Borg, and H.L. Janssen, *Early on-treatment prediction of response to peginterferon alfa-2a for HBeAg-negative chronic hepatitis B using HBsAg and HBV DNA levels.* Hepatology, 2010. **52**(2): p. 454-61.
 106. Yuen, M.F. and C.L. Lai, *Treatment of chronic hepatitis B: Evolution over two decades.* J Gastroenterol Hepatol, 2011. **26 Suppl 1**: p. 138-43.
 107. Chang, T.T., C.L. Lai, S. Kew Yoon, S.S. Lee, H.S. Coelho, F.J. Carrilho, F. Poordad, W. Halota, Y. Horsmans, N. Tsai, H. Zhang, D.J. Tenney, R. Tamez, and U. Iloeje, *Entecavir treatment for up to 5 years in patients with hepatitis B e antigen-positive chronic hepatitis B.* Hepatology, 2010. **51**(2): p. 422-30.
 108. Yokosuka, O., K. Takaguchi, S. Fujioka, M. Shindo, K. Chayama, H. Kobashi, N. Hayashi, C. Sato, K. Kiyosawa, K. Tanikawa, H. Ishikawa, N. Masaki, T. Seriu, and M. Omata, *Long-term use of entecavir in nucleoside-naive Japanese patients with chronic hepatitis B infection.* J Hepatol, 2010. **52**(6): p. 791-9.
 109. Snow-Lampart, A., B. Chappell, M. Curtis, Y. Zhu, F. Myrick, J. Schawalder, K. Kitrinis, E.S. Svarovskaia, M.D. Miller, J. Sorbel, J. Heathcote, P. Marcellin, and K. Borroto-Esoda, *No resistance to tenofovir disoproxil fumarate detected after up to 144 weeks of therapy in patients monoinfected with chronic hepatitis B virus.* Hepatology, 2011. **53**(3): p. 763-73.
 110. Lee, B., W.X. Luo, S. Suzuki, M.J. Robins, and D.L. Tyrrell, *In vitro and in vivo comparison of the abilities of purine and pyrimidine 2',3'-dideoxynucleosides to inhibit duck hepadnavirus.* Antimicrob Agents Chemother, 1989. **33**(3): p. 336-9.

111. Suzuki, S., B. Lee, W. Luo, D. Tovell, M.J. Robins, and D.L. Tyrrell, *Inhibition of duck hepatitis B virus replication by purine 2',3'-dideoxynucleosides*. *Biochem Biophys Res Commun*, 1988. **156**(3): p. 1144-51.
112. Howe, A.Y., M.J. Robins, J.S. Wilson, and D.L. Tyrrell, *Selective inhibition of the reverse transcription of duck hepatitis B virus by binding of 2',3'-dideoxyguanosine 5'-triphosphate to the viral polymerase*. *Hepatology*, 1996. **23**(1): p. 87-96.
113. Lapinski, T.W., J. Pogorzelska, and R. Flisiak, *HBV mutations and their clinical significance*. *Adv Med Sci*, 2012. **57**(1): p. 18-22.
114. Svicher, V., V. Cento, R. Salpini, F. Mercurio, M. Fraune, B. Beggel, Y. Han, C. Gori, L. Wittkop, A. Bertoli, V. Micheli, G. Gubertini, R. Longo, S. Romano, M. Visca, V. Gallinaro, N. Marino, F. Mazzotta, G.M. De Sanctis, H. Fleury, P. Trimoulet, M. Angelico, G. Cappiello, X.X. Zhang, J. Verheyen, F. Ceccherini-Silberstein, and C.F. Perno, *Role of hepatitis B virus genetic barrier in drug-resistance and immune-escape development*. *Dig Liver Dis*, 2011. **43**(12): p. 975-83.
115. Locarnini, S.A. and L. Yuen, *Molecular genesis of drug-resistant and vaccine-escape HBV mutants*. *Antivir Ther*, 2010. **15**(3 Pt B): p. 451-61.
116. Wieland, S., R. Thimme, R.H. Purcell, and F.V. Chisari, *Genomic analysis of the host response to hepatitis B virus infection*. *Proc Natl Acad Sci U S A*, 2004. **101**(17): p. 6669-74.
117. Dunn, C., D. Peppia, P. Khanna, G. Nebbia, M. Jones, N. Brendish, R.M. Lascar, D. Brown, R.J. Gilson, R.J. Tedder, G.M. Dusheiko, M. Jacobs, P. Klenerman, and M.K. Maini, *Temporal analysis of early immune responses in patients with acute hepatitis B virus infection*. *Gastroenterology*, 2009. **137**(4): p. 1289-300.
118. Fisicaro, P., C. Valdatta, C. Boni, M. Massari, C. Mori, A. Zerbini, A. Orlandini, L. Sacchelli, G. Missale, and C. Ferrari, *Early kinetics of innate and adaptive immune responses during hepatitis B virus infection*. *Gut*, 2009. **58**(7): p. 974-82.

119. Wu, J., Z. Meng, M. Jiang, R. Pei, M. Trippler, R. Broering, A. Bucchi, J.P. Sowa, U. Dittmer, D. Yang, M. Roggendorf, G. Gerken, M. Lu, and J.F. Schlaak, *Hepatitis B virus suppresses toll-like receptor-mediated innate immune responses in murine parenchymal and nonparenchymal liver cells*. *Hepatology*, 2009. **49**(4): p. 1132-40.
120. Kumar, M., S.Y. Jung, A.J. Hodgson, C.R. Madden, J. Qin, and B.L. Slagle, *Hepatitis B virus regulatory HBx protein binds to adaptor protein IPS-1 and inhibits the activation of beta interferon*. *J Virol*, 2011. **85**(2): p. 987-95.
121. Wang, H. and W.S. Ryu, *Hepatitis B virus polymerase blocks pattern recognition receptor signaling via interaction with DDX3: implications for immune evasion*. *PLoS Pathog*, 2010. **6**(7): p. e1000986.
122. Yu, S., J. Chen, M. Wu, H. Chen, N. Kato, and Z. Yuan, *Hepatitis B virus polymerase inhibits RIG-I- and Toll-like receptor 3-mediated beta interferon induction in human hepatocytes through interference with interferon regulatory factor 3 activation and dampening of the interaction between TBK1/IKKepsilon and DDX3*. *J Gen Virol*, 2010. **91**(Pt 8): p. 2080-90.
123. Lutgehetmann, M., T. Bornscheuer, T. Volz, L. Allweiss, J.H. Bockmann, J.M. Pollok, A.W. Lohse, J. Petersen, and M. Dandri, *Hepatitis B virus limits response of human hepatocytes to interferon-alpha in chimeric mice*. *Gastroenterology*, 2011. **140**(7): p. 2074-83, 2083 e1-2.
124. Chen, J., M. Wu, X. Zhang, W. Zhang, Z. Zhang, L. Chen, J. He, Y. Zheng, C. Chen, F. Wang, Y. Hu, X. Zhou, C. Wang, Y. Xu, M. Lu, and Z. Yuan, *Hepatitis B virus polymerase impairs interferon-alpha-induced STAT activation through inhibition of importin-alpha5 and protein kinase C-delta*. *Hepatology*, 2013. **57**(2): p. 470-82.
125. Rosmorduc, O., H. Sirma, P. Soussan, E. Gordien, P. Lebon, M. Horisberger, C. Brechot, and D. Kremsdorf, *Inhibition of interferon-inducible MxA protein expression by hepatitis B virus capsid protein*. *J Gen Virol*, 1999. **80** (Pt 5): p. 1253-62.

126. Isogawa, M., M.D. Robek, Y. Furuichi, and F.V. Chisari, *Toll-like receptor signaling inhibits hepatitis B virus replication in vivo*. J Virol, 2005. **79**(11): p. 7269-72.
127. Guo, H., D. Jiang, D. Ma, J. Chang, A.M. Dougherty, A. Cuconati, T.M. Block, and J.T. Guo, *Activation of pattern recognition receptor-mediated innate immunity inhibits the replication of hepatitis B virus in human hepatocyte-derived cells*. J Virol, 2009. **83**(2): p. 847-58.
128. Wieland, S.F., L.G. Guidotti, and F.V. Chisari, *Intrahepatic induction of alpha/beta interferon eliminates viral RNA-containing capsids in hepatitis B virus transgenic mice*. J Virol, 2000. **74**(9): p. 4165-73.
129. Wieland, S.F., R.G. Vega, R. Muller, C.F. Evans, B. Hilbush, L.G. Guidotti, J.G. Sutcliffe, P.G. Schultz, and F.V. Chisari, *Searching for interferon-induced genes that inhibit hepatitis B virus replication in transgenic mouse hepatocytes*. J Virol, 2003. **77**(2): p. 1227-36.
130. Mao, R., J. Zhang, D. Jiang, D. Cai, J.M. Levy, A. Cuconati, T.M. Block, J.T. Guo, and H. Guo, *Indoleamine 2,3-dioxygenase mediates the antiviral effect of gamma interferon against hepatitis B virus in human hepatocyte-derived cells*. J Virol, 2011. **85**(2): p. 1048-57.
131. Baumert, T.F., C. Rosler, M.H. Malim, and F. von Weizsacker, *Hepatitis B virus DNA is subject to extensive editing by the human deaminase APOBEC3C*. Hepatology, 2007. **46**(3): p. 682-9.
132. Nguyen, D.H., S. Gummuluru, and J. Hu, *Deamination-independent inhibition of hepatitis B virus reverse transcription by APOBEC3G*. J Virol, 2007. **81**(9): p. 4465-72.
133. Biermer, M., R. Puro, and R.J. Schneider, *Tumor necrosis factor alpha inhibition of hepatitis B virus replication involves disruption of capsid Integrity through activation of NF-kappaB*. J Virol, 2003. **77**(7): p. 4033-42.
134. Puro, R. and R.J. Schneider, *Tumor necrosis factor activates a conserved innate antiviral response to hepatitis B virus that destabilizes*

- nucleocapsids and reduces nuclear viral DNA.* J Virol, 2007. **81**(14): p. 7351-62.
135. Choo, Q.L., G. Kuo, A.J. Weiner, L.R. Overby, D.W. Bradley, and M. Houghton, *Isolation of a cDNA clone derived from a blood-borne non-A, non-B viral hepatitis genome.* Science, 1989. **244**(4902): p. 359-62.
136. Kuiken, C. and P. Simmonds, *Nomenclature and numbering of the hepatitis C virus.* Methods Mol Biol, 2009. **510**: p. 33-53.
137. Nakano, T., G.M. Lau, G.M. Lau, M. Sugiyama, and M. Mizokami, *An updated analysis of hepatitis C virus genotypes and subtypes based on the complete coding region.* Liver Int, 2012. **32**(2): p. 339-45.
138. Domingo, E., V. Martin, C. Perales, A. Grande-Perez, J. Garcia-Arriaza, and A. Arias, *Viruses as quasispecies: biological implications.* Curr Top Microbiol Immunol, 2006. **299**: p. 51-82.
139. Bartenschlager, R., F. Penin, V. Lohmann, and P. Andre, *Assembly of infectious hepatitis C virus particles.* Trends Microbiol, 2011. **19**(2): p. 95-103.
140. Chevaliez, S. and J.M. Pawlotsky, *Hepatitis C virus: virology, diagnosis and management of antiviral therapy.* World J Gastroenterol, 2007. **13**(17): p. 2461-6.
141. Kolykhalov, A.A., K. Mihalik, S.M. Feinstone, and C.M. Rice, *Hepatitis C virus-encoded enzymatic activities and conserved RNA elements in the 3' nontranslated region are essential for virus replication in vivo.* J Virol, 2000. **74**(4): p. 2046-51.
142. Moradpour, D. and F. Penin, *Hepatitis C virus proteins: from structure to function.* Curr Top Microbiol Immunol, 2013. **369**: p. 113-42.
143. Chevaliez, S. and J.M. Pawlotsky, *Virology of hepatitis C virus infection.* Best Pract Res Clin Gastroenterol, 2012. **26**(4): p. 381-9.
144. Barth, H., E.K. Schnober, F. Zhang, R.J. Linhardt, E. Depla, B. Boson, F.L. Cosset, A.H. Patel, H.E. Blum, and T.F. Baumert, *Viral and cellular determinants of the hepatitis C virus envelope-heparan sulfate interaction.* J Virol, 2006. **80**(21): p. 10579-90.

145. Albecka, A., S. Belouzard, A. Op de Beeck, V. Descamps, L. Goueslain, J. Bertrand-Michel, F. Terce, G. Duverlie, Y. Rouille, and J. Dubuisson, *Role of low-density lipoprotein receptor in the hepatitis C virus life cycle*. *Hepatology*, 2012. **55**(4): p. 998-1007.
146. Suzuki, T., K. Ishii, H. Aizaki, and T. Wakita, *Hepatitis C viral life cycle*. *Adv Drug Deliv Rev*, 2007. **59**(12): p. 1200-12.
147. Lohmann, V., *Hepatitis C virus RNA replication*. *Curr Top Microbiol Immunol*, 2013. **369**: p. 167-98.
148. Gosert, R., D. Egger, V. Lohmann, R. Bartenschlager, H.E. Blum, K. Bienz, and D. Moradpour, *Identification of the hepatitis C virus RNA replication complex in Huh-7 cells harboring subgenomic replicons*. *J Virol*, 2003. **77**(9): p. 5487-92.
149. Bartenschlager, R., F.L. Cosset, and V. Lohmann, *Hepatitis C virus replication cycle*. *J Hepatol*, 2010. **53**(3): p. 583-5.
150. Ferraris, P., E. Blanchard, and P. Roingard, *Ultrastructural and biochemical analyses of hepatitis C virus-associated host cell membranes*. *J Gen Virol*, 2010. **91**(Pt 9): p. 2230-7.
151. Romero-Brey, I., A. Merz, A. Chiramel, J.Y. Lee, P. Chlanda, U. Haselman, R. Santarella-Mellwig, A. Habermann, S. Hoppe, S. Kallis, P. Walther, C. Antony, J. Krijnse-Locker, and R. Bartenschlager, *Three-dimensional architecture and biogenesis of membrane structures associated with hepatitis C virus replication*. *PLoS Pathog*, 2012. **8**(12): p. e1003056.
152. Neufeldt, C.J., M.A. Joyce, A. Levin, R.H. Steenbergen, D. Pang, J. Shields, D.L. Tyrrell, and R.W. Wozniak, *Hepatitis C virus-induced cytoplasmic organelles use the nuclear transport machinery to establish an environment conducive to virus replication*. *PLoS Pathog*, 2013. **9**(10): p. e1003744.
153. Brass, V., D. Moradpour, and H.E. Blum, *Molecular virology of hepatitis C virus (HCV): 2006 update*. *Int J Med Sci*, 2006. **3**(2): p. 29-34.
154. WHO, H.f., <http://www.who.int/mediacentre/factsheets/fs164/en/>, 2013.

155. Lavanchy, D., *The global burden of hepatitis C*. Liver Int, 2009. **29 Suppl 1**: p. 74-81.
156. Maasoumy, B. and H. Wedemeyer, *Natural history of acute and chronic hepatitis C*. Best Pract Res Clin Gastroenterol, 2012. **26**(4): p. 401-12.
157. Modi, A.A. and T.J. Liang, *Hepatitis C: a clinical review*. Oral Dis, 2008. **14**(1): p. 10-4.
158. Thomas, D.L. and L.B. Seeff, *Natural history of hepatitis C*. Clin Liver Dis, 2005. **9**(3): p. 383-98, vi.
159. Tanaka, Y., F. Kurbanov, S. Mano, E. Orito, V. Vargas, J.I. Esteban, M.F. Yuen, C.L. Lai, A. Kramvis, M.C. Kew, H.E. Smuts, S.V. Netesov, H.J. Alter, and M. Mizokami, *Molecular tracing of the global hepatitis C virus epidemic predicts regional patterns of hepatocellular carcinoma mortality*. Gastroenterology, 2006. **130**(3): p. 703-14.
160. Liang, T.J. and M.G. Ghany, *Current and future therapies for hepatitis C virus infection*. N Engl J Med, 2013. **368**(20): p. 1907-17.
161. Chen, L., I. Borozan, J. Feld, J. Sun, L.L. Tannis, C. Coltescu, J. Heathcote, A.M. Edwards, and I.D. McGilvray, *Hepatic gene expression discriminates responders and nonresponders in treatment of chronic hepatitis C viral infection*. Gastroenterology, 2005. **128**(5): p. 1437-44.
162. Asselah, T., I. Bieche, S. Narguet, A. Sabbagh, I. Laurendeau, M.P. Ripault, N. Boyer, M. Martinot-Peignoux, D. Valla, M. Vidaud, and P. Marcellin, *Liver gene expression signature to predict response to pegylated interferon plus ribavirin combination therapy in patients with chronic hepatitis C*. Gut, 2008. **57**(4): p. 516-24.
163. Bibert, S., T. Roger, T. Calandra, M. Bochud, A. Cerny, N. Semmo, F.H. Duong, T. Gerlach, R. Malinverni, D. Moradpour, F. Negro, B. Mullhaupt, and P.Y. Bochud, *IL28B expression depends on a novel TT/-G polymorphism which improves HCV clearance prediction*. J Exp Med, 2013. **210**(6): p. 1109-16.
164. McFarland, A.P., S.M. Horner, A. Jarret, R.C. Joslyn, E. Bindewald, B.A. Shapiro, D.A. Delker, C.H. Hagedorn, M. Carrington, M. Gale, Jr., and R.

- Savan, *The favorable IFNL3 genotype escapes mRNA decay mediated by AU-rich elements and hepatitis C virus-induced microRNAs*. Nat Immunol, 2014. **15**(1): p. 72-9.
165. Fried, M.W., M.L. Shiffman, K.R. Reddy, C. Smith, G. Marinus, F.L. Goncalves, Jr., D. Haussinger, M. Diago, G. Carosi, D. Dhumeaux, A. Craxi, A. Lin, J. Hoffman, and J. Yu, *Peginterferon alfa-2a plus ribavirin for chronic hepatitis C virus infection*. N Engl J Med, 2002. **347**(13): p. 975-82.
166. Hadziyannis, S.J., H. Sette, Jr., T.R. Morgan, V. Balan, M. Diago, P. Marcellin, G. Ramadori, H. Bodenheimer, Jr., D. Bernstein, M. Rizzetto, S. Zeuzem, P.J. Pockros, A. Lin, and A.M. Ackrill, *Peginterferon-alpha2a and ribavirin combination therapy in chronic hepatitis C: a randomized study of treatment duration and ribavirin dose*. Ann Intern Med, 2004. **140**(5): p. 346-55.
167. Manns, M.P., J.G. McHutchison, S.C. Gordon, V.K. Rustgi, M. Shiffman, R. Reindollar, Z.D. Goodman, K. Koury, M. Ling, and J.K. Albrecht, *Peginterferon alfa-2b plus ribavirin compared with interferon alfa-2b plus ribavirin for initial treatment of chronic hepatitis C: a randomised trial*. Lancet, 2001. **358**(9286): p. 958-65.
168. Martinot-Peignoux, M., N. Boyer, M. Pouteau, C. Castelnau, N. Giuily, V. Duchatelle, A. Auperin, C. Degott, J.P. Benhamou, S. Erlinger, and P. Marcellin, *Predictors of sustained response to alpha interferon therapy in chronic hepatitis C*. J Hepatol, 1998. **29**(2): p. 214-23.
169. Martinot-Peignoux, M., S. Maylin, R. Moucari, M.P. Ripault, N. Boyer, A.C. Cardoso, N. Giuily, C. Castelnau, M. Pouteau, C. Stern, A. Auperin, P. Bedossa, T. Asselah, and P. Marcellin, *Virological response at 4 weeks to predict outcome of hepatitis C treatment with pegylated interferon and ribavirin*. Antivir Ther, 2009. **14**(4): p. 501-11.
170. Maylin, S., M. Martinot-Peignoux, M.P. Ripault, R. Moucari, A.C. Cardoso, N. Boyer, N. Giuily, C. Castelnau, M. Pouteau, T. Asselah, M.H. Nicolas-Chanoine, and P. Marcellin, *Sustained virological response is*

- associated with clearance of hepatitis C virus RNA and a decrease in hepatitis C virus antibody.* Liver Int, 2009. **29**(4): p. 511-7.
171. Moucari, R., M.P. Ripault, V. Oules, M. Martinot-Peignoux, T. Asselah, N. Boyer, A. El Ray, D. Cazals-Hatem, D. Vidaud, D. Valla, M. Bourliere, and P. Marcellin, *High predictive value of early viral kinetics in retreatment with peginterferon and ribavirin of chronic hepatitis C patients non-responders to standard combination therapy.* J Hepatol, 2007. **46**(4): p. 596-604.
172. Murakami, T., N. Enomoto, M. Kurosaki, N. Izumi, F. Marumo, and C. Sato, *Mutations in nonstructural protein 5A gene and response to interferon in hepatitis C virus genotype 2 infection.* Hepatology, 1999. **30**(4): p. 1045-53.
173. Enomoto, N., I. Sakuma, Y. Asahina, M. Kurosaki, T. Murakami, C. Yamamoto, Y. Ogura, N. Izumi, F. Marumo, and C. Sato, *Mutations in the nonstructural protein 5A gene and response to interferon in patients with chronic hepatitis C virus 1b infection.* N Engl J Med, 1996. **334**(2): p. 77-81.
174. Okanoue, T., Y. Itoh, H. Hashimoto, K. Yasui, M. Minami, T. Takehara, E. Tanaka, M. Onji, J. Toyota, K. Chayama, K. Yoshioka, N. Izumi, N. Akuta, and H. Kumada, *Predictive values of amino acid sequences of the core and NS5A regions in antiviral therapy for hepatitis C: a Japanese multi-center study.* J Gastroenterol, 2009. **44**(9): p. 952-63.
175. Akuta, N., F. Suzuki, Y. Kawamura, H. Yatsuji, H. Sezaki, Y. Suzuki, T. Hosaka, M. Kobayashi, M. Kobayashi, Y. Arase, K. Ikeda, and H. Kumada, *Predictive factors of early and sustained responses to peginterferon plus ribavirin combination therapy in Japanese patients infected with hepatitis C virus genotype 1b: amino acid substitutions in the core region and low-density lipoprotein cholesterol levels.* J Hepatol, 2007. **46**(3): p. 403-10.
176. Kanazawa, Y., N. Hayashi, E. Mita, T. Li, H. Hagiwara, A. Kasahara, H. Fusamoto, and T. Kamada, *Influence of viral quasispecies on effectiveness*

- of interferon therapy in chronic hepatitis C patients. Hepatology, 1994. 20(5): p. 1121-30.*
177. Nasu, A., H. Marusawa, Y. Ueda, N. Nishijima, K. Takahashi, Y. Osaki, Y. Yamashita, T. Inokuma, T. Tamada, T. Fujiwara, F. Sato, K. Shimizu, and T. Chiba, *Genetic heterogeneity of hepatitis C virus in association with antiviral therapy determined by ultra-deep sequencing. PLoS One, 2011. 6(9): p. e24907.*
178. Chambers, T.J., X. Fan, D.A. Droll, E. Hembrador, T. Slater, M.W. Nickells, L.B. Dustin, and A.M. Dibisceglie, *Quasispecies heterogeneity within the E1/E2 region as a pretreatment variable during pegylated interferon therapy of chronic hepatitis C virus infection. J Virol, 2005. 79(5): p. 3071-83.*
179. McHutchison, J.G., G.T. Everson, S.C. Gordon, I.M. Jacobson, M. Sulkowski, R. Kauffman, L. McNair, J. Alam, and A.J. Muir, *Telaprevir with peginterferon and ribavirin for chronic HCV genotype 1 infection. N Engl J Med, 2009. 360(18): p. 1827-38.*
180. Hezode, C., N. Forestier, G. Dusheiko, P. Ferenci, S. Pol, T. Goeser, J.P. Bronowicki, M. Bourliere, S. Gharakhanian, L. Bengtsson, L. McNair, S. George, T. Kieffer, A. Kwong, R.S. Kauffman, J. Alam, J.M. Pawlotsky, and S. Zeuzem, *Telaprevir and peginterferon with or without ribavirin for chronic HCV infection. N Engl J Med, 2009. 360(18): p. 1839-50.*
181. Jacobson, I.M., J.G. McHutchison, G. Dusheiko, A.M. Di Bisceglie, K.R. Reddy, N.H. Bzowej, P. Marcellin, A.J. Muir, P. Ferenci, R. Flisiak, J. George, M. Rizzetto, D. Shouval, R. Sola, R.A. Terg, E.M. Yoshida, N. Adda, L. Bengtsson, A.J. Sankoh, T.L. Kieffer, S. George, R.S. Kauffman, and S. Zeuzem, *Telaprevir for previously untreated chronic hepatitis C virus infection. N Engl J Med, 2011. 364(25): p. 2405-16.*
182. Zeuzem, S., P. Andreone, S. Pol, E. Lawitz, M. Diago, S. Roberts, R. Focaccia, Z. Younossi, G.R. Foster, A. Horban, P. Ferenci, F. Nevens, B. Mullhaupt, P. Pockros, R. Terg, D. Shouval, B. van Hoek, O. Weiland, R. Van Heeswijk, S. De Meyer, D. Luo, G. Boogaerts, R. Polo, G. Picchio,

- and M. Beumont, *Telaprevir for retreatment of HCV infection*. N Engl J Med, 2011. **364**(25): p. 2417-28.
183. Kwo, P.Y., E.J. Lawitz, J. McCone, E.R. Schiff, J.M. Vierling, D. Pound, M.N. Davis, J.S. Galati, S.C. Gordon, N. Ravendhran, L. Rossaro, F.H. Anderson, I.M. Jacobson, R. Rubin, K. Koury, L.D. Pedicone, C.A. Brass, E. Chaudhri, and J.K. Albrecht, *Efficacy of boceprevir, an NS3 protease inhibitor, in combination with peginterferon alfa-2b and ribavirin in treatment-naive patients with genotype 1 hepatitis C infection (SPRINT-1): an open-label, randomised, multicentre phase 2 trial*. Lancet, 2010. **376**(9742): p. 705-16.
184. Poordad, F., J. McCone, Jr., B.R. Bacon, S. Bruno, M.P. Manns, M.S. Sulkowski, I.M. Jacobson, K.R. Reddy, Z.D. Goodman, N. Boparai, M.J. DiNubile, V. Sniukiene, C.A. Brass, J.K. Albrecht, and J.P. Bronowicki, *Boceprevir for untreated chronic HCV genotype 1 infection*. N Engl J Med, 2011. **364**(13): p. 1195-206.
185. Afdhal, N., S. Zeuzem, P. Kwo, M. Chojkier, N. Gitlin, M. Puoti, M. Romero-Gomez, J.P. Zarski, K. Agarwal, P. Buggisch, G.R. Foster, N. Brau, M. Buti, I.M. Jacobson, G.M. Subramanian, X. Ding, H. Mo, J.C. Yang, P.S. Pang, W.T. Symonds, J.G. McHutchison, A.J. Muir, A. Mangia, and P. Marcellin, *Ledipasvir and sofosbuvir for untreated HCV genotype 1 infection*. N Engl J Med, 2014. **370**(20): p. 1889-98.
186. Liang, T.J., *Current progress in development of hepatitis C virus vaccines*. Nat Med, 2013. **19**(7): p. 869-78.
187. Loo, Y.M., D.M. Owen, K. Li, A.K. Erickson, C.L. Johnson, P.M. Fish, D.S. Carney, T. Wang, H. Ishida, M. Yoneyama, T. Fujita, T. Saito, W.M. Lee, C.H. Hagedorn, D.T. Lau, S.A. Weinman, S.M. Lemon, and M. Gale, Jr., *Viral and therapeutic control of IFN-beta promoter stimulator 1 during hepatitis C virus infection*. Proc Natl Acad Sci U S A, 2006. **103**(15): p. 6001-6.
188. You, S. and C.M. Rice, *3' RNA elements in hepatitis C virus replication: kissing partners and long poly(U)*. J Virol, 2008. **82**(1): p. 184-95.

189. Li, K., N.L. Li, D. Wei, S.R. Pfeffer, M. Fan, and L.M. Pfeffer, *Activation of chemokine and inflammatory cytokine response in hepatitis C virus-infected hepatocytes depends on Toll-like receptor 3 sensing of hepatitis C virus double-stranded RNA intermediates*. *Hepatology*, 2012. **55**(3): p. 666-75.
190. Wang, N., Y. Liang, S. Devaraj, J. Wang, S.M. Lemon, and K. Li, *Toll-like receptor 3 mediates establishment of an antiviral state against hepatitis C virus in hepatoma cells*. *J Virol*, 2009. **83**(19): p. 9824-34.
191. Arnaud, N., S. Dabo, D. Akazawa, M. Fukasawa, F. Shinkai-Ouchi, J. Hugon, T. Wakita, and E.F. Meurs, *Hepatitis C virus reveals a novel early control in acute immune response*. *PLoS Pathog*, 2011. **7**(10): p. e1002289.
192. Kang, J.I., S.N. Kwon, S.H. Park, Y.K. Kim, S.Y. Choi, J.P. Kim, and B.Y. Ahn, *PKR protein kinase is activated by hepatitis C virus and inhibits viral replication through translational control*. *Virus Res*, 2009. **142**(1-2): p. 51-6.
193. Shimoike, T., S.A. McKenna, D.A. Lindhout, and J.D. Puglisi, *Translational insensitivity to potent activation of PKR by HCV IRES RNA*. *Antiviral Res*, 2009. **83**(3): p. 228-37.
194. Garaigorta, U. and F.V. Chisari, *Hepatitis C virus blocks interferon effector function by inducing protein kinase R phosphorylation*. *Cell Host Microbe*, 2009. **6**(6): p. 513-22.
195. Horner, S.M. and M. Gale, Jr., *Regulation of hepatic innate immunity by hepatitis C virus*. *Nat Med*, 2013. **19**(7): p. 879-88.
196. Foy, E., K. Li, C. Wang, R. Sumpter, Jr., M. Ikeda, S.M. Lemon, and M. Gale, Jr., *Regulation of interferon regulatory factor-3 by the hepatitis C virus serine protease*. *Science*, 2003. **300**(5622): p. 1145-8.
197. Foy, E., K. Li, R. Sumpter, Jr., Y.M. Loo, C.L. Johnson, C. Wang, P.M. Fish, M. Yoneyama, T. Fujita, S.M. Lemon, and M. Gale, Jr., *Control of antiviral defenses through hepatitis C virus disruption of retinoic acid-*

- inducible gene-I signaling*. Proc Natl Acad Sci U S A, 2005. **102**(8): p. 2986-91.
198. Li, K., E. Foy, J.C. Ferreon, M. Nakamura, A.C. Ferreon, M. Ikeda, S.C. Ray, M. Gale, Jr., and S.M. Lemon, *Immune evasion by hepatitis C virus NS3/4A protease-mediated cleavage of the Toll-like receptor 3 adaptor protein TRIF*. Proc Natl Acad Sci U S A, 2005. **102**(8): p. 2992-7.
199. Otsuka, M., N. Kato, M. Moriyama, H. Taniguchi, Y. Wang, N. Dharel, T. Kawabe, and M. Omata, *Interaction between the HCV NS3 protein and the host TBK1 protein leads to inhibition of cellular antiviral responses*. Hepatology, 2005. **41**(5): p. 1004-12.
200. Tasaka, M., N. Sakamoto, Y. Itakura, M. Nakagawa, Y. Itsui, Y. Sekine-Osajima, Y. Nishimura-Sakurai, C.H. Chen, M. Yoneyama, T. Fujita, T. Wakita, S. Maekawa, N. Enomoto, and M. Watanabe, *Hepatitis C virus non-structural proteins responsible for suppression of the RIG-I/Cardif-induced interferon response*. J Gen Virol, 2007. **88**(Pt 12): p. 3323-33.
201. Abe, T., Y. Kaname, I. Hamamoto, Y. Tsuda, X. Wen, S. Taguwa, K. Moriishi, O. Takeuchi, T. Kawai, T. Kanto, N. Hayashi, S. Akira, and Y. Matsuura, *Hepatitis C virus nonstructural protein 5A modulates the toll-like receptor-MyD88-dependent signaling pathway in macrophage cell lines*. J Virol, 2007. **81**(17): p. 8953-66.
202. Lan, K.H., K.L. Lan, W.P. Lee, M.L. Sheu, M.Y. Chen, Y.L. Lee, S.H. Yen, F.Y. Chang, and S.D. Lee, *HCV NS5A inhibits interferon-alpha signaling through suppression of STAT1 phosphorylation in hepatocyte-derived cell lines*. J Hepatol, 2007. **46**(5): p. 759-67.
203. Lin, W., S.S. Kim, E. Yeung, Y. Kamegaya, J.T. Blackard, K.A. Kim, M.J. Holtzman, and R.T. Chung, *Hepatitis C virus core protein blocks interferon signaling by interaction with the STAT1 SH2 domain*. J Virol, 2006. **80**(18): p. 9226-35.
204. Bigger, C.B., K.M. Brasky, and R.E. Lanford, *DNA microarray analysis of chimpanzee liver during acute resolving hepatitis C virus infection*. J Virol, 2001. **75**(15): p. 7059-66.

205. Major, M.E., H. Dahari, K. Mihalik, M. Puig, C.M. Rice, A.U. Neumann, and S.M. Feinstone, *Hepatitis C virus kinetics and host responses associated with disease and outcome of infection in chimpanzees*. *Hepatology*, 2004. **39**(6): p. 1709-20.
206. Nanda, S., M.B. Havert, G.M. Calderon, M. Thomson, C. Jacobson, D. Kastner, and T.J. Liang, *Hepatic transcriptome analysis of hepatitis C virus infection in chimpanzees defines unique gene expression patterns associated with viral clearance*. *PLoS One*, 2008. **3**(10): p. e3442.
207. Yu, C., D. Boon, S.L. McDonald, T.G. Myers, K. Tomioka, H. Nguyen, R.E. Engle, S. Govindarajan, S.U. Emerson, and R.H. Purcell, *Pathogenesis of hepatitis E virus and hepatitis C virus in chimpanzees: similarities and differences*. *J Virol*, 2010. **84**(21): p. 11264-78.
208. Su, A.I., J.P. Pezacki, L. Wodicka, A.D. Brideau, L. Supekova, R. Thimme, S. Wieland, J. Bukh, R.H. Purcell, P.G. Schultz, and F.V. Chisari, *Genomic analysis of the host response to hepatitis C virus infection*. *Proc Natl Acad Sci U S A*, 2002. **99**(24): p. 15669-74.
209. Dill, M.T., Z. Makowska, F.H. Duong, F. Merkofer, M. Filipowicz, T.F. Baumert, L. Tornillo, L. Terracciano, and M.H. Heim, *Interferon-gamma-stimulated genes, but not USP18, are expressed in livers of patients with acute hepatitis C*. *Gastroenterology*, 2012. **143**(3): p. 777-86 e1-6.
210. Jaeckel, E., M. Cornberg, H. Wedemeyer, T. Santantonio, J. Mayer, M. Zankel, G. Pastore, M. Dietrich, C. Trautwein, and M.P. Manns, *Treatment of acute hepatitis C with interferon alfa-2b*. *N Engl J Med*, 2001. **345**(20): p. 1452-7.
211. Gerlach, J.T., H.M. Diepolder, R. Zachoval, N.H. Gruener, M.C. Jung, A. Ulsenheimer, W.W. Schraut, C.A. Schirren, M. Waechtler, M. Backmund, and G.R. Pape, *Acute hepatitis C: high rate of both spontaneous and treatment-induced viral clearance*. *Gastroenterology*, 2003. **125**(1): p. 80-8.
212. Makowska, Z. and M.H. Heim, *Interferon signaling in the liver during hepatitis C virus infection*. *Cytokine*, 2012. **59**(3): p. 460-6.

213. Sarasin-Filipowicz, M., E.J. Oakeley, F.H. Duong, V. Christen, L. Terracciano, W. Filipowicz, and M.H. Heim, *Interferon signaling and treatment outcome in chronic hepatitis C*. Proc Natl Acad Sci U S A, 2008. **105**(19): p. 7034-9.
214. Darling, J.M., J. Aerssens, G. Fanning, J.G. McHutchison, D.B. Goldstein, A.J. Thompson, K.V. Shianna, N.H. Afdhal, M.L. Hudson, C.D. Howell, W. Talloen, J. Bollekens, M. De Wit, A. Scholliers, and M.W. Fried, *Quantitation of pretreatment serum interferon-gamma-inducible protein-10 improves the predictive value of an IL28B gene polymorphism for hepatitis C treatment response*. Hepatology, 2011. **53**(1): p. 14-22.
215. Lagging, M., G. Askarieh, F. Negro, S. Bibert, J. Soderholm, J. Westin, M. Lindh, A. Romero, G. Missale, C. Ferrari, A.U. Neumann, J.M. Pawlotsky, B.L. Haagmans, S. Zeuzem, P.Y. Bochud, and K. Hellstrand, *Response prediction in chronic hepatitis C by assessment of IP-10 and IL28B-related single nucleotide polymorphisms*. PLoS One, 2011. **6**(2): p. e17232.
216. Takahashi, K., S. Asabe, S. Wieland, U. Garaigorta, P. Gastaminza, M. Isogawa, and F.V. Chisari, *Plasmacytoid dendritic cells sense hepatitis C virus-infected cells, produce interferon, and inhibit infection*. Proc Natl Acad Sci U S A, 2010. **107**(16): p. 7431-6.
217. Stone, A.E., S. Giugliano, G. Schnell, L. Cheng, K.F. Leahy, L. Golden-Mason, M. Gale, Jr., and H.R. Rosen, *Hepatitis C virus pathogen associated molecular pattern (PAMP) triggers production of lambda-interferons by human plasmacytoid dendritic cells*. PLoS Pathog, 2013. **9**(4): p. e1003316.
218. Naggie, S., A. Osinusi, A. Katsounas, R. Lempicki, E. Herrmann, A.J. Thompson, P.J. Clark, K. Patel, A.J. Muir, J.G. McHutchison, J.F. Schlaak, M. Trippler, B. Shivakumar, H. Masur, M.A. Polis, and S. Kottlil, *Dysregulation of innate immunity in hepatitis C virus genotype 1 IL28B-unfavorable genotype patients: impaired viral kinetics and therapeutic response*. Hepatology, 2012. **56**(2): p. 444-54.

219. Teijaro, J.R., C. Ng, A.M. Lee, B.M. Sullivan, K.C. Sheehan, M. Welch, R.D. Schreiber, J.C. de la Torre, and M.B. Oldstone, *Persistent LCMV infection is controlled by blockade of type I interferon signaling*. *Science*, 2013. **340**(6129): p. 207-11.
220. Wilson, E.B., D.H. Yamada, H. Elsaesser, J. Herskovitz, J. Deng, G. Cheng, B.J. Aronow, C.L. Karp, and D.G. Brooks, *Blockade of chronic type I interferon signaling to control persistent LCMV infection*. *Science*, 2013. **340**(6129): p. 202-7.
221. Sells, M.A., M.L. Chen, and G. Acs, *Production of hepatitis B virus particles in Hep G2 cells transfected with cloned hepatitis B virus DNA*. *Proc Natl Acad Sci U S A*, 1987. **84**(4): p. 1005-9.
222. Ladner, S.K., M.J. Otto, C.S. Barker, K. Zaifert, G.H. Wang, J.T. Guo, C. Seeger, and R.W. King, *Inducible expression of human hepatitis B virus (HBV) in stably transfected hepatoblastoma cells: a novel system for screening potential inhibitors of HBV replication*. *Antimicrob Agents Chemother*, 1997. **41**(8): p. 1715-20.
223. Sureau, C., J.L. Romet-Lemonne, J.I. Mullins, and M. Essex, *Production of hepatitis B virus by a differentiated human hepatoma cell line after transfection with cloned circular HBV DNA*. *Cell*, 1986. **47**(1): p. 37-47.
224. Galle, P.R., J. Hagelstein, B. Kommerell, M. Volkmann, P. Schranz, and H. Zentgraf, *In vitro experimental infection of primary human hepatocytes with hepatitis B virus*. *Gastroenterology*, 1994. **106**(3): p. 664-73.
225. Gripon, P., C. Diot, and C. Guguen-Guillouzo, *Reproducible high level infection of cultured adult human hepatocytes by hepatitis B virus: effect of polyethylene glycol on adsorption and penetration*. *Virology*, 1993. **192**(2): p. 534-40.
226. Gripon, P., C. Diot, N. Theze, I. Fourel, O. Loreal, C. Brechot, and C. Guguen-Guillouzo, *Hepatitis B virus infection of adult human hepatocytes cultured in the presence of dimethyl sulfoxide*. *J Virol*, 1988. **62**(11): p. 4136-43.

227. Schulze-Bergkamen, H., A. Untergasser, A. Dax, H. Vogel, P. Buchler, E. Klar, T. Lehnert, H. Friess, M.W. Buchler, M. Kirschfink, W. Stremmel, P.H. Krammer, M. Muller, and U. Protzer, *Primary human hepatocytes--a valuable tool for investigation of apoptosis and hepatitis B virus infection*. J Hepatol, 2003. **38**(6): p. 736-44.
228. Gripon, P., S. Rumin, S. Urban, J. Le Seyec, D. Glaise, I. Cannie, C. Guyomard, J. Lucas, C. Trepo, and C. Guguen-Guillouzo, *Infection of a human hepatoma cell line by hepatitis B virus*. Proc Natl Acad Sci U S A, 2002. **99**(24): p. 15655-60.
229. Billioud, G., C. Pichoud, R. Parent, and F. Zoulim, *Decreased infectivity of nucleoside analogs-resistant hepatitis B virus mutants*. J Hepatol, 2012. **56**(6): p. 1269-75.
230. Beard, M.R., G. Abell, M. Honda, A. Carroll, M. Gartland, B. Clarke, K. Suzuki, R. Lanford, D.V. Sangar, and S.M. Lemon, *An infectious molecular clone of a Japanese genotype 1b hepatitis C virus*. Hepatology, 1999. **30**(1): p. 316-24.
231. Kolykhalov, A.A., E.V. Agapov, K.J. Blight, K. Mihalik, S.M. Feinstone, and C.M. Rice, *Transmission of hepatitis C by intrahepatic inoculation with transcribed RNA*. Science, 1997. **277**(5325): p. 570-4.
232. Lanford, R.E., H. Lee, D. Chavez, B. Guerra, and K.M. Brasky, *Infectious cDNA clone of the hepatitis C virus genotype 1 prototype sequence*. J Gen Virol, 2001. **82**(Pt 6): p. 1291-7.
233. Yanagi, M., R.H. Purcell, S.U. Emerson, and J. Bukh, *Transcripts from a single full-length cDNA clone of hepatitis C virus are infectious when directly transfected into the liver of a chimpanzee*. Proc Natl Acad Sci U S A, 1997. **94**(16): p. 8738-43.
234. Lohmann, V., F. Korner, J. Koch, U. Herian, L. Theilmann, and R. Bartenschlager, *Replication of subgenomic hepatitis C virus RNAs in a hepatoma cell line*. Science, 1999. **285**(5424): p. 110-3.

235. Nakabayashi, H., K. Taketa, K. Miyano, T. Yamane, and J. Sato, *Growth of human hepatoma cells lines with differentiated functions in chemically defined medium*. *Cancer Res*, 1982. **42**(9): p. 3858-63.
236. Kato, T., T. Date, M. Miyamoto, A. Furusaka, K. Tokushige, M. Mizokami, and T. Wakita, *Efficient replication of the genotype 2a hepatitis C virus subgenomic replicon*. *Gastroenterology*, 2003. **125**(6): p. 1808-17.
237. Kato, T., A. Furusaka, M. Miyamoto, T. Date, K. Yasui, J. Hiramoto, K. Nagayama, T. Tanaka, and T. Wakita, *Sequence analysis of hepatitis C virus isolated from a fulminant hepatitis patient*. *J Med Virol*, 2001. **64**(3): p. 334-9.
238. Lindenbach, B.D., M.J. Evans, A.J. Syder, B. Wolk, T.L. Tellinghuisen, C.C. Liu, T. Maruyama, R.O. Hynes, D.R. Burton, J.A. McKeating, and C.M. Rice, *Complete replication of hepatitis C virus in cell culture*. *Science*, 2005. **309**(5734): p. 623-6.
239. Lindenbach, B.D., P. Meuleman, A. Ploss, T. Vanwolleghem, A.J. Syder, J.A. McKeating, R.E. Lanford, S.M. Feinstone, M.E. Major, G. Leroux-Roels, and C.M. Rice, *Cell culture-grown hepatitis C virus is infectious in vivo and can be recultured in vitro*. *Proc Natl Acad Sci U S A*, 2006. **103**(10): p. 3805-9.
240. Wakita, T., T. Pietschmann, T. Kato, T. Date, M. Miyamoto, Z. Zhao, K. Murthy, A. Habermann, H.G. Krausslich, M. Mizokami, R. Bartenschlager, and T.J. Liang, *Production of infectious hepatitis C virus in tissue culture from a cloned viral genome*. *Nat Med*, 2005. **11**(7): p. 791-6.
241. Zhong, J., P. Gastaminza, G. Cheng, S. Kapadia, T. Kato, D.R. Burton, S.F. Wieland, S.L. Uprichard, T. Wakita, and F.V. Chisari, *Robust hepatitis C virus infection in vitro*. *Proc Natl Acad Sci U S A*, 2005. **102**(26): p. 9294-9.
242. Yi, M., R.A. Villanueva, D.L. Thomas, T. Wakita, and S.M. Lemon, *Production of infectious genotype 1a hepatitis C virus (Hutchinson strain)*

- in cultured human hepatoma cells*. Proc Natl Acad Sci U S A, 2006. **103**(7): p. 2310-5.
243. Pietschmann, T., M. Zayas, P. Meuleman, G. Long, N. Appel, G. Koutsoudakis, S. Kallis, G. Leroux-Roels, V. Lohmann, and R. Bartenschlager, *Production of infectious genotype 1b virus particles in cell culture and impairment by replication enhancing mutations*. PLoS Pathog, 2009. **5**(6): p. e1000475.
244. Steenbergen, R.H., M.A. Joyce, B.S. Thomas, D. Jones, J. Law, R. Russell, M. Houghton, and D.L. Tyrrell, *Human serum leads to differentiation of human hepatoma cells, restoration of very-low-density lipoprotein secretion, and a 1000-fold increase in HCV Japanese fulminant hepatitis type 1 titers*. Hepatology, 2013. **58**(6): p. 1907-17.
245. Yang, D., C. Zuo, X. Wang, X. Meng, B. Xue, N. Liu, R. Yu, Y. Qin, Y. Gao, Q. Wang, J. Hu, L. Wang, Z. Zhou, B. Liu, D. Tan, Y. Guan, and H. Zhu, *Complete replication of hepatitis B virus and hepatitis C virus in a newly developed hepatoma cell line*. Proc Natl Acad Sci U S A, 2014.
246. Cooper, S., A.L. Erickson, E.J. Adams, J. Kansopon, A.J. Weiner, D.Y. Chien, M. Houghton, P. Parham, and C.M. Walker, *Analysis of a successful immune response against hepatitis C virus*. Immunity, 1999. **10**(4): p. 439-49.
247. Thimme, R., J. Bukh, H.C. Spangenberg, S. Wieland, J. Pemberton, C. Steiger, S. Govindarajan, R.H. Purcell, and F.V. Chisari, *Viral and immunological determinants of hepatitis C virus clearance, persistence, and disease*. Proc Natl Acad Sci U S A, 2002. **99**(24): p. 15661-8.
248. Bertoni, R., A. Sette, J. Sidney, L.G. Guidotti, M. Shapiro, R. Purcell, and F.V. Chisari, *Human class I supertypes and CTL repertoires extend to chimpanzees*. J Immunol, 1998. **161**(8): p. 4447-55.
249. Berthelot, P., A.M. Courouce, A. Eyquem, G. Feldmann, J. Jacob, P. Ravisse, B. Vacher, J. Moor-Jankowski, E. Muchmore, and A. Prince, *Hepatitis B vaccine safety monitoring in the chimpanzee: interpretation of results*. J Med Primatol, 1984. **13**(3): p. 119-33.

250. Ohmura, T., A. Ohmizu, A. Sumi, W. Ohtani, Y. Uemura, H. Arimura, M. Nishida, Y. Kohama, M. Okabe, T. Mimura, and et al., *Properties of recombinant hepatitis B vaccine*. *Biochem Biophys Res Commun*, 1987. **149**(3): p. 1172-8.
251. Fujisawa, Y., S. Kuroda, P.M. Van Eerd, H. Schellekens, and A. Kakinuma, *Protective efficacy of a novel hepatitis B vaccine consisting of M (pre-S2 + S) protein particles (a third generation vaccine)*. *Vaccine*, 1990. **8**(3): p. 192-8.
252. Ogata, N., P.J. Cote, A.R. Zanetti, R.H. Miller, M. Shapiro, J. Gerin, and R.H. Purcell, *Licensed recombinant hepatitis B vaccines protect chimpanzees against infection with the prototype surface gene mutant of hepatitis B virus*. *Hepatology*, 1999. **30**(3): p. 779-86.
253. Folgori, A., S. Capone, L. Ruggeri, A. Meola, E. Sporeno, B.B. Ercole, M. Pezzanera, R. Tafi, M. Arcuri, E. Fattori, A. Lahm, A. Luzzago, A. Vitelli, S. Colloca, R. Cortese, and A. Nicosia, *A T-cell HCV vaccine eliciting effective immunity against heterologous virus challenge in chimpanzees*. *Nat Med*, 2006. **12**(2): p. 190-7.
254. Choo, Q.L., G. Kuo, R. Ralston, A. Weiner, D. Chien, G. Van Nest, J. Han, K. Berger, K. Thudium, C. Kuo, and et al., *Vaccination of chimpanzees against infection by the hepatitis C virus*. *Proc Natl Acad Sci U S A*, 1994. **91**(4): p. 1294-8.
255. Frey, S.E., M. Houghton, S. Coates, S. Abrignani, D. Chien, D. Rosa, P. Pileri, R. Ray, A.M. Di Bisceglie, P. Rinella, H. Hill, M.C. Wolff, V. Schultze, J.H. Han, B. Scharschmidt, and R.B. Belshe, *Safety and immunogenicity of HCV E1E2 vaccine adjuvanted with MF59 administered to healthy adults*. *Vaccine*, 2010. **28**(38): p. 6367-73.
256. Rollier, C.S., G. Paranhos-Baccala, E.J. Verschoor, B.E. Verstrepen, J.A. Drexhage, Z. Fagrouch, J.L. Berland, F. Komurian-Pradel, B. Duverger, N. Himoudi, C. Staib, M. Meyr, M. Whelan, J.A. Whelan, V.C. Adams, E. Larrea, J.I. Riezu, J.J. Lasarte, B. Bartosch, F.L. Cosset, W.J. Spaan, H.M. Diepolder, G.R. Pape, G. Sutter, G. Inchauspe, and J.L. Heeney, *Vaccine-*

- induced early control of hepatitis C virus infection in chimpanzees fails to impact on hepatic PD-1 and chronicity.* Hepatology, 2007. **45**(3): p. 602-13.
257. Habersetzer, F., G. Honnet, C. Bain, M. Maynard-Muet, V. Leroy, J.P. Zarski, C. Feray, T.F. Baumert, J.P. Bronowicki, M. Doffoel, C. Trepo, D. Agathon, M.L. Toh, M. Baudin, J.Y. Bonnefoy, J.M. Limacher, and G. Inchauspe, *A poxvirus vaccine is safe, induces T-cell responses, and decreases viral load in patients with chronic hepatitis C.* Gastroenterology, 2011. **141**(3): p. 890-899 e1-4.
258. in *Chimpanzees in Biomedical and Behavioral Research: Assessing the Necessity*, B.M. Altevogt, et al., Editors. 2011: Washington (DC).
259. Amako, Y., K. Tsukiyama-Kohara, A. Katsume, Y. Hirata, S. Sekiguchi, Y. Tobita, Y. Hayashi, T. Hishima, N. Funata, H. Yonekawa, and M. Kohara, *Pathogenesis of hepatitis C virus infection in Tupaia belangeri.* J Virol, 2010. **84**(1): p. 303-11.
260. Yan, R.Q., J.J. Su, D.R. Huang, Y.C. Gan, C. Yang, and G.H. Huang, *Human hepatitis B virus and hepatocellular carcinoma. I. Experimental infection of tree shrews with hepatitis B virus.* J Cancer Res Clin Oncol, 1996. **122**(5): p. 283-8.
261. Yan, R.Q., J.J. Su, D.R. Huang, Y.C. Gan, C. Yang, and G.H. Huang, *Human hepatitis B virus and hepatocellular carcinoma. II. Experimental induction of hepatocellular carcinoma in tree shrews exposed to hepatitis B virus and aflatoxin B1.* J Cancer Res Clin Oncol, 1996. **122**(5): p. 289-95.
262. Bukh, J., C.L. Apgar, and M. Yanagi, *Toward a surrogate model for hepatitis C virus: An infectious molecular clone of the GB virus-B hepatitis agent.* Virology, 1999. **262**(2): p. 470-8.
263. Beames, B., D. Chavez, and R.E. Lanford, *GB virus B as a model for hepatitis C virus.* ILAR J, 2001. **42**(2): p. 152-60.
264. Kapoor, A., P. Simmonds, G. Gerold, N. Qaisar, K. Jain, J.A. Henriquez, C. Firth, D.L. Hirschberg, C.M. Rice, S. Shields, and W.I. Lipkin,

- Characterization of a canine homolog of hepatitis C virus.* Proc Natl Acad Sci U S A, 2011. **108**(28): p. 11608-13.
265. Lenhoff, R.J., C.A. Luscombe, and J. Summers, *Acute liver injury following infection with a cytopathic strain of duck hepatitis B virus.* Hepatology, 1999. **29**(2): p. 563-71.
266. Summers, J., J.M. Smolec, and R. Snyder, *A virus similar to human hepatitis B virus associated with hepatitis and hepatoma in woodchucks.* Proc Natl Acad Sci U S A, 1978. **75**(9): p. 4533-7.
267. Chisari, F.V., C.A. Pinkert, D.R. Milich, P. Filippi, A. McLachlan, R.D. Palmiter, and R.L. Brinster, *A transgenic mouse model of the chronic hepatitis B surface antigen carrier state.* Science, 1985. **230**(4730): p. 1157-60.
268. Kim, C.M., K. Koike, I. Saito, T. Miyamura, and G. Jay, *HBx gene of hepatitis B virus induces liver cancer in transgenic mice.* Nature, 1991. **351**(6324): p. 317-20.
269. Guidotti, L.G., B. Matzke, H. Schaller, and F.V. Chisari, *High-level hepatitis B virus replication in transgenic mice.* J Virol, 1995. **69**(10): p. 6158-69.
270. Isogawa, M., K. Kakimi, H. Kamamoto, U. Protzer, and F.V. Chisari, *Differential dynamics of the peripheral and intrahepatic cytotoxic T lymphocyte response to hepatitis B surface antigen.* Virology, 2005. **333**(2): p. 293-300.
271. Sprinzl, M.F., H. Oberwinkler, H. Schaller, and U. Protzer, *Transfer of hepatitis B virus genome by adenovirus vectors into cultured cells and mice: crossing the species barrier.* J Virol, 2001. **75**(11): p. 5108-18.
272. Yang, P.L., A. Althage, J. Chung, and F.V. Chisari, *Hydrodynamic injection of viral DNA: a mouse model of acute hepatitis B virus infection.* Proc Natl Acad Sci U S A, 2002. **99**(21): p. 13825-30.
273. Kremsdorf, D. and N. Brezillon, *New animal models for hepatitis C viral infection and pathogenesis studies.* World J Gastroenterol, 2007. **13**(17): p. 2427-35.

274. Dorner, M., J.A. Horwitz, J.B. Robbins, W.T. Barry, Q. Feng, K. Mu, C.T. Jones, J.W. Schoggins, M.T. Catanese, D.R. Burton, M. Law, C.M. Rice, and A. Ploss, *A genetically humanized mouse model for hepatitis C virus infection*. *Nature*, 2011. **474**(7350): p. 208-11.
275. Hikosaka, K., H. Noritake, W. Kimura, N. Sultana, M.T. Sharkar, Y. Tagawa, T. Uezato, Y. Kobayashi, T. Wakita, and N. Miura, *Expression of human factors CD81, claudin-1, scavenger receptor, and occludin in mouse hepatocytes does not confer susceptibility to HCV entry*. *Biomed Res*, 2011. **32**(2): p. 143-50.
276. Bitzegeio, J., D. Bankwitz, K. Hueging, S. Haid, C. Brohm, M.B. Zeisel, E. Herrmann, M. Iken, M. Ott, T.F. Baumert, and T. Pietschmann, *Adaptation of hepatitis C virus to mouse CD81 permits infection of mouse cells in the absence of human entry factors*. *PLoS Pathog*, 2010. **6**: p. e1000978.
277. Mercer, D.F., D.E. Schiller, J.F. Elliott, D.N. Douglas, C. Hao, A. Rinfret, W.R. Addison, K.P. Fischer, T.A. Churchill, J.R. Lakey, D.L. Tyrrell, and N.M. Kneteman, *Hepatitis C virus replication in mice with chimeric human livers*. *Nat Med*, 2001. **7**(8): p. 927-33.
278. Lacek, K., K. Vercauteren, K. Grzyb, M. Naddeo, L. Verhoye, M.P. Slowikowski, S. Fafi-Kremer, A.H. Patel, T.F. Baumert, A. Folgari, G. Leroux-Roels, R. Cortese, P. Meuleman, and A. Nicosia, *Novel human SR-BI antibodies prevent infection and dissemination of HCV in vitro and in humanized mice*. *J Hepatol*, 2012. **57**(1): p. 17-23.
279. Meuleman, P., M.T. Catanese, L. Verhoye, I. Desombere, A. Farhoudi, C.T. Jones, T. Sheahan, K. Grzyb, R. Cortese, C.M. Rice, G. Leroux-Roels, and A. Nicosia, *A human monoclonal antibody targeting scavenger receptor class B type I precludes hepatitis C virus infection and viral spread in vitro and in vivo*. *Hepatology*, 2012. **55**(2): p. 364-72.
280. Vanwolleghem, T., J. Bukh, P. Meuleman, I. Desombere, J.C. Meunier, H. Alter, R.H. Purcell, and G. Leroux-Roels, *Polyclonal immunoglobulins from a chronic hepatitis C virus patient protect human liver-chimeric mice*

- from infection with a homologous hepatitis C virus strain. Hepatology*, 2008. **47**(6): p. 1846-55.
281. Steenbergen, R.H., M.A. Joyce, G. Lund, J. Lewis, R. Chen, N. Barsby, D. Douglas, L.F. Zhu, D.L. Tyrrell, and N.M. Kneteman, *Lipoprotein profiles in SCID/uPA mice transplanted with human hepatocytes become human-like and correlate with HCV infection success. Am J Physiol Gastrointest Liver Physiol*, 2010. **299**(4): p. G844-54.
282. Hiraga, N., M. Imamura, T. Hatakeyama, S. Kitamura, F. Mitsui, S. Tanaka, M. Tsuge, S. Takahashi, H. Abe, T. Maekawa, H. Ochi, C. Tateno, K. Yoshizato, T. Wakita, and K. Chayama, *Absence of viral interference and different susceptibility to interferon between hepatitis B virus and hepatitis C virus in human hepatocyte chimeric mice. J Hepatol*, 2009. **51**(6): p. 1046-54.
283. Tsuge, M., Y. Fujimoto, N. Hiraga, Y. Zhang, M. Ohnishi, T. Kohno, H. Abe, D. Miki, M. Imamura, S. Takahashi, H. Ochi, C.N. Hayes, F. Miya, T. Tsunoda, and K. Chayama, *Hepatitis C virus infection suppresses the interferon response in the liver of the human hepatocyte chimeric mouse. PLoS One*, 2011. **6**(8): p. e23856.
284. Walters, K.A., M.A. Joyce, J.C. Thompson, M.W. Smith, M.M. Yeh, S. Prohl, L.F. Zhu, T.J. Gao, N.M. Kneteman, D.L. Tyrrell, and M.G. Katze, *Host-specific response to HCV infection in the chimeric SCID-beige/Alb-uPA mouse model: role of the innate antiviral immune response. PLoS Pathog*, 2006. **2**(6): p. e59.
285. Bosma, M.J. and A.M. Carroll, *The SCID mouse mutant: definition, characterization, and potential uses. Annu Rev Immunol*, 1991. **9**: p. 323-50.
286. Roder, J.C., *The beige mutation in the mouse. I. A stem cell predetermined impairment in natural killer cell function. J Immunol*, 1979. **123**(5): p. 2168-73.
287. Hoopes, B.C. and W.R. McClure, *Studies on the selectivity of DNA precipitation by spermine. Nucleic Acids Res*, 1981. **9**(20): p. 5493-504.

288. Welzel, T.M., W.J. Miley, T.L. Parks, J.J. Goedert, D. Whitby, and B.A. Ortiz-Conde, *Real-time PCR assay for detection and quantification of hepatitis B virus genotypes A to G*. J Clin Microbiol, 2006. **44**(9): p. 3325-33.
289. Livak, K.J. and T.D. Schmittgen, *Analysis of Relative Gene Expression Data Using Real-Time Quantitative PCR and the $2^{-\Delta\Delta CT}$ Method*. Methods, 2001. **25**(4): p. 402-408.
290. Livak, K.J. and T.D. Schmittgen, *Analysis of relative gene expression data using real-time quantitative PCR and the $2^{-\Delta\Delta C(T)}$ Method*. Methods, 2001. **25**(4): p. 402-8.
291. Koopman, R., G. Schaart, and M.K. Hesselink, *Optimisation of oil red O staining permits combination with immunofluorescence and automated quantification of lipids*. Histochem Cell Biol, 2001. **116**(1): p. 63-8.
292. Li, K. and S.M. Lemon, *Innate immune responses in hepatitis C virus infection*. Semin Immunopathol, 2013. **35**(1): p. 53-72.
293. Cheng, G., J. Zhong, and F.V. Chisari, *Inhibition of dsRNA-induced signaling in hepatitis C virus-infected cells by NS3 protease-dependent and -independent mechanisms*. Proc Natl Acad Sci U S A, 2006. **103**(22): p. 8499-504.
294. Murayama, M., Y. Katano, I. Nakano, M. Ishigami, K. Hayashi, T. Honda, Y. Hirooka, A. Itoh, and H. Goto, *A mutation in the interferon sensitivity-determining region is associated with responsiveness to interferon-ribavirin combination therapy in chronic hepatitis patients infected with a Japan-specific subtype of hepatitis C virus genotype 1B*. J Med Virol, 2007. **79**(1): p. 35-40.
295. Enomoto, N., I. Sakuma, Y. Asahina, M. Kurosaki, T. Murakami, C. Yamamoto, N. Izumi, F. Marumo, and C. Sato, *Comparison of full-length sequences of interferon-sensitive and resistant hepatitis C virus 1b. Sensitivity to interferon is conferred by amino acid substitutions in the NS5A region*. J Clin Invest, 1995. **96**(1): p. 224-30.

296. Hayashi, K., Y. Katano, M. Ishigami, A. Itoh, Y. Hirooka, I. Nakano, F. Urano, K. Yoshioka, H. Toyoda, T. Kumada, and H. Goto, *Mutations in the core and NS5A region of hepatitis C virus genotype 1b and correlation with response to pegylated-interferon-alpha 2b and ribavirin combination therapy*. J Viral Hepat, 2011. **18**(4): p. 280-6.
297. El-Shamy, A., M. Nagano-Fujii, N. Sasase, S. Imoto, S.R. Kim, and H. Hotta, *Sequence variation in hepatitis C virus nonstructural protein 5A predicts clinical outcome of pegylated interferon/ribavirin combination therapy*. Hepatology, 2008. **48**(1): p. 38-47.
298. Berg, T., A. Mas Marques, M. Hohne, B. Wiedenmann, U. Hopf, and E. Schreier, *Mutations in the E2-PePHD and NS5A region of hepatitis C virus type 1 and the dynamics of hepatitis C viremia decline during interferon alfa treatment*. Hepatology, 2000. **32**(6): p. 1386-95.
299. Kohashi, T., S. Maekawa, N. Sakamoto, M. Kurosaki, H. Watanabe, Y. Tanabe, C.H. Chen, N. Kanazawa, M. Nakagawa, S. Kakinuma, T. Yamashiro, Y. Itsui, T. Koyama, N. Enomoto, and M. Watanabe, *Site-specific mutation of the interferon sensitivity-determining region (ISDR) modulates hepatitis C virus replication*. J Viral Hepat, 2006. **13**(9): p. 582-90.
300. Sarrazin, C., E. Herrmann, K. Bruch, and S. Zeuzem, *Hepatitis C virus nonstructural 5A protein and interferon resistance: a new model for testing the reliability of mutational analyses*. J Virol, 2002. **76**(21): p. 11079-90.
301. Macquillan, G.C., X. Niu, D. Speers, S. English, G. Garas, G.B. Harnett, W.D. Reed, J.E. Allan, and G.P. Jeffrey, *Does sequencing the PKRBD of hepatitis C virus NS5A predict therapeutic response to combination therapy in an Australian population?* J Gastroenterol Hepatol, 2004. **19**(5): p. 551-7.
302. Xu, Z., X. Fan, Y. Xu, and A.M. Di Bisceglie, *Comparative analysis of nearly full-length hepatitis C virus quasispecies from patients experiencing viral breakthrough during antiviral therapy: clustered*

- mutations in three functional genes, E2, NS2, and NS5a.* J Virol, 2008. **82**(19): p. 9417-24.
303. Farci, P., R. Strazzera, H.J. Alter, S. Farci, D. Degioannis, A. Coiana, G. Peddis, F. Usai, G. Serra, L. Chessa, G. Diaz, A. Balestrieri, and R.H. Purcell, *Early changes in hepatitis C viral quasispecies during interferon therapy predict the therapeutic outcome.* Proc Natl Acad Sci U S A, 2002. **99**(5): p. 3081-6.
304. Zhang, S., K. Kodys, G.J. Babcock, and G. Szabo, *CD81/CD9 tetraspanins aid plasmacytoid dendritic cells in recognition of hepatitis C virus-infected cells and induction of interferon-alpha.* Hepatology, 2012.
305. Lau, D.T., A. Negash, J. Chen, N. Crochet, M. Sinha, Y. Zhang, J. Guedj, S. Holder, T. Saito, S.M. Lemon, B.A. Luxon, A.S. Perelson, and M. Gale, Jr., *Innate immune tolerance and the role of kupffer cells in differential responses to interferon therapy among patients with HCV genotype 1 infection.* Gastroenterology, 2013. **144**(2): p. 402-413 e12.
306. Chen, L., I. Borozan, J. Sun, M. Guindi, S. Fischer, J. Feld, N. Anand, J. Heathcote, A.M. Edwards, and I.D. McGilvray, *Cell-type specific gene expression signature in liver underlies response to interferon therapy in chronic hepatitis C infection.* Gastroenterology, 2010. **138**(3): p. 1123-33 e1-3.
307. McGilvray, I., J.J. Feld, L. Chen, V. Pattullo, M. Guindi, S. Fischer, I. Borozan, G. Xie, N. Selzner, E.J. Heathcote, and K. Siminovitch, *Hepatic cell-type specific gene expression better predicts HCV treatment outcome than IL28B genotype.* Gastroenterology, 2012. **142**(5): p. 1122-1131 e1.
308. Watanabe, T., F. Sugauchi, Y. Tanaka, K. Matsuura, H. Yatsunami, S. Murakami, S. Iijima, E. Iio, M. Sugiyama, T. Shimada, M. Kakuni, M. Kohara, and M. Mizokami, *Hepatitis C virus kinetics by administration of pegylated interferon-alpha in human and chimeric mice carrying human hepatocytes with variants of the IL28B gene.* Gut, 2012.
309. Hiraga, N., H. Abe, M. Imamura, M. Tsuge, S. Takahashi, C.N. Hayes, H. Ochi, C. Tateno, K. Yoshizato, Y. Nakamura, N. Kamatani, and K.

- Chayama, *Impact of viral amino acid substitutions and host interleukin-28b polymorphism on replication and susceptibility to interferon of hepatitis C virus*. *Hepatology*, 2011. **54**(3): p. 764-71.
310. Sonneveld, M.J., V. Rijckborst, S. Zeuzem, E.J. Heathcote, K. Simon, H. Senturk, S.D. Pas, B.E. Hansen, and H.L. Janssen, *Presence of precore and core promoter mutants limits the probability of response to peginterferon in hepatitis B e antigen-positive chronic hepatitis B*. *Hepatology*, 2012. **56**(1): p. 67-75.
311. Bode, J.G., S. Ludwig, C. Ehrhardt, U. Albrecht, A. Erhardt, F. Schaper, P.C. Heinrich, and D. Haussinger, *IFN-alpha antagonistic activity of HCV core protein involves induction of suppressor of cytokine signaling-3*. *FASEB J*, 2003. **17**(3): p. 488-90.
312. Melen, K., R. Fagerlund, M. Nyqvist, P. Keskinen, and I. Julkunen, *Expression of hepatitis C virus core protein inhibits interferon-induced nuclear import of STATs*. *J Med Virol*, 2004. **73**(4): p. 536-47.
313. de Lucas, S., J. Bartolome, and V. Carreno, *Hepatitis C virus core protein down-regulates transcription of interferon-induced antiviral genes*. *J Infect Dis*, 2005. **191**(1): p. 93-9.
314. Kneteman, N.M., A.J. Weiner, J. O'Connell, M. Collett, T. Gao, L. Aukerman, R. Kovelsky, Z.J. Ni, Q. Zhu, A. Hashash, J. Kline, B. Hsi, D. Schiller, D. Douglas, D.L. Tyrrell, and D.F. Mercer, *Anti-HCV therapies in chimeric scid-Alb/uPA mice parallel outcomes in human clinical application*. *Hepatology*, 2006. **43**(6): p. 1346-53.
315. Christen, V., F. Duong, C. Bernsmeier, D. Sun, M. Nassal, and M.H. Heim, *Inhibition of alpha interferon signaling by hepatitis B virus*. *J Virol*, 2007. **81**(1): p. 159-65.
316. Fernandez, M., J.A. Quiroga, and V. Carreno, *Hepatitis B virus downregulates the human interferon-inducible MxA promoter through direct interaction of precore/core proteins*. *J Gen Virol*, 2003. **84**(Pt 8): p. 2073-82.

317. Wu, M., Y. Xu, S. Lin, X. Zhang, L. Xiang, and Z. Yuan, *Hepatitis B virus polymerase inhibits the interferon-inducible MyD88 promoter by blocking nuclear translocation of Stat1*. J Gen Virol, 2007. **88**(Pt 12): p. 3260-9.
318. Lin, W., W.H. Choe, Y. Hiasa, Y. Kamegaya, J.T. Blackard, E.V. Schmidt, and R.T. Chung, *Hepatitis C virus expression suppresses interferon signaling by degrading STAT1*. Gastroenterology, 2005. **128**(4): p. 1034-41.
319. Sumpter, R., Jr., Y.M. Loo, E. Foy, K. Li, M. Yoneyama, T. Fujita, S.M. Lemon, and M. Gale, Jr., *Regulating intracellular antiviral defense and permissiveness to hepatitis C virus RNA replication through a cellular RNA helicase, RIG-I*. J Virol, 2005. **79**(5): p. 2689-99.
320. Lau, D.T., P.M. Fish, M. Sinha, D.M. Owen, S.M. Lemon, and M. Gale, Jr., *Interferon regulatory factor-3 activation, hepatic interferon-stimulated gene expression, and immune cell infiltration in hepatitis C virus patients*. Hepatology, 2008. **47**(3): p. 799-809.
321. Jiang, F., A. Ramanathan, M.T. Miller, G.Q. Tang, M. Gale, Jr., S.S. Patel, and J. Marcotrigiano, *Structural basis of RNA recognition and activation by innate immune receptor RIG-I*. Nature, 2011. **479**(7373): p. 423-7.
322. Kumar, H., T. Kawai, H. Kato, S. Sato, K. Takahashi, C. Coban, M. Yamamoto, S. Uematsu, K.J. Ishii, O. Takeuchi, and S. Akira, *Essential role of IPS-1 in innate immune responses against RNA viruses*. J Exp Med, 2006. **203**(7): p. 1795-803.
323. Suthar, M.S., D.Y. Ma, S. Thomas, J.M. Lund, N. Zhang, S. Daffis, A.Y. Rudensky, M.J. Bevan, E.A. Clark, M.K. Kaja, M.S. Diamond, and M. Gale, Jr., *IPS-1 is essential for the control of West Nile virus infection and immunity*. PLoS Pathog, 2010. **6**(2): p. e1000757.
324. Alvarez-Garcia, I. and E.A. Miska, *MicroRNA functions in animal development and human disease*. Development, 2005. **132**(21): p. 4653-62.

325. Bushati, N. and S.M. Cohen, *microRNA functions*. Annu Rev Cell Dev Biol, 2007. **23**: p. 175-205.
326. Schickel, R., B. Boyerinas, S.M. Park, and M.E. Peter, *MicroRNAs: key players in the immune system, differentiation, tumorigenesis and cell death*. Oncogene, 2008. **27**(45): p. 5959-74.
327. Garzon, R., G.A. Calin, and C.M. Croce, *MicroRNAs in Cancer*. Annu Rev Med, 2009. **60**: p. 167-79.
328. Gottwein, E. and B.R. Cullen, *Viral and cellular microRNAs as determinants of viral pathogenesis and immunity*. Cell Host Microbe, 2008. **3**(6): p. 375-87.
329. Lagos-Quintana, M., R. Rauhut, A. Yalcin, J. Meyer, W. Lendeckel, and T. Tuschl, *Identification of tissue-specific microRNAs from mouse*. Curr Biol, 2002. **12**(9): p. 735-9.
330. Chang, J., E. Nicolas, D. Marks, C. Sander, A. Lerro, M.A. Buendia, C. Xu, W.S. Mason, T. Moloshok, R. Bort, K.S. Zaret, and J.M. Taylor, *miR-122, a mammalian liver-specific microRNA, is processed from hcr mRNA and may downregulate the high affinity cationic amino acid transporter CAT-1*. RNA Biol, 2004. **1**(2): p. 106-13.
331. Jopling, C.L., M. Yi, A.M. Lancaster, S.M. Lemon, and P. Sarnow, *Modulation of hepatitis C virus RNA abundance by a liver-specific MicroRNA*. Science, 2005. **309**(5740): p. 1577-81.
332. Randall, G., M. Panis, J.D. Cooper, T.L. Tellinghuisen, K.E. Sukhodolets, S. Pfeffer, M. Landthaler, P. Landgraf, S. Kan, B.D. Lindenbach, M. Chien, D.B. Weir, J.J. Russo, J. Ju, M.J. Brownstein, R. Sheridan, C. Sander, M. Zavolan, T. Tuschl, and C.M. Rice, *Cellular cofactors affecting hepatitis C virus infection and replication*. Proc Natl Acad Sci U S A, 2007. **104**(31): p. 12884-9.
333. Murakami, Y., H.H. Aly, A. Tajima, I. Inoue, and K. Shimotohno, *Regulation of the hepatitis C virus genome replication by miR-199a*. J Hepatol, 2009. **50**(3): p. 453-60.

334. Banaudha, K., M. Kaliszewski, T. Korolnek, L. Florea, M.L. Yeung, K.T. Jeang, and A. Kumar, *MicroRNA silencing of tumor suppressor DLC-1 promotes efficient hepatitis C virus replication in primary human hepatocytes*. Hepatology, 2011. **53**(1): p. 53-61.
335. Hou, W., Q. Tian, J. Zheng, and H.L. Bonkovsky, *MicroRNA-196 represses Bach1 protein and hepatitis C virus gene expression in human hepatoma cells expressing hepatitis C viral proteins*. Hepatology, 2010. **51**(5): p. 1494-504.
336. Harvala, H., I. Robertson, T. Chieochansin, E.C. McWilliam Leitch, K. Templeton, and P. Simmonds, *Specific association of human parechovirus type 3 with sepsis and fever in young infants, as identified by direct typing of cerebrospinal fluid samples*. J Infect Dis, 2009. **199**(12): p. 1753-60.
337. Cheng, J.C., Y.J. Yeh, C.P. Tseng, S.D. Hsu, Y.L. Chang, N. Sakamoto, and H.D. Huang, *Let-7b is a novel regulator of hepatitis C virus replication*. Cell Mol Life Sci, 2012. **69**(15): p. 2621-33.
338. Bhanja Chowdhury, J., S. Shrivastava, R. Steele, A.M. Di Bisceglie, R. Ray, and R.B. Ray, *Hepatitis C virus infection modulates expression of interferon stimulatory gene IFITM1 by upregulating miR-130A*. J Virol, 2012. **86**(18): p. 10221-5.
339. Pezacki, J.P., R. Singaravelu, and R.K. Lyn, *Host-virus interactions during hepatitis C virus infection: a complex and dynamic molecular biosystem*. Mol Biosyst, 2010. **6**(7): p. 1131-42.
340. Herker, E. and M. Ott, *Unique ties between hepatitis C virus replication and intracellular lipids*. Trends Endocrinol Metab, 2011. **22**(6): p. 241-8.
341. Kapadia, S.B. and F.V. Chisari, *Hepatitis C virus RNA replication is regulated by host geranylgeranylation and fatty acids*. Proc Natl Acad Sci U S A, 2005. **102**(7): p. 2561-6.
342. Agnello, V., G. Abel, M. Elfahal, G.B. Knight, and Q.X. Zhang, *Hepatitis C virus and other flaviviridae viruses enter cells via low density lipoprotein receptor*. Proc Natl Acad Sci U S A, 1999. **96**(22): p. 12766-71.

343. Germi, R., J.M. Crance, D. Garin, J. Guimet, H. Lortat-Jacob, R.W. Ruigrok, J.P. Zarski, and E. Drouet, *Cellular glycosaminoglycans and low density lipoprotein receptor are involved in hepatitis C virus adsorption*. J Med Virol, 2002. **68**(2): p. 206-15.
344. Triyatni, M., B. Saunier, P. Maruvada, A.R. Davis, L. Ulianich, T. Heller, A. Patel, L.D. Kohn, and T.J. Liang, *Interaction of hepatitis C virus-like particles and cells: a model system for studying viral binding and entry*. J Virol, 2002. **76**(18): p. 9335-44.
345. Shi, S.T., K.J. Lee, H. Aizaki, S.B. Hwang, and M.M. Lai, *Hepatitis C virus RNA replication occurs on a detergent-resistant membrane that cofractionates with caveolin-2*. J Virol, 2003. **77**(7): p. 4160-8.
346. Miyanari, Y., K. Atsuzawa, N. Usuda, K. Watashi, T. Hishiki, M. Zayas, R. Bartenschlager, T. Wakita, M. Hijikata, and K. Shimotohno, *The lipid droplet is an important organelle for hepatitis C virus production*. Nat Cell Biol, 2007. **9**(9): p. 1089-97.
347. Huang, H., F. Sun, D.M. Owen, W. Li, Y. Chen, M. Gale, Jr., and J. Ye, *Hepatitis C virus production by human hepatocytes dependent on assembly and secretion of very low-density lipoproteins*. Proc Natl Acad Sci U S A, 2007. **104**(14): p. 5848-53.
348. Shirasaki, T., M. Honda, T. Shimakami, R. Horii, T. Yamashita, Y. Sakai, A. Sakai, H. Okada, R. Watanabe, S. Murakami, M. Yi, S.M. Lemon, and S. Kaneko, *MicroRNA-27a regulates lipid metabolism and inhibits hepatitis C virus replication in human hepatoma cells*. J Virol, 2013. **87**(9): p. 5270-86.
349. Barad, O., E. Meiri, A. Avniel, R. Aharonov, A. Barzilai, I. Bentwich, U. Einav, S. Gilad, P. Hurban, Y. Karov, E.K. Lobenhofer, E. Sharon, Y.M. Shibolet, M. Shtutman, Z. Bentwich, and P. Einat, *MicroRNA expression detected by oligonucleotide microarrays: system establishment and expression profiling in human tissues*. Genome Res, 2004. **14**(12): p. 2486-94.

350. Chen, W.J., K. Yin, G.J. Zhao, Y.C. Fu, and C.K. Tang, *The magic and mystery of microRNA-27 in atherosclerosis*. *Atherosclerosis*, 2012. **222**(2): p. 314-23.
351. Alisi, A., L. Da Sacco, G. Bruscalupi, F. Piemonte, N. Panera, R. De Vito, S. Leoni, G.F. Bottazzo, A. Masotti, and V. Nobili, *Mirnome analysis reveals novel molecular determinants in the pathogenesis of diet-induced nonalcoholic fatty liver disease*. *Lab Invest*, 2011. **91**(2): p. 283-93.
352. Her, G.M., C.C. Hsu, J.R. Hong, C.Y. Lai, M.C. Hsu, H.W. Pang, S.K. Chan, and W.Y. Pai, *Overexpression of gankyrin induces liver steatosis in zebrafish (Danio rerio)*. *Biochim Biophys Acta*, 2011. **1811**(9): p. 536-48.
353. Vickers, K.C., B.M. Shoucri, M.G. Levin, H. Wu, D.S. Pearson, D. Osei-Hwedieh, F.S. Collins, A.T. Remaley, and P. Sethupathy, *MicroRNA-27b is a regulatory hub in lipid metabolism and is altered in dyslipidemia*. *Hepatology*, 2013. **57**(2): p. 533-42.
354. Pezacki, J.P., J.A. Blake, D.C. Danielson, D.C. Kennedy, R.K. Lyn, and R. Singaravelu, *Chemical contrast for imaging living systems: molecular vibrations drive CARS microscopy*. *Nat Chem Biol*, 2011. **7**(3): p. 137-45.
355. Lyn, R.K., D.C. Kennedy, S.M. Sagan, D.R. Blais, Y. Rouleau, A.F. Pegoraro, X.S. Xie, A. Stolow, and J.P. Pezacki, *Direct imaging of the disruption of hepatitis C virus replication complexes by inhibitors of lipid metabolism*. *Virology*, 2009. **394**(1): p. 130-42.
356. Singaravelu, R., R. Chen, R.K. Lyn, D.M. Jones, S. O'Hara, Y. Rouleau, J. Cheng, P. Srinivasan, N. Naseri, R.S. Russell, D.L. Tyrrell, and J.P. Pezacki, *Hepatitis C virus induced up-regulation of microRNA-27: a novel mechanism for hepatic steatosis*. *Hepatology*, 2014. **59**(1): p. 98-108.
357. Schoonjans, K., B. Staels, and J. Auwerx, *Role of the peroxisome proliferator-activated receptor (PPAR) in mediating the effects of fibrates and fatty acids on gene expression*. *J Lipid Res*, 1996. **37**(5): p. 907-25.
358. Conklin, D., D. Gilbertson, D.W. Taft, M.F. Maurer, T.E. Whitmore, D.L. Smith, K.M. Walker, L.H. Chen, S. Wattler, M. Nehls, and K.B. Lewis,

- Identification of a mammalian angiopoietin-related protein expressed specifically in liver.* Genomics, 1999. **62**(3): p. 477-82.
359. Clark, H.F., A.L. Gurney, E. Abaya, K. Baker, D. Baldwin, J. Brush, J. Chen, B. Chow, C. Chui, C. Crowley, B. Currell, B. Deuel, P. Dowd, D. Eaton, J. Foster, C. Grimaldi, Q. Gu, P.E. Hass, S. Heldens, A. Huang, H.S. Kim, L. Klimowski, Y. Jin, S. Johnson, J. Lee, L. Lewis, D. Liao, M. Mark, E. Robbie, C. Sanchez, J. Schoenfeld, S. Seshagiri, L. Simmons, J. Singh, V. Smith, J. Stinson, A. Vagts, R. Vandlen, C. Watanabe, D. Wieand, K. Woods, M.H. Xie, D. Yansura, S. Yi, G. Yu, J. Yuan, M. Zhang, Z. Zhang, A. Goddard, W.I. Wood, P. Godowski, and A. Gray, *The secreted protein discovery initiative (SPDI), a large-scale effort to identify novel human secreted and transmembrane proteins: a bioinformatics assessment.* Genome Res, 2003. **13**(10): p. 2265-70.
360. Shimizugawa, T., M. Ono, M. Shimamura, K. Yoshida, Y. Ando, R. Koishi, K. Ueda, T. Inaba, H. Minekura, T. Kohama, and H. Furukawa, *ANGPTL3 decreases very low density lipoprotein triglyceride clearance by inhibition of lipoprotein lipase.* J Biol Chem, 2002. **277**(37): p. 33742-8.
361. Clark, P.J., A.J. Thompson, M. Zhu, D.M. Vock, Q. Zhu, D. Ge, K. Patel, S.A. Harrison, T.J. Urban, S. Naggie, J. Fellay, H.L. Tillmann, K. Shianna, S. Noviello, L.D. Pedicone, R. Esteban, P. Kwo, M.S. Sulkowski, N. Afdhal, J.K. Albrecht, D.B. Goldstein, J.G. McHutchison, and A.J. Muir, *Interleukin 28B polymorphisms are the only common genetic variants associated with low-density lipoprotein cholesterol (LDL-C) in genotype-1 chronic hepatitis C and determine the association between LDL-C and treatment response.* J Viral Hepat, 2012. **19**(5): p. 332-40.
362. Tillmann, H.L., K. Patel, A.J. Muir, C.D. Guy, J.H. Li, X.Q. Lao, A. Thompson, P.J. Clark, S.D. Gardner, J.G. McHutchison, and J.J. McCarthy, *Beneficial IL28B genotype associated with lower frequency of*

- hepatic steatosis in patients with chronic hepatitis C. J Hepatol*, 2011. **55**(6): p. 1195-200.
363. Petta, S., C. Rosso, R. Leung, M.L. Abate, D. Booth, F. Salomone, R. Gambino, M. Rizzetto, P. Caviglia, A. Smedile, S. Grimaudo, C. Camma, A. Craxi, J. George, and E. Bugianesi, *Effects of IL28B rs12979860 CC genotype on metabolic profile and sustained virologic response in patients with genotype 1 chronic hepatitis C. Clin Gastroenterol Hepatol*, 2013. **11**(3): p. 311-7 e1.
364. Stattermayer, A.F., K. Rutter, S. Beinhardt, T.M. Scherzer, A. Stadlmayr, H. Hofer, F. Wrba, P. Steindl-Munda, M. Krebs, C. Datz, M. Trauner, and P. Ferenci, *Association of the IL28B genotype with insulin resistance in patients with chronic hepatitis C. J Hepatol*, 2012. **57**(3): p. 492-8.
365. Ohnishi, M., M. Tsuge, T. Kohno, Y. Zhang, H. Abe, H. Hyogo, Y. Kimura, D. Miki, N. Hiraga, M. Imamura, S. Takahashi, H. Ochi, C.N. Hayes, S. Tanaka, K. Arihiro, and K. Chayama, *IL28B polymorphism is associated with fatty change in the liver of chronic hepatitis C patients. J Gastroenterol*, 2012. **47**(7): p. 834-44.